Characterization of Molecular and Antigenic Determinants of FIKK Kinase(s) to Detect *Plasmodium falciparum*

A Thesis Submitted in Partial Fulfillment of the Requirements for the Degree

of

Doctor of Philosophy

by

M. Rajendra Prasad

196106103

Department of Biosciences and Bioengineering

Indian Institute of Technology Guwahati

Guwahati, Assam, 781039, India

Indian Institute of Technology Guwahati

Department of Biosciences and Bioengineering

Declaration

I, **M. Rajendra Prasad**, declare that the thesis entitled **"Characterization of Molecular and Antigenic Determinants of FIKK Kinase(s) to Detect *Plasmodium falciparum*",** culminating my research efforts regarding the diagnosis of *P. falciparum* malaria targeting FIKK kinase(s) that selectively identifies during mixed and co-infection with a greater sensitivity represents a novel biomarker in making it a reliable and potential diagnostic tool. Throughout this research endeavor, I have adhered to the highest standards of academic integrity and ethics. All sources of information, including data, ideas, and concepts, have been duly acknowledged and referenced, following the guidelines provided by my institution. I have not plagiarized or misrepresented the work of others in any form and did not use any AI tools for writing or preparing figures and tables. I affirm that this thesis is the result of my original research work conducted under the supervision of **Prof. Vishal Trivedi**, and in compliance with the regulations of my academic institution, the **Department of Biosciences and Bioengineering, Indian Institute of Technology Guwahati.** I declare that this work has not been submitted for any other degree or examination at any other university or institution.

June 26, 2025

M. Rajendra Prasad

(196106103)

Indian Institute of Technology Guwahati

Department of Biosciences and Bioengineering

Certificate

This is to certify that the thesis entitled **"Characterization of Molecular and Antigenic Determinants of FIKK Kinase(s) to Detect *Plasmodium falciparum*"**, submitted by M. Rajendra Prasad, bearing registration number **196106103**, has been prepared under my supervision and is a record of the original research work carried out by the student. This thesis fulfills the requirements for the Doctor of Philosophy degree at the **Indian Institute of Technology Guwahati.** The findings presented in this thesis are original and contribute to the existing knowledge in the explored area of research. To the best of my knowledge, I certify that this thesis represents original work and has not been submitted for any degree or examination at any other institute or university. The research follows the ethical standards outlined by the Indian Institute of Technology and relevant regulatory bodies. Additionally, we emphasize that the thesis has meticulously acknowledged all research materials obtained from external sources. Moreover, we have diligently cited and attributed any textual content, illustrations, tables, figures, and other elements borrowed from external sources to the best of our knowledge and following scholarly conventions.

June 26, 2025

Prof. Vishal Trivedi

(Supervisor)

Acknowledgements

I have been fortunate to receive invaluable guidance, thoughtful critiques, and encouraging support from many remarkable individuals. Their ideas, challenges, and unwavering belief in my work have not only shaped the outcome of this research but also helped me grow, both intellectually and personally. Words may never fully capture the depth of my gratitude, but I would like to take this moment to sincerely thank each and every person.

At the foundation of every meaningful journey lies the presence of a guiding force, one who illuminates the path when the way forward is uncertain. I extend my deepest gratitude to my supervisor, Prof. Vishal Trivedi, whose wisdom, patience, and steady guidance have been that force throughout my research. His encouragement to explore independently, yet with purpose and discipline, has been instrumental in shaping both my academic path and my growth as a researcher. The training I received under his mentorship is a lasting strength that I shall carry forward with responsibility.

With deep respect, I thank the current Head of the Department Prof. Utpal Bora, and the former heads, Prof. Rakhi Chaturvedi and Prof. Latha Rangan, for their unwavering support and encouragement. It is with great respect that I thank my Doctoral Committee, Prof. Nitin Chaudhary, Prof. Sachin Kumar, and Prof. Tharmalingam Punniyamurthy, for being the wise stewards of my academic path. Their support, like silent guardians, has quietly elevated my journey.

I owe a special note of thanks to all those who have been part of the Malaria Research Group over the years, including Dr. Sooram Banesh, Dr. Anil Kumar, Dr. Rafi Uz Zama Khan, Dr. Alok Kumar Pandey, Dr. Siddharth Neog, Mr. Shirish Bhagwan Kathane, Ms. Eena Dodwani, Mr. Pitam Chakrabarty, Ms. Simran, Mr. Sai, Mr. Shyamji, Ms. Neha, Mr. Sandeep, Mr. Divyanshu, Ms. Arunima, Ms. Mansi Biswas, Mr. Partha Pratim Sikdar, Ms. Harshini Krishna Sai Devalla, Mr. Surya Prakash, Ms. Mitra, and Mr. Mohit Sharma. This journey was made meaningful by their companionship and unwavering support. The friendships we nurtured will forever be a part of my story. I also extend my gratitude to all past and current members in each lab of the department for their invaluable support and contributions. I am grateful to my friends, Rafi, Samara, Sai Chander, Yeshwanth, Venkatesh, Srinivas, Shiva Kumar, Keerthana, Vidya, Shilpa, Anjaneyulu, Pradeep, Chandragiri, Prabhakar, Sosmitha, Noor, Vignesh, Bharatheeswaran, Rohan, Rashmi Singh, Himanshi, Bhoomika, Mouli, Kalpana, Meenakshi, Renuka, Eshwari, Sunitha, Niteesh, Vijay, Anshuman, Arman, Ajith, Raghavan, Nikhil, Sonia, Sahil, Muthuvel, Krishna, Ajay, Ambika, and Krishnakant, for the strong ties that have endured throughout this endeavor. No matter how far apart we were, they found ways to stay close, always ready with encouragement and support when it mattered most.

The soul that steadied my storm, my boundless gratitude to My younger sibling Chinna, My cousins Himasri, Tejaswini, Madhuri, Sri Ramulu, Neelavathi, Kavitha, Rukmini, Swetha, Revathi, Ramu, Balu, Kurumurthy, Mahesh, Sai, Dinesh, Bunty, Bunny, & Bhanu. My aunt's Naga Laxmi garu, Sujatha garu, Bhagya Jyothi garu,Syamala garu, Thirupathamma garu, Lakshmi Devamma garu, and Shantha Kumari garu, for their firm and reliable presence at every step.

My heartfelt thanks extend to my dear childhood friends Pranay, Surendar, Vamsi, Aditya, Srikanth, Sandeep, Kotesh, Amreeth, Sai Charan, Naga Raju, and Harish, whose unwavering support and friendship have been a pillar of strength throughout this journey.

Lastly, with a humble heart, I thank the Divine above, the hands that raised me, and the minds that shaped me.

I am also grateful to the Department of Biosciences and Bioengineering and the Central Instrument Facility (CIF) for providing the essential analytical instruments crucial to my research. I am thankful to my institute, the Indian Institute of Technology, Guwahati, for offering me the opportunity to conduct my research and for providing a fellowship during my Ph.D. tenure.

This acknowledgment is a modest reflection of the deep gratitude I hold for all those, near and far, known and unknown, whose encouragement, kindness, or simply their presence, helped light the way.

Table of Contents

Table of Contents i

List of Figures iv

List of Tables vi

Abbreviations viii

Units ix

Chapter I: Malaria: A Global Health Challenge

1.1	Introduction	3
1.2	The Global Prevalence, and Burden	4
1.3	The Causative Agent of Malaria	6
1.3.1	The Life cycle of *Plasmodium* parasite	7
1.3.2	Erythrocytic Schizogony	8
1.4	The role of Mosquito vectors in transmission	11
1.5	Risk Factors and Vulnerable Populations	12
1.6	Diagnosis and Treatment	14
1.7	References	18

Chapter II: Systematic Analysis of Diagnostic Tools for Malaria Detection

2.1	Malaria Diagnosis	23
2.1.1	Microscopy	23
2.1.2	PCR based methods	24
2.1.3	Rapid Diagnostic Tests (RDTs)	25
2.1.4	Comparative analysis of diagnostic methods	26
2.2	Biomarkers in Malaria Diagnosis	28
2.3	Ongoing Diagnostic Innovations	29
2.4	FIKK Kinases	30
2.4.1	Distribution of FIKK kinase(s)	31
2.4.2	The Functional Properties, Expression profile, and Localization of FIKK kinase(s) in iRBCs	32

2.4.3	Evolutionary Relationship of FIKK kinase(s)	34
2.5	Importance of FIKK Kinase(s)	35
2.6	Objectives of the study	37
2.8	References	38

Chapter III: Experimental Procedures

3.1	Materials and Strains	46
3.2	Bioinformatics Analysis of *P. falciparum* FIKK Kinase(s) for Primer Designing and In-silico PCR	48
3.3	*Plasmodium falciparum 3D7* strain culture	49
3.4	Isolation of genomic DNA from *Plasmodium falciparum, Homo sapiens and other organisms*	49
3.5	PCR Amplification and Gel-Based DNA Analysis	49
3.6	Evaluation of analytical sensitivity and specificity of the *fikk* kinase-based PCR assay	51
3.7	Densitometry and Statistical Analysis	51
3.8	Computational Design of *Chimeric*-FIKK Protein and Plasmid Assembly	52
3.8.1	Comparative Analysis of *FIKK* Kinase Proteins: Retrieval from PlasmoDB and Protein BLAST Evaluation	52
3.8.2	Computational Prediction of Linear B-Cell Epitopes in *FIKK* Kinase Proteins	52
3.8.3	Computational Prediction of MHC Class I and II Binding Epitopes for T-Cell Immunogenicity	53
3.9	Recombinant Expression and Purification of *Chimeric*-FIKK	54
3.9.1	Recombinant C-FIKK Expression: Optimization and Analysis	54
3.9.2	Evaluation of C-FIKK Protein Expression in Different *E. coli* Hosts	54
3.9.3	Effect of Temperature on C-FIKK Protein Expression	55
3.9.4	Optimization of C-FIKK Expression Using Ethanol and Glucose in TB Media	55
3.9.5	Optimization of Culture Media for C-FIKK Protein Expression	55
3.9.6	Optimization of IPTG Concentration for C-FIKK Protein Expression	55

3.9.7	Optimization of Induction Time for C-FIKK Protein Expression	56
3.9.8	Large-Scale Expression and Purification of C-FIKK	56
3.10	Protein Expression Analysis Using SDS-PAGE and Western Blotting	56
3.11	Electro Elution-Based Extraction of C-FIKK Protein	57
3.12	SDS Removal and Protein Fractionation by Ammonium Sulphate Precipitation	57
3.13	Protein Quantification	57
3.14	Generation of Polyclonal Antibody in Rabbit	58
3.15	Purification of Polyclonal antibody of C-FIKK by Ammonium Sulphate Precipitation	58
3.16	Evaluation of Purified Anti-C-FIKK Polyclonal Antibody Titre	58
3.17	Evaluation of Sensitivity of Anti-*Chimeric*-FIKK Polyclonal Antibody	59
3.18	Evaluation of *P. falciparum* Protein using Purified Anti-*Chimeric*-FIKK Polyclonal Antibody	59
3.19	Evaluation of the Selectivity of Anti-*Chimeric*-FIKK during other Organisms by Mocking Coinfection	60
3.20	References	61
	Annexure I	63

Chapter IV: FIKK-Based Molecular Detection of *Plasmodium falciparum*

4.1	Introduction	67
4.2	Experimental Procedures	69
4.3	Results	70
4.4	Discussion	83
4.5	References	87
	Annexure I	91
	Annexure II	97

Chapter V: Characterization of Antigenic Determinants of FIKK Kinase(s) to Detect *Plasmodium falciparum*

5.1	Introduction	100

5.2 Experimental Procedures 102
5.3 Results 103
5.4 Discussion 118
5.5 References 120
Annexure I 122

Chapter VI: Diagnostic Validation of *Chimeric*-FIKK in *Plasmodium falciparum* Malaria Detection

6.1 Introduction 130
6.2 Experimental Procedures 132
6.3 Results 133
6.4 Discussion 139
6.5 References 141
Annexure I 143

Chapter VII: Conclusions

7.1 Conclusions 150
7.2 Future Directions 151

List of Figures

Fig. No.	Figure Description	Page No.
Figure 1.1	The enduring threat of malaria from ancient times	2
Figure 1.2	Global distribution of malaria cases and deaths in 2023	5
Figure 1.3	Life cycle of *Plasmodium falciparum*	7
Figure 1.4	Invasion and Egress of malaria parasite	8
Figure 1.5	Surface antigens of *Plasmodium* species in malaria diagnosis	9
Figure 1.6	Mosquito vectors in malaria transmission	10
Figure 1.7	Risk Factors in Malaria Transmission	12
Figure 1.8	Impact of misdiagnosis on survival during co-infection and mixed malaria infections	14
Figure 2.1	Microscopic identification of malarial parasites using thick and thin blood smears	24

Figure 2.2	PCR-based identification of *Plasmodium* parasites	25
Figure 2.3	Lateral flow Rapid Diagnostic Tests (RDTs) for identifying *Plasmodium* infections	26
Figure 2.4	Stage-specific expression and intracellular localization of FIKK kinases in *P. falciparum*-infected red blood cells (iRBCs).	33
Figure 2.5	Comparison of kinome composition in Apicomplexan parasites, & *Homo sapiens* along with the phylogenetic analysis of the *P. falciparum* kinome	35
Figure 4.1	Research design provides a visual representation of the sequential steps involved in the research and development process, from gene selection to the final validation in developing PCR-based malaria diagnosis	70
Figure 4.2	Flowchart of the in-silico analysis and primer design for *fikk* kinases that illustrates the comprehensive in silico analysis and rigorous selection process undertaken to identify highly specific primers for the accurate detection of *P. falciparum*	71
Figure 4.3	The primers designed for specific amplification from the *Plasmodium falciparum* genome do not show any amplification with host DNA	73
Figure 4.4	Shortlisted *fikk* primers specifically detect *Plasmodium falciparum* DNA at the molecular level	74
Figure 4.5	Shortlisted *fikk* primers are specific to detect *Plasmodium falciparum* infected RBCs at the organism/cellular level	76
Figure 4.6	Shortlisted *fikk* primers are specific to detect *Plasmodium falciparum* infected RBCs in the presence of virus infected mammalian cells	77
Figure 4.7	Sensitivity analysis of shortlisted primers for the detection of *Plasmodium falciparum*	78
Figure 4.8	Validation of shortlisted primers (*fikk3*) in mock patient samples	82
Figure 5.1	The illustration of the research design visually outlines the step-by-step process, starting from FIKK selection and progressing to final C-FIKK design	103

Figure 5.2	FIKK9.1 includes distinctive regions with potential applications in malaria detection	104
Figure 5.3	Sequential and overlapping analysis of predicted linear B-cell epitopes to identify their surface accessibility and antigenic potential	115
Figure 5.4	Sequential and overlapping analysis of predicted linear T-cell epitopes to identify potential MHC-1 & II with greater binding affinities	116
Figure 5.5	The design of the chimeric FIKK involved selecting suitable FIKK proteins based on the physicochemical properties of B and T-cells	117
Figure 6.1	*Chimeric*-FIKK Expression.	133
Figure 6.2	Purification, and Antibody Generation of C-FIKK	134
Figure 6.3	Antibody Titration and Specificity Validation of Anti-C-FIKK Sera by ELISA and Western Blot	135
Figure 6.4	Sensitivity of *Chimeric*-FIKK	136
Figure 6.5	Selectivity of *Chimeric*-FIKK	137

List of Tables

Table. No.	**Table Description**	**Page No.**
Table 1.1	Treatment strategies for malaria with co-infections	15
Table 1.2	Treatment strategies for infections having mixed *Plasmodium* species	16
Table 2.1	Comparative Assessment of Malaria Diagnostic Techniques: Microscopy, PCR, and Rapid Diagnostic Tests	27
Table 2.2	Limitations of Commonly Used Malaria Diagnostic Markers	28
Table 2.3	Comparison of Emerging Diagnostic Techniques	29
Table 2.4	Distribution of FIKK Kinases in *Plasmodium species*	32

Table 2.5	Localization and Expression Stages of 21 FIKK kinases of *P. falciparum*	34
Table 3.1	List of various pathogens and their source used in the study	47
Table 3.2	Primer details for *fikk* kinase-based PCR assay	50
Table 4.1	Shortlisted primer sequences specific to *Plasmodium falciparum*	72
Table 4.2	Validation of *fikk3* for detecting *P.falciparum* malaria via blind test.	80
Table 5.1	Analysis of *Plasmodium falciparum* 3D7 FIKK kinase(s) protein sequence	105
Table 5.2	Characterization of predicted B-cell epitopes of FIKK kinase from *P. falciparum*	106
Table 5.3	Characterization of predicted 21 FIKK kinase B-cell epitopes of *P. falciparum* 3D7 strain (PF3D7) based on their innate physiochemical properties (surface accessibility and antigenicity).	107
Table 5.4	Predicted linear B-cell epitopes of antigenic FIKK proteins of *P. falciparum* (*PF3D7* strain)	109
Table 5.5	Prediction of potential T-cell epitopes (MHC-I binding predictions) of FIKK kinases of *P. falciparum* 3D7 strain (PF3D7)	111
Table 5.6	Prediction of potential T-cell epitopes (MHC-II binding predictions) of FIKK kinases of *P. falciparum* 3D7 strain (PF3D7)	113

Abbreviations

18S rRNA- 18S ribosomal RNA

BLAST- Basic Local Alignment Search Tool

bp- base pair

cDNA- complementary DNA

C-terminus- Carboxyl-terminus

DEV- Duck Enteritis Virus

DNA- Deoxyribose Nucleic acid

E. coli- Escherichia coli

FIKK- Phenylalanine, Isoleucine, Lysine, Lysine

f 3- fikk 3 gene

f 4.2- fikk 4.2 gene

f 8- fikk 8 gene

f 10.2- fikk 10.2 gene

f 12- fikk 12 gene

f 14- fikk 14 gene

FP- Forward Primer

gDNA- genomic DNA

GC- Guanine-Cytosine content

Hb- Haemoglobin

HSV- Herpes Simplex Virus

P. m- Plasmodium malariae

HuGAPDH- Human Specific Glyceraldehyde-3-Phosphate Dehydrogenase

P. k- Plasmodium knowlesi

RBCs- Red Blood Cells

RPMI 1640- Roswell Park Memorial Institute 1640 medium

RNA- Ribo Nucleic acid

RPA- Recombinase Polymerase Amplification

RDTs- Rapid Diagnostic Tests

RP- Reverse Primer

SD- Syphilis Duo

tHDA- Isothermal Thermophilic Helicase–Dependent Amplification

WHO- World Health Organization

*Pf*EMP1 - *Plasmodium falciparum* Erythrocytic Membrane Protein 1

MSP1 - Merozoite Surface Protein 1

*Pf*Rh5 - *Plasmodium falciparum* Reticulocyte Binding Protein Homologue 5

*Pf*Rhs - *Plasmodium falciparum* Reticulocyte-binding Protein Homologs

PCR - Polymerase Chain Reaction

PFA - Paraformaldehyde

PEG - Polyethylene Glycol

TBST - Tris-Buffered Saline with Tween

TNF-α - Tumor Necrosis Factor Alpha

JEV- Japanese Encephalitis Virus

LAMP- Loop-Mediated

Isothermal Amplification

M- Marker

NC/N- Negative Control

NCBI- National Centre for Biotechnology

Information

NDV- Newcastle Disease Virus

N-terminus- Amino-terminal

OD- Optical Density

PCR- Polymerase Chain Reaction

PC/P- Positive Control

Pf-ldh- Plasmodium falciparum Specific

Lactate Dehydrogenase

Pf-hrp-2- Plasmodium falciparum specific

Histidine Rich Protein 2

pLDH- *Plasmodium* Lactate Dehydrogenase

P. v- Plasmodium vivax

P. o- Plasmodium ovale

pI - Isoelectric Point

PR8 - Influenza A Virus (strain PR8)

qPCR - Quantitative Polymerase Chain Reaction

ROS - Reactive Oxygen Species

Units

Å	angstrom	**nm**	nanometer
°C	degree celsius	**kcal/mole**	kilocalories per mole
%	percent	**kJ/mole**	kilojoule per mole
µM	micro molar	**mg**	milligram
µW	microwatt	**kV**	kilovolt
µg/ml	microgram per milliliter	**mm**	millimeter
µmole/min	micromoles per minute	**U/L**	units per Liter
µl	micro liter	**g**	gram
µg	micro gram	**fg**	femtogram
mM	mill molar	**mL**	milliliter
mg/ml	milligram per milliliter	**pg**	picogram
ns	nanosecond	**nM**	nano molar

Chapter 1

Malaria: A Global Health Challenge

SUMMARY

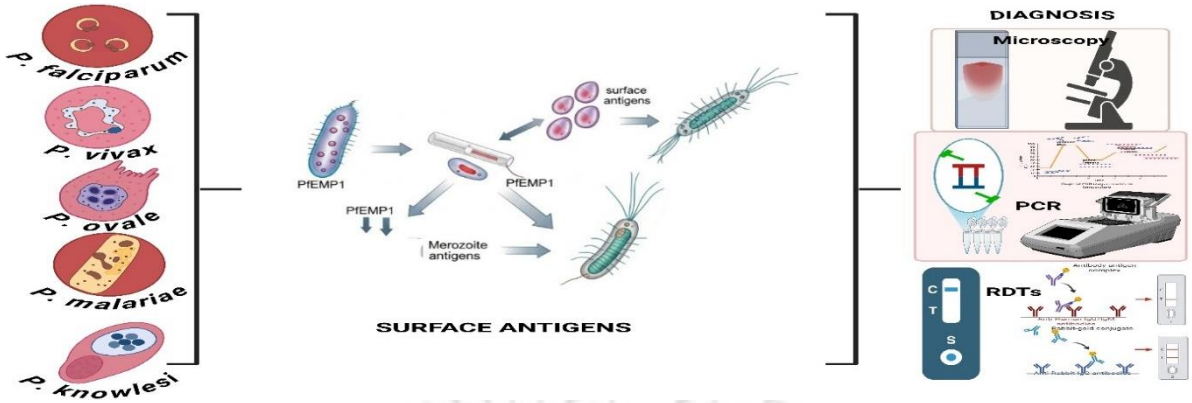

Figure: A representation of Surface antigens of *Plasmodium* species in malaria diagnosis.

Malaria, caused by *Plasmodium* parasites and transmitted by *Anopheles* mosquitoes, remains a global health challenge, with *Plasmodium falciparum* responsible for most severe and fatal infections (WHO, 2024; CDC, 2023). Historical advancements include the discovery of qquinine, Laveran's identification of the *Plasmodium* parasite in 1880, and the development of Artemisinin-based therapies have shaped the global response to malaria (Laveran, 1880; Najera et al., 2011; & Tu, 2011). Despite progress through vector control strategies like insecticide-treated nets (ITNs), indoor residual spraying (IRS), and improved treatment, malaria elimination remains challenging. The rise of drug- and insecticide-resistant strains, diagnostic limitations, and weak surveillance systems continue to impede progress (Najera et al., 2011; Menard & Dondorp, 2017; Genton et al., 2021; & Global Fund, 2023). According to the *World Malaria Report 2024*, 249 million cases were reported globally, with sub-Saharan Africa bearing the highest burden. India, however, achieved over a 90% reduction in cases since 2000 through integrated interventions (WHO, 2024). The persistence of malaria is further reinforced by the parasite's ability to evade host immunity and adapt to environmental and epidemiological pressures (Phillips et al., 2017; Sinden, 2017). Climate variability, poverty, and healthcare disparities further complicate eradication efforts (Ryan et al., 2020; Kwiatkowski, 2005). In this context, strengthening early and accurate diagnosis remains critical, as timely detection directly influences treatment efficacy and transmission control. Advances in molecular and biomarker-based diagnostics, including the exploration of *Plasmodium* proteins such as FIKK kinase(s), offer promising avenues for improving sensitivity, specificity, and field applicability. Continued innovation in these areas, coupled with vaccine research, vector management, and international collaboration, is essential in achieving the WHO's 2030 malaria elimination goals (Feachem et al., 2019; Greenwood et al., 2019).

1.1 Introduction

Malaria is a life-threatening infectious disease caused by *Plasmodium* parasites and transmitted to humans through the bites of infected *Anopheles* mosquitoes (Koella 1998). Among the five *Plasmodium* species that infect humans, *Plasmodium falciparum* is the most virulent (Larson, B. (2019)) and is responsible for the majority of malaria-related deaths worldwide (Sankineni, S 2023). The disease manifests with recurrent fever, chills, and flu-like symptoms, but severe cases can lead to complications such as cerebral malaria, multi-organ failure, and fatal outcomes (El-Radhi, A. S. (2019)).

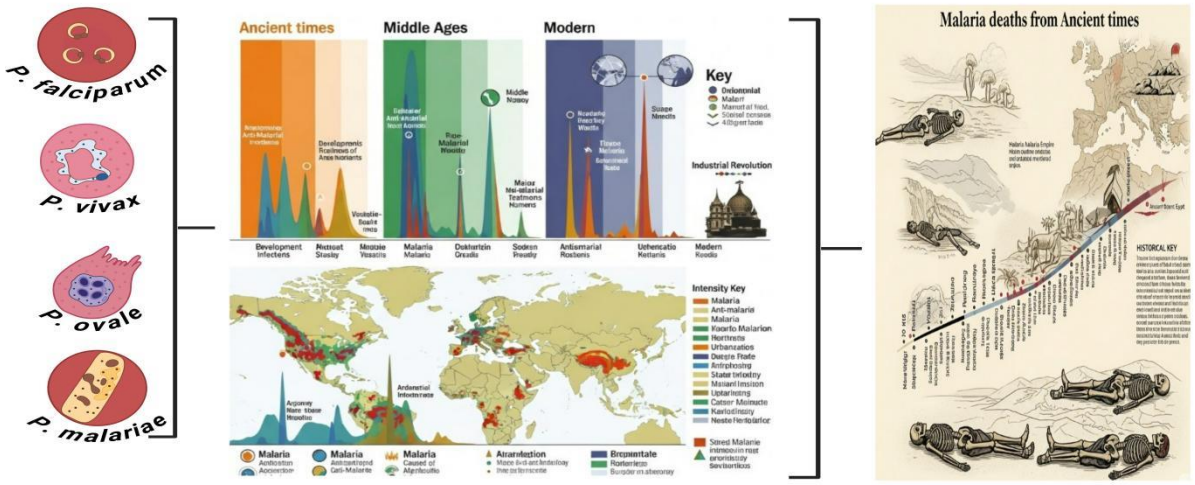

Figure 1.1: The enduring threat of malaria from ancient times. The figure represents the persistent and evolving burden of malaria, from ancient civilizations to modern day endemic regions with higher mortality rates. (Prepared using BioRender)

Malaria has afflicted human populations for millennia (Figure 1.1), with early descriptions of periodic fever found in ancient Chinese medical texts dating back to 2700 BC and Greek writings from around 800 BC (Neghina 2010). The disease was historically prevalent in Egypt, India, and Rome, where it was commonly associated with marshy environments, giving rise to the term *mal aria* ("bad air") (Packard, R. M. 2021). However, scientific understanding of malaria remained rudimentary until the 17th century when the medicinal properties of cinchona bark, which contains quinine, were recognized as the first effective treatment (Foley, M., & Tilley, L. (1998)). A pivotal breakthrough occurred in 1880, when Alphonse Laveran first identified *Plasmodium* parasites in the blood of a febrile patient, marking the discovery of the causative agent of malaria and establishing the foundation of modern parasitology (Laveran, 1880; Bruce-Chwatt, 1988). This discovery set the stage for decades of research culminating in the development of Artemisinin-based Combination

Therapies (ACTs), which today serve as the first-line treatment for *uncomplicated Plasmodium falciparum* malaria (WHO, 2024). Despite these advancements, malaria remains a major global health challenge, causing an estimated 608,000 deaths and 249 million cases in 2024, with over 94% of fatalities occurring in sub-Saharan Africa, particularly among children under five and pregnant women (WHO, 2024; CDC, 2023)

The 21st century has seen intensified malaria elimination initiatives, including the Roll Back Malaria (RBM) Partnership, the Global Technical Strategy for Malaria 2016–2030 (GTS), and the E-2025 initiative, all aiming to reduce malaria incidence and mortality by at least 90% by 2030 (Feachem et al., 2019; WHO, 2021). However, challenges such as drug and insecticide resistance, diagnostic limitations, health system gaps, climate change, and socioeconomic inequality continue to hinder progress toward malaria elimination (interruption of local transmission) and the longer-term goal of eradication (global cessation of transmission) (Menard & Dondorp, 2017; Feachem et al., 2019). Addressing these multilayered obstacles requires sustained innovation in diagnostics, therapeutics, vector control, and surveillance.

Despite these advancements, malaria remains a significant global health challenge, with huge deaths, predominantly in sub-Saharan Africa (WH0 2023). Although vaccines such as RTS, S (Mosquirix) and R21 have been developed, their efficacy remains modest and requires further optimization (Barrett, J. R, 2024). Additionally, emerging challenges, including *pfhrp2* gene deletions that compromise rapid diagnostic tests (RDTs), drug-resistant *Plasmodium* strains, insecticide-resistant mosquitoes, and the expansion of malaria-endemic regions due to climate change, continue to pose significant obstacles to eradication efforts (Musyoka, K. B. (2021); Stabler, T. C. (2024)). Ongoing efforts aimed at improving diagnostic methods, developing novel therapeutics, enhancing vaccine efficacy, and implementing innovative vector control strategies will be crucial in advancing malaria elimination efforts globally (Takala-Harrison & Laufer, 2015).

1.2 Global Prevalence and Burden

The World Malaria Report 2024, published by the World Health Organization (WHO) in December 2024, estimated approximately 249 million malaria cases worldwide (Figure 1.2-A), reflecting a decrease from 252 million cases reported in 2022. However, malaria-related deaths exhibited a slight decline, decreasing from 600,000 in 2022 to 597,000 in 2023 but increased to 608,000 in 2024 (Figure 1.2-B). The WHO African Region remains the most severely affected, accounting for 94% of all malaria cases, with approximately 234 million cases reported in 2024. While malaria transmission is also significant in other regions, such as

Southeast Asia, its prevalence remains considerably lower compared to sub-Saharan Africa (WHO, 2024).

India, despite being the highest malaria-burden country in the WHO South-East Asia Region, has made substantial progress in malaria control. According to the World Malaria Report 2024, India has reduced its malaria incidence by 93% since 2000, with cases declining from 20 to 1.5 per 1,000 people at risk, translating to 17.7 million fewer malaria cases (WHO, 2024). Between 2015 and 2022, the country recorded an 85.1% reduction in malaria cases and an 83.3% decline in malaria-related deaths. More recently, reported malaria cases in India fell by 49%, accompanied by a 50.5% reduction in malaria-related fatalities (WHO, 2024). While these statistics highlight substantial progress, they also emphasize the need for sustained efforts and strengthened public health interventions to achieve global malaria eradication.

Malaria continues to disproportionately affect children under five years and pregnant women, who represent the most vulnerable groups in endemic regions. In young children, underdeveloped immunity increases the risk of severe and fatal malaria (Snow et al., 2017). In pregnant women, particularly primigravidae, immunological modulation during pregnancy reduces protection against *Plasmodium falciparum* infection (Desai et al., 2007; Rogerson et al., 2018). Placental malaria arises when infected erythrocytes expressing VAR2CSA adhere to chondroitin sulfate A (CSA) in the placenta, impairing nutrient transfer and provoking inflammation (Fried & Duffy, 1996; Sharma et al., 2020). This contributes to maternal anemia, preterm delivery, and low-birth-weight infants—major causes of neonatal morbidity and mortality. In 2022, approximately 12 million pregnancies in sub-Saharan Africa were exposed to malaria, resulting in over 900,000 low-birth-weight infants (WHO, 2024). These findings highlight the need for improved diagnostics, intermittent preventive treatment in pregnancy (IPTp), and strengthened vector control. Sustained interventions are crucial for achieving malaria elimination—the interruption of local transmission—while the long-term global goal remains the eradication of malaria infection (Feachem et al., 2019; WHO, 2021).

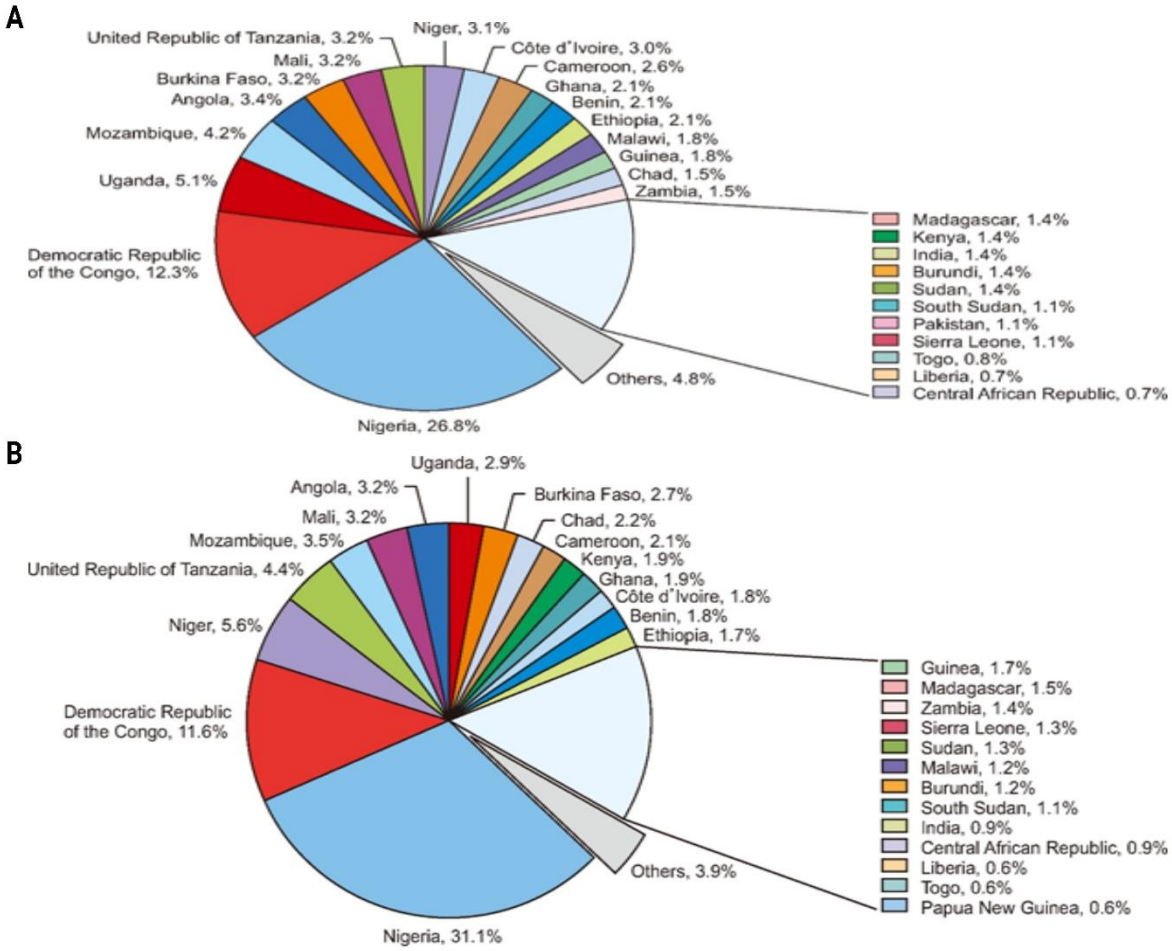

Figure 1.2: Global distribution of malaria cases and deaths in 2024. This illustrate the geographical burden of malaria with panel **(A)** showing the estimated cases and panel **(B)** depicting the deaths reported. (Source: World Health Organization)

1.3 The Causative Agent of Malaria

The *Plasmodium* genus comprises protozoan parasites that cause malaria, a major global health concern. Of the more than 200 identified *Plasmodium* species, five are known to infect humans: *Plasmodium falciparum, Plasmodium vivax, Plasmodium malariae, Plasmodium ovale,* and *Plasmodium knowlesi* (Sato, S. (2021)). While the first four species are human-specific, *P. knowlesi* primarily infects macaque monkeys but can also be transmitted to humans, particularly in Southeast Asia, where zoonotic transmission has been increasingly documented (Singh & Daneshvar, 2013). Among these species, *P. falciparum* is the most virulent, frequently leading to severe complications and high mortality rates, particularly in sub-Saharan Africa (Venugopal et al., 2020).

The *Plasmodium* parasite follows a complex life cycle involving two hosts: a vertebrate (such as humans) and an insect vector (female *Anopheles* mosquitoes). Recent studies suggest that the bone marrow serves as a critical site for both asexual replication and gametocyte development, providing a protected niche that facilitates parasite survival and contributes to disease persistence (Venugopal et al., 2020). This sequestration in specific tissues presents a challenge for malaria treatment, as these hidden parasite reservoirs can evade immune responses and antimalarial therapies. Consequently, targeting these protected sites and disrupting the parasite's life cycle at multiple stages is an essential strategy for malaria eradication (Venugopal et al., 2020).

A comprehensive understanding of *Plasmodium* biology and transmission dynamics is crucial for developing effective malaria control and prevention strategies. Current research efforts focus on identifying novel diagnostic biomarkers, improving vector control measures, and developing next-generation antimalarial drugs and vaccines that target different stages of the parasite's life cycle (Sato, 2021). These integrated approaches are vital in the ongoing battle against malaria, supporting global efforts to reduce transmission and ultimately achieve disease eradication.

1.3.1 The Lifecycle of *Plasmodium* Parasite

The *Plasmodium* parasite, the causative agent of malaria, follows a complex life cycle involving both human and mosquito hosts (Figure 1.3). Transmission occurs when an infected female *Anopheles* mosquito (in the figure 1.3) bites a human, introducing sporozoites into the bloodstream (*Ghosh et al., 2019*). These sporozoites rapidly migrate to the liver, where they invade hepatocytes and undergo asexual replication, forming schizonts. Upon maturation, the schizonts rupture, releasing merozoites into the bloodstream and initiating the erythrocytic stage (*Prudêncio et al., 2011*). Merozoites invade red blood cells (RBCs) and progress through distinct developmental phases, ring, trophozoite, and schizont stages, culminating in RBC rupture and the release of new merozoites. This cycle perpetuates the infection and is responsible for the characteristic periodic fevers and chills associated with malaria (Warrell, D. A. (2017)). Some merozoites differentiate into sexual forms, known as gametocytes, which are essential for transmission back to the mosquito vector (Josling, G. A *2018*).

When a mosquito ingests gametocyte-infected blood, the parasite undergoes sexual reproduction in the mosquito's midgut. The gametocytes mature into male and female gametes, which fuse to form a zygote (*Bousema & Drakeley, 2011*). The zygote develops into a motile ookinete, which traverses the mosquito's midgut wall and forms an oocyst on the external

surface. Inside the oocyst, thousands of sporozoites develop and eventually migrate to the mosquito's salivary glands, enabling transmission to a new human host during the mosquito's next blood meal *(*Sinden, 2017*).*

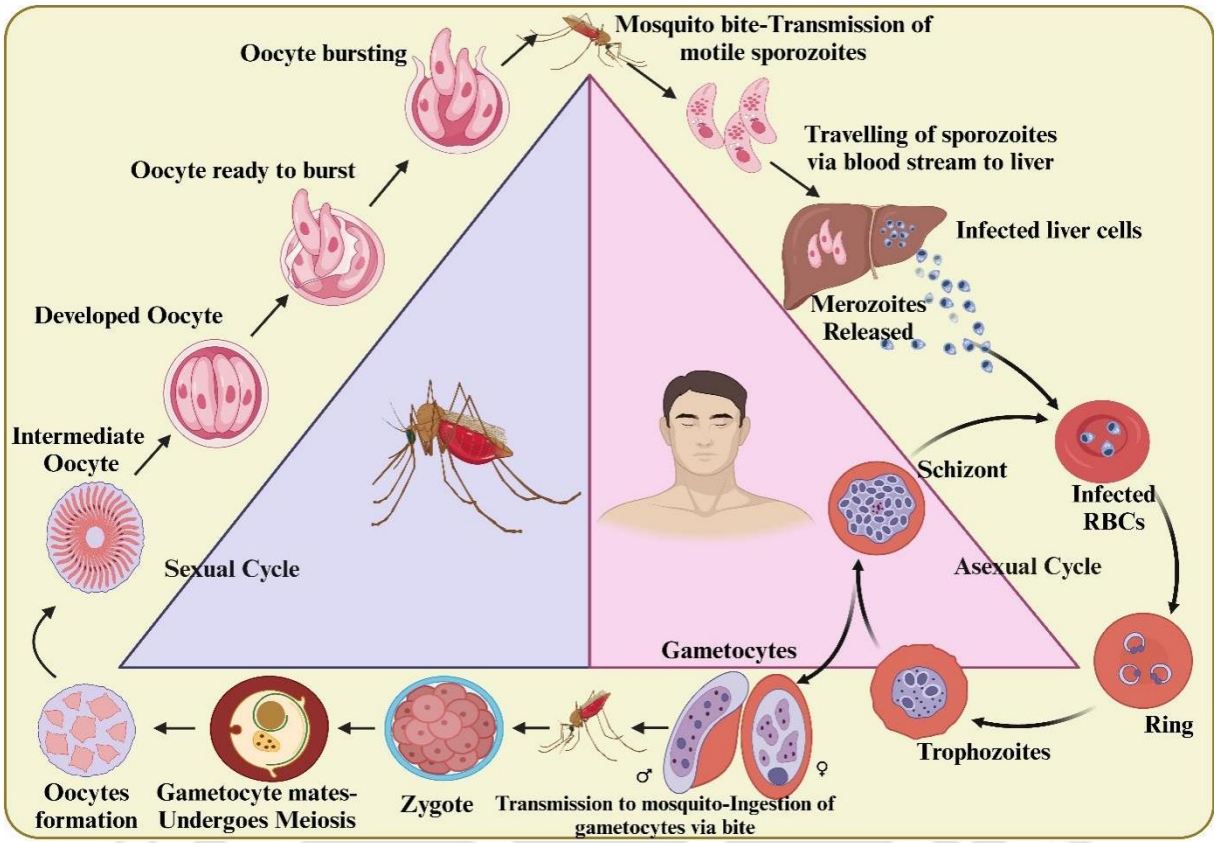

Figure 1.3: Life cycle of *Plasmodium falciparum.* The figure represents the digenetic life cycle of *P. falciparum* involving the human host and female *Anopheles* mosquito. (Prepared using BioRender)

Understanding the intricate life cycle of *Plasmodium* is critical for developing targeted malaria control strategies. By identifying key vulnerabilities in the parasite's developmental stages, researchers can design interventions to disrupt transmission and disease progression, including innovative diagnostic approaches, vaccines, vector control measures, and antimalarial therapies (Cable, J., Barber, *2017*).

1.3.2 Erythrocytic Schizogony

The parasite is transmitted through infected *Anopheles* mosquitoes, initiating infection in the liver before invading red blood cells (RBCs), where most of the disease pathology arises (*Chandley et al., 2023*). While the host immune system can often clear invading parasites

(*Sierro & Grau, 2019*), *Plasmodium* species have evolved sophisticated mechanisms to evade immune detection and destruction.

During transmission, *Plasmodium* sporozoites must bypass skin defenses before reaching the liver. To achieve this, they employ motility-associated proteins such as SPECT-1, SPECT-2, PLP1, and TRAP, facilitating migration through the dermis (*Ejigiri & Sinnis, 2009; Guerra & Carruthers, 2017; Patarroyo et al., 2011; Wilson et al., 2016*). Additionally, sporozoites manipulate neutrophils to evade immune clearance (*Waisberg et al., 2014; Aitken et al., 2018*). Once in the liver, parasites modulate Kupffer cell activity by suppressing Th1 cytokines and enhancing Th2 cytokine responses to facilitate hepatocyte invasion (*Tweedell et al., 2018*). Further, the parasite exploits the host's cholesterol uptake pathway for intracellular survival (*Deroost et al., 2016*) and utilizes its circumsporozoite protein (CSP) to regulate inflammatory responses and the mTOR pathway (*Belachew, 2018; Dimasuay et al., 2017; Rashidi et al., 2021*).

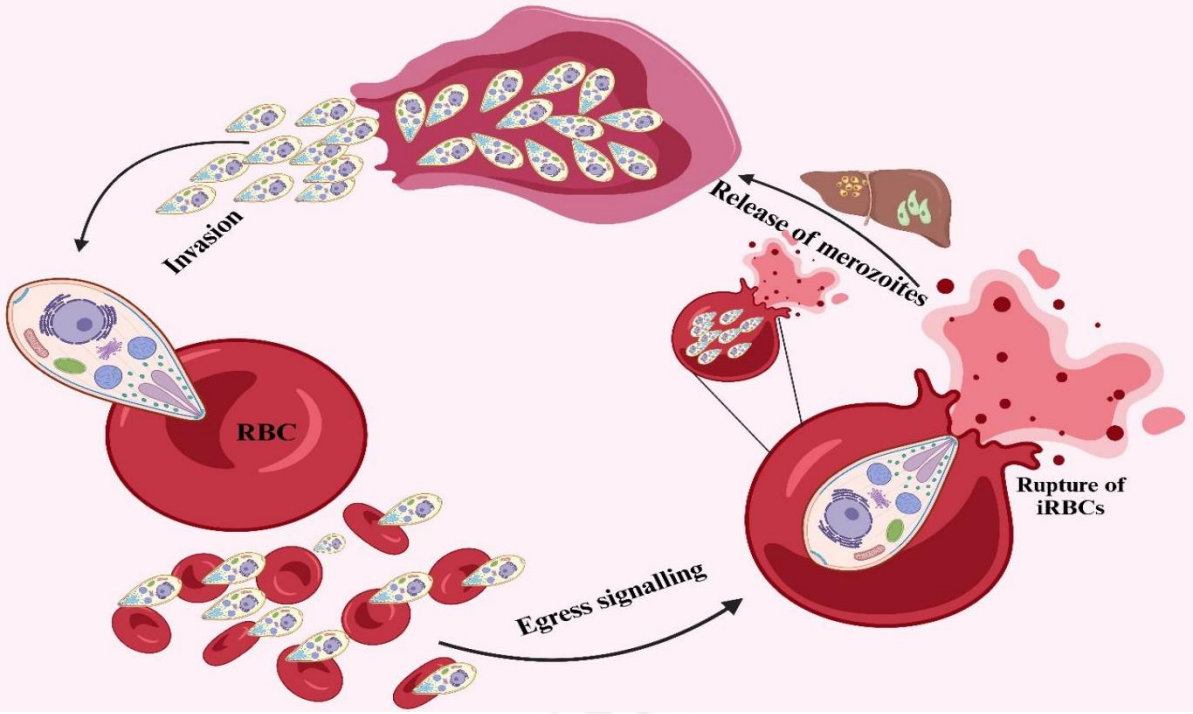

Figure 1.4: Invasion and Egress of malaria parasite. The figure illustrates the step by step processes of invasion and egress during the intraerythrocytic cycle of *P. falciparum*. (Prepared using BioRender)

In the bloodstream, *P. falciparum* merozoites utilize surface proteins such as MSP-1 and EBL to invade RBCs (*Nosjean et al., 1997*), while schizogony enables rapid proliferation (*Belachew, 2018; Rund et al., 2016*). To evade immune clearance, parasites employ rosetting

(*Moll et al., 2015*) and sequestration within the microvasculature via PfEMP-1, which binds endothelial receptors (*Abdi et al., 2016; Wahlgren & Goel, 2017; Sakoguchi et al., 2021; Chew et al., 2022*). The parasite further evades immunity by shedding the antigenic protein EBA-175 (*Jaskiewicz et al., 2019; Paing et al., 2018*), secreting extracellular vesicles containing HRF and EF-1α to suppress CD4+ T-cell activation (*Demarta-Gatsi et al., 2019*), and acquiring host plasminogen to degrade complement components (*Reiss et al., 2021*) as seen in the figure 1.4. Additionally, *Plasmodium* induces regulatory T cells to release sFGL2, inhibiting macrophage activity (*Fu et al., 2020*), and utilizes microRNAs to trigger lymphocyte apoptosis (*Dieng et al., 2020*).

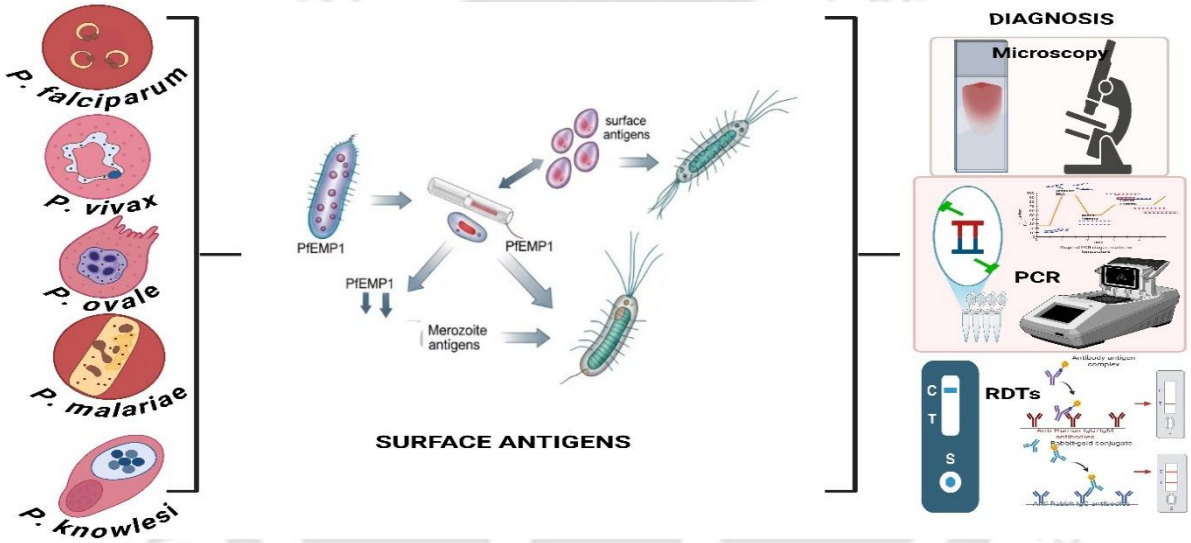

Figure 1.5: Surface antigens of *Plasmodium* species in malaria diagnosis. The figure represents the role of key surface antigens expressed in *Plasmodium* species serving as diagnostic targets. (Prepared using BioRender)

Surface antigens like *Plasmodium falciparum* erythrocyte membrane protein 1 (PfEMP1) and merozoite surface antigens (MSAs) are vital for malaria diagnosis (figure 1.5), offering accessible and distinct targets. Merozoite surface proteins (MSPs), such as MSP1 and MSP2, are crucial for serological detection of past or current infections due to the development and persistence of antibodies against them (Fowkes et al., 2010; Richards et al., 2010). While PfEMP1's variability poses challenges, its role in pathogenesis (Tembo et al., 2014) highlights its diagnostic potential. However, rapid diagnostic tests (RDTs) primarily rely on the abundant Histidine-Rich Protein II (HRP2) (CDC, n.d.), despite issues with antigen persistence and *Pfhrp2/3* gene deletions that can lead to false results (CDC, n.d.; WHO, 2023) pressing the need for novel targets.

Malaria, primarily caused by *P. falciparum*, presents with symptoms such as fever, chills, headache, and gastrointestinal disturbances that may mimic influenza-like illness (WHO, 2023). The fever pattern in *P. falciparum* infections is typically irregular due to asynchronous erythrocytic schizogony, while *P. vivax* and *P. ovale* infections often exhibit a 48-hour ("tertian") periodicity and *P. malariae* a 72-hour ("quartan") cycle (White et al., 2014; Collins & Jeffery, 2005). The progression from uncomplicated to severe disease underscores the critical importance of early diagnosis and prompt, effective treatment to prevent mortality and long-term sequelae (WHO, 2024).

1.4 The Role of Mosquito Vectors in Transmission

Mosquitoes are the primary vectors of numerous infectious diseases, with malaria exclusively transmitted by female *Anopheles* species through their bites (Sinka et al., 2012). Key vectors include *Anopheles gambiae* and *Anopheles funestus* in sub-Saharan Africa, known for their high vectorial capacity (Takken & Verhulst, 2013). In the Americas, *Anopheles darlingi* is the main vector, while *Anopheles dirus* and *Anopheles minimus* are crucial in Southeast Asia (Manguin et al., 2013). The distribution and prevalence of these mosquito species are significantly influenced by ecological and climatic factors like temperature, humidity, and breeding site availability, which impact their survival, feeding behaviour, and transmission potential (Guerra et al., 2006).

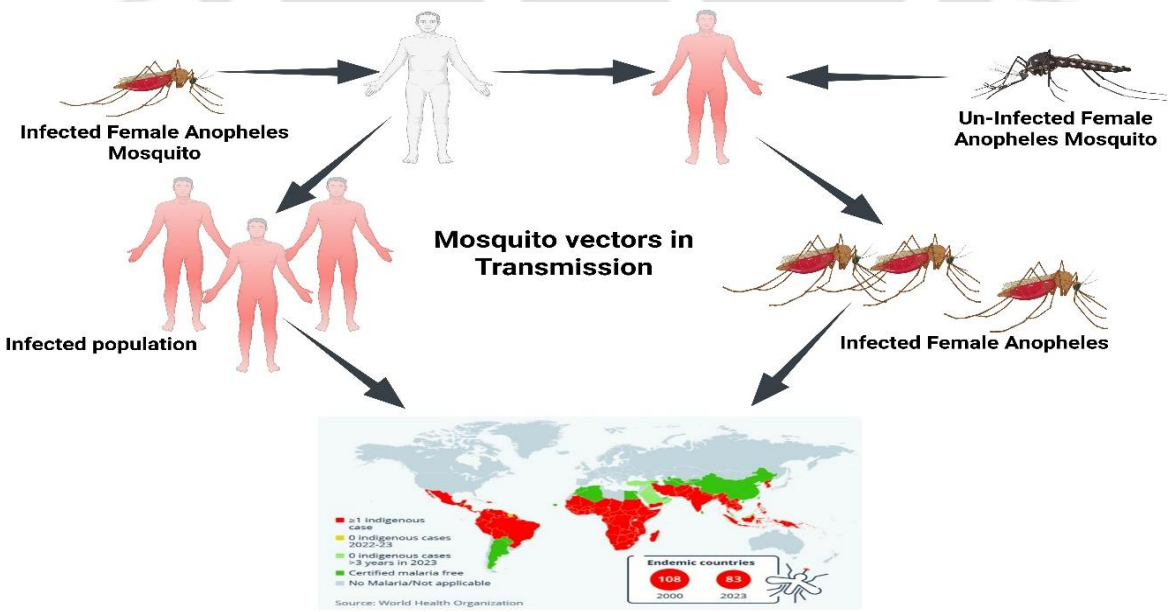

Figure 1.6: Mosquito vectors in malaria transmission. This figure represents the essential role of infected and un-infected female *Anopheles* mosquitoes for global burden in the transmission of malaria. (Prepared using BioRender)

Malaria transmission is closely tied to the presence and behavior of dominant vector species (DVS), with 41 mosquito species contributing to global malaria transmission (Sinka et al., 2012). In Africa, *Anopheles gambiae*, *Anopheles arabiensis*, and *Anopheles funestus* are highly efficient due to their adaptability (Sinka et al., 2012). The Asia-Pacific region, however, presents a more complex scenario with multiple coexisting *Anopheles* species, including *Anopheles dirus*, *Anopheles minimus*, and *Anopheles sundaicus*, each possessing unique traits that influence transmission patterns (Sinka et al., 2012). This diversity in vector species creates challenges for malaria control, necessitating targeted interventions that consider regional vector ecology and behavior. When the mosquito bites another human, it injects saliva containing sporozoites, initiating a new infection (Figure 1.6). Several factors influence transmission efficiency, including the mosquito's lifespan, feeding frequency, and environmental conditions that affect both mosquito survival and parasite development (Smith et al., 2004).

Understanding the global distribution and behavioral patterns of malaria vectors is crucial for designing effective disease control strategies. Studies such as those by Sinka et al. (2012) provide valuable insights into the geographic distribution of malaria vectors, forming a foundational basis for public health interventions. By identifying the dominant mosquito species responsible for malaria transmission in different regions, researchers and policymakers can implement more effective vector control measures, ultimately reducing the global burden of malaria (WHO, 2021).

1.5 Risk Factors and Vulnerable Populations

Malaria transmission and severity are shaped by a complex interplay of environmental, socioeconomic, and biological factors. Environmental conditions, including temperature, rainfall, and humidity, are critical in determining mosquito breeding and survival patterns (Figure 1.7). *Anopheles* mosquitoes thrive in warm, humid climates, with peak transmission typically occurring during and after the rainy season (Yamana & Eltahir, 2013). Geographic features such as proximity to water bodies, dense forests, and inadequate housing further exacerbate malaria risk (Weiss et al., 2019). Additionally, human-induced environmental changes, including urbanization and deforestation, can alter mosquito habitats, sometimes increasing malaria transmission in certain regions (Reid et al., 2019).

Socioeconomic conditions also play a significant role in malaria prevalence. Poverty restricts access to healthcare, insecticide-treated bed nets (ITNs), and other preventive measures, increasing vulnerability among affected populations (Tusting et al., 2013).

Education and awareness are equally critical, as a lack of knowledge about malaria prevention and treatment often leads to delayed medical intervention (Okaka et al., 2021). Occupational exposure is another key factor, with farmers, miners, and forest workers at higher risk due to prolonged outdoor activity during peak mosquito feeding times (Haque et al., 2020). Additionally, inadequate infrastructure, poor sanitation, and limited access to electricity create conditions conducive to mosquito breeding and increase nighttime exposure (Castro et al., 2017).

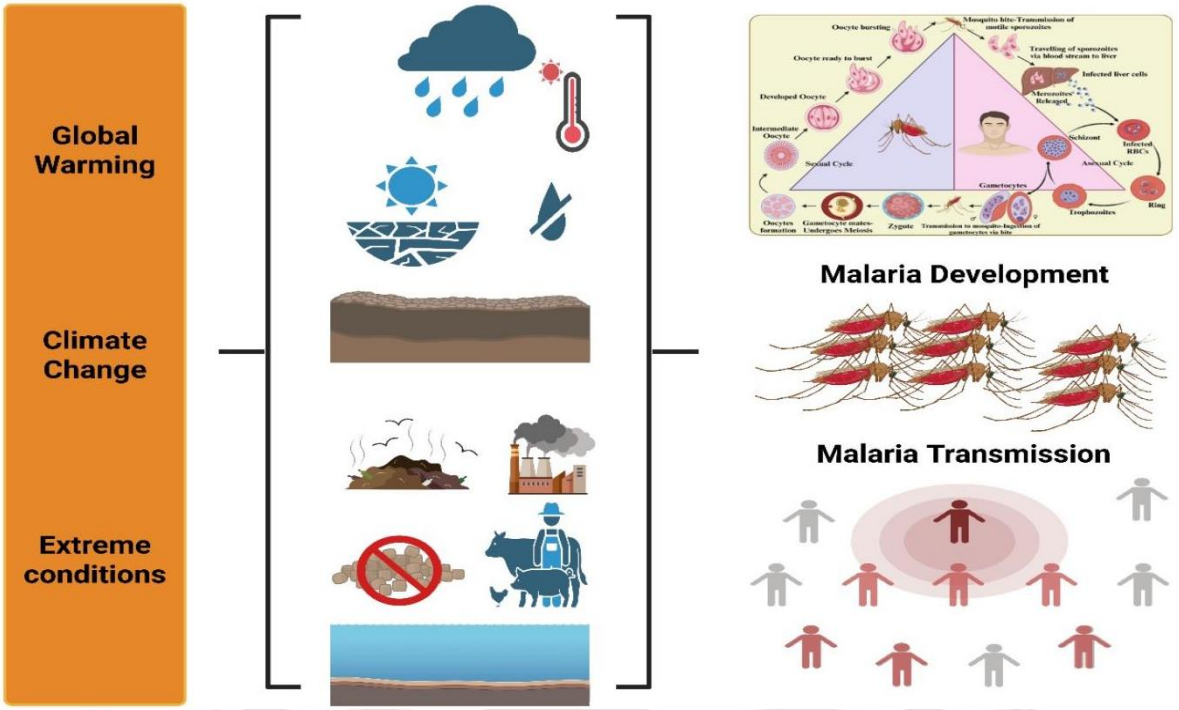

Figure 1.7: Risk Factors in Malaria Transmission. This figure represents how rising temperatures, altered rainfall patterns, and extreme environmental conditions contribute to the expanded mosquito breeding habitats, enhanced development of *Plasmodium* species, extended transmission seasons, and altered geographic distribution of *Anopheles* vectors. (Prepared using BioRender)

Biological, environmental, and demographic factors significantly influence malaria susceptibility. The most vulnerable groups are children under five years of age and pregnant women, due to their limited or altered immune responses. Children develop only partial and non-sterilizing immunity after repeated exposure, while pregnant women especially primigravidae experience reduced immune responses due to physiological and hormonal changes during pregnancy (Desai et al., 2007). Placental sequestration of *P. falciparum*-

infected erythrocytes expressing the VAR2CSA variant of PfEMP1 leads to placental malaria, which contributes to maternal anemia, preterm birth, and low birth weight—key factors in neonatal and infant mortality (Desai et al., 2007; Walker et al., 2020).

Partial immunity to malaria develops only in areas of stable, high-intensity transmission, typically defined as ≥10 infective mosquito bites per person per year (Snow & Marsh, 2002; Doolan et al., 2009). This immunity reduces the severity of infection among residents of endemic regions compared to non-immune travelers. However, changes in transmission intensity, urbanization, and vector adaptation can alter these dynamics.Recent findings have identified the spread of *Anopheles stephensi*, an efficient urban malaria vector traditionally found in South Asia, into parts of Africa, including Ethiopia, Sudan, and Somalia. This invasion poses a major biological threat to malaria control due to the species' ability to breed in urban water sources and transmit both *P. falciparum* and *P. vivax* (WHO, 2024; Sinka et al., 2020). Its establishment in the Horn of Africa has been recognized by the WHO as a significant obstacle to malaria elimination efforts. Addressing these risk factors requires a multi-faceted approach involving vector control, improved healthcare access, community education, and targeted interventions for high-risk populations. By identifying and mitigating these influences, public health strategies can be more effective in reducing malaria transmission and associated mortality worldwide.

1.6 Diagnosis and Treatment

Accurate diagnosis is fundamental to the effective treatment and control of malaria, especially in complex scenarios involving co-infections (e.g., malaria with tuberculosis, HIV, or dengue) and mixed-species infections such as *P. falciparum* and *P. vivax*. Prompt and precise identification of the *Plasmodium* species not only guides targeted treatment but also prevents drug resistance and serious complications due to inappropriate therapy (WHO, 2021; Lalloo et al., 2016). Diagnostic methods include microscopy, rapid diagnostic tests (RDTs), and molecular approaches such as PCR, each offering varying levels of sensitivity and applicability. Microscopy remains the gold standard for quantifying parasitemia, whereas RDTs are widely used for quick, point-of-care results. Molecular tools, with their high sensitivity, are essential for detecting low-density and mixed infections that are often missed by conventional methods (Singh & Daneshvar, 2013).

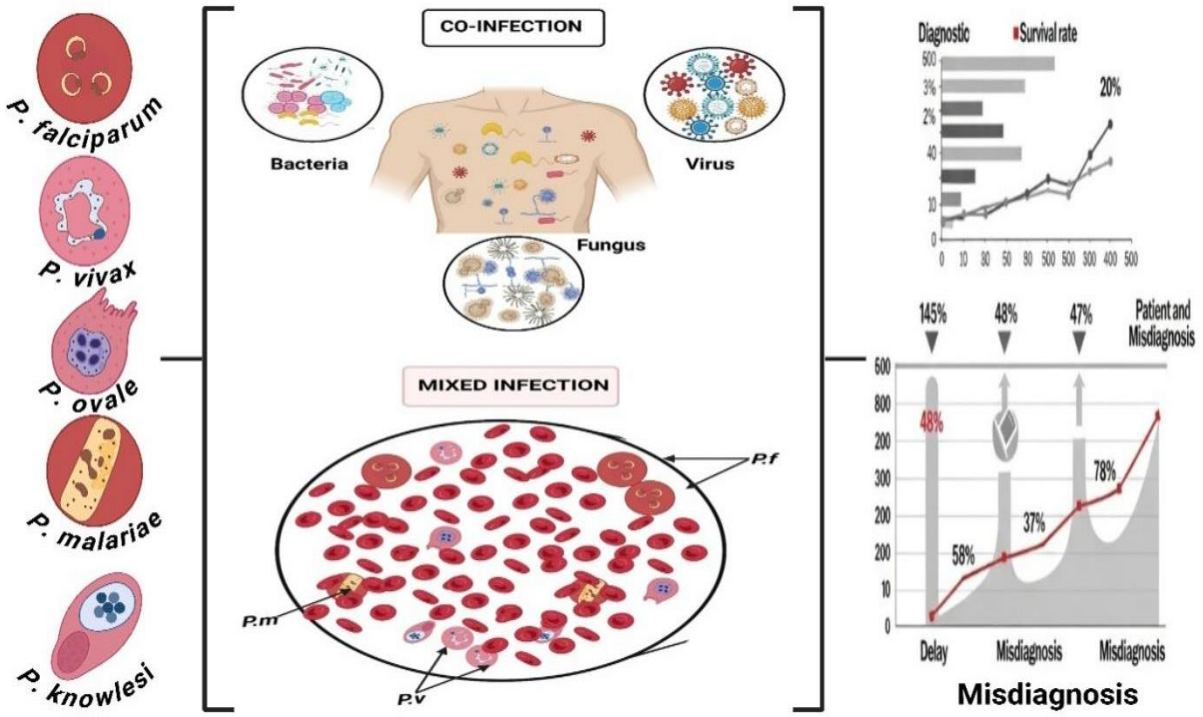

Figure 1.8: Impact of misdiagnosis on survival during co-infection and mixed malaria infections. This figure represents the impact of misdiagnosis on patient survival rates and mortality during malaria co-infections (e.g., *P. falciparum* + bacterial/viral/fungal pathogens) and mixed-species infections (e.g., *P. falciparum* + *P. vivax/P. ovale*) (Prepared using BioRender)

Misdiagnosis of malaria remains a major challenge, especially in cases involving co-infections with bacterial (e.g., typhoid, tuberculosis), viral (e.g., dengue, COVID-19, HIV), or fungal pathogens, and mixed *Plasmodium* species infections such as *P. falciparum* with *P. vivax* or *P. malariae* (Figure 1.8). Overlapping clinical symptoms like fever, fatigue, and gastrointestinal distress can obscure the true etiology, leading to incorrect treatment and increased morbidity (Hänscheid, 2003; Duedu et al., 2016). Studies show that misdiagnosis contributes to inappropriate treatment and delayed care for bacterial or viral infections, particularly in high-burden African regions (D'Acremont et al., 2014; WHO, 2024). Co-infections with HIV, dengue virus, and invasive non-typhoidal Salmonella (iNTS) are epidemiologically important, as they modify clinical severity and can confound diagnosis (Scott et al., 2011; Onyango et al., 2021). Not all co-infections exacerbate malaria outcomes; interactions depend on host immunity and infection dynamics.

Table 1.1: Treatment strategies for malaria with co-infections.				
Co-infection Type	**Malaria Treatment**	**Co-infection Treatment**	**Considerations**	**References**
Malaria + Tuberculosis	ACT + Antitubercular therapy (HRZE)	HRZE: isoniazid, rifampin, pyrazinamide, ethambutol	Rifampin reduces ACT efficacy, monitor closely	Murphy ME et al., 2012 ; WHO 2024
Malaria + Typhoid Fever	ACT + Ceftriaxone or Azithromycin	Ceftriaxone preferred in severe typhoid	Avoid overlapping hepatotoxic drugs	Rufai, T et al., (2022) ; WHO 2024
Malaria + Dengue	ACT + Supportive therapy	Fluids, antipyretics (avoid NSAIDs)	Overlapping symptoms, careful differential diagnosis	Anders, K. L., & Hay, S.I. (2012) ; WHO 2024
Malaria + Influenza	ACT + Antivirals (e.g., oseltamivir)	Use if within 48 hours of symptoms	Avoid misdiagnosis, manage fever carefully	Chuma, J., et al., (2009); WHO 2024
Malaria + Fungal Skin Infection	ACT + Topical/oral antifungals	Ketoconazole, terbinafine, etc.	No major drug interactions	Muturi, E. J., et al. (2006); WHO 2024
Malaria + HIV	ACT or artesunate + ART	Dolutegravir-based regimens preferred	Monitor drug interactions (e.g., efavirenz)	Banda, C. G., et al. (2022); WHO 2024

Mixed infections are often underdiagnosed due to the limitations of microscopy and antigen-based rapid diagnostic tests (RDTs), which may preferentially detect the dominant species or fail entirely in the presence of gene deletions such as *pfhrp2* (Gamboa et al., 2010; Singh & Daneshvar, 2013). This diagnostic uncertainty can result in the administration of incomplete or inappropriate therapies, such as omission of primaquine for *P. vivax*, thereby contributing to relapse, drug resistance, and continued transmission. Advanced molecular diagnostics like PCR offer greater sensitivity and specificity, particularly for detecting sub microscopic and mixed infections, but remain underutilized in endemic settings due to resource constraints (Snounou & Singh, 2002; Tadesse et al., 2017). Improved diagnostic strategies are essential for accurate case management and the implementation of effective, species-specific treatment protocols during co-infection as shown in the table 1.1 and table 1.2 for mixed infection scenarios.

Table 1.2: Treatment strategies for infections having mixed *Plasmodium* species			
Mixed Infection	**Primary Treatment**	**Additional Considerations**	**Citations**
P. falciparum + *P. vivax*	ACT + Primaquine	ACT for blood stages; Primaquine for hypnozoites (G6PD test needed)	Ahmed et al. 2011 ; Douglas et al. 2011
P. falciparum + *P. ovale*	ACT + Primaquine	Similar to *P. vivax*	Dinko et al. 2013
P. falciparum + *P. malariae*	ACT	P. malariae does not require radical cure	Dinko et al. 2013
P. falciparum + *P. knowlesi*	ACT	ACT effective	Singh & Daneshvar (2013)
P. vivax + *P. ovale*	Chloroquine + Primaquine	Both species need radical cure	Dinko et al. 2013
P. vivax + *P. malariae*	ACT or Chloroquine + Primaquine	Consider ACT if resistance suspected	Genton et al. 2005
P. vivax + *P. knowlesi*	ACT + Primaquine	Same as for *P. falciparum* + *P. vivax*	Singh & Daneshvar (2013)
P. ovale + *P. malariae*	Chloroquine + Primaquine	*P. ovale* needs radical cure	Dinko et al. 2013
P. falciparum + any species	ACT + Primaquine (if hypnozoites present)	Screen for G6PD before primaquine	Lalloo et al. (2016) ; Lubis et al. 2020

Treatment of malaria should only follow laboratory confirmation, except in severe cases with high clinical suspicion where immediate intervention is necessary (WHO, 2024; CDC, 2023). Therapy is tailored based on species identification, clinical severity, and local drug resistance patterns. For uncomplicated infections caused by chloroquine-sensitive *P. falciparum*, chloroquine or hydroxychloroquine is used, whereas *P. vivax* or *P. ovale* infections require the addition of primaquine to clear dormant liver stages (John et al., 2015). In cases of chloroquine resistance, artemisinin-based combination therapies (ACTs) like artemether-lumefantrine or atovaquone-proguanil are recommended (Ashley et al., 2022). Severe *P. falciparum* malaria warrants intravenous artesunate or quinidine, supplemented by antibiotics if needed. Screening for G6PD deficiency is essential prior to primaquine administration to prevent hemolysis. Adverse effects such as gastrointestinal upset, QT prolongation, and neuropsychiatric symptoms necessitate close monitoring and interprofessional care (CDC, 2021).

The accurate and timely malaria diagnosis is crucial for guiding species-specific treatment, especially in co-infection and mixed-infection contexts. ACTs remain the cornerstone of blood-stage treatment, while primaquine plays an essential role in preventing relapses associated with *P. vivax* and *P. ovale* (table 1.2). Artemisinin-based Combination Therapies (ACTs) remain the first-line treatment for uncomplicated *P. falciparum*, with a single low-dose primaquine (0.25 mg/kg) recommended in selected settings to reduce transmission. For *P. vivax* and *P. ovale*, radical cure with primaquine targets dormant hypnozoites, and quinine remains a second-line option in some African policies. Tailored treatment protocols considering co-morbidities, drug interactions, and G6PD status are critical for optimizing clinical outcomes, reducing disease burden, and supporting global malaria elimination strategies. Misidentification, particularly in co-endemic regions where *P. ovale* and *P. vivax* coexist, can lead to inappropriate therapy and relapse due to unaddressed liver-stage hypnozoites. Microscopy and RDTs remain standard diagnostic tools, their limited sensitivity for mixed or low-density infections underscores the importance of molecular methods like PCR. These high-sensitivity techniques enable species-specific detection, which is critical for guiding treatment decisions, especially for initiating radical cure with primaquine or tafenoquine in *P. ovale* infections. Thus, as we delve deeper into the diagnostic literature, achieving robust diagnostic accuracy, particularly through the use of novel molecular targets that proves essential for enabling species-specific treatment and advancing effective malaria elimination strategies.

1.7 References

1. Abdi, A., et al. (2016). *Molecular and Biochemical Parasitology*.
2. Ahmed S, Adil F, Shahzad T, Yahiya Y. Severe malaria in children: Factors predictive of outcome and response to Quinine. J Pak Med Assoc. 2011;61:54–8.
3. Aitken, E. H., et al. (2018). *PLoS Pathogens*.
4. Anders, K. L., & Hay, S. I. (2012). Lessons from malaria control to help meet the rising challenge of dengue. *The Lancet Infectious Diseases*, *12*(12), 977-984.
5. Ashley, E. A., et al. (2022). *Nature Reviews Disease Primers*, 8(1), 58.
6. Banda, C. G., Nkosi, D., Allen, E., Workman, L., Madanitsa, M., Chirwa, M., ... & Barnes, K. I. (2022). Impact of dolutegravir-based antiretroviral therapy on piperaquine exposure following dihydroartemisinin-piperaquine intermittent preventive treatment of malaria in pregnant women living with HIV. *Antimicrobial agents and chemotherapy*, *66*(12), e00584-22.
7. Barrett, J. R. (2024). *Environmental Health Perspectives*, 132(1), 014002.
8. Belachew, E. (2018). *Journal of Clinical & Cellular Immunology*, 9(1).
9. Bhatt, S., et al. (2015). *Nature*, 526(7572), 314–318.
10. Bousema, T., & Drakeley, C. (2011). *Trends in Parasitology*, 27(9), 427–434.
11. Cable, J., & Barber, I. (2017). *Molecular Ecology*, 26(17), 4381–4383.
12. Castro, M. C., et al. (2017). *Trends in Parasitology*, 33(3), 163–172.
13. Centers for Disease Control and Prevention (CDC). (2021). *CDC Yellow Book 2020: Health Information for International Travel*. Oxford University Press.
14. Centers for Disease Control and Prevention (CDC). (2023). *Malaria*. https://www.cdc.gov/malaria/index.html
15. Centers for Disease Control and Prevention (CDC). (2024). *Malaria: About Malaria*. https://www.cdc.gov/malaria/about/
16. Chandley, P., et al. (2023). *eLife*, 12, e86221.
17. Chew, W. H., et al. (2022). *Frontiers in Cellular and Infection Microbiology*, 12, 856019.
18. Chuma, J., Abuya, T., Memusi, D., Juma, E., Akhwale, W., Ntwiga, J., ... & Amin, A. (2009). Reviewing the literature on access to prompt and effective malaria treatment in Kenya: implications for meeting the Abuja targets. *Malaria journal*, *8*, 1-13.
19. Demarta-Gatsi, C., et al. (2019). *PLoS Pathogens*, 15(4), e1007621.
20. Deroost, N., et al. (2016). *Nature Communications*, 7(1), 11634.
21. Desai, M., et al. (2007). *PLoS Medicine*, 4(10), e275.
22. Dieng, S., et al. (2020). *EBioMedicine*, 51, 102570.
23. Dimasuay, K. G., et al. (2017). *PLoS Pathogens*, 13(10), e1006692.
24. Dinko B, Oguike MC, Larbi JA, Bousema T, Sutherland CJ. Persistent detection of *Plasmodium falciparum*, *P. malariae*, *P. ovale curtisi* and *P. ovale wallikeri* after ACT treatment of asymptomatic Ghanaian school-children. Int J Parasitol Drugs Drug Resist. 2013;3:45–50.
25. Doolan, D. L., et al. (2009). *Annual Review of Immunology*, 27, 1–32.
26. Douglas NM, Nosten F, Ashley EA, Phaiphun L, Van Vugt M, Singhasivanon P, et al. *Plasmodium vivax* recurrence following falciparum and mixed species malaria: risk factors and effect of antimalarial kinetics. Clin Infect Dis. 2011;52:612–20.
27. Duedu, K. O., et al. (2016). *Malaria Research and Treatment*, 2016, 5021038.
28. Ejigiri, I., & Sinnis, P. (2009). *Cell Host & Microbe*, 6(3), 268–275.

29. El-Radhi, A. S. (2019). *Clinical infectious diseases in children*. Springer.
30. Feachem, R. G. A., et al. (2019). *The Lancet*, 394(10200), 735–740.
31. Foley, M., & Tilley, L. (1998). *Pharmacology & Therapeutics*, 79(2), 165–191.
32. Fowkes, F. J. I., et al. (2010). *PLoS Medicine*, 7(1), e1000218.
33. Fu, W. Y., et al. (2020). *Cell Reports*, 31(7), 107663.
34. Gamboa, D., et al. (2010). *PLoS ONE*, 5(1), e8091.
35. Genton B, Baea K, Lorry K, Ginny M, Wines B, Alpers MP. Parasitological and clinical efficacy of standard treatment regimens against *Plasmodium falciparum*, *P. vivax* and *P. malariae* in Papua New Guinea. P N G Med J. 2005;48:141–50.
36. Ghosh, A. K., et al. (2019). *PLoS Biology*, 17(1), e3000072.
37. Gilles, H. M., & Warrell, D. A. (1993). *Bruce-Chwatt's Essential Malariology*. Edward Arnold.
38. Global Fund. (2023). *Impact*. https://www.theglobalfund.org/en/impact/
39. Grassi, B. (1924). *Journal of Tropical Medicine and Hygiene*, 27(13), 166–170.
40. Greenwood, B., et al. (2019). *The Lancet*, 394(10200), 741–752.
41. Guerra, C. A., et al. (2006). *Trends in Parasitology*, 22(12), 569–575.
42. Guerra, M. M., & Carruthers, V. B. (2017). *Trends in Parasitology*, 33(3), 232–242.
43. Hänscheid, T. (2003). *Clinical Microbiology and Infection*, 9(6), 497–504.
44. Haque, U., et al. (2020). *Parasites & Vectors*, 13(1), 1–13.
45. Jaskiewicz, M., et al. (2019). *PLoS Pathogens*, 15(11), e1008082.
46. John, C. C., et al. (2015). *Malaria Journal*, 11, 280.
47. Josling, G. A. (2018). *Trends in Parasitology*, 34(5), 363–366.
48. Koella, J. C. (1998). *Parasitology Today*, 14(10), 400–404.
49. Kwiatkowski, D. P. (2005). *Nature Genetics*, 37(12), 1297–1298.
50. Lalloo, D. G., et al. (2016). *The Lancet. Infectious Diseases*, 16(11), e256–e266.
51. Larson, B. (2019). *Trends in Parasitology*, 35(1), 7–9.
52. Laveran, A. (1880). *Bulletin de l'Académie de médecine*, 9(45), 1235–1236.
53. Manguin, S., et al. (2013). *Malaria Journal*, 12(1), 405.
54. Menard, D., & Dondorp, A. M. (2017). *New England Journal of Medicine*, 377(18), 1779–1781.
55. Moll, K., et al. (2015). *Trends in Parasitology*, 31(11), 543–554.
56. Murphy, M. E., Singh, K. P., Laurenzi, M., Brown, M., & Gillespie, S. H. (2012). Managing malaria in tuberculosis patients on fluoroquinolone-containing regimens: assessing the risk of QT prolongation. *The international journal of tuberculosis and lung disease*, *16*(2), 144-149.
57. Musyoka, K. B. (2021). *Current Opinion in Insect Science*, 47, 100800.
58. Muturi, E. J., Mbogo, C. M., Mwangangi, J. M., Ng'ang'a, Z. W., Kabiru, E. W., Mwandawiro, C., & Beier, J. C. (2006). Concomitant infections of Plasmodium falciparum and Wuchereria bancrofti on the Kenyan coast. *Filaria Journal*, *5*, 1-8.
59. Najera, J. A., et al. (2011). *Malaria Journal*, 10(1), 24.
60. Neghina, R. (2010). *Journal of Medicine and Life*, 3(4), 438–440.
61. Nosjean, O., et al. (1997). *European Journal of Biochemistry*, 247(2), 654–661.
62. Nye, E. R. (2002). *The Lancet*, 359(9303), 346.
63. Okaka, F. O., et al. (2021). *BMC Public Health*, 21(1), 1–13.
64. Packard, R. M. (2021). *The Making of a Tropical Disease: A Short History of Malaria*. Johns Hopkins University Press.

65. Paing, S. S., et al. (2018). *Infection and Immunity*, 86(7), e00898-17.
66. Patarroyo, M. A., et al. (2011). *PLoS ONE*, 6(12), e28932.
67. Phillips, M. A., et al. (2017). *Nature Reviews Drug Discovery*, 16(2), 119–134.
68. Prudêncio, M., et al. (2011). *Current Opinion in Microbiology*, 14(4), 461–469.
69. Rashidi, F., et al. (2021). *Molecular and Cellular Proteomics*, 20, 100067.
70. Reid, M. C., et al. (2019). *Environmental Research Letters*, 14(8), 084024.
71. Reiss, M., et al. (2021). *Frontiers in Immunology*, 12, 706425.
72. Richards, J. S., et al. (2010). *PLoS Medicine*, 7(1), e1000218.
73. Rufai, T., Aninagyei, E., Akuffo, K. O., Ayin, C. T. M., Nortey, P., Quansah, R., ... & Danso-Appiah, A. (2022). Malaria and typhoid fever coinfection among patients presenting with febrile illnesses in Ga West Municipality, Ghana. *medRxiv*, 2022-04.
74. Rund, S. S. C., et al. (2016). *Current Opinion in Insect Science*, 16, 103–109.
75. Ryan, S. J., et al. (2020). *Lancet Planetary Health*, 4(9), e438–e447.
76. Sakoguchi, A., et al. (2021). *Frontiers in Cellular and Infection Microbiology*, 11, 663189.
77. Sankineni, S. (2023). *Journal of Vector Borne Diseases*, 60(2), 85–87.
78. Sato, S. (2021). *Parasitology International*, 80, 102213.
79. Sierro, F., & Grau, G. E. (2019). *Trends in Parasitology*, 35(3), 253–264.
80. Sinden, R. E. (2017). *Trends in Parasitology*, 33(5), 374–387.
81. Singh, B., & Daneshvar, C. (2013). *Clinical Microbiology Reviews*, 26(2), 165–184.
82. Sinka, M. E., et al. (2012). *Parasites & Vectors*, 5, 67.
83. Smith, T., et al. (2004). *Trends in Parasitology*, 20(9), 433–440.
84. Snounou, G., & Singh, B. (2002). *Methods in Molecular Medicine*, 72, 189–203.
85. Stabler, T. C. (2024). *Frontiers in Immunology*, 15.
86. Stratton, J. A. (2008). *Public Health Reports*, 123(5), 629–633.
87. Tadesse, F. G., et al. (2017). *Trends in Parasitology*, 33(7), 603–615.
88. Takala-Harrison, S., & Laufer, M. K. (2015). *Current Opinion in Infectious Diseases*, 28(5), 442–448.
89. Takken, W., & Verhulst, N. O. (2013). *Malaria Journal*, 12(1), 1–11.
90. Tembo, D. L., et al. (2014). *PLoS Pathogens*, 10(12), e1004537.
91. Tu, Y. (2011). *Nature Medicine*, 17(10), 1217–1218.
92. Tusting, L. S., et al. (2013). *Malaria Journal*, 12(1), 1–12.
93. Tweedell, R. E., et al. (2018). *PLoS Pathogens*, 14(9), e1007287.
94. Venugopal, K., et al. (2020). *Trends in Parasitology*, 36(12), 999–1011.
95. Waisberg, M., et al. (2014). *Cell Host & Microbe*, 15(4), 517–525.
96. Wahlgren, M., & Goel, S. (2017). *Microbes and Infection*, 19(2), 110–121.
97. Walker, P. G., et al. (2020). *The Lancet. Global Health*, 8(3), e341–e348.
98. Wang, J. (2019). *Trends in Biotechnology*, 37(1), 1–4.
99. Warrell, D. A. (2017). *Journal of Travel Medicine*, 24(suppl_1), S18–S35.
100. Weber, S. E. (2011). *New England Journal of Medicine*, 364(7), 633–643.
101. Weiss, D. J., et al. (2019). *Nature*, 569(7758), 536–542.
102. White, N. J., et al. (2014). *The Lancet*, 383(9918), 723–735.
103. World Health Organization (WHO). (2019-2024). *World Malaria Report 2019-2024*.
104. Wilson, D. W., et al. (2016). *PLoS Pathogens*, 12(11), e1006001.
105. Yamana, T., & Eltahir, E. A. B. (2013). *Environmental Research Letters*, 8(3), 035025.

Chapter 2

Systematic Analysis of Diagnostic Tools for Malaria Detection

SUMMARY

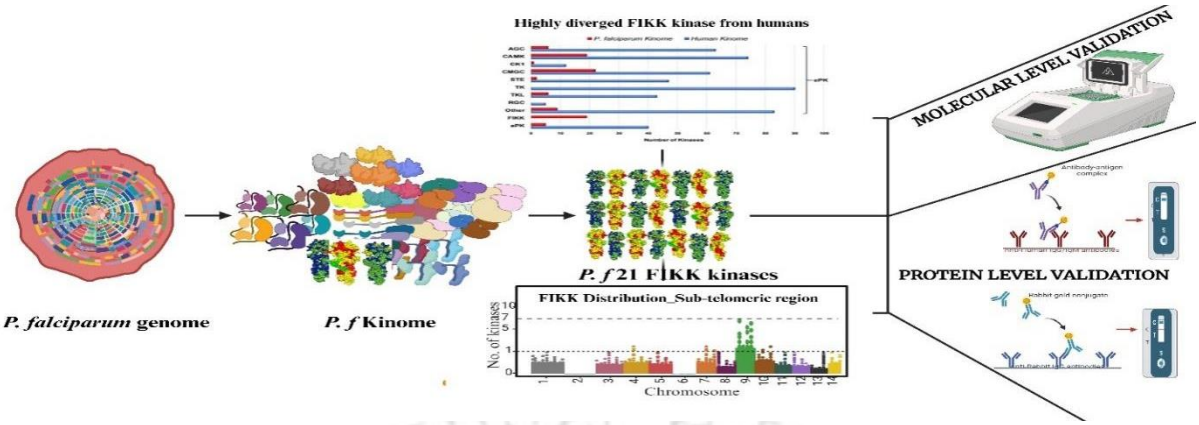

Figure: Schematic representation of the systematic pipeline used for identifying diagnostic FIKK kinase candidates from the *P. falciparum* genome.

Accurate diagnosis of malaria is vital for effective treatment and disease control. Traditional diagnostic methods include microscopy, Rapid Diagnostic Tests (RDTs), and Polymerase Chain Reaction (PCR). While microscopy is effective, it requires skilled personnel, making it less accessible in resource-limited settings. PCR provides high sensitivity and specificity for detecting low parasitemia and mixed infections, but cross-amplification due to conserved genetic regions shared among *Plasmodium* species, and humans can hinder species-specific detection and lower diagnostic accuracy. RDTs offer a rapid and accessible alternative but face reliability issues, particularly in cases with low parasite densities, coinfection, mixed infections, and *pfhrp2* gene deletions. Missed or incorrect diagnoses can result in disease progression, ineffective treatment, sustained community-level transmission, resistant to the drugs, and can result in severe complications like multi-organ failure, and ultimately death. This highlights the urgent need for novel, species-specific targets that can offer improved sensitivity, reliability, and adaptability across diverse clinical settings. The significance of FIKK kinase-based diagnostics extends beyond primary detection, offering potential applications in malaria surveillance, treatment monitoring, and elimination strategies (Figure). Through enhanced sensitivity, these markers support the detection of submicroscopic, and asymptomatic malaria cases, while also enabling accurate species-specific diagnosis in complex infections involving multiple pathogens, which are crucial for malaria eradication efforts. Integrating FIKK kinase-based assays with portable diagnostic platforms such as loop-mediated isothermal amplification (LAMP) or CRISPR-based detection could enhance field applicability and enable point-of-care testing in endemic regions. Given their potential for accurate, species-specific, and ultra-sensitive malaria detection, FIKK kinases can be further

explored and integrated into modern diagnostic frameworks to improve global malaria control efforts.

2.1 Malaria Diagnosis

Accurate and reliable diagnostic testing is essential for effective malaria management, as it allows for correct identification of *Plasmodium* parasites and ensures timely and appropriate treatment (Perkins et al., 2017). Malaria is a life-threatening disease transmitted by *Anopheles* mosquitoes, and early diagnosis is critical to prevent complications and limit transmission (WHO, 2023). Diagnostic tests must be sensitive, specific, affordable, and accessible, particularly in remote or resource-limited settings (Udhayakumar et al., 2016). Children under five years of age are especially vulnerable, accounting for around 80% of malaria-related deaths in Africa in 2021 (WHO, 2021). Early detection in high-risk groups is vital to reduce disease severity and mortality. Identifying the infecting *Plasmodium* species and quantifying parasitemia are essential steps in assessing disease severity and selecting appropriate treatment (CDC, 2021). In non-endemic regions, imported cases of malaria present diagnostic challenges, often due to a lack of skilled microscopists and limited diagnostic capacity during emergencies or outside normal working hours (Lalloo et al., 2016; Moody, 2002). These limitations highlight the importance of using standardized protocols and alternative diagnostic tools such as Rapid Diagnostic Tests (RDTs) and Polymerase Chain Reaction (PCR) to improve diagnostic speed and accuracy (WHO, 2022). Ultimately, to achieve malaria elimination, there is a pressing need for novel diagnostic tools that are not constrained by infrastructure and can provide reliable, rapid results across all clinical settings (Tadesse et al., 2017).

2.1.1 Microscopy

Microscopy remains the gold standard for malaria diagnosis due to its ability to detect and quantify parasites, identify *Plasmodium* species, and assesses disease severity through parasite density measurements (WHO, 2021; Moody, 2002). The procedure involves preparing and staining thick and thin blood smears with Giemsa, followed by examination under light microscopy to detect and stage parasites (WHO, 2016). When performed correctly, microscopy achieves a sensitivity of up to 95% and specificity of 98%, with a detection limit of approximately 50–200 parasites per µL of blood (John et al., 2015; WHO, 2022). It is cost-effective and widely accessible, even in remote areas, provided trained personnel and well-maintained equipment are available (Warhurst & Williams, 1996; Björkman & Mårtensson, 2010).

Figure 2.1 Microscopic identification of malarial parasites using thick and thin blood smears. The thick smears help in quantifying parasitemia, while the thin smears provide parasite morphology for differentiating species. (Prepared using BioRender)

Microscopy also enables monitoring of treatment response by tracking parasitemia and detecting drug-induced changes in parasite morphology (WHO, 2015). However, the method is labor-intensive, time-consuming, and its accuracy depends heavily on smear quality, technician skill, and adherence to standardized guidelines (CDC, 2019; WHO, 2020). Challenges include difficulty in detecting low parasitemia, misidentification of species (e.g., *P. knowlesi* vs. *P. malariae*), false positives from artifacts, and underdiagnosis in poorly prepared smears (Singh & Daneshvar, 2013; Hänscheid, 2003; Duedu et al., 2016). Mixed infections are also often missed, and parasite sequestration in *P. falciparum* may hinder full detection (Nguyen et al., 2019).

2.1.2 PCR based Methods

Polymerase Chain Reaction (PCR) is a highly sensitive and specific method for malaria diagnosis, capable of detecting low parasitemia levels and mixed infections that are often missed by microscopy and Rapid Diagnostic Tests (RDTs) (Snounou & Singh, 2002; Haanshuijsen et al., 2020). Various formats such as nested PCR, multiplex PCR, and real-time PCR (qPCR) enable precise detection and species differentiation, with sensitivity ranging from 98% to 100% and specificity between 88% and 94% compared to microscopy (Cordray & Richards-Kortum, 2012). Real-time PCR also quantifies parasite load, supporting treatment decisions and monitoring (Perera et al., 2020), while genotyping capabilities help identify drug resistance markers for surveillance (Schultz et al., 2022). The detection limit of PCR is as low

as 0.5–5 parasites/mL, making it effective for identifying submicroscopic and asymptomatic infections (WHO,2018;Imwongetal.,2014).

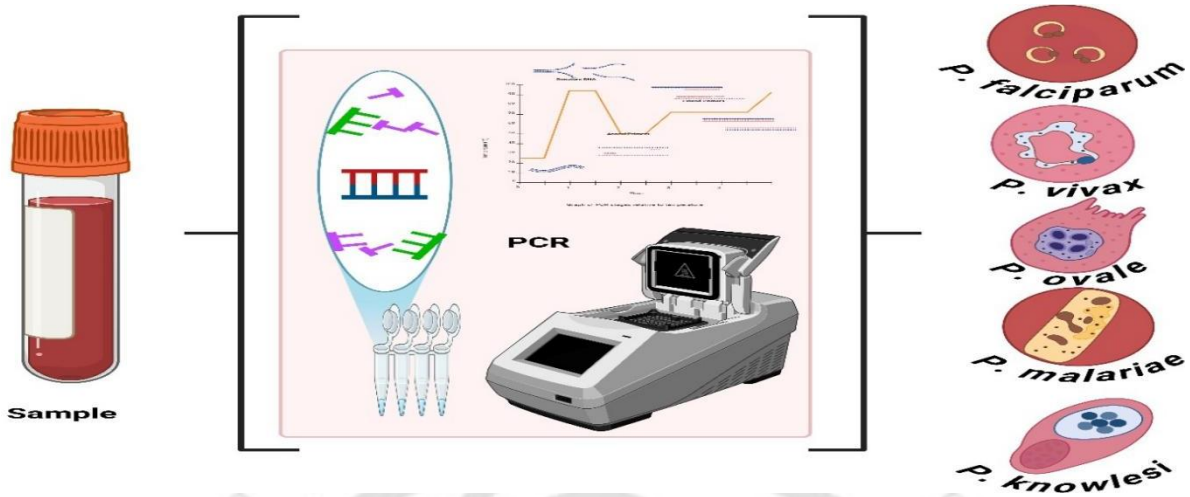

Figure 2.2 PCR-based identification of *Plasmodium* parasites. The assay shows the specificity of primer sets in quantifying and species differentiation. (Prepared using BioRender)

Although PCR requires skilled personnel, reliable electricity, and longer processing time, it remains the gold standard in research and reference laboratories for its accuracy and utility in epidemiological monitoring (WHO, 2021). To address infrastructure limitations, alternative molecular methods such as Loop-Mediated Isothermal Amplification (LAMP) and Recombinase Polymerase Amplification (RPA) have been developed, offering comparable sensitivity without the need for thermal cycling equipment (Notomi et al., 2000; Tsalik et al., 2010).

2.1.3 Rapid Diagnostic Tests (RDTs)

Rapid Diagnostic Tests (RDTs) are widely used for malaria detection due to their ease of use, speed, and suitability in resource-limited settings (WHO, 2021). These lateral flow immunochromatographic assays detect malaria antigens by capturing them with dye-labeled antibodies on a nitrocellulose strip, producing visible test lines within 15 minutes (Moody, 2002; Maltha et al., 2013). RDTs offer a sensitivity of 85–95% and specificity of 95–99%, with a detection limit of approximately 50–100 parasites per microliter of blood (WHO, 2018; Ochola et al., 2016). They are especially valuable in rural or remote areas lacking microscopy. However, their accuracy can decline with low parasitemia, and false negatives may occur due to the prozone effect in hyperparasitemia or genetic deletions (Gillet et al., 2009; Gamboa et

al., 2010). False positives may also result from persistent antigens after parasite clearance, making it difficult to distinguish current from past infections (Dalrymple et al., 2018).

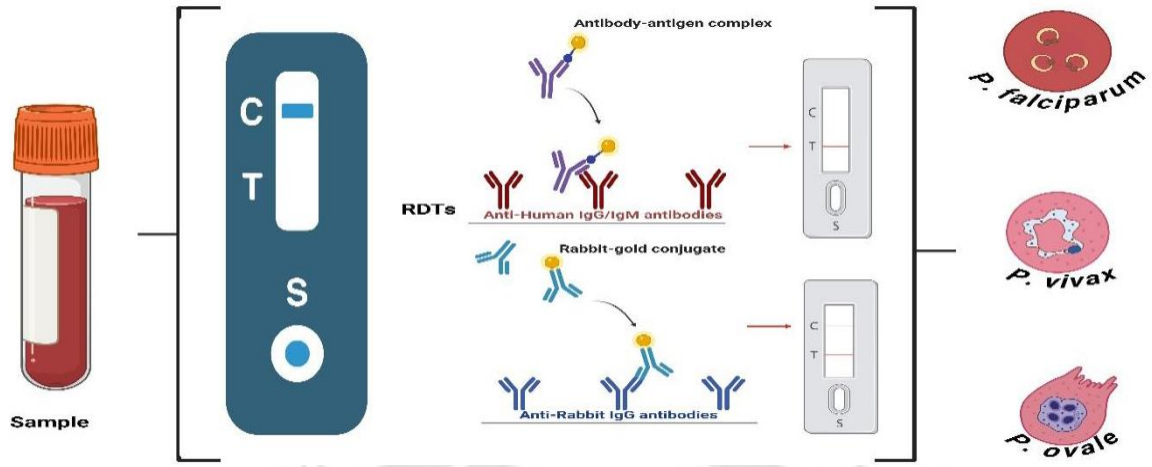

Figure 2.3 Lateral flow Rapid Diagnostic Tests (RDTs) for identifying *Plasmodium* infections. These strips demonstrate antigen detection from various *Plasmodium* species where control line indicates test validity and test bands confirm the presence of species-specific antigens. (Prepared using BioRender)

Variability in performance across brands and settings highlights the importance of confirmatory testing with microscopy or PCR (Ashley et al., 2022) and most commercially available RDTs do not reliably detect *P. knowlesi* and *P. ovale* infections due to antigenic similarity with other *Plasmodium* species and lack of species-specific test lines. RDTs remain cost-effective and accessible, but continuous quality control and integration with complementary diagnostic tools are essential for improving malaria management, particularly in low-resource environments (Mukherjee et al., 2017; Mekonnen et al., 2021; Chiodini et al., 2019).

2.1.4 Comparative analysis of diagnostic methods:

The diagnostic methods have their own strengths and limitations and it becomes evident that microscopy, PCR, and RDTs play complementary yet imperfect roles in malaria diagnosis. Light microscopy remains the traditional gold standard, capable of species differentiation and parasite quantification, yet its reliability declines at parasite densities below 50 parasites/µL and is highly operator-dependent (Poostchi et al., 2018; WHO, 2024). RDTs, which detect parasite antigens such as *P. falciparum* Histidine-Rich Protein 2 (PfHRP2) and *Plasmodium* Lactate Dehydrogenase (pLDH), provide rapid and accessible diagnosis but are limited by antigenic variability, HRP2/3 gene deletions, and the prozone effect, where excessive antigen concentrations cause false-negative results (Gillet et al., 2009; Mouatcho & Goldring, 2013;

Gatton et al., 2017). A comparative evaluation (Table2.1) of microscopy, PCR, and RDTs reveals distinct advantages and limitations in malaria diagnostics.

Table 2.1: Comparative Assessment of Malaria Diagnostic Techniques: Microscopy, PCR, and Rapid Diagnostic Tests

Property	Microscopy	PCR	RDTs
Sensitivity	50–200 parasites/µL; up to 95%	0.5–5 parasites/mL; 98–100%	50–100 parasites/µL; 85–95%
Specificity	~98%	88–94%	95–99%
Species Identification	Limited in mixed infections	Precise, including mixed infections	Limited
Quantification	Possible	Possible (qPCR)	Not Possible
Time	~30–60 minutes	Several hours	~15 minutes
Requirements	Microscope, trained personnel	Thermocycler/qPCR machine, skilled personnel, reliable electricity	Minimal equipment, user-friendly
Field Suitability	Moderate	Low	High
Limitations	Skill-dependent ; Labor-intensive ; Poor performance in low parasitemia ; Species misidentification	Infrastructure-heavy ; Expensive ; Long processing time	Reduced sensitivity in low parasitemia ; False negatives (e.g., *pfhrp2* deletions) ; Antigen persistence causes false positives
Cost	Moderate	High	Low–Moderate
Reference Use	Gold standard in endemic regions	Gold standard in research	Field-level surveillance
References	Moody (2002); John et al. (2015); Singh & Daneshvar (2013)	WHO (2023–2024), Genton (2021), Lucchi (2019), Gatton (2017)	Mukherjee et al. (2017) WHO, 2024; Genton et al., 2021

2.2 Biomarkers in Malaria Diagnosis

A wide range of target antigens and genes are currently used in malaria diagnostics, each with specific advantages and limitations. The most commonly targeted protein biomarkers include *Plasmodium falciparum* Histidine-Rich Proteins 2 and 3 (PfHRP2**,** PfHRP3), *Plasmodium* Lactate Dehydrogenase (pLDH), and Aldolase, which are detected by Rapid Diagnostic Tests (RDTs) (Maltha et al., 2013; WHO, 2021). PfHRP2 is highly abundant and widely used, but gene deletions in endemic regions like India and Africa have led to false-negative results, prompting the need for alternative markers like PfLDH and Aldolase (Parr et al., 2017; Berhane et al., 2018). pLDH is essential for Plasmodium glycolysis and is species-specific, enabling discrimination between *P. falciparum* and *P. vivax*, but shows reduced sensitivity at low parasitemia and is unstable at high temperatures (Chiodini et al., 2007; Cheng et al., 2021).

Table 2.2: Limitations of Commonly Used Malaria Diagnostic Markers.

S. No	Marker	Type	Drawbacks	Reference
1	PfHRP2/HRP3	Antigen (RDT)	Gene deletions, antigen persistence	Houzé, S., et al., 2011
2	pLDH	Antigen (RDT)	Lower sensitivity, stage-dependent expression	Jelinek, T., et al., 1999
3	Aldolase	Antigen (RDT)	Cross-reactivity between species	Cho, C. H., et al., 2011
4	18S rRNA	Gene (PCR)	Cross-species amplification	Das., Ashis, et al., 1995
5	Cox1/Cox3	Gene (PCR)	Limited species resolution	Berná, L., et al., 2021
6	PfLDH	Gene (PCR)	Genetic variability	Simpalipan, P., et al., 2018

Other promising protein markers include Glutamate-Rich Protein (GLURP)**,** Hypoxanthine-Guanine Phosphoribosyltransferase (HGPRT)**,** Phosphoglycerate Mutase (PGM)**,** and Heat Shock Protein 70 (HSP70)**,** all involved in parasite metabolism and survival (Acharya et al., 2017). Hemozoin, a byproduct of hemoglobin digestion, is also being explored through techniques like Raman spectroscopy and magneto-optical detection (Sullivan et al., 1996; Newton et al., 2019). At the genetic level, diagnostic methods commonly target 18S rRNA, cox-I/cox-III**,** Pf-LDH**,** and PfHRP2 genes using PCR-based techniques, which offer high sensitivity (detection limit: 0.5–5 parasites/mL) and specificity for species identification and drug resistance surveillance (Snounou & Singh, 2002; WHO, 2018). Emerging strategies include biosensors (e.g., electrochemical, optical, nanomaterial-based), saliva-based detection

of topoisomerases, and microRNA markers like miR-1246, which show high specificity and stability in body fluids (Dutta et al., 2015; Bertolotti et al., 2020). However, all these methods face challenges such as low sensitivity at low parasite density, antigen variability, heat instability, and cross-reactivity as shown in the table 2.1. A combined diagnostic approach integrating antigen, and gene is needed to overcome these limitations and improve diagnostic accuracy in diverse settings (Poostchi et al., 2018; Kasoju et al., 2021).

2.3 Ongoing Diagnostic Innovations

Several innovative diagnostic techniques are under development to improve malaria detection across diverse clinical and field settings. The key features, detection targets, limits of detection, and limitations of these innovative diagnostic methods are summarized for clearer comparison and evaluation as listed in the table 2.3. Microscopy-based methods are being enhanced through digital imaging and artificial intelligence (AI) to automate parasite identification and quantification, though they remain dependent on skilled personnel and are less reliable at low parasite densities (Rajpurkar et al., 2018; Poostchi et al., 2018).

Table 2.3: Comparison of Emerging Diagnostic Techniques.

S. No	Method	LoD	Advantages	Disadvantages	Reference
1	AI Microscopy	~50 parasites/µL	Automated, scalable	Cost, & training	Rajpurkar et al., 2018; Poostchi et al., 2018
2	High-sensitivity RDT	~50–100/µL	Improved low parasitemia detection	Still affected by antigen persistence	Chiodini et al., 2019; El-Bishbishi et al., 2011
3	LAMP	~1 parasite/µL	Isothermal, portable	Primer design complexity and Susceptible to contamination	Notomi et al., 2000 ; Riley et al., 2011
5	CRISPR-based	<1 parasite/µL	Ultra-sensitive, species-specific	Experimental, & costly	(Gunalan et al., 2021;
6	Hemozoin-based	~50 parasites/µL	No reagents, rapid	Costly, & Specialised Equipment-dependent	Kappe et al., 2004

Among field-adapted molecular tools, Loop-Mediated Isothermal Amplification (LAMP) has transitioned from innovation to an established diagnostic method, offering sensitivity comparable to PCR but with minimal equipment requirements. Commercial kits such as the Loopamp™ MALARIA Pan/Pf detection system have demonstrated high sensitivity and specificity in detecting low-density and asymptomatic infections, making LAMP a practical alternative for resource-limited environments (Polley et al., 2010; Hopkins et al., 2013; WHO, 2023). Other isothermal amplification platforms, including Nucleic Acid Sequence-Based Amplification (NASBA) and Thermophilic Helicase-Dependent Amplification (tHDA), also amplify targets like 18S rRNA and mitochondrial DNA at constant temperatures, reducing dependency on thermocyclers while maintaining diagnostic accuracy (Compton, 1991; Riley et al., 2011). In addition to nucleic acid–based techniques, non-invasive sample matrices such as saliva and urine are being evaluated for parasite antigen or nucleic acid detection, offering patient-friendly alternatives though often with variable sensitivity (Singh et al., 2008; Martínez et al., 2009). Transdermal hemozoin detection, which uses ultrasound-induced vapor bubbles to identify crystalline hemozoin, represents a further innovation that enables non-blood-based malaria screening (Kappe et al., 2004). Collectively, these evolving and established molecular tools complement standard microscopy and RDTs, addressing critical diagnostic gaps in detecting low-parasitemia, mixed-species, and asymptomatic infections in malaria-endemic regions (Genton et al., 2021).

2.4 FIKK Kinase(s)

The genome of *P. falciparum*, the most lethal human malaria parasite, spans approximately 23.3 megabases across 14 chromosomes and encodes around 5,300 genes, with a notable adenine-thymine (A+T) content of 80.6% (Gardner et al., 2002; Carlton et al., 2008). Among these genes, a subset codes for the parasite's complete set of protein kinases, known as the kinome, which plays a central role in regulating vital cellular processes. Despite its complexity, the *P. falciparum* kinome is relatively small compared to other eukaryotes, comprising about 99 protein kinases, of which 65 belong to conserved eukaryotic kinase groups, and 21 are highly divergent, classified as orphan kinases (Doerig et al., 2002; Anamika et al., 2005). These kinases fall into various families, including AGC, CMGC, Casein Kinase (CK), CDPK, TKL**,** and other families **(**Talevich et al., 2012) as shown in the figure 2.4.

FIKK kinase(s) are a distinct family of protein kinases unique to apicomplexan parasites, with a notable expansion in *P. falciparum*, which encodes 21 FIKK genes compared to only one or none in other *Plasmodium* species (Sargeant et al., 2006; Tewari et al., 2010).

Named after a conserved phenylalanine-isoleucine-lysine-lysine motif, FIKKs are categorized as orphan kinases due to their lack of similarity to known eukaryotic kinase families (Talevich et al., 2012). These kinases are exported to the cytoplasm and membrane of infected red blood cells (iRBCs), where they contribute to host cell remodeling, immune evasion, and parasite survival (Kaviratne et al., 2009; Pease et al., 2013). Structurally, they diverge from conventional serine/threonine kinases through unique N-terminal domains that may support parasite-specific functions (Sargeant et al., 2006). The FIKKs even facilitate sequestration of iRBCs in host microvasculature, contributing to malaria pathogenesis (Miller et al., 2018), highlighting their potential as key regulators in *P. falciparum* biology. Their absence in humans and specialized role in parasite-host interactions make FIKK kinase(s) a promising candidates for species-specific diagnostic tools.

2.4.1 Distribution of FIKK kinase(s)

In *P. falciparum*, the FIKK kinase gene family is unusually expanded, with 21 genes distributed across 11 of its 14 chromosomes, primarily localized within telomeric and subtelomeric regions associated with genes involved in antigenic variation and immune evasion (Gardner et al., 2002; Nunes et al., 2010). These genes are often found near *var*, *rifin*, *stevor*, and *PfHISTb* loci, suggesting a potential role in red blood cell surface modification and malaria pathogenesis (Schneider & Puijalon, 2005). Genomic clustering is particularly prominent on chromosome 9, and all *P. falciparum* FIKK genes, except FIKK8, contain three exons rich in A+T sequences, reflecting the parasite's overall high A+T genome bias (Carlton et al., 2008). FIKK kinases have undergone lineage-specific expansion within *Plasmodium*, with *P. falciparum* and *P. reichenowi* (human and ape parasites) encoding 21 FIKKs, while *P. gaboni* (chimpanzee parasite) encodes 22, including the unique non-orthologous FIKK9.15, likely acquired before the divergence of the Laverania subgenus (Sundararaman et al., 2016). Among these, FIKK8 is the only gene conserved across multiple *Plasmodium* species and is exported to the host erythrocyte cytosol, indicating an evolutionarily conserved role in host-cell modification (Nunes et al., 2010). In contrast, some FIKKs have become pseudogenes in certain species like FIKK7.2 and FIKK14 are nonfunctional in *P. falciparum* but remain intact in *P. gaboni*, and *P. reichenowi*, while FIKK9.5 is a pseudogene in *P. gaboni* but functional in the other two (Sundararaman et al., 2016) as given in the table 2.3. This distribution and functional divergence reflect the evolutionary flexibility of FIKK kinases and support their role in host-parasite interactions and species-specific adaptations.

Table 2.4: Distribution of FIKK Kinases in *Plasmodium species.*				
***Plasmodium* Species**	**No. of FIKK Genes**	**Syntenic/Orthologous Genes**	**Unique/Pseudogenes**	**References**
P. falciparum	21	Conserved FIKK8 across species	FIKK7.2 and FIKK14 are pseudogenes	Gardner et al., 2002
P. reichenowi	21	Most orthologous to *P. falciparum*	Functional FIKK7.2, FIKK14	Sundararaman et al., 2016
P. gaboni	22	All except FIKK9.15	FIKK9.15 is unique; FIKK9.5 is pseudogene	Sundararaman et al., 2016
P. vivax	1	FIKK8 (only)	No expansion observed	Sargeant et al., 2006; Tewari et al., 2010
P. ovale	1	FIKK8 (only)	No expansion	Sargeant et al., 2006
P. malariae	1	FIKK8 (only)	No expansion	Sargeant et al., 2006
P. knowlesi	1	FIKK8 (only)	No expansion	Sargeant et al., 2006

2.4.2 The Functional Properties, Expression profile, and Localization of FIKK kinase(s) in iRBCs

FIKK kinases play a critical role in remodeling the host erythrocyte during *Plasmodium falciparum* infection. They phosphorylate a variety of host and parasite proteins, influencing membrane rigidity, surface antigen trafficking, and immune evasion. For example, FIKK1 regulates the phosphorylation of adducin, a cytoskeletal protein involved in membrane stability, while FIKK4.1 modulates the 4.1R complex, which affects cytoadhesion and PfEMP1 trafficking. These kinases generate distinct phosphorylation signatures, suggesting non-redundant and specialized functions across the family. Though single gene deletions may not impact parasite growth in vitro, FIKKs are essential for long-term parasite survival and virulence in vivo (Davies et al., 2020; Ghoneim et al., 2022).

FIKK kinases are predominantly expressed during the late trophozoite and schizont stages of the intraerythrocytic developmental cycle in *P. falciparum* (Figure 2.4-A, & Table 2.4). This stage-specific expression aligns with the timing of major host cell remodeling processes, such as increased rigidity, knob formation, and antigen export. Transcriptomic and proteomic studies confirm that several FIKKs, including FIKK4.1, FIKK8, and FIKK10.2, are highly expressed during these stages. Their expression patterns support their roles in preparing

iRBCs for cytoadhesion and evading splenic clearance (Sargeant et al., 2006; Tewari et al., 2010).

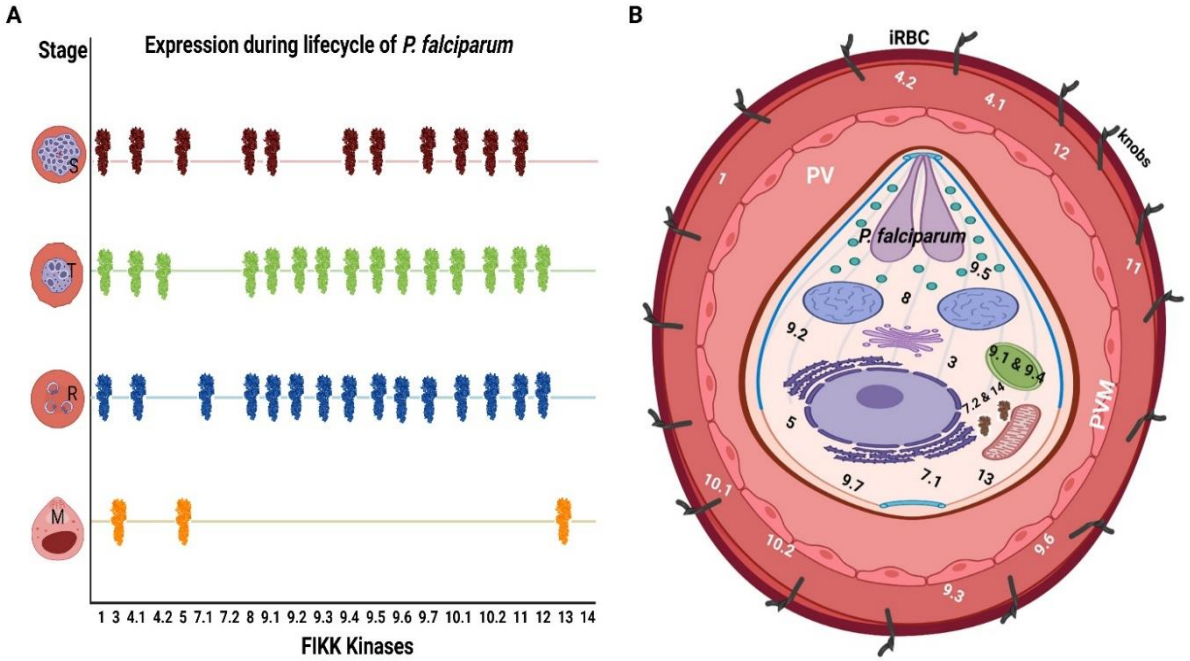

Figure 2.4: Stage-specific expression and intracellular localization of FIKK kinases in *P. falciparum*-infected red blood cells (iRBCs). The left panel **(A)** represents the stage-specific expression profiles of the 21 FIKK kinases across the parasite life cycle, including ring, trophozoite, schizont, and merozoite stages, based on transcriptomic data. The right panel **(B)** depicts the subcellular localization of FIKK kinases within infected red blood cells (iRBCs). **(**Prepared using BioRender**)**

Most FIKK kinases are exported into the host erythrocyte cytoplasm and membrane through the parasite's PTEX (*Plasmodium* Translocon of Exported proteins) export machinery (Figure 2.4-B and Table 2.4). Specific kinases localize to different subcellular compartments: FIKK4.1 and FIKK10.2 associate with the erythrocyte periphery and Maurer's clefts, while FIKK1 localizes to the cytoskeleton and Co-localized to Maurer's cleft. In contrast, FIKK8 remains within the parasite cytoplasm and is not exported. This differential localization reflects the functional diversity of FIKKs, with some involved in direct remodeling of host structures and others in intracellular signaling pathways (Davies et al., 2020; Miller et al., 2013).

Table 2.5: Localization and Expression Stages of 21 FIKK kinases of *P. falciparum*.				
FIKK Name	**Gene ID**	**Localization**	**Expression stage**	**References**
FIKK1	PF3D7_0102600	Co-localized to Maurer's cleft	R, T, & Sc	Davies et al., 2021 ; Nunes et al., 2007 & 2010 ; Ward et al.,(2004) ; Sargeant et al., 2006; Tewari et al., 2010 ; Ghoneim et al., 2022 ; & Miller et al., 2013
FIKK3	PF3D7_0301200	Not defined	Mz	
FIKK4.1	PF3D7_0424500	RBC periphery	R, T, & Sc	
FIKK4.2	PF3D7_0424700	RBC periphery	T	
FIKK5	PF3D7_0500900	Not defined	Sc (Mz formation)	
FIKK7.1	PF3D7_0726200	Not defined	R	
FIKK7.2	PF3D7_0731400	Not functional (pseudogene)	-	
FIKK8	PF3D7_0805700	Parasite cytoplasm (not exported)	R, T, & Sc	
FIKK9.1	PF3D7_0902000	Not defined	R, T, & Sc	
FIKK9.2	PF3D7_0902100	Parasite cytoplasm (not exported)	R, & T	
FIKK9.3	PF3D7_0902200	Maurer's cleft	R, & T	
FIKK9.4	PF3D7_0902300	Not defined	R, T, & Sc	
FIKK9.5	PF3D7_0902400	Not defined	R, T, & Sc	
FIKK9.6	PF3D7_0902500	Maurer's cleft	R, & T	
FIKK9.7	PF3D7_0902600	Not defined	R, T, & Sc	
FIKK10.1	PF3D7_1016400	Co-localized to Maurer's cleft	R, T, & Sc	
FIKK10.2	PF3D7_1039000	Co-localized to Maurer's cleft	R, T, & Sc	
FIKK11	PF3D7_1149300	RBC periphery	R, T, & Sc	
FIKK12	PF3D7_1200800	Maurer's cleft/RBC membrane	R, & T	
FIKK13	PF3D7_1371700	Not defined	Mz	
FIKK14	PF3D7_1476400	Not functional (pseudogene)	-	

2.4.3 Evolutionary Relationship of FIKK kinase(s)

FIKK kinases exhibit a distinct evolutionary trajectory, diverging significantly from other eukaryotic kinases, as shown through phylogenetic analyses (Figure 2.5-A). When compared with the broader eukaryotic kinome, FIKKs cluster separately, lacking homology to conventional kinase families found in humans and other model organisms, highlighting their apicomplexan-specific evolution (Talevich et al., 2012). A phylogenetic tree constructed within the *P. falciparum* kinome (Figure 2.5-B) further reveals that FIKKs form a unique clade distinct from conserved kinase groups like AGC, CMGC, and CDPK, reinforcing their classification as orphan kinases (Anamika et al., 2005). Notably, comparative analysis with the human kinome shows no direct orthologs, underlining the absence of structural or sequence similarity, which supports their potential as selective drug targets with minimal risk of host cross-reactivity (Doerig et al., 2004). This evolutionary uniqueness, reflected in both inter- and intra-kinome phylogenies, suggests that FIKK kinases have undergone lineage-specific

expansion and functional specialization in *P. falciparum*, likely driven by host adaptation and immune evasion requirements.

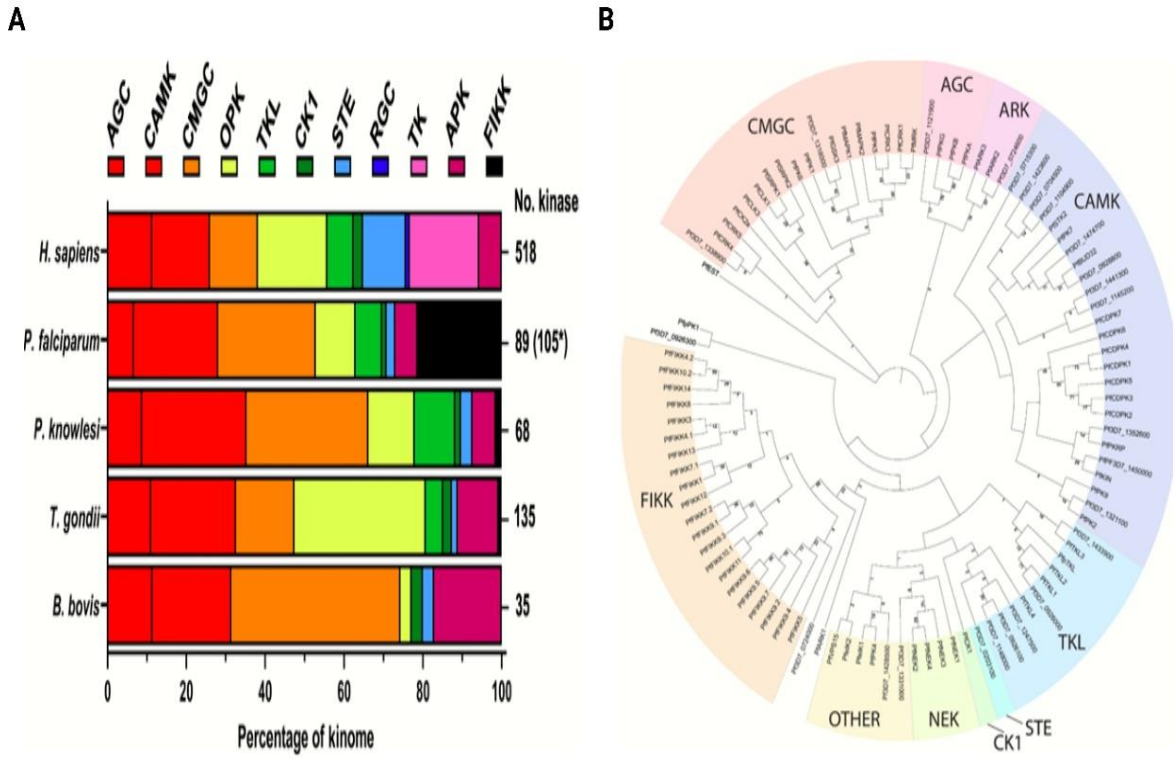

Figure 2.5: Comparison of kinome composition in Apicomplexan parasites, & *Homo sapiens* along with the phylogenetic analysis of the *P. falciparum* kinome. The Panel **(A)** illustrates the distribution and classification of kinases in *Plasmodium* species, and *Homo sapiens*, highlighting the lineage-specific expansions such as the FIKK kinase family unique to *P. falciparum*. The panel **(B)** presents a phylogenetic tree of *P. falciparum* kinases, grouped into ePK families (like CMGC, TKL, ARK, and FIKK). (Source: Jack Adderley et al. 2021)

Overall, FIKK kinase(s) display a high degree of evolutionary specialization, forming a unique lineage within the *Plasmodium* kinome, and are functionally differentiated from the human kinome, emphasizing their potential as species-specific therapeutic or diagnostic targets.

2.5 Importance of FIKK kinase(s)

FIKK kinase(s), exclusive to *P. falciparum*, hold strong potential as highly specific biomarkers for malaria diagnosis due to their absence in the human host and other *Plasmodium* species (Sargeant et al., 2006; Kaviratne et al., 2009). Unlike conventional markers such as HRP2 or

LDH, which are prone to gene deletions and diagnostic failures, FIKK kinases exhibit high sequence conservation across *P. falciparum* strains, enhancing their reliability (Tewari et al., 2010). Their expression during intraerythrocytic stages and localization within infected red blood cells (iRBCs) allow early detection of low-density and asymptomatic infections that is critical for timely treatment and transmission control (Miller et al., 2018). Moreover, their role in parasite survival, host cell remodeling, and immune evasion underscores their diagnostic significance (Ghoneim et al., 2022). As they are species-specific, FIKK-based assays can reduce cross-reactivity in co-infection and mixed infections, enabling precise identification and tailored treatments (Josling et al., 2015).

The development of PCR and rapid diagnostic tests (RDTs) using in silico-designed primers and immunoinformatic tools such as the Immune Epitope Database (IEDB) to characterize B-cell and T-cell epitopes targeting unique regions of FIKK kinases presents a promising approach for creating highly specific diagnostic tools (Singh et al., 2020). These tools, validated for cross-reactivity and sensitivity, could be optimized for reliable field deployment. Moreover, the incorporation of FIKK targets into portable molecular platforms such as loop-mediated isothermal amplification (LAMP) could significantly improve point-of-care testing, particularly in low-resource settings. Due to their species-specific expression and critical roles in parasite survival and host cell remodeling, FIKK kinase(s) represent valuable candidates for advanced molecular diagnostics in malaria surveillance, early detection, and eradication efforts highlighting the need for continued research to achieve these objectives.

2.6 Objectives of the study

Objective 1: - Screening and Selection of Suitable Molecular Marker for *P. falciparum* Malaria Diagnosis

1. Selection of suitable genes of *P. falciparum* for PCR based *P. falciparum* malaria diagnosis
2. Selection of suitable FIKK kinase for PCR based malaria diagnosis
3. Identification of FIKK kinase region to perform species specific detection of malaria
4. Designing and Validation of primer sequences to perform species specific detection of malaria
5. Development of suitable malaria diagnostic kit based on PCR and its validation

Objective 2: - Development of Rapid Antigen Test for *P. falciparum* Malaria Diagnosis

1. Selection of suitable proteins of *P. falciparum* genome for antigen based diagnosis
2. Selection of suitable FIKK kinase for malaria diagnosis
3. Generation of chimeric proteins to develop antibodies for different FIKK kinases
4. Cloning, Over-expression, purification and antibody development against chimeric protein in suitable animal
5. Purification of anti-C-FIKK antibodies and Validation for *P. falciparum* detection of malaria

2.7 References

1. Abba, K., Deeks, J. J., Olliaro, P. L., Naing, C. M., Jackson, S. M., Takwoingi, Y., ... & Garner, P. (2011). Rapid diagnostic tests for diagnosing uncomplicated *P. falciparum* malaria in endemic countries. *Cochrane Database of Systematic Reviews*, (7), CD008122. https://doi.org/10.1002/14651858.CD008122.pub2
2. Acharya, P., Chaubey, S., & Grover, M. (2017). *Plasmodium falciparum* biology: Glimpses from post-genomics studies. *Pathogens and Global Health*, 111(8), 421–432.
3. Aidoo, M., Kanyok, T. P., & Gokool, S. (2021). Novel antigens and technologies in malaria rapid diagnostics: Future prospects. *Expert Review of Molecular Diagnostics*, 21(2), 195–207.
4. Anamika, K., Srinivasan, N., & Krupa, A. (2005). A genomic perspective of protein kinases in *Plasmodium falciparum*. *Proteins: Structure, Function, and Bioinformatics*, 58(1), 180–189.
5. Ashley, E. A., Phyo, A. P., & Woodrow, C. J. (2022). Malaria. *The Lancet*, 400(10355), 965–979. https://doi.org/10.1016/S0140-6736(22)01381-0
6. Berhane, A., et al. (2018). Major threat to malaria control programs: Deletion of *PfHRP2* and *PfHRP3* genes in *Plasmodium falciparum* from Ethiopia. *PLOS ONE*, 13(2), e0193127.
7. Berná, L., Rego, N., & Francia, M. E. (2021). The elusive mitochondrial genomes of Apicomplexa: where are we now?. *Frontiers in microbiology*, *12*, 751775.
8. Bertolotti, A., et al. (2020). miRNA expression as a biomarker for malaria: A microarray study of miR-1246 in blood. *Scientific Reports*, 10, 1353.
9. Beshir, K. B., Gatton, M. L., Lewis, M. D., et al. (2017). Assessing *Plasmodium falciparum* HRP2 and HRP3 gene deletions in symptomatic patients from Ghana. *Scientific Reports*, 7, 11222.
10. Björkman, A., & Mårtensson, A. (2010). Risks and benefits of targeted malaria treatment based on rapid diagnostic test results. *Clinical Infectious Diseases*, 51(5), 512–514. https://doi.org/10.1086/655152
11. Bousema, T., & Drakeley, C. (2011). Epidemiology and infectivity of *Plasmodium falciparum* and *Plasmodium vivax* gametocytes in relation to malaria control and elimination. *Clinical Microbiology Reviews*, 24(2), 377–410. https://doi.org/10.1128/CMR.00051-10
12. Carlton, J. M., et al. (2008). Comparative genomics of the neglected human malaria parasite *Plasmodium vivax*. *Nature*, 455(7214), 757–763.
13. Carter, J. Y., et al. (2006). Reduction of malaria morbidity and mortality in Kisii District, Kenya, by improved diagnosis and treatment: A pilot project. *The American Journal of Tropical Medicine and Hygiene*, 75(6), 972–977.
14. Centers for Disease Control and Prevention. (2019). *Malaria diagnosis (U.S.) - Procedure manual for the laboratory diagnosis of malaria*. https://www.cdc.gov/dpdx/malaria/index.html
15. Centers for Disease Control and Prevention. (2021). *Malaria diagnosis & treatment in the United States*. https://www.cdc.gov/malaria/diagnosis_treatment/index.html
16. Cheng, Q., et al. (2021). Protein-based and molecular malaria diagnostics: Overview of current limitations and future needs. *Diagnostics*, 11(9), 1626.
17. Chiodini, P. L., Bowers, K., Jorgensen, P., Barnwell, J. W., Grady, K. K., Luchavez, J., ... & Bell, D. (2019). The heat stability of malaria rapid diagnostic tests. *Malaria Journal*, 18, 387. https://doi.org/10.1186/s12936-019-2994-3
18. Chiodini, P. L., et al. (2007). Impact of heat and transport on malaria RDT performance. *Tropical Medicine & International Health*, 12(1), 1–8.

19. Cho, C. H., Nam, M. H., Kim, J. S., Han, E. T., Lee, W. J., Oh, J. S., ... & Lim, C. S. (2011). Genetic variability in Plasmodium vivax aldolase gene in Korean isolates and the sensitivity of the Binax Now malaria test. *Tropical Medicine & International Health*, *16*(2), 223-226.
20. Compton, J. (1991). Nucleic acid sequence-based amplification. *Nature*, 350(6313), 91–92. https://doi.org/10.1038/350091a0
21. Cordray, M. S., & Richards-Kortum, R. R. (2012). Emerging nucleic acid-based tests for point-of-care detection of malaria. *The American Journal of Tropical Medicine and Hygiene*, 87(2), 223–230. https://doi.org/10.4269/ajtmh.2012.11-0685
22. Dalrymple, U., Arambepola, R., Gething, P. W., & Cameron, E. (2018). How long do rapid diagnostic tests remain positive after anti-malarial treatment? *Malaria Journal*, 17, 228. https://doi.org/10.1186/s12936-018-2360-8
23. Das, Ashis ; Holloway, Brian ; Collins, William E. ; Shama, V. P. ; Ghosh, Sushanta K. ; Sinha, Subrata ; Hasnain, Seyed E. ; Talwar, Gursaran P. ; Lal, Altaf A. (1995) *Species-specific 18S rRNA gene amplification for the detection of P. falciparum and P. vivax malaria parasites* Molecular and Cellular Probes, 9 (3). pp. 161-165. ISSN 0890-8508
24. Davies, D. H., et al. (2020). Protein kinases regulate red blood cell remodeling and virulence in *Plasmodium falciparum*. *Nature Microbiology*, 5(12), 1609–1623. https://doi.org/10.1038/s41564-020-00800-9
25. Doerig, C., et al. (2002). Protein kinases of *Plasmodium falciparum*: Kinomics and biology. *Trends in Parasitology*, 18(12), 570–577.
26. Doerig, C., Meijer, L., & Mottram, J. C. (2002). Protein kinases as drug targets in parasitic protozoa. *Trends in Parasitology*, 18(8), 365–371.
27. Dorin-Semblat, D., et al. (2015). Functional characterization of a NIMA-related kinase in *Plasmodium falciparum*. *PLOS ONE*, 10(3), e0121465.
28. Duedu, K. O., et al. (2016). False positive diagnosis of malaria in children in a malaria endemic zone: A case study of clinical versus laboratory diagnosis at a teaching hospital in Ghana. *Malaria Research and Treatment*, 2016, 1–5. https://doi.org/10.1155/2016/5021038
29. Dutta, S., et al. (2015). Detection of *Plasmodium* Topoisomerase activity in human saliva. *Malaria Journal*, 14, 97.
30. El-Bishbishi, E. A., et al. (2011). Non-invasive detection of *P. falciparum* gametocytes using saliva. *Tropical Medicine & International Health*, 16(4), 437–440.
31. Gadia, C. L., et al. (2017). Functional characterization of FIKK kinases in *Plasmodium falciparum*. *Molecular and Biochemical Parasitology*, 211, 42–50.
32. Gamboa, D., Ho, M. F., Bendezu, J., Torres, K., Chiodini, P. L., Barnwell, J. W., ... & Bell, D. (2010). A large proportion of *P. falciparum* isolates in the Amazon region of Peru lack *pfhrp2* and *pfhrp3*. *PLoS ONE*, 5(1), e8091. https://doi.org/10.1371/journal.pone.0008091
33. Gardner, M. J., et al. (2002). Genome sequence of the human malaria parasite *Plasmodium falciparum*. *Nature*, 419(6906), 498–511.
34. Ghoneim, M. A., et al. (2022). Parasite-specific protein kinases regulate red blood cell remodeling in *Plasmodium falciparum*. *Nature Communications*, 13(1), 3821.
35. Gillet, P., Mori, M., Van Esbroeck, M., Van den Ende, J., & Jacobs, J. (2009). Assessment of the prozone effect in malaria rapid diagnostic tests. *Malaria Journal*, 8, 271. https://doi.org/10.1186/1475-2875-8-271
36. Haanshuijsen, S. J., van Rosmalen, J., Keuter, M., & Mens, P. F. (2020). Clinical relevance of low-density *Plasmodium falciparum* infections. *Malaria Journal*, 19, 173. https://doi.org/10.1186/s12936-020-03265-w

37. Hänscheid, T. (2003). Current strategies to avoid misdiagnosis of malaria. *Clinical Microbiology and Infection*, 9(6), 497–504. https://doi.org/10.1046/j.1469-0691.2003.00699.x
38. Houzé, S., Hubert, V., Le Pessec, G., Le Bras, J., & Clain, J. (2011). Combined deletions of pfhrp2 and pfhrp3 genes result in Plasmodium falciparum malaria false-negative rapid diagnostic test. *Journal of clinical microbiology*, *49*(7), 2694-2696.
39. Imwong, M., Hanchana, S., Malleret, B., Rénia, L., Day, N. P. J., Dondorp, A. M., & White, N. J. (2014). High-throughput ultrasensitive molecular techniques for quantifying low-density malaria parasitemias. *Journal of Clinical Microbiology*, 52(9), 3303–3309. https://doi.org/10.1128/JCM.01057-14
40. Jelinek, T., Grobusch, M. P., Schwenke, S., Steidl, S., Von Sonnenburg, F., Nothdurft, H. D., ... & Loscher, T. (1999). Sensitivity and specificity of dipstick tests for rapid diagnosis of malaria in nonimmune travelers. *Journal of clinical microbiology*, *37*(3), 721-723.
41. John, G. K., Douglas, N. M., von Seidlein, L., Nosten, F., Baird, J. K., & Price, R. N. (2015). Primaquine radical cure of *Plasmodium vivax*: A critical review of the literature. *Malaria Journal*, 11, 280. https://doi.org/10.1186/1475-2875-11-280
42. Josling, G. A., et al. (2015). Gene regulation and epigenetic control in *Plasmodium falciparum*. *Biochimica et Biophysica Acta (BBA) - Gene Regulatory Mechanisms*, 1849(1), 1–10.
43. Kappe, S. H. I., Vaughan, A. M., Boddey, J. A., & Cowman, A. F. (2004). That was then but this is now: Malaria research in the time of an eradication agenda. *Science*, 328(5980), 862–866.
44. Kaviratne, M., et al. (2009). Remodeling of host erythrocyte cytoskeleton by *Plasmodium falciparum*: The role of exported kinases. *Cellular Microbiology*, 11(10), 1604–1616.
45. Lalloo, D. G., Shingadia, D., Pasvol, G., Chiodini, P. L., Whitty, C. J., Beeching, N. J., ... & Hill, D. R. (2016). UK malaria treatment guidelines. *Journal of Infection*, 72(6), 635–649. https://doi.org/10.1016/j.jinf.2016.02.001
46. Maltha, J., Gillet, P., & Jacobs, J. (2013). Malaria rapid diagnostic tests in travel medicine. *Clinical Microbiology and Infection*, 19(5), 408–415.
47. Mangold, K. A., Manson, R. U., Koay, E. S. C., Stephens, L., Regner, M., Thomson, R. B., ... & Peterson, L. R. (2005). Real-time PCR for detection and identification of *Plasmodium spp*. *Journal of Clinical Microbiology*, 43(5), 2435–2440. https://doi.org/10.1128/JCM.43.5.2435-2440.2005
48. Martínez, M. J., et al. (2009). *Plasmodium* detection in saliva: Future of non-invasive diagnostics? *Malaria Journal*, 8, 211. https://doi.org/10.1186/1475-2875-8-211
49. Mekonnen, Z., Ali, S., Belachew, T., Suleman, S., & Medhin, G. (2021). Performance of malaria rapid diagnostic tests in Ethiopia: A systematic review and meta-analysis. *Malaria Journal*, 20, 322. https://doi.org/10.1186/s12936-021-03879-1
50. Miller, L. H., Baruch, D. I., Marsh, K., & Doumbo, O. K. (2018). The pathogenic basis of malaria. *Nature*, 415(6872), 673–679.
51. Moody, A. (2002). Rapid diagnostic tests for malaria parasites. *Clinical Microbiology Reviews*, 15(1), 66–78. https://doi.org/10.1128/CMR.15.1.66-78.2002
52. Mukherjee, A., Diop, M., Sarr, F. D., & Loucoubar, C. (2017). Diagnostic performance of malaria RDTs under real conditions: A review. *Malaria Research and Treatment*, 2017, 1–10. https://doi.org/10.1155/2017/4209821
53. Newton, P. N., et al. (2019). Hemozoin and malaria: Emerging diagnostic techniques. *Trends in Parasitology*, 35(7), 579–591.

54. Notomi, T., Okayama, H., Masubuchi, H., Yonekawa, T., Watanabe, K., Amino, N., & Hase, T. (2000). Loop-mediated isothermal amplification of DNA. *Nucleic Acids Research*, 28(12), e63. https://doi.org/10.1093/nar/28.12.e63
55. Nunes, M. C., et al. (2010). Targeting the exported FIKK kinases of *Plasmodium falciparum*. *Molecular Microbiology*, 78(3), 578–595.
56. Ochola, L. B., Vounatsou, P., Smith, T., Mabaso, M. L. H., & Newton, C. R. J. C. (2016). The reliability of diagnostic techniques in the diagnosis and management of malaria in the absence of a gold standard. *The Lancet Infectious Diseases*, 6(9), 582–588.
57. Parr, J. B., et al. (2017). *PfHRP2/3* deletions in *Plasmodium falciparum* and the impact on rapid diagnostic tests. *The Lancet Infectious Diseases*, 17(10), 1028–1036.
58. Pease, B. N., et al. (2013). The *P. falciparum* kinome: Functional analysis reveals roles in erythrocyte remodeling. *Cell Host & Microbe*, 14(5), 534–546.
59. Perera, R. S., Ding, X. C., Thriemer, K., Salazar, C. L., Clark, T. G., & Kobayashi, T. (2020). Real-time PCR for malaria diagnosis: Evaluating diagnostic performance and patient outcomes. *Malaria Journal*, 19, 373. https://doi.org/10.1186/s12936-020-03518-w
60. Perkins, M. D., Bell, D. R., & Totty, H. (2017). New diagnostics for malaria elimination. *Transactions of the Royal Society of Tropical Medicine and Hygiene*, 111(1), 13–17. https://doi.org/10.1093/trstmh/trx010
61. PlasmoDB. (2017). *The Plasmodium Genomics Resource*. http://plasmodb.org
62. Poostchi, M., et al. (2018). Image analysis and machine learning for detecting malaria. *Malaria Journal*, 17, 122. https://doi.org/10.1186/s12936-018-2260-1
63. Rajpurkar, P., et al. (2018). Deep learning for malaria parasite detection. *Nature Biomedical Engineering*, 2(10), 730–738. https://doi.org/10.1038/s41551-018-0309-5
64. Riley, L. F., et al. (2011). Helicase-dependent amplification of malaria parasite DNA for diagnostic applications. *Analytical Biochemistry*, 414(2), 215–220. https://doi.org/10.1016/j.ab.2011.03.024
65. Rougemont, M., Van Saanen, M., Sahli, R., Hinrikson, H. P., Bille, J., & Jaton, K. (2004). Detection of four *Plasmodium* species in blood from humans by 18S rRNA gene subunit-based and species-specific real-time PCR assays. *Journal of Clinical Microbiology*, 42(12), 5636–5643. https://doi.org/10.1128/JCM.42.12.5636-5643.2004
66. Sargeant, T. J., et al. (2006). Lineage-specific expansion of proteins exported to erythrocytes in malaria parasites. *Genome Biology*, 7(2), R12. https://doi.org/10.1186/gb-2006-7-2-r12
67. Schneider, A. G., & Puijalon, O. M. (2005). A new Apicomplexa-specific protein kinase family: Multiple members in *Plasmodium falciparum*, but not in other Apicomplexa. *Trends in Parasitology*, 21(10), 470–473.
68. Schultz, L., Wellems, T. E., & Volkman, S. K. (2022). *Plasmodium* drug resistance in the post-genomic era. *Nature Reviews Microbiology*, 20(6), 401–414. https://doi.org/10.1038/s41579-021-00636-w
69. Simpalipan, P., Pattaradilokrat, S., & Harnyuttanakorn, P. (2018). Global sequence diversity of the lactate dehydrogenase gene in Plasmodium falciparum. *Malaria journal*, *17*, 1-12.
70. Singh, B., & Daneshvar, C. (2013). Human infections and detection of *Plasmodium knowlesi*. *Clinical Microbiology Reviews*, 26(2), 165–184. https://doi.org/10.1128/CMR.00079-12
71. Singh, B., Bobogare, A., Cox-Singh, J., Snounou, G., Abdullah, M. S., & Rahman, H. A. (1999). A genus- and species-specific nested polymerase chain reaction malaria detection assay for epidemiologic studies. *The American Journal of Tropical Medicine and Hygiene*, 60(4), 687–692. https://doi.org/10.4269/ajtmh.1999.60.687

72. Singh, B., et al. (2008). Saliva-based diagnostics for malaria detection. *Transactions of the Royal Society of Tropical Medicine and Hygiene*, 102(12), 1145–1150. https://doi.org/10.1016/j.trstmh.2008.03.017
73. Singh, B., et al. (2020). Targeting protein kinases in malaria: Opportunities and challenges. *Pharmacology & Therapeutics*, 211, 107527.
74. Snounou, G., & Singh, B. (2002). Nested PCR analysis of *Plasmodium* parasites. *Methods in Molecular Medicine*, 72, 189–203. https://doi.org/10.1385/1-59259-271-6:189
75. Sullivan, D. J., Gluzman, I. Y., & Goldberg, D. E. (1996). Hemozoin formation and malaria. *Proceedings of the National Academy of Sciences*, 93(21), 11865–11870.
76. Sundararaman, S. A., et al. (2016). Genomic variation in malaria parasites from chimpanzees and gorillas: Insights into cross-species transmission. *Genome Biology and Evolution*, 8(5), 1551–1563.
77. Tadesse, F. G., Slater, H. C., Chali, W., Teelen, K., Lanke, K., Belachew, M., ... & Bousema, T. (2017). The quest for persistent malaria transmission: How low can we go? *Trends in Parasitology*, 33(7), 603–615. https://doi.org/10.1016/j.pt.2017.04.004
78. Talevich, E., Mirza, A., & Kannan, N. (2012). Structural and evolutionary divergence of eukaryotic protein kinases in *Plasmodium falciparum*. *BMC Evolutionary Biology*, 11, 321. https://doi.org/10.1186/1471-2148-12-321
79. Tewari, R., et al. (2010). The systematic functional analysis of *Plasmodium* protein kinases identifies essential regulators of mosquito transmission. *Cell Host & Microbe*, 8(4), 377–387. https://doi.org/10.1016/j.chom.2010.09.006
80. Tsalik, E. L., Bonomo, R. A., & Fowler, V. G. (2010). New molecular diagnostic approaches to bacterial infections and antibacterial resistance. *Annual Review of Medicine*, 61, 379–394. https://doi.org/10.1146/annurev.med.080708.082451
81. Udhayakumar, V., Lucchi, N. W., & Srivastava, P. (2016). Challenges in malaria diagnosis and detection of drug resistance. *The Journal of Infectious Diseases*, 213(Supplement_1), S135–S143. https://doi.org/10.1093/infdis/jiv576
82. Warhurst, D. C., & Williams, J. E. (1996). Laboratory diagnosis of malaria. *Journal of Clinical Pathology*, 49(7), 533–538. https://doi.org/10.1136/jcp.49.7.533
83. Wilson, R. J. M., et al. (1996). Complete gene map of the plastid-like DNA of *Plasmodium falciparum*. *Journal of Molecular Biology*, 261(2), 155–172.
84. World Health Organization. (2015). *Guidelines for the treatment of malaria* (3rd ed.). https://apps.who.int/iris/handle/10665/162441
85. World Health Organization. (2016). *Microscopy for the detection, identification and quantification of malaria parasites on stained thick and thin blood films in research settings*. https://www.who.int/publications/i/item/9789241549462
86. World Health Organization. (2018). *Malaria rapid diagnostic test performance – Results of WHO product testing of malaria RDTs: Round 8 (2016–2018)*. https://apps.who.int/iris/handle/10665/276231
87. World Health Organization. (2020). *Malaria microscopy quality assurance manual – Version 2*. https://www.who.int/publications/i/item/9789240012639
88. World Health Organization. (2021). *World malaria report 2021*. https://www.who.int/teams/global-malaria-programme/reports/world-malaria-report-2021
89. World Health Organization. (2022). *Malaria diagnostics*. https://www.who.int/teams/global-malaria-programme/prevention/diagnosis
90. World Health Organization. (2023). *Malaria*. https://www.who.int/news-room/fact-sheets/detail/malaria

Chapter 3

Experimental Procedures

METHODOLOGICAL FRAMEWORK

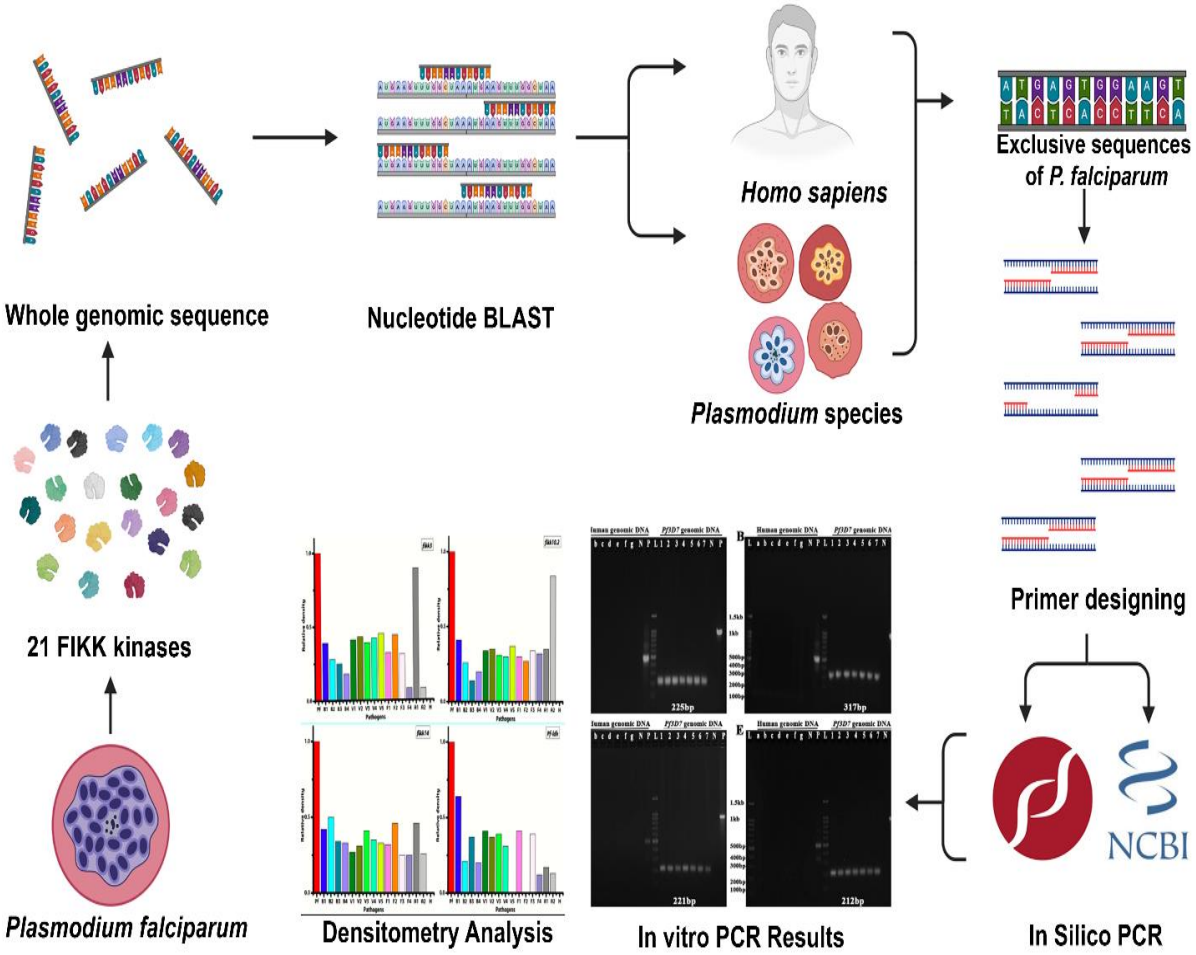

Figure: Schematic representation of PCR-based assay with various methods employed for genomic detection of *P. falciparum*.

The study employed a PCR-based assay targeting FIKK kinase genes for the sensitive and selective detection of *Plasmodium falciparum* by employing the various methods as described in this chapter. Primer specificity was validated using the NCBI-Primer BLAST and FastPCRtools. PCR amplification was optimized to enhance specificity, and gel electrophoresis verified DNA integrity. The assay's analytical sensitivity was evaluated using serially diluted genomic DNA from *P. falciparum*, while specificity was tested against non-target species, including bacteria, fungi, and viruses. The optimized assay demonstrated sensitivity, and selectivity, making it a reliable molecular diagnostic tool.

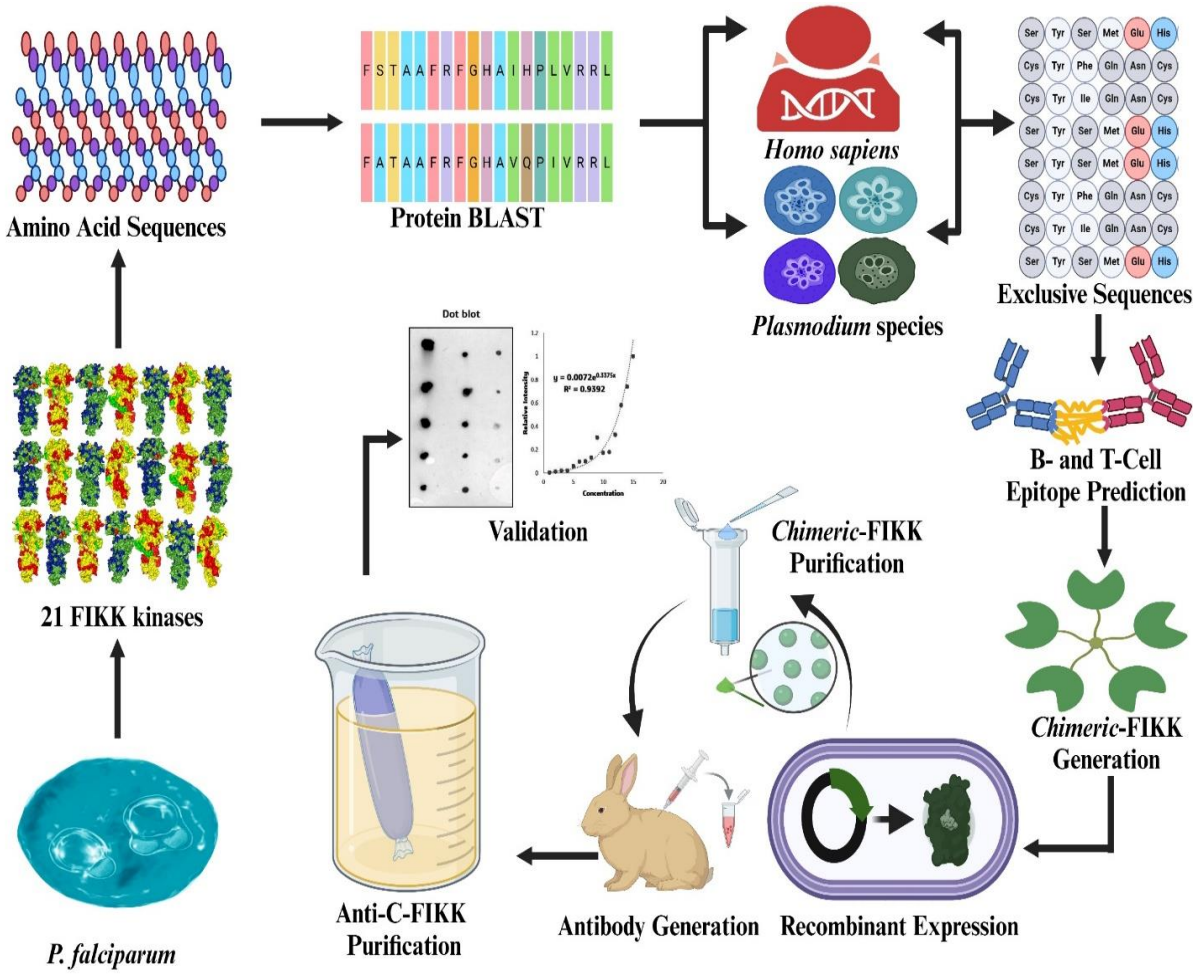

Figure: Schematic representation of RAT-based assay with various methods employed for detection of *P. falciparum*.

A rapid diagnostic test (RDT) based on recombinant C-FIKK protein using PSI-BLAST, and computational tools such as IEDB (NetMHCpan EL 4.1) predicted antigenic epitopes and MHC-binding affinities for field-applicable malaria detection. Recombinant protein expression was optimized in *E. coli* by employing various strategies and purified using electro elution and ammonium sulfate precipitation. SDS-PAGE and Western blotting confirmed protein integrity, followed by polyclonal antibody generation in rabbits. ELISA was used to determine antibody titers. The sensitivity, and specificity was evaluated by performing dot blot assay along with the co-infection models. The anti-C-FIKK antibody selectivity was assessed for *P. falciparum* specific RDT development. Thus the chapter contribute to the various molecular and immunodiagnostic methods for malaria detection and surveillance.

3.1 MATERIALS AND STRAINS

The various reagents, consumables, and equipment were utilized in this study. Like the EmeraldAmp GT PCR Master Mix (Cat. RR310B) was sourced from Takara, Shiga, Japan, while Agarose (CAS No. 9012-36-6) and the 100 bp DNA Ladder (Cat. N3231S) were procured from New England Biolabs. The Precision Plus Protein Dual Color Standards (Cat. 1610374) were obtained from Bio-Rad, and RPMI 1640 medium and gentamycin were purchased from Sigma, St. Louis, MO, USA. Additionally, Albumax II (lipid-rich bovine serum albumin) was sourced from GIBCO, Grand Island, NY, USA. The PCR tubes (Cat. AB0620) were supplied by Thermo Scientific, Waltham, Massachusetts, USA, while nitrocellulose blotting sheets were acquired from Bio-Rad Laboratories, Hercules, California, USA.

The equipment used in this study included the T100 Thermal Cycler and Gel Documentation Unit from Bio-Rad, a bacterial orbital shaking incubator from Remi, a high-speed refrigerated centrifuge from HEMA, and a Spin-Win Mini Centrifuge from Tarsons. The Trans-Blot Turbo Transfer System was obtained from Bio-Rad, while the Cooling Centrifuge C-24 Plus and the Swinging Bucket Centrifuge were sourced from Remi. Other laboratory instruments included the Spinex Vortex from Tarsons, the I-Wave Microwave Oven from LG, and the Quintix Weighing Balance (mg) and BSA223S Weighing Balance (gm) from Sartorius.

Additional equipment included the Microtiter Plate Reader (SpectraMax M2), Mini-PROTEAN Electrophoresis Tank (Bio-Rad), DNA Electrophoresis Tank (Genaxy), Vacuum Pump (Millipore), and pH Meter (pH Tutor) from EUTECH. The Electrophoresis Power Supply Pack, Spinet Magnetic Stirrer, and Hot Plate were acquired from Tarsons, while the Spectrophotometer was obtained from Shimadzu. The Water Bath (Equitron), Compound Light Microscope (Nikon YS100), and Inverted Light Microscope (Nikon Eclipse TC100) were also employed in the study.

Furthermore, the Fixed Rotor Cooling Centrifuge (Sigma 2-16 PK), Dry Bath Heat Block (Genei), 3D Gyratory Rocker (Benchtop Lab System), and Rocking Max Shaker (Tarsons) were used for experimental procedures. Cold storage was maintained using a Twin Cooling Refrigerator (Samsung), a -80°C Deep Freezer (Eppendorf U410 Premium), and an Ice Maker (Labman). Heat-based equipment included the Hot Air Oven (Universal Hot Air Oven) and the Heat Plastic Sealer (Sepack).

For cell culture, a CO_2 Incubator for Parasites (Galaxy 170 S) and a CO_2 Incubator for Mammalian Cells (Thermo Scientific) were used. The Laminar Hood for culturing parasites and mammalian cells was sourced from Esco Airstream and Thermo Scientific respectively,

while sterilization procedures were carried out using an Autoclave (Equitron)**.** The media components for cultivating various strains were prepared following standard protocols. All other reagents and buffer salts used in this study were of high analytical purity. This study includes a variety of pathogens, which are systematically listed in the following table P, along with their respective sources.

Table 3.1: List of various pathogens and their source used in the study

S. No	Strain Name	Source
1	*S. cerevisiae* (BY4742 WT)	Procured from Dharmacon
2	*Scenedesmus abundans* NCIM 2897	Procured from National Collection of Industrial Microorganisms, NCL, Pune, India.
3	*Rodococcus opacus* strain PD630	Procured from Microbial Type Culture Collection and Gene Bank (MTCC), Chandigarh, India
4	*Neurospora crassa* 74-OR23-1V A (FGSC 2489)	Procured from Fungal Genetics Stock Center (FGSC), University of Missouri, Kansas City, MO 64110
5	*Pichia pastoris* X33 strain	Procured from Biogrammatics Inc., USA,
6	*Acinetobacter baylyi* sp SRL_72524	Procured from Biogrammatics Inc., USA,
7	*Bacillus megaterium* strain 18-2	Procured from Bose Institute, Kolkata, India
8	*E. coli strains* (DH5α, BL21CodonPlus)	Procured from Invitrogen
9	Herpes simplex virus (AnHV-1)	Procured from the College of Veterinary Sciences, Guwahati, India
10	Duck plague virus (IVRI-19)	Procured from National Veterinary Services Laboratory, (Ames, IA)
11	Influenza virus (PR8 Strain)	Procured from Centers for Disease Control and Prevention (CDC; Atlanta, GA)
12	Japanese encephalitis strain (SA14-14-2)	Procured from the Department of health and family welfare, Government of Assam, India.
13	Newcastle disease virus (R2B strain)	Procured from the College of Veterinary Science, Khanapara, Assam, India
14	*Aspergillus terreus-10831*	Procured from National Center for Industrial Microorganisms (NCIM), Pune, India
15	*Mycobacterium smegmatis* (ATCC14468)	Procured from Institute of Microbial Technology, (IMTECH), Chandigarh, India (MTCC)
16	*Bacillus subtilis* RSL-2 strain	Water from oil contaminated Isolates (Swati Sharma, Lalit M. Pandey, et al., 2020)
17	*Bacillus vallismortis IS1*	Sea water Isolates (M. Pandey, et al., 2017)
18	*Staphylococcus aureus* -SA	Procured from Institute of Microbial Technology, (IMTECH), Chandigarh, India (MTCC)
19	*Listeria monocytogenes* 5260	Procured from Institute of Microbial Technology, (IMTECH), Chandigarh, India (MTCC)
20	*Bacillus tequilensisMK 729017*	Soil sample of Assam Oil reserve field Isolates (Poulami Datta, Lalit M. Pandey, et al., 2020)
21	*Methylobacterium extorquens* L2-4	Procured from Institute of Microbial Technology, (IMTECH), Chandigarh, India (MTCC)
22	*Lactobacillus lactis* strain A3	Procured from Institute of Microbial Technology, (IMTECH), Chandigarh, India (MTCC)

METHODS

3.2 Bioinformatics Analysis of *P. falciparum* FIKK Kinase(s) for Primer Designing and In-silico PCR

The Basic Local Alignment Search Tool (BLAST) was utilized to compare the nucleotide sequences of individual *fikk* kinase genes from *Plasmodium falciparum* with those of *Homo sapiens* and four other human-infecting *Plasmodium* species (*P. vivax, P. ovale, P. malariae,* and *P. knowlesi*) using the blastn algorithm. Nucleotide sequences of each *fikk* kinase gene from *P. falciparum* and one conserved *fikk* kinase from each of the four *Plasmodium* species were retrieved from PlasmoDB, a specialized database for *Plasmodium* species.

For the Nucleotide BLAST (blastn) search, each *fikk* kinase sequence was entered into the query sequence field one at a time, and the standard databases (nr/nt) were selected for comparison. The target organism (*Homo sapiens* or a specific *Plasmodium* species) was designated according to the intended analysis. The BLAST search was performed using the blastn algorithm to identify sequences with significant similarity. The BLAST hits were analyzed to assess sequence homology with humans, identify species-specific regions, and determine the exclusive sequences of each individual *fikk* kinase genes**.**

Exclusive nucleotide sequences of the 21 *fikk* kinase genes of *Plasmodium falciparum* that were identified through *blastn* were selected as potential target regions for primer design with sequences ranging from 200 to 400 base pairs. Primers were designed using NCBI Primer-BLAST and FastPCR, version 6.9.11 (Kalendar, R., 2022) ensuring optimal characteristics such as 30 to 60 % GC content, 55 to 60 °C melting temperature (Tm), 18 to 25 base pairs (bp) primer length, low self-complementarity, and expected product size, the set of primers were designed for the possible *fikk* kinase genes. To validate the specificity of the designed primers, in silico PCR was performed using NCBI Primer-BLAST and fastPCR tool. The analysis was conducted by selecting *P. falciparum* as the target organism from the NCBI database or by uploading the respective genome files in the FASTA format including the human genome and other *Plasmodium* species causing malaria in humans. This approach enabled the identification of potential non-specific amplifications in the human genome while confirming specific amplification in *P. falciparum*. The results from both tools were cross-verified to ensure the reliability of the designed primers and thus shortlisted the primers in the *fikk* kinases of *P. falciparum*.

3.3 *Plasmodium falciparum 3D7* Strain Culture

Plasmodium falciparum (3D7), a drug-sensitive strain, was maintained in continuous culture using human red blood cells (RBCs) of the O+ blood group under controlled conditions. The parasites were cultured at 37°C in RPMI 1640 medium, which was supplemented with 5% Albumax (a lipid-rich bovine serum albumin substitute) and 5% sodium bicarbonate to maintain physiological pH and osmolarity. The culture was incubated under a controlled gas environment consisting of 90% nitrogen (N_2), 5% carbon dioxide (CO_2), and 5% oxygen (O_2) to mimic in vivo conditions conducive to parasite growth. The culturing method followed established protocols for in vitro propagation of *P. falciparum*, as previously described (Trivedi, V., et al., 2005).

3.4 Isolation of Genomic DNA from *Plasmodium falciparum, Homo sapiens and other Organisms*

The genomic DNA from the cultured flask (*Plasmodium falciparum 3D7* strain) was isolated using the traditional phenol-chloroform method as described (Chan, S., et al., 2013). The genomic DNA of *Plasmodium vivax* from the field isolates that contain trace amounts of human genomic DNA was gifted by Prof. Vishal Saxena of BITS Pilani. The genomic DNA from healthy volunteers *(Homo sapiens)* with informed consent was drawn and used to isolate the genomic DNA by Non-Enzymatic Salting-out method (Bharatha, A., S., et al., 2014). The genomic DNA from bacterial species (*Acinetobacter baylyi*, *Rhodococcus opacus*, *Bacillus megaterium*, & *E. coli-DH5α*), algae (*Scenedesmus*), fungi (*Aspergillus terreus*, *Pichia pastoris*, & *Saccharomyces cerevisiae*) and virus (Herpes simplex virus, Duck enteritis virus, Influenza virus, Japanese encephalitis, & Newcastle disease virus) were isolated as per established protocol (Bhardwaj, B., et al., 2019 ; Pattern, R.,et al., 2019 ; Lõoke, M., et al., 2011 ; Mahesh, R., et al., 2019)

3.5 Polymerase Chain Reaction (PCR) Amplification and Gel-Based DNA Analysis

The PCR was carried out in a reaction volume of 10–20 µL with primers, PCR master mix and template DNA in a thermal cycler (Bio-Rad, *Berkeley, California*). Initially gradient PCR was set up to optimise the annealing temperature of the designed primers (primer details in Table M) from a range of 50 °C to 56 °C based on the melting temperature of each forward and reverse primer with 1X PCR master mix(5µL), forward and reverse primers (1µL i. e ~10 pico moles each), ~10 ng DNA template (1µL) and Nuclease free water (3µL) for a total reaction volume of 10 µL. The final conditions for PCR are as follows: an initial denaturation at 95°C

for 5 minutes to unwind DNA, followed by 30 cycles of denaturation at 95°C for 30 seconds, optimised annealing at 54°C (from a range of 50 °C to 56 °C) for 30 seconds, and extension at 72°C for 30-60 seconds. The final step is a cycle of extension at 72°C for 7 minutes to complete the amplification. *Pf-ldh* primers reported in the previous studies were used as a positive control (Keluskar, P., et al., 2014). The details of the primer pairs used in the study is given in the table 3.2.

Table 3.2: Primer details for *fikk* kinase-based PCR assay.

S. No	Target Gene Name	Primer Name	Sequence (5' - 3')	Product Size (bp)	Melting Temperature (°C)	GC Content (%)
1	*fikk3*	S1_*f3*_Set9_FP S1_*f3*_Set9_RP	TACAAGCGTCTCATCATATCAA CGTTTGTTCTTACTCCATTTATCCT	225	55.11 57.39	36.36 36.00
2	*fikk4.2*	S2_*f4.2*_Set48_FP S2_*f4.2*_Set48_RP	GTTTTAGGGGTAAAAGTGCGT CTCCCCCTGATCAATTAAACCT	317	56.73 57.47	42.86 45.45
3	*fikk8*	S3_*f8*_Set97_FP S3_*f8*_Set97_RP	GATGGAAGAAGAAAAATACCGTG CATATCATTTTGACCTGCTCC	277	57.10 55.80	39.13 42.86
4	*fikk10.2*	S4_*f10.2*_Set152_FP S4_*f10.2*_Set152_RP	GACGGAGATCAAGAAAATATTACA TCTTCGCTACCATACCCATT	221	54.80 56.02	33.33 45.00
5	*fikk12*	S5_*f12*_Set167_FP S5_*f12*_Set167_RP	GCATCACGTGAACTCTGATA TACAAGTACCTTCTACACTCTC	212	55.31 54.10	45.00 40.91
6	*fikk14*	S6_*f14*_Set185_FP S6_*f14*_Set185_RP	TCAAGATATTCGAGGGGTCT GTACTTCTATTCGTACTTTTCTGT	203	55.03. 54.47	45.00 33.33

The PCR-amplified products were assessed using 2% agarose gel electrophoresis to verify amplification specificity and product size. A 2% (w/v) agarose gel was prepared in 1X TAE buffer (40 mM Tris-acetate, 1 mM EDTA, pH 8.0) and allowed to solidify before loading the samples. Electrophoresis was conducted at a constant voltage of 80 V for 60 minutes in 1X TAE buffer to facilitate DNA migration. After electrophoresis, the gel was visualized under UV light using a transilluminator (Bio-Rad Gel Doc System, USA), and images were captured for documentation. The presence of distinct bands at the expected fragment size confirmed successful PCR amplification, while the appearance of primer-dimer formations indicated potential off-target amplification.

3.6 Evaluation of Analytical Sensitivity and Specificity of the *fikk* Kinase-based PCR Assay

Genomic DNA from *Plasmodium falciparum* was extracted from cultured parasites to evaluate the sensitivity and specificity of the *fikk* kinase-based PCR assay. The concentration of extracted DNA was quantified using OD_{260} measurements, and the percentage of parasitemia was determined microscopically. To assess the assay's sensitivity, tenfold serial dilutions of the DNA (ranging from 10^{2} ng to 10^{-5} ng) and infected red blood cells (iRBCs) from *P. falciparum* cultures with parasitemia levels between 5% and 0.0003% were tested. For specificity analysis, the assay was conducted using genomic DNA (100 ng) extracted from various non-target species, including *Plasmodium vivax*, bacteria (*Acinetobacter baylyi*, *Rhodococcus opacus*, *Bacillus megaterium*, and *E. coli-DH5α*), algae (*Scenedesmus*), fungi (*Aspergillus terreus*, *Pichia pastoris*, and *Saccharomyces cerevisiae*), and viruses (Herpes simplex, Duck enteritis, Influenza, Japanese encephalitis, and Newcastle disease). PCR reactions were performed both with pure DNA from these pathogens and with mixed samples containing 1 ng of *P. falciparum* DNA contaminated with 100 ng of DNA from other pathogens at the molecular level. At the cellular level, approximately 8,000 to 10,000 cells of each pathogen type were tested alone and in combination with *P. falciparum* iRBCs at 0.5% parasitemia. DNA extracted from these mixed samples was then used as templates in the PCR assay to evaluate its specificity thoroughly.

3.7 Densitometry and Statistical Analysis

The intensity of PCR product present in agarose gel was densitometrically analysed using ImageLab 4.1 (Bio-Rad) and ImageJ 1.54j. Background subtraction was performed uniformly across the lanes of a selected gel, ensuring the background was consistently subtracted from the PCR product. The obtained data was graphed using the OriginLab 9.0 version for further analysis.

To assess the assay's specificity, band intensities from unknown or cross-reactivity samples were compared against a positive control containing a known amount of *P. falciparum* genomic DNA. This comparison helped determine whether the presence of DNA from other pathogens interfered with the assay. Positive and negative samples were quantified by evaluating their band intensities and verifying them against known results (true positives and true negatives). The accuracy of each mock patient sample was then calculated using standard metrics: sensitivity (true positives / [true positives + false negatives]) and specificity (true

negatives / [true negatives + false positives]), providing a clear percentage accuracy for each tested mock sample.

3.8 Computational Design of *Chimeric*-FIKK Protein and Plasmid Assembly

3.8.1 Comparative Analysis of *FIKK* Kinase Proteins: Retrieval from PlasmoDB and Protein BLAST Evaluation

The protein sequences of FIKK kinases were retrieved from the PlasmoDB database v54 (August 2021) & v58 (December 2022) (Alvarez-Jarreta *et al.*, 2023) in FASTA format for subsequent antigenic epitope predictions. Protein BLAST (BLASTp) was conducted using the PSI-BLAST algorithm to identify homologous sequences (Altschul, S. F. *et al.*, 1997). Each *FIKK* kinase protein sequence from PlasmoDB was used as a query in the PSI-BLAST search. The standard non-redundant (nr) protein database of *Homo sapiens* (taxid: 9606) was selected as the search set to compare against a comprehensive protein dataset. Similarly performed with other *Plasmodium* species causing malaria in humans.

PSI-BLAST was executed, and the first iteration of the search generated a results page displaying the protein superfamily of the query sequence. Two sets of aligned hits were obtained: one with an E-value below the predefined threshold (0.05) and another with a higher E-value. All hits with E-values below the threshold were selected, and three additional PSI-BLAST iterations were performed (totaling four iterations) to enhance search sensitivity and refine significant homologous sequences.

Following this iterative process, hits with the highest sensitivity and lowest E-values were identified. The search strategy was then downloaded in ASN.1 format, and the Position-Specific Scoring Matrix (PSSM) was extracted. The PSSM file was uploaded onto the Protein BLAST page under the algorithm parameters section, and PSI-BLAST was re-run to generate specific hits from the Protein Data Bank (PDB), enabling to generate exclusive regions for individual FIKK kinases of *P. falciparum*, along with the conserved FIKK kinase of other *Plasmodium* species causing malaria in humans and a homologous region among *Plasmodium* species for further analysis.

3.8.2 Computational Prediction of Linear B-Cell Epitopes in *FIKK* Kinase Proteins

Linear (continuous) B-cell epitopes were predicted from the retrieved antigenic *FIKK* kinase protein sequences using integrative computational approaches. These predictions were based on key physicochemical properties of antigenic sequences, including surface accessibility,

structural flexibility, antigenicity, and hydrophilicity. These attributes were analyzed using predictive tools available on the Immune Epitope Database (IEDB) analysis resource, v2.26 (24 Feb 2022), & v2.27 (25 May 2023) specifically Emini Surface Accessibility (Emini et al., 1985), Karplus & Schulz Flexibility (Karplus & Schulz, 1985), Kolaskar & Tongaonkar Antigenicity (Kolaskar & Tongaonkar, 1990), and Parker Hydrophilicity (Parker et al., 1986). A high-threshold range was selected to enhance the specificity of predicted epitopes.

Additionally, the Bepipred Linear Epitope Prediction 2.0 tool (Jespersen et al., 2017) was utilized to further refine the prediction and scoring of linear B-cell epitopes. The predicted epitope lengths were systematically varied between 9 and 16 amino acids to identify epitopes that met the stringent threshold criteria for potential immunogenicity.

3.8.3 Computational Prediction of MHC Class I and II Binding Epitopes for T-Cell Immunogenicity

Identifying T-cell epitopes from antigenic protein sequences is crucial for distinguishing immunogenic from non-immunogenic peptides. This distinction determines their potential to be recognized by T cells and elicit an immune response. To predict T-cell epitopes, the NetMHCI-4.0 & NetMHCII-4.1 method was employed, leveraging stabilized neural networks (SNN), weight matrices, and artificial neural networks (ANNs) to evaluate binding affinities between major histocompatibility complex (MHC) class I molecules and human leukocyte antigen (HLA) alleles (Reynisson et al., 2020).

The analysis prioritized common HLA haplotypes across diverse populations to identify potential T-cell epitopes. Binding affinities and percentile ranks were determined for key HLA class I supertypes, including HLA-A01:01, HLA-A02:01, HLA-A03:01, HLA-A24:02, HLA-B07:02, HLA-B08:01, HLA-B27:05, HLA-B40:01, HLA-B58:01, and HLA-B15:01 **(**Hoof et al., 2009). These supertypes collectively represent a significant proportion of the global human population. Previous studies have demonstrated that amino acid residues with large aromatic side chains enhance T-cell immunogenicity, particularly at critical positions P4–P6, which are essential for effective immune recognition (Sette et al., 2013). To assess the immunogenic potential of predicted epitopes, an integrated Immune Epitope Database (IEDB**)** method was used (Paul et al., 2013). This approach evaluates peptide-MHC (pMHC) complexes based on amino acid properties and their position within the peptide sequence, providing a comprehensive analysis of immunogenicity.

For MHC class II epitope prediction, T-cell epitope clusters were identified based on their ability to bind multiple HLA-DRB1 alleles. The selected alleles HLA-DRB1*03:01, HLA-*

*DRB1*07:01, HLA-DRB1*15:01*, *HLA-DRB3*01:01, HLA-DRB3*02:02*, *HLA-DRB4*01:01, and HLA-DRB5*01:01—were chosen as they represent the most prevalent HLA-DRB1 supertypes, covering over 95% of the global human population (Southwood et al., 1998). This strategy eliminates the need for exhaustive haplotype analysis while ensuring broad population coverage.

The selected FIKK kinases were analyzed to identify overlapping residues forming linear B-cell epitopic peptides, as predicted by the Emini Surface Accessibility method (Emini et al., 1985), and the Kolaskar & Tongaonkar(Kolaskar & Tongaonkar, 1990) Antigenicity method . These B-cell epitopes were further compared with predicted T-cell epitopes (Sette et al., Year) to assess their surface accessibility and antigenic properties. Overlapping residues constituting both B-cell and T-cell epitopes (MHC-I and MHC-II Immunogenicity) with the highest antigenicity were selected for incorporation into a chimeric FIKK (C-FIKK) design. To construct the chimeric protein, peptides from six selected FIKK kinase proteins were fused using appropriate peptide linkers. The recombinant gene sequence (575 base pairs) was then codon-optimized for expression in *Escherichia coli* using tools such as OPTIMIZER (Puigbò et al., 2007) and the GeneScript rare codon analysis tool to enhance expression efficiency. The optimized gene was subsequently synthesized (by Gene Script) which was cloned into the pET28a (+) expression vector for further experimental analysis.

3.9 Recombinant Expression and Purification of *Chimeric*-FIKK

3.9.1 Recombinant C-FIKK Expression: Optimization and Analysis

The expression of C-FIKK protein was optimized by testing different expression hosts, growth media, inducer concentrations, additives, and incubation temperatures. These factors were tested and adjusted at multiple time points following induction to achieve C-FIKK protein expression as follows.

3.9.2 Evaluation of C-FIKK Protein Expression in Different *E. coli* Hosts

The expression of the recombinant C-FIKK protein was assessed in various *E. coli* expression hosts. To achieve this, the recombinant plasmid (pET28a+_C-FIKK) was transformed into multiple *E. coli* strains, including BL21(DE3), BL21(DE3) pLysS, Rosetta(DE3), BL21(DE3) A1, C41, and BL21(DE3) CodonPlus. Transformants were selected on LB agar plates supplemented with 50 µg/mL kanamycin. For *E. coli* Rosetta(DE3) and *E. coli* BL21(DE3) pLysS, an additional 50 µg/mL chloramphenicol was included in the selection medium.

Following successful transformation, the selected clones were cultured in Terrific Broth (TB) and Super Broth (SB) along with LB broth at 37°C until the optical density at 600 nm (OD600) reached 0.6. Protein expression was induced by the addition of 1 mM isopropyl-β-D-thiogalacto pyranoside (IPTG). After 3.5 hours of induction, recombinant cell pellets were harvested and analyzed.

3.9.3 Effect of Temperature on C-FIKK Protein Expression

To evaluate the effect of temperature on recombinant C-FIKK protein expression, the *E. coli* BL21(DE3) CodonPlus strain was used. Following the standard expression protocol, cultures were induced with IPTG and incubated at varying temperatures (18, 21, 24, 27, 30, 33, and 37°C). For lower temperatures, incubation was extended overnight (16 hours' post-induction). The following day, cell pellets were collected and analyzed to assess protein expression levels.

3.9.4 Optimization of C-FIKK Expression Using Ethanol and Glucose in TB Media

To assess the effect of media additives on *C-FIKK* expression in *E. coli* Rosetta(DE3) and *E. coli* BL21(DE3) transformants, three variations of TB media were tested: one supplemented with 3% ethanol, another with 0.2% glucose, and a combination containing both 3% ethanol and 0.2% glucose. Each medium included the appropriate antibiotics based on the host strain. *C-FIKK* expression was induced following the standard protocol, and cell pellets were collected before and after IPTG induction for analysis.

3.9.5 Optimization of Culture Media for C-FIKK Protein Expression

Following the confirmation of C-FIKK expression in *E. coli* BL21(DE3) CodonPlus, the impact of different culture media on protein yield was assessed. To evaluate this, recombinant transformants were inoculated into three different media—Luria Bertani (LB), Super Broth (SB), and Terrific Broth (TB). Protein expression was induced, and samples were collected 3.5 hours' post-induction at 37°C for further analysis.

3.9.6 Optimization of IPTG Concentration for C-FIKK Protein Expression

To determine the optimal IPTG concentration for inducing protein expression, recombinant transformants were cultured in Terrific Broth (TB) and grown at 37°C until the optical density at 600 nm (OD600) reached 0.6. Various concentrations of IPTG (ranging from 0.1 to 2 mM) were added to induce protein expression, followed by incubation at 37°C. Induced cell pellets were collected 3.5 hours' post-induction and analyzed to assess expression levels.

3.9.7 Optimization of Induction Time for C-FIKK Protein Expression

To identify the optimal time point for maximum C-FIKK protein expression, post-induction time intervals were examined. A single colony of the recombinant *E. coli* BL21(DE3) CodonPlus strain was inoculated into Terrific Broth (TB) containing the appropriate antibiotic and incubated at 37°C. Protein expression was induced by adding 1 mM IPTG. At various time points post-induction (1, 2, 3, 4, and 5 hours), 5 mL of culture was harvested, and the collected cell pellets were analyzed to assess expression levels.

3.9.8 Large-Scale Expression and Purification of C-FIKK

Following the optimization of host strain, media, inducer concentration, and induction time, *E. coli* BL21(DE3) CodonPlus transformants were used for large-scale *C-FIKK* expression in a 500 mL culture, following the established protocol. For purification, the induced cell pellets were resuspended in lysis buffer (20 mM Tris, 300 mM NaCl, pH 7.8) and lysed via sonication (3 s pulse on, 18 s off) for 45 minutes. The lysate was centrifuged at 13,000 rpm for 15 minutes at 4°C to remove cell debris. The resulting supernatant was incubated with pre-equilibrated Nickel-Nitrilo Triacetic Acid (Ni-NTA) agarose at 4°C for 45 minutes. Unbound proteins were removed through sequential washes with wash buffer, followed by elution of the C-FIKK protein. The purified fractions were analyzed to confirm C-FIKK presence and assess the removal of non-specific proteins.

3.10 Protein Expression Analysis Using SDS-PAGE and Western Blotting

The bacterial pellets were resuspended in 200 µL of lysis buffer (20 mM Tris, 300 mM NaCl, pH 7.8, 4% SDS, 20% glycerol, 0.5% bromophenol blue, and 10% 2-mercaptoethanol) and incubated at 95°C for 10 minutes to ensure complete protein denaturation, and 30 µL of the prepared sample was loaded into each well for electrophoresis. The lysed samples were then collected, and the expression of the recombinant protein was analyzed using 15% SDS-PAGE followed by staining with Coomassie Brilliant Blue.

Western blotting was performed to confirm the expression of the 6xHis-tagged C-FIKK protein. The SDS-PAGE gel was transferred onto a nitrocellulose membrane (Hybond Amersham) using the Turbo-Blot system (Bio-Rad, USA) at 25 V for 15 minutes. The membrane was then blocked with 5% BSA for 1 hour, followed by three washes with 1X TBST and 1X TBS. It was incubated overnight at 4°C with a primary anti-His antibody (1:7,000 dilution), then washed and incubated with an HRP-conjugated secondary antibody (1: 5,000

dilution) for 45 minutes at room temperature. After final washes, the blot was visualized using chemiluminescence under UV light.

3.11 Electro Elution-Based Extraction of C-FIKK Protein

Following SDS-PAGE separation on a 15% polyacrylamide gel (1.5 mm thick), the C-FIKK protein band (~23 kDa), located between the 20 kDa and 25 kDa molecular weight markers, was precisely excised using a sterile scalpel from the wash 1 (W1) of Ni-NTA purified sample. The gel fragment was then placed in a dialysis bag along with the buffer in an electro elution chamber containing an elution buffer (25 mM Tris-HCl, pH 7.8; 192 mM glycine; 0.1% SDS). Electro elution was performed under controlled conditions at 4°C for 5 hours to facilitate the efficient extraction of the C-FIKK protein. The procedure ensured optimal recovery for subsequent analysis, following the manufacturer's protocol (Vázquez-Iglesias, L., et al., 2017).

3.12 SDS Removal and Protein Fractionation by Ammonium Sulfate Precipitation

To remove SDS and other impurities, ammonium sulfate precipitation was performed (Wingfield, P., et al., 1998). The electro eluted C-FIKK protein was fractionated between ~25–100% saturation; as lower molecular weight proteins require higher salt concentrations for precipitation. The sample was centrifuged at 9,000 g for 30 minutes at 4°C, then transferred to a beaker on a magnetic stirrer at 4°C. While stirring, 25% saturated ammonium sulfate was gradually added over an hour for complete dissolution. After centrifugation under the same conditions, the supernatant was discarded, and the pellet was resuspended in 30–50% of the original volume using 1X PBS. The solution was then transferred to dialysis tubing and dialyzed with four buffer changes, ensuring adequate space for expansion.

3.13 Protein Quantification

The concentration of the purified C-FIKK protein was determined using the Bradford assay, a colorimetric method based on the binding of Coomassie Brilliant Blue dye to protein molecules (Bradford, 1976). The absorbance of the protein-dye complex was measured at 595 nm using a spectrophotometer. A standard curve was generated using known concentrations of bovine serum albumin (BSA) (Sigma-Aldrich, Madrid, Spain) to calculate the protein concentration in the samples.

3.14 Generation of Polyclonal Antibody in Rabbit

A single 4-month-old New Zealand White rabbit was used as the animal model for generating polyclonal antibodies against the *chimeric* FIKK protein. The immunization protocol was approved by the Institutional Animal Ethics Committee and conducted in accordance with guidelines. For the primary immunization, ~450 µg of purified, heat-inactivated C-FIKK protein (in 500 µL volume) was emulsified with an equal volume of Freund's Complete Adjuvant (FCA) and administered subcutaneously into the thigh of the rabbit. One month later, a booster dose containing the same amount of antigen (~450 µg) emulsified with Freund's Incomplete Adjuvant (FIA) was administered using the same route. Blood was collected 12 days after the first booster to evaluate the antibody response. A second booster dose of identical composition was administered following the first blood collection, and a second blood sample was collected 12 days after the second booster for titre assessment. The collected blood samples were centrifuged at 2000 rpm for 10 minutes at 4°C to separate the serum. The clear serum containing anti-C-FIKK antibodies was carefully stored at −20 °C until further use. Antibody titres from the first and second boosters were determined by ELISA.

3.15 Purification of Polyclonal antibody of C-FIKK by Ammonium Sulphate Precipitation

A 100 µL sample was initially centrifuged at 9,000 × g for 30 minutes at 4°C. The pellet was transferred to a beaker containing a stir bar and placed on a magnetic stirrer at 4°C. While stirring, saturated ammonium sulphate (25%) was slowly added over one hour to ensure complete dissolution. The mixture was then transferred to a conical tube and centrifuged again at 9,000 × g for 30 minutes at 4°C. The supernatant was carefully discarded by inverting the tube. The pellet was resuspended in 30–50% of the initial volume using 1× PBS and transferred to dialysis tubing, allowing sufficient space for expansion during dialysis. The solution underwent three PBS buffer exchanges (Wingfield, P., et al., 1998). After dialysis, the solution was recovered, centrifuged, and the purified anti-C-FIKK protein was confirmed by western blotting.

3.16 Evaluation of Purified Anti-C-FIKK Polyclonal Antibody Titer

An ELISA (Enzyme-Linked Immunosorbent Assay) was performed to evaluate the titration of purified anti-C-FIKK polyclonal antibodies. A 96-well ELISA plate was coated with 200 µL per well of coating buffer containing 10 µg/mL of purified C-FIKK protein and incubated overnight at 4 °C. The next day, the wells were washed three times with phosphate-buffered

saline (PBS) and blocked with 5% Bovine Serum Albumin (BSA) in PBS for 2 hours at room temperature to prevent nonspecific binding. Following blocking, serial dilutions of rabbit antisera from 1:100 to 1: 80,000 from two separate serum batches (S1 and S2) were prepared in PBS for both the titres and added to the wells. The plates were incubated for 2 hours at room temperature. Subsequently, the wells were washed three times with PBST (PBS with 0.05% Tween-20) followed by PBS alone. For detection, goat anti-rabbit IgG HRP-conjugated secondary antibody (Cell Signaling Technology, Cat# 7074P2) was used at a 1:5000 dilutions in PBS. The antibody was added to each well and incubated for 1 hour at room temperature. After a final set of washes (PBST followed by PBS), TMB (3,3′,5,5′-Tetramethylbenzidine) substrate was added, and the enzymatic reaction was stopped by adding 50 µL of 0.1 N H_2SO_4 per well. The optical density (OD) was measured at 450 nm using a microplate reader. A cut-off value of OD ≥ 0.15 was used to define a positive result, with detectable signal maintained at dilutions up to 1: 80,000, indicating a strong antibody response.

3.17 Evaluation of Sensitivity of Anti-*Chimeric*-FIKK Polyclonal Antibody

To assess the sensitivity of purified anti-C-FIKK antibody, a dot blot was performed with varying concentrations of purified C-FIKK protein, each probed separately with the respective antibody (anti-C-FIKK). The proteins were dotted onto a nitrocellulose membrane, air-dried, and blocked with a solution of PBS (pH 7.4) containing 3% BSA for 1 hour at room temperature. After blocking, the membrane was washed three times each with 1X PBST and 1X PBS, then incubated overnight at 4°C with the respective primary antibody at a 1:5000 dilutions. Following probing, the membrane was washed three times with PBST and PBS (5 minutes each) and incubated with a goat anti-rabbit HRP-conjugated secondary antibody at a 1:6000 dilutions for 45 minutes at room temperature. Finally, a chemiluminescent substrate was applied, and the signal was captured using a Gel Doc system (Bio-Rad, USA).

3.18 Evaluation of *P. falciparum* Protein using Purified Anti-*Chimeric*-FIKK Polyclonal Antibody

The specificity of the anti-C-FIKK antibody was evaluated by probing them against various samples, including complete media, human serum, parasite culture media, and parasite culture. Samples were dotted onto a blotting membrane and blocked with a 3% BSA solution to prevent nonspecific binding. After blocking, the blots were sequentially probed with the primary antibodies (anti-C-FIKK, each at a 1:5000 dilution) and a secondary antibody (1:6000 dilution),

with thorough washing steps between each stage. The results were assessed by comparing the chemiluminescence intensities of the samples to those of purified C-FIKK as control.

3.19 Evaluation of the Selectivity of Anti-*Chimeric*-FIKK during other Organisms by Mocking Coinfection

To determine the specificity of anti-C-FIKK antibody during co-infection, parasites were detected in human blood samples contaminated with laboratory strains of various infectious agents, including *Bacillus vallismortis*, *Bacillus subtilis*, *Staphylococcus aureus*, *Listeria monocytogenes*, *Bacillus tequilensis*, *Lactobacillus*, *Rhodococcus opacus*, *E. coli* (BL21(DE3), BL21(DE3) CodonPlus, Rosetta(DE3), DH5α), yeast (*Aspergillus terreus*, *Neurospora crassa*, *Saccharomyces cerevisiae*, *Pichia pastoris*), viruses (Influenza virus, Newcastle disease virus, Japanese encephalitis virus, Duck enteritis virus), and algae (*Scenedesmus*). Human blood with 0.5% parasitemia was contaminated with varying concentrations of these infectious agents to mimic co-infection conditions. As controls, human blood without malaria parasites but containing infectious agents served as the negative control, while blood with malaria parasites alone was the positive control. All mock co-infection samples and controls were processed and blotted onto a nitrocellulose membrane. The blotting procedure and subsequent steps were performed following standard protocols to evaluate antibody specificity.

3.20 REFERENCES

1. Sharma, S., & Pandey, L. M. (2020). Production of biosurfactant by Bacillus subtilis RSL-2 isolated from sludge and biosurfactant mediated degradation of oil. *Bioresource Technology*, *307*, 123261.
2. Datta, P., Tiwari, P., & Pandey, L. M. (2020). Oil washing proficiency of biosurfactant produced by isolated Bacillus tequilensis MK 729017 from Assam reservoir soil. *Journal of Petroleum Science and Engineering*, *195*, 107612.
3. Kalendar, R., *A guide to using FASTPCR software for PCR, in silico PCR, and oligonucleotide analysis.* PCR Primer Design, 2022: p. 223-243.

4. Trivedi, V., et al., *Clotrimazole inhibits hemoperoxidase of Plasmodium falciparum and induces oxidative stress: proposed antimalarial mechanism of clotrimazole.* Journal of Biological Chemistry, 2005. **280**(50): p. 41129-41136.

5. Chan, S., *I. DNA isolation from Plasmodium falciparum.* METHODS IN MALARIA RESEARCH, 2013: p. 259.
6. Bharatha, A., S. Suguna, and N.D.S.K.R. Kunkulol, *Genomic DNA isolation from human whole blood samples by non enzymatic salting out method.* 2014.
7. Bhardwaj, B., et al., *An efficient method for DNA extraction from cyanobacteria isolated from hypersaline and marine environments.* Journal of Phycology, 2019. **55**(3): p. 733-737.
8. Pattern, R., *RNA isolation and reverse transcription protocol: Cells in culture.* Boston: Abcam, 2019.
9. Lõoke, M., K. Kristjuhan, and A. Kristjuhan, *Extraction of genomic DNA from yeasts for PCR-based applications.* Biotechniques, 2011. **50**(5): p. 325-328.
10. Mahesh, R., V.R. Naira, and S.K. Maiti, *Concomitant production of fatty acid methyl ester (biodiesel) and exopolysaccharides using efficient harvesting technology in flat panel photobioreactor with special sparging system via Scenedesmus abundans.* Bioresource technology, 2019. **278**: p. 231-241.
11. Keluskar, P., et al., *Plasmodium falciparum and Plasmodium vivax specific lactate dehydrogenase: genetic polymorphism study from Indian isolates.* Infection, Genetics and Evolution, 2014. **26**: p. 313-322.

12. Alvarez-Jarreta *et al.*, VEuPathDB: the eukaryotic pathogen, vector and host bioinformatics resource center in 2023, *Nucleic Acids Research*, Nucleic Acids Research, Volume 52, Issue D1, 5 January 2024, Pages D808–D816 https://doi.org/10.1093/nar/gkad1003

13. Altschul, S. F., Madden, T. L., Schäffer, A. A., Zhang, J., Zhang, Z., Miller, W., & Lipman, D. J. (1997). Gapped BLAST and PSI-BLAST: a new generation of protein database search programs. *Nucleic acids research*, *25*(17), 3389-3402.

14. Jespersen, M.C., et al., *BepiPred-2.0: improving sequence-based B-cell epitope prediction using conformational epitopes.* Nucleic acids research, 2017. **45**(W1): p. W24-W29.

15. Parker, J., D. Guo, and R. Hodges, *New hydrophilicity scale derived from high-performance liquid chromatography peptide retention data: correlation of predicted surface residues with antigenicity and X-ray-derived accessible sites.* Biochemistry, 1986. **25**(19): p. 5425-5432.

16. Karplus, P. and G. Schulz, *Prediction of chain flexibility in proteins: a tool for the selection of peptide antigens.* Naturwissenschaften, 1985. **72**(4): p. 212-213.

17. Emini, E.A., et al., *Induction of hepatitis A virus-neutralizing antibody by a virus-specific synthetic peptide.* Journal of virology, 1985. **55**(3): p. 836-839.

18. Karosiene, E., et al., *NetMHCcons: a consensus method for the major histocompatibility complex class I predictions.* Immunogenetics, 2012. **64**: p. 177-186.

19. Nielsen, M., C. Lundegaard, and O. Lund, *Prediction of MHC class II binding affinity using SMM-align, a novel stabilization matrix alignment method.* BMC bioinformatics, 2007. **8**: p. 1-12.

20. Kolaskar, A.S. and P.C. Tongaonkar, *A semi-empirical method for prediction of antigenic determinants on protein antigens.* FEBS letters, 1990. **276**(1-2): p. 172-174.

21. Puigbo, P., Guzmán, E., Romeu, A., & Garcia-Vallvé, S. (2007). OPTIMIZER: a web server for optimizing the codon usage of DNA sequences. *Nucleic acids research*, *35*(suppl_2), W126-W131.

22. Vázquez-Iglesias, L., et al., *A simple electroelution method for rapid protein purification: isolation and antibody production of alpha toxin from Clostridium septicum.* PeerJ, 2017. **5**: p. e3407.

23. Wingfield, P., *Protein precipitation using ammonium sulfate.* Current protocols in protein science, 1998. **13**(1): p. A. 3F. 1-A. 3F. 8.

24. Singh, G., et al., *Development of an indirect competitive ELISA for analysis of alternariol in bread and bran samples.* Food analytical methods, 2018. **11**: p. 1444-1450.

Annexure I

Preparation of Reagents and Buffers

i. **50X TAE Buffer**
0.50 M EDTA, 2 M Tris-HCl, and 1 M glacial acetic acid, pH 8.5

ii. **TKM1 Buffer for RBC lysis**
10 mM Tris-HCl, 10 mM NaCl, 10 mM MgCl2, and 2 mM EDTA, pH 7.6

iii. **TKM2 Buffer for WBC lysis**
10 mM Tris-HCl, 400 mM NaCl, 10 mM MgCl2, and 2 mM EDTA, pH 7.6

iv. **Reagents for freezing malaria parasite (*Pf3D7* strain)**
28 % glycerol, 3 % sorbitol, 0.65 % NaCl, and complete media (CM)

v. **Reagents for malaria parasite revival (*Pf3D7* strain)**
10 % NaCl, 1.6 % / 1.8 % NaCl, 0.9 % NaCl +0.2 % glucose

vi. **Reaction mixture for PCR (10 µL)**

S. No	Component	Quantity
1	Nuclease free Water	2.6-3.6 µL
2	Master Mix (2X)	5 µL
3	Forward primer	0.2 µL (10 Pico moles)
4	Reverse primer	0.2 µL (10 Pico moles)
5	Template	1-2 µL (10 fg to 100 ng)

vii. **JSB I Staining**
Per 500 mL, Medicinal methylene blue: 0.5 grams, 3 mL of 1 % H2SO4, and Na2HPO4.2H2O: 3.5 grams

viii. **JSB II Staining**
Per 500 mL, 1 gram of yellow eosin

ix. **Incomplete media (ICM) for malaria parasite (*Pf3D7* strain)**
Per 500 mL, RPMI1640: 8.2 grams, glucose: 1 gram, gentamycin (40 mg/mL): 500 µL, Hypoxanthine (0.1M): 500 µL

x. **Complete media (CM) for malaria parasite (*Pf3D7* strain)**
Per 10 mL, 8.6 mL of ICM, 1 mL of 5 % Albumax, and 0.4 mL of 5% Sodium Bicarbonate

xi. **Lysis buffer for malaria parasite (*Pf3D7* strain) DNA isolation**
40 mM Tris-HCl, 80 mM EDTA, and 2 % SDS (w/v), pH 8.0

xii. **DNA Elution buffer**
10 mM Tris-HCl, and 1 mM EDTA, pH 8.3

xiii. **Extraction buffer for DNA isolation from algae**
200 mM Tris-HCl, 25 mM EDTA, 400 mM LiCl, and 1 % SDS (w/v), pH 8.0

xiv. **DNA Gel Loading Dye**
10% w/v SDS, 500mM EDTA, 50% Glycerol, and 0.2% bromophenol blue dye

xv. **Reagent for lysing RBCs during malaria parasite (*Pf3D7* strain) DNA isolation**
A stock of 5 % Saponin

xvi. **Reagent for precipitating malaria parasite (*Pf3D7* strain) DNA**
3 M Sodium Acetate and absolute ethanol

xvii. **Reagent for digesting proteins during malaria parasite (*Pf3D7* strain) DNA isolation**
20 mg/mL Proteinase K stock solution

xviii. **Reagent for digesting RNA during malaria parasite (*Pf3D7* strain) DNA isolation**
20 mg/mL RNAse A stock solution

xix. **Lysis buffer for DNA isolation from bacteria**
50 mM Tris-HCl, 25 mM EDTA, 250 U/mL lysozyme, and 0.5 % Tween 20, pH 8.0

xx. **Reagent for separating biomolecules (like DNA and RNA) through gel**
2 % agarose in 1X-TAE buffer

xxi. **Reagent for visualizing biomolecules (like DNA and RNA) through gel**
10 mg/mL stock of ethidium bromide (EtBr)

Chapter 4

FIKK-Based Molecular Detection of *Plasmodium falciparum*

*The contents of this chapter are published as **Prasad, M. R., & Trivedi, V.** (2024). **Molecular Investigation of FIKK Kinase Family to Develop PCR-Based Diagnosis of *Plasmodium falciparum*.** *Molecular Biotechnology*, 1-17.

SUMMARY

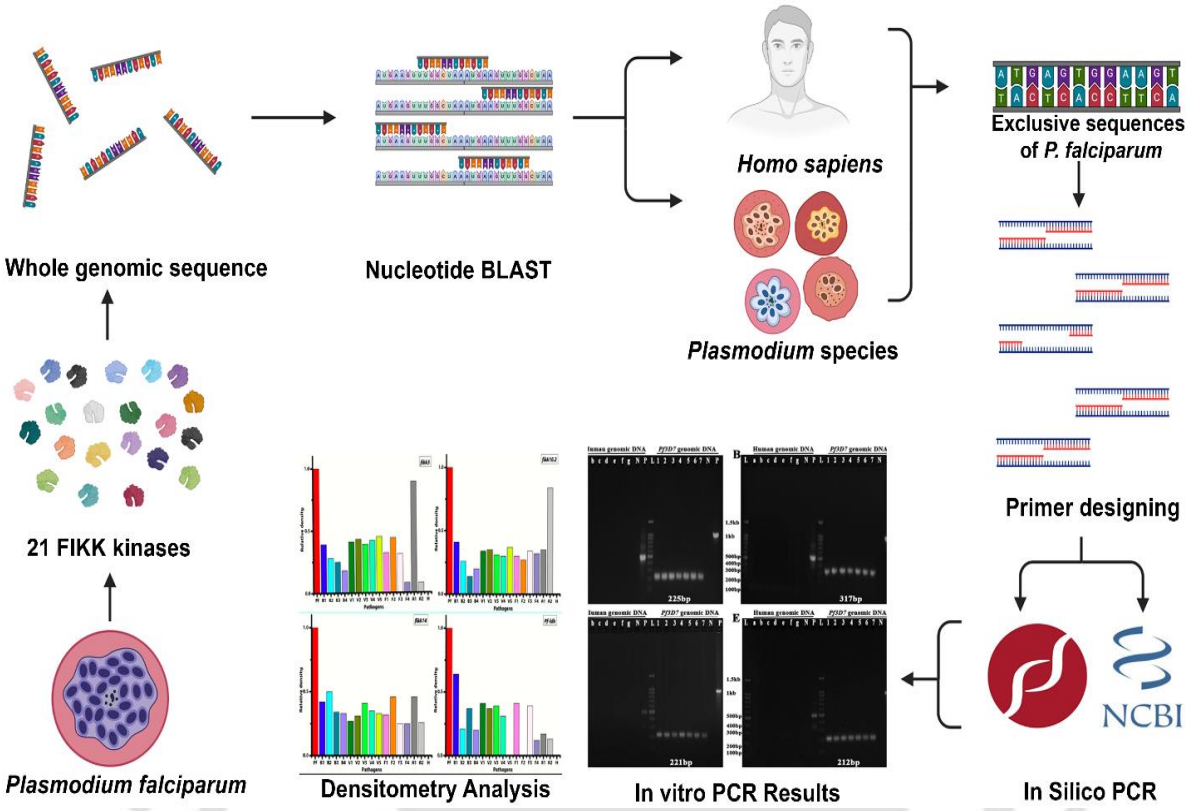

Figure: The sequential workflow in the development of a FIKK-based molecular detection of *P. falciparum.*

Accurate malaria diagnosis is crucial for effective disease management as different *Plasmodium* species require specific treatment regimens. Current detection methods have limitations related to sensitivity and specificity. This is mainly due to employing similar targets such as 18S rRNA, *Pf-ldh, Pf-hrp-2,* and aldolase with significant homology to human counterparts. Targeting *Plasmodium fikk* kinases, that are unique to *P. falciparum* offers a novel approach for developing potential biomarkers. We have identified exclusive regions of *fikk* kinases using in-silico PCR and later validated our findings using in-vitro PCR. We observed exceptional sensitivity with our designed primers of the targeted *fikk* kinases, with the detection limit going as low as 10^{-5} ng level of parasite DNA and 0.0003 % parasitemia. The shortlisted primers also selectively identified *P. falciparum* in the presence of *Plasmodium vivax* or several other bacterial, viral, & fungal pathogens. Detection of mock patient samples indicates that the *fikk*-based PCR diagnosis is giving accurate results, and it is much better than the existing method. Thus, we show that the *fikk* kinases from *P. falciparum* are excellent targets for developing novel biomarkers with high sensitivity and specificity.

4.1 INTRODUCTION

Malaria carries a significant disease burden affecting over 200 million people, resulting in over half a million deaths each year [1]. The disease is caused by obligate intracellular parasites from the genus *Plasmodium*, transmitted to humans through the bite of infected female Anopheles mosquitoes [2]. The five most common species that infect humans are *Plasmodium falciparum*, *Plasmodium vivax*, *Plasmodium ovale*, *Plasmodium malariae*, & *Plasmodium knowlesi*. The *P. falciparum* accounts for more than 90% of morbidity and mortality, particularly in children below five years [3]. Currently, there are different diagnostic tests available to detect malaria parasites, but they have several drawbacks. The current malaria detection systems like microscopy, Rapid Diagnostic Tests (RDTs), Polymerase Chain Reaction (PCR), Loop-Mediated Isothermal *Amplification* (LAMP), and serology tests face significant limitations related to sensitivity, specificity, cost, complexity, and infrastructure requirements [4]. Microscopy, the 'Gold Standard' for examining blood smears to detect malaria parasites, suffers from significant drawbacks today. It exhibits low sensitivity, often missing low-density infections and resulting in false negatives. The method depends on technicians' skill, with varying accuracy based on their expertise, leading to inconsistent results. Microscopy also struggles with detecting mixed *Plasmodium* species infections, identifying only 5% compared to 15% by RDTs and 20% by PCR in a study conducted in conflict-affected regions [5].

The RDTs for malaria diagnosis, such as First Response Malaria Antigen, *Plasmodium falciparum* antigen histidine-rich protein 2 (HRP2) [6] / *Plasmodium* lactate dehydrogenase (pLDH) [7], Syphilis Duo (SD) and Bioline Malaria Antigen *Pf* / pLDH [8], and BinaxNOW Malaria Test [9], vary in their strengths and limitations compared to Polymerase Chain Reaction [10, 11]. First Response and SD Bioline RDTs have drawbacks, including limited ability to differentiate current infection from past exposure [12], potentially leading to false positives, and reduced sensitivity for detecting low parasite density infections or non-*P. falciparum* species [11]. The emergence of mutations, particularly deletions in the *hrp2* gene [13], poses a significant challenge in malaria diagnosis using RDTs of HRP2, a protein produced by *P. falciparum* targeted by many RDTs to detect malaria infections. However, mutations or deletions in the *hrp2* gene can lead to false-negative results, where the parasite is present but goes undetected [13]. This issue has been documented in various regions, particularly in areas with high malaria transmission rates and extensive RDT use. A notable study investigated the prevalence of *pfhrp2* gene deletions in *P. falciparum* strains from Honduras, revealing a significant proportion of such deletions [14]. This genetic variation

compromises the sensitivity and reliability of HRP2-based RDTs, highlighting the need for continuous surveillance and quality control of diagnostic tools. BinaxNOW also faces challenges with sensitivity, particularly in low-transmission areas, and may not detect all *Plasmodium* species accurately [15]. Accurate diagnostic tools like PCR are crucial in malaria diagnosis due to their high sensitivity and specificity, allowing detection of low levels of parasites in the blood. PCR can identify multiple *Plasmodium* species in a single sample, enabling appropriate treatment, and can detect malaria parasites before symptoms appear, facilitating early intervention [16]. Additionally, PCR helps monitor drug resistance by identifying genetic markers and guiding treatment decisions and public health strategies. It also aids in epidemiological studies by providing precise data on malaria prevalence and transmission [17]. PCR detected malaria in 95% of cases, while microscopy and RDTs detected 75% and 80%, respectively [18]. It also identified mixed infections in 20% of cases missed by other methods and detected asymptomatic infections, allowing early treatment and reducing transmission. The study concludes that integrating PCR into malaria diagnosis, especially in endemic areas, can significantly improve patient outcomes and support malaria control efforts.

In the case of the malaria parasite, FIKK (Phe-Ile-Lys-Lys) kinases are a unique family of protein kinases predominantly found exclusively within the Apicomplexan phylum, particularly in the malaria-causing parasite *P. falciparum*. Unlike other kinases, they exhibit a distinct structural domain characterized by a conserved C-terminal motif and are notably absent in humans, making them highly specific to the parasite. This uniqueness provides a selective advantage for targeting in both diagnostic and therapeutic applications [19]. Functionally, *FIKK* kinases are involved in modifying host red blood cells (RBCs) after infection. These kinases are strategically localized to various sites within infected RBCs, including the erythrocyte membrane and Maurer's clefts structures associated with protein trafficking. Through phosphorylation of host and parasite proteins, *FIKK* kinases contribute to antigenic variation, cytoadhesion, and remodelling of the RBC surface, enabling immune evasion and prolonged survival of the parasite within the host [20-24]. So, the FIKKs in *Plasmodium falciparum* have a specific group of 21 kinase enzymes that have no homology with the human kinases with highly antigenic features and could be explored for developing a potential biomarker. In the present study, we explored the utility of primers designed against different FIKK kinases to detect malaria parasites using PCR. In-silico PCR allowed us to select FIKK primers, and they were found to give no amplification with human DNA, as well as genomic DNA from different bacterial, fungal, viral and algal species. In addition, these organisms are not interfering into detection of *P. falciparum* DNA or are present in the culture. The PCR

detection using FIKK primers is very sensitive, and it is very accurate to detect mock patient samples. Hence, early detection of the parasite and species-specific diagnosis plays a major role in the control and elimination of malaria.

4.2 EXPERIMENTAL PROCEDURES

4.2.1 Materials and Strains

The various materials and reagents used in this study are comprehensively detailed in the section 3.1, with specific strains employed for the study as listed in Table 3.1 of the same section of chapter 3: Experimental Procedures.

4.2.2 In-silico PCR

The in-silico PCR was performed as detailed in the section 3.2 of chapter 3: Experimental Procedures.

4.2.3 *Plasmodium falciparum 3D7* strain culture

The *Plasmodium falciparum 3D7* strain was cultured as described in the section 3.3 of chapter 3: Experimental Procedures.

4.2.4 Isolation of genomic DNA from *Plasmodium falciparum*, *Plasmodium vivax*, *Homo sapiens and other organisms*

The genomic DNA from the cultured flask of *Plasmodium falciparum 3D7* strain, humans, bacterial species (*Acinetobacter baylyi*, *Rhodococcus opacus*, *Bacillus megaterium*, & *E. coli-DH5α*), algae (*Scenedesmus*), fungi (*Aspergillus terreus*, *Pichia pastoris*, & *Saccharomyces cerevisiae*) and virus (Herpes simplex virus, Duck enteritis virus, Influenza virus, Japanese encephalitis, & Newcastle disease virus) were isolated as described in the section 3.4 of chapter 3: Experimental Procedures.

4.2.5 Polymerase Chain Reaction (PCR)

The PCR was carried out as detailed in the section 3.5 of chapter 3: Experimental Procedures.

4.2.6 Evaluation of analytical sensitivity and specificity of the *fikk* kinase-based PCR assay

The procedure for evaluating the analytical sensitivity and specificity was detailed in the section 3.6 of chapter 3: Experimental Procedures

4.2.7 Densitometry and Statistical Analysis

The intensity of PCR product present in agarose gel was densitometrically analysed as detailed in the section 3.7 of chapter 3: Experimental Procedures

4.3 RESULTS

4.3.1 FIKK kinases have the potential to develop into a diagnostic marker for malaria detection

FIKK kinases are exclusive protein kinases present in the *Plasmodium* species with no homology to the existing proteins in the host [19, 20]. A total of 21 FIKK kinases are present in the *P. falciparum* and we explored the suitability of these molecules for diagnosis of malaria especially detection of *P. falciparum* in biological samples. In the designed study strategy (**Figure 4.1**), we have used genomic sequence to identify the region of nucleotide sequence exclusive to the *fikk* kinases. We have designed primers to amplify the gene and screened these primers using *Homo sapiens* genome. The selected primer set was used to detect *P. falciparum* in an in-vitro PCR (**Figure4.2**).

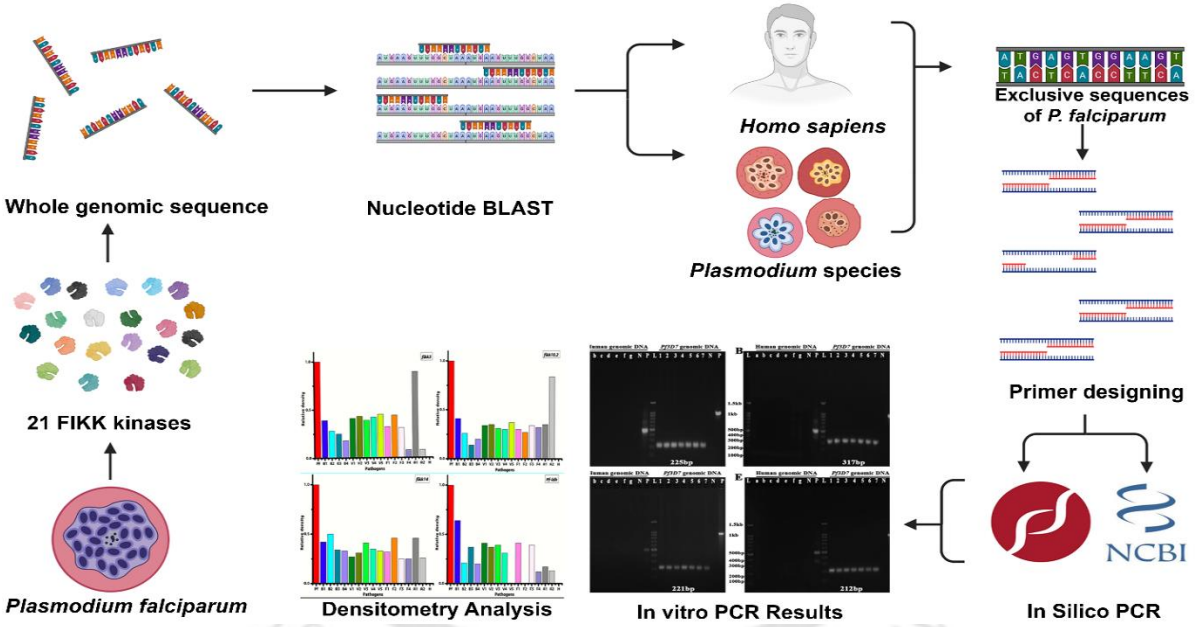

Figure 4.1: Research design provides a visual representation of the sequential steps involved in the research and development process, from gene selection to the final validation in developing PCR-based malaria diagnosis.

The nucleotide sequence of individual *fikk* kinase was retrieved from the *Plasmodium* genome and then these sequence was blasted into Human genome to identify nucleotide sequence exclusive to the *Plasmodium* species. Similar analysis was done to identify the nucleotide sequence specific to the individual *Plasmodium* species like *P. vivax, P. ovale, P. malariae* and *P. knowlesi*. Based on the blast analysis, a total of 6 *fikk* kinases (*fikk 3, fikk4.2, fikk 8, fikk 10.2, fikk 12* and *fikk 14*) were found suitable for further analysis. A total of 36 pairs

of primers were designed from the *fikk 3* nucleotide sequence. These primers are giving amplified product in the range of 200-300 bp in *P. falciparum* whereas 21 primer sets were giving no amplification in human host (**Table S1 in Annexure II**).

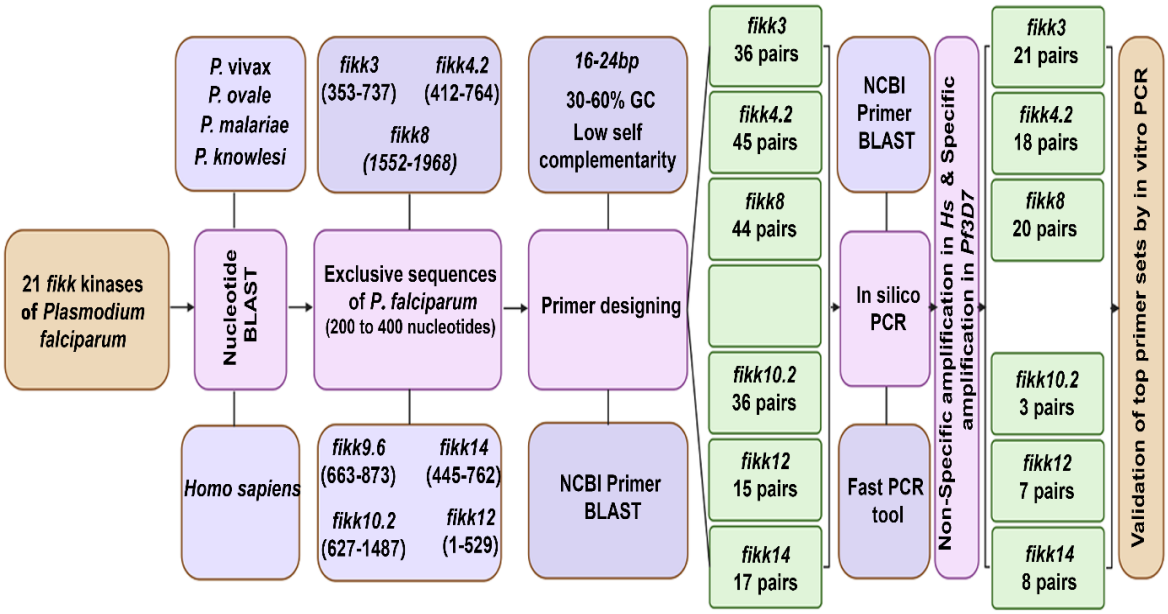

Figure 4.2: Flowchart of the in-silico analysis and primer design for *fikk* kinases that illustrates the comprehensive in silico analysis and rigorous selection process undertaken to identify highly specific primers for the accurate detection of *P. falciparum*.

Similarly, we performed primer analysis for *fikk 4.2* (using 45 primer pairs), *fikk 8* (using 44 primer pairs), *fikk 10.2* (using 36 primer pairs), *fikk 12* (using 15 primer pairs) and *fikk 14* (using 17 primer pairs). The result of primer screening was presented in the supplementary **Table S2-S6 in Annexure II**. Based on the screening, 21 primer pairs from *fikk 3*, 24 primer pairs from *fikk 4.2*, 20 primer pairs from *fikk 8*, 3 primer pairs from *fikk 10.2*, 7 primer pairs from *fikk 12* and 8 primer pairs from *fikk 14* were found suitable based on the insilico PCR (**Figure 4.2**). Further analysis of primer sequence based on GC content, primer dimer formation, and thorough comparison of the target sequence with the database of other *Plasmodium* species causing malaria in humans, we have selected 6 primer sets from *fikk 3, fikk 4.2, fikk 8, fikk 10.2* and *fikk 14* (**Table 4.1**) that are exclusively targeting the *fikks* of *P. falciparum*.

4.3.2 Screening and selection of primers for *Plasmodium falciparum* detection

First we tested the suitability of designed and selected primers for malaria diagnosis by testing the ability of these primers to give no amplification with human genome and give desirable

amplicon with *P. falciparum* genome (**Table 4.1**). The gradient PCR with annealing temperature in the range of 50-56ºC was used and genomic DNA isolated from the *P. falciparum 3D7*strain or human genomic DNA isolated from lymphocytes was used as template.

Table 4.1: Shortlisted primer sequences specific to *Plasmodium falciparum*.

S. No	Primer Name	Primers (5'->3')	Amplicon Size (bp)	
			Plasmodium falciparum	***Other Plasmodium species causing malaria in humans***
1	S1_*f3*_Set9_FP S1_*f3*_Set9_RP	TACAAGCGTCTCATCATATCAA CGTTTGTTCTTACTCCATTTATCCT	225	NO
2	S2_*f4.2*_Set48_FP S2_*f4.2*_Set48_RP	GTTTTAGGGGTAAAAGTGCGT CTCCCCCTGATCAATTAAACCT	317	NO
3	S3_*f8*_Set97_FP S3_*f8*_Set97_RP	GATGGAAGAAGAAAAATACCGTG CATATCATTTTGACCTGCTCC	277	NO
4	S4_*f10.2*_Set152_FP S4_*f10.2*_Set152_RP	GACGGAGATCAAGAAAATATTACA TCTTCGCTACCATACCCATT	221	NO
5	S5_*f12*_Set167_FP S5_*f12*_Set167_RP	GCATCACGTGAACTCTGATA TACAAGTACCTTCTACACTCTC	212	NO
6	S6_*f14*_Set185_FP S6_*f14*_Set185_RP	TCAAGATATTCGAGGGGTCT GTACTTCTATTCGTACTTTTCTGT	203	NO
7	PC_Pf-ldh_FP PC_Pf-ldh_RP	ATGGCACCAAAAGCAAAAATC TTAAGCTAATGCCTTCATTCTC	951	-
8	PC_Humans_FP PC_Humans_RP	TGTAAAACGACGGCCAGT CAGGAAACAGCTATGACC	-	

The *Pf-ldh* serve as positive control for *P. falciparum 3D7* whereas human-specific glyceraldehyde 3-phosphate dehydrogenase (HuGAPDH) serve as positive control for human. Gradient PCR with primers for *fikk 3* (S1_*f3*_Set9_FP/S1_*f3*_Set9_RP) gives amplified product of size ~225bp (Lanes 8: 56.0 ºC, Lanes 9: 55.5 ºC, Lanes 10: 54.8 ºC, Lanes 11: 53.7 ºC, Lanes 12: 52.3 ºC, Lanes 13: 51.1 ºC, Lanes 14: 50.4 ºC) with *P. falciparum* genome whereas no amplified product (Lanes 1: 56.0 ºC, Lanes 2: 55.5 ºC, Lanes 3: 54.8 ºC, Lanes 4: 53.7 ºC, Lanes 5: 52.3 ºC, Lanes 6: 51.1 ºC, Lanes 7: 50.4 ºC) was observed with Human genome (**Figure 4.3-A**). Negative PCR with no primer leads to no amplification product clearly indicate no contamination in the reaction mixture (Lane N). Similarly, gradient PCR with other primer sets (**Table 4.3**) were conducted and we found that specific amplification was observed with *P. falciparum* genomic DNA but no amplification was seen in human genomic DNA (**Figure 4.3-B to F**). The PCR using primer for HuGAPDH or *Pf-ldh* gives desirable amplified product indicate that the PCR from respective template is possible.

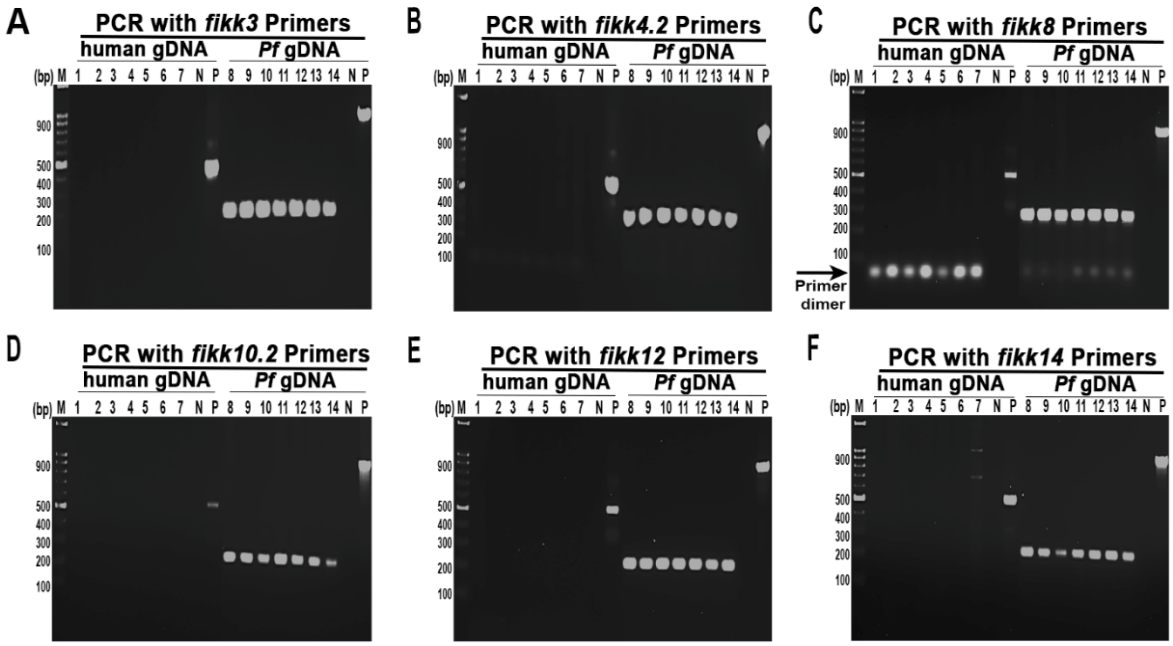

Figure 4.3: The primers designed for specific amplification from the *Plasmodium falciparum* genome do not show any amplification with host DNA. Gradient PCR (50 to 56ºC) was set up with 6 primers using *Pf* or human genomic DNA as templates. No non-specific amplification was seen with human genomic DNA from Lane 1 to 7, and specific amplification was observed with *Pf* genomic DNA from Lane 8 to 14 using the primers designed for **(A)** *fikk 3*, **(B)** *fikk 4.2*, **(C)** *fikk 8*, **(D)** *fikk 10.2*, **(E)** *fikk 12* & **(F)** *fikk 14.* Lane N and P in each panel denote negative (no primers) and positive (huGAPDH for humans and *Pf-ldh* primers for *Pf*) controls, respectively and 'M' as 100 bp DNA marker.

4.3.3 Shortlisted primers are highly selective in detecting *Plasmodium falciparum* in presence of other organisms.

Malaria co-infection with other infectious organisms belonging to different classes like fungi, viruses and bacterial species is reported [34-36]. Since designed primers were good to recognize *P. falciparum* in presence of human genomic DNA, we further explored the utility of these primers to detect *P. falciparum* in presence of other infectious organisms. First we tested the amplification from different pathogens alone. Genomic DNA or cDNA (in case of RNA virus) was isolated from the pathogens and used as a template in the PCR reaction containing the selected *fikk* primers. PCR with bacterial species (*Acinetobacter baylyi* as B1, *Rhodococcus opacus* as B2, *Bacillus megaterium* as B3, & *E. coli-DH5α* as B4), Viral species (Herpes simplex virus as V1, Duck enteritis virus as V2, Influenza virus as V3, Japanese encephalitis as V4, & Newcastle disease virus as V5), Fungal species (*Aspergillus terreus* as

F1, *Pichia pastoris* as F2, & *Saccharomyces cerevisiae* as F3), and algae (*Scenedesmus* as A1) using *fikk* 3 primers (S1_*f3*_Set9_FP/S1_*f3*_Set9_RP) gives no amplification except primer dimer (**Figure 4.4, Panel a**, lanes B1-B4, V1-V5, F1-F3 and Algae). *P. falciparum* genome was used as positive control and it gives amplified product at ~225bp (**Figure 4.4, Panel a**, lane PC).

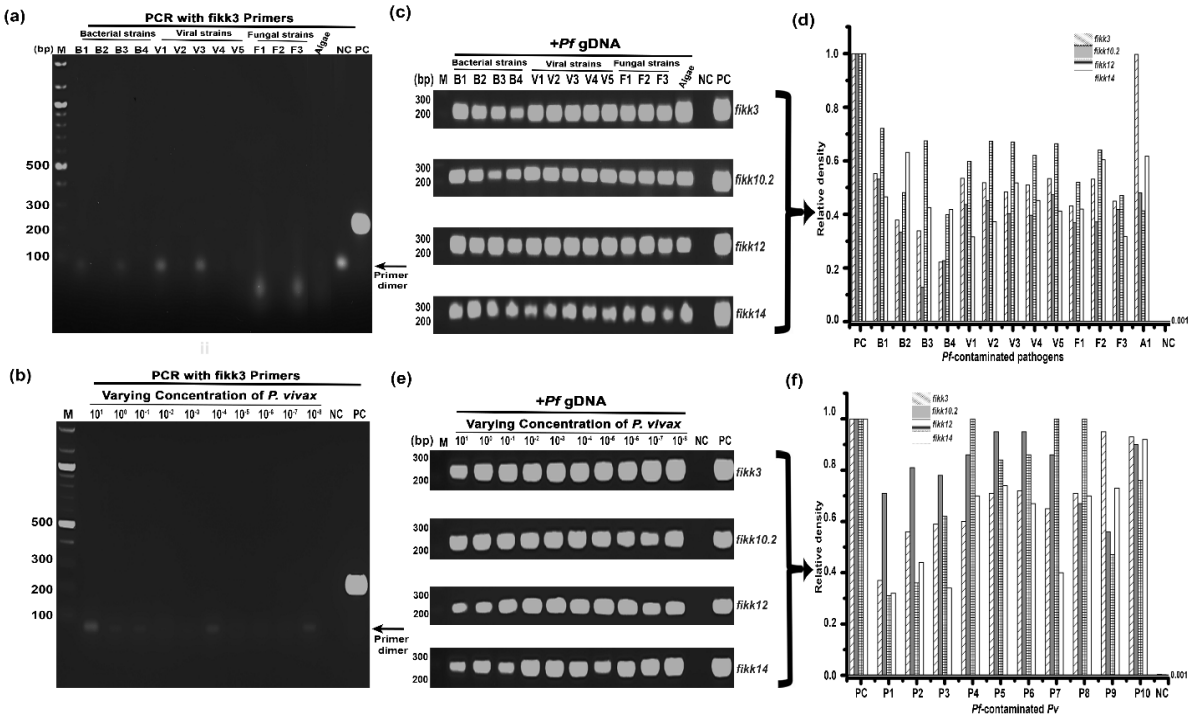

Figure 4.4: Shortlisted *fikk* primers specifically detect *Plasmodium falciparum* DNA at the molecular level. (a) PCR reactions were set up with *fikk 3* primer (S1_f3_Set9_FP/S1_f3_Set9_RP) and template DNA from different bacterial species, fungal species, viral species, and algae. Amplified product was loaded into the agarose gel from different PCR reactions where template DNA was used as follows: *Acinetobacter baylyi* DNA in lane B1, *Rhodococcus opacus* DNA in lane B2, *Bacillus megaterium* DNA in lane B3, & *E. coli-DH5α* DNA in lane B4, DNA/cDNA from Herpes simplex virus in lane V1, Duck enteritis virus in lane V2, Influenza virus in lane V3, Japanese encephalitis virus in lane V4, & Newcastle disease virus in lane V5, genomic DNA from fungal species as *Aspergillus terreus* in lane F1, *Pichia pastoris* in lane F2, & *Saccharomyces cerevisiae* in lane F3 & genomic DNA from Algae, *Scenedesmus* in lane Algae. **(b)** PCR reactions were set up with *fikk 3* primer (S1_f3_Set9_FP/S1_f3_Set9_RP), and *Plasmodium vivax* gDNA (varying concentration from 10 ng to 10 ag) as a template, and the amplified product were loaded into the agarose gel. **(c)** Shortlisted primers gives amplified product from *P. falciparum* genome in the presence of DNA from other pathogens. PCR reactions were setup with *fikk 3 / fikk 10.2 / fikk 12 / fikk 14*

primers and *P. falciparum* genome mixed with DNA from other organisms in the ratio of 1:100 and resulting mixture was used as template DNA. Amplified product was loaded into the agarose gel from different PCR reactions into different lanes in the same manner as described in panel **"a"**. **(d)** Densiometeric analysis of reaction product from the PCR reaction in panel "c". **(e)** PCR reactions were setup with *fikk 3 / fikk 10.2 / fikk 12 / fikk 14* primers and *P. falciparum* genome mixed with *P. vivax* gDNA (varying concentration from 10 ng to 10 ag) as template DNA and amplified product was loaded into the agarose gel. **(f)** Densitometric analysis of reaction product from the PCR reaction in panel "e".

Similarly, we have tested the utility of remaining primer sets and all these primer sets are not giving any amplification with these organisms (**Supplementary Figure S1 in Annexure I**). Next, we tested the specificity of *fikk 3* primers (S1_*f3*_Set9_FP/S1_*f3*_Set9_RP) to amplify *P. vivax* DNA, *fikk 3* primers (S1_*f3*_Set9_FP/S1_*f3*_Set9_RP) gives no amplification except primer dimer (**Figure 4.4, panel b**). Next, we tested the impact of DNA from other pathogens on the amplification from the *P. falciparum* genome using *fikk* primers. We have contaminated 1 ng *P. falciparum* with 100 ng of DNA from other pathogens and then PCR was performed. As expected, there was no interference of DNA from the other pathogens to get desirable amplified product with primers from *fikk* kinases (**Figure 4.4, panel c**). Densitometric measurement of the amplified product indicates a little or no reduction of amplification in the presence of DNA from other pathogens, and amplification was found good enough to detect *P. falciparum* in the presence of these pathogens (**Figure 4.4, Panel d**). Even with contamination of 1ng *P. falciparum* genome with varying concentration (10 nanogram to 10 attogram) of *P. vivax*, there was no interference of DNA from other *Plasmodium* species (**Figure 4.4, panel e, f**).

Most commonly during mixture of infections (like malaria with viral infection) the symptoms are indistinguishable, and the diagnostic results are often false positive or false negative [34-36]. It is important to mimic these complex disease conditions and test the robustness of *fikk* based PCR detection of malaria parasite. Malaria parasite culture was mixed with infectious organisms like different bacterial species (*Acinetobacter baylyi* as B1, *Rhodococcus opacus* as B2, *Bacillus megaterium* as B3, & *E. coli-DH5α* as B4), Viral infected mammalian cells (Herpes simplex virus as V1, Duck enteritis virus as V2, Influenza virus as V3, Japanese encephalitis as V4, & Newcastle disease virus as V5), Fungal species (*Aspergillus terreus* as F1, *Pichia pastoris* as F2, & *Saccharomyces cerevisiae* as F3) and algae

(*Scenedesmus* as A1). PCR using *fikk* 3 primers (S1_*f3*_Set9_FP/S1_*f3*_Set9_RP) with different bacterial species (*Acinetobacter baylyi* as B1, *Rhodococcus opacus* as B2, *Bacillus megaterium* as B3, & *E. coli-DH5α* as B4), Viral infected mammalian cells (Herpes simplex virus as V1, Duck enteritis virus as V2, Influenza virus as V3, Japanese encephalitis as V4, & Newcastle disease virus as V5), Fungal species (*Aspergillus terreus* as F1, *Pichia pastoris* as F2, & *Saccharomyces cerevisiae* as F3) and algae (*Scenedesmus* as A1) alone does not give any amplification except primer dimer (**Figure 4.5, panel a**).

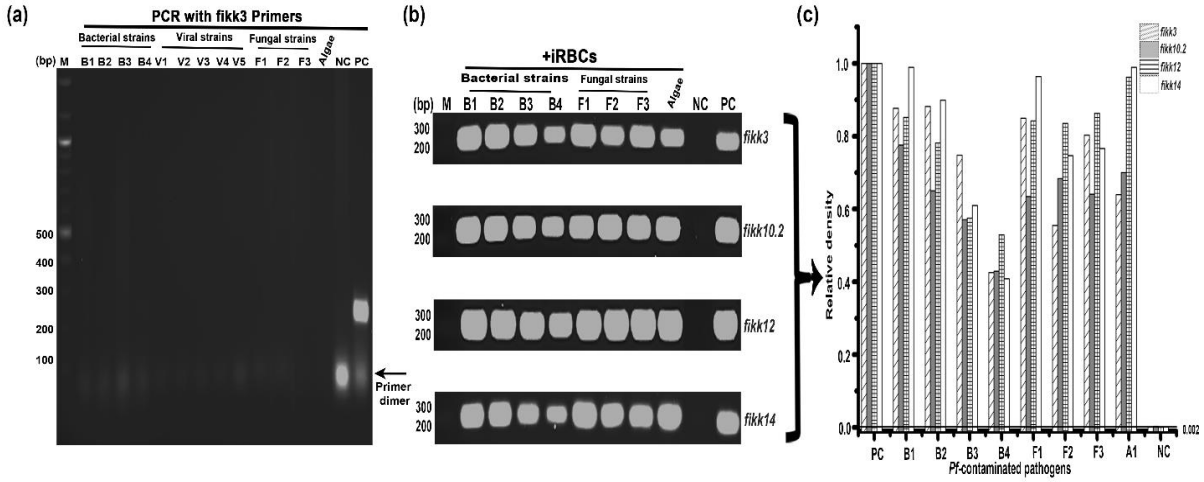

Figure 4.5: Shortlisted *fikk* primers are specific to detect *Plasmodium falciparum* infected RBCs at the organism/cellular level. (a) PCR reactions were setup using *fikk 3* primer (S1_*f3*_Set9_FP/S1_*f3*_Set9_RP) with culture from different bacterial species, fungal species, viral species, and algae. Amplified product was analysed on 2% agarose gel with *Acinetobacter baylyi* in lane B1, *Rhodococcus opacus* in lane B2, *Bacillus megaterium* in lane B3, & *E. coli-DH5α* in lane B4, fungal species as *Aspergillus terreus* in lane F1, *Pichia pastoris* in lane F2, & *Saccharomyces cerevisiae* in lane F3 & Algae, *Scenedesmus* in lane Algae. **(b)** Shortlisted primers gives amplified product from *Plasmodium falciparum* infected RBCs in the presence of cells from other pathogens. PCR reactions were setup with *fikk 3 / fikk 10.2 / fikk 12 / fikk 14* primers and *Plasmodium falciparum* infected RBCs in the presence of other pathogens, extracted and used as a template DNA. Amplified product was loaded into the agarose gel from different PCR reactions into different lanes in the same manner as described in panel **"a"**. (c) Densitometric analysis of reaction product from the PCR reaction in panel "b".

PCR using selected *fikk* primers with *P. falciparum* culture gives desirable amplified product (**Figure 4.5, panel b**, lane PC). PCR using selected *fikk* primers with *P. falciparum*

culture mixed with other pathogens gives desirable amplified product (**Figure 4.5, panel b**, lane B1-B4, F1-F3 and algae). Quantification of amplified product further confirm the no significant interference from other pathogens to the PCR mediated malaria detection (**Figure 4.5, panel c**).

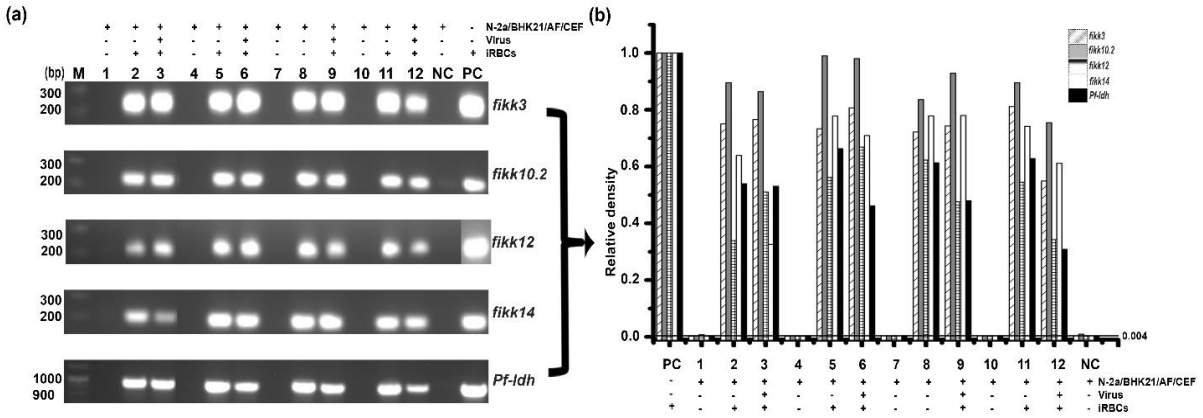

Figure 4.6: Shortlisted *fikk* primers are specific to detect *Plasmodium falciparum* infected RBCs in the presence of virus infected mammalian cells. (a) Shortlisted *fikk* primer gives amplified product from *Plasmodium falciparum* infected RBCs in the presence of mammalian cells (mammalian cells alone in Lane 1, 4, 7, & 10, or in combination with iRBCs in Lane 2, 5, 8, & 11 as denoted in the respective lane of each image) infected with different viruses (Lanes 3: Herpes simplex virus+iRBCs, Lanes 6: Influenza virus+iRBCs, Lanes 9: Japanese encephalitis virus+iRBCs, Lanes 12: Newcastle disease virus+iRBCs). **(b)** Densitometric analysis of reaction product from the PCR reaction in panel **"a"**. Lane NC and PC in each panel denote negative (no template used) and positive (*Pf* gDNA of 1 ng / *Pf* gDNA of 0.2 % parasitemia used) controls, respectively and 'M' as 100 bp DNA marker.

Similarly, we have mixed parasite culture with mammalian cells infected with different strains of viral species (Herpes simplex virus as V1, Duck enteritis virus as V2, Influenza virus as V3, Japanese encephalitis as V4, & Newcastle disease virus as V5) and test the robustness of PCR detection methods using *fikk* primers. PCR using *fikk* primers with different Viral infected mammalian cells (Herpes simplex virus as V1, Duck enteritis virus as V2, Influenza virus as V3, Japanese encephalitis as V4, & Newcastle disease virus as V5) mixed with *P. falciparum* infected RBCs gives desirable amplified product (**Figure 4.6, panel a**). Quantification of amplified product further confirm the no significant interference from other organisms to the PCR mediated malaria detection (**Figure 4.6, panel b**). The results from

Figure 4.4-4.6 clearly highlight the selectivity of designed primers from *fikk* kinases to detect *P. falciparum* in presence of other pathogens including viral species.

4.3.4 Shortlisted primers are highly sensitive in detecting *Plasmodium falciparum:*

The selectivity and sensitivity of PCR based detection of pathogenic organism is desirable. The designed primers are highly selective compared to their host, *P. vivax* and other pathogens. Now we tested the sensitivity of these primers to detect the released *P. falciparum* genome or DNA present inside the infected RBCs. PCR was performed with template DNA in a series of reaction with serial dilution of the *P. falciparum 3D7* genomic DNA from 100 nanogram (ng) to 10^{-5} nanogram (i.e., 10 femtogram) using selected *fikk* primers and *Pf-ldh* primers. *fikk* kinase primers are giving detectable PCR product in the range of 10^{-3} ng to 10^{-5} ng (**Figure 4.7A**). The Gold Standard *Pf-ldh* used in commercial setting gives detectable PCR product till 10^{-3} ng (**Figure 4.7A**) whereas *fikk 3, fikk 10.2, fikk 12, and fikk 14* primers give detectable PCR product till 10^{-5} ng (**Figure 4.7A**).

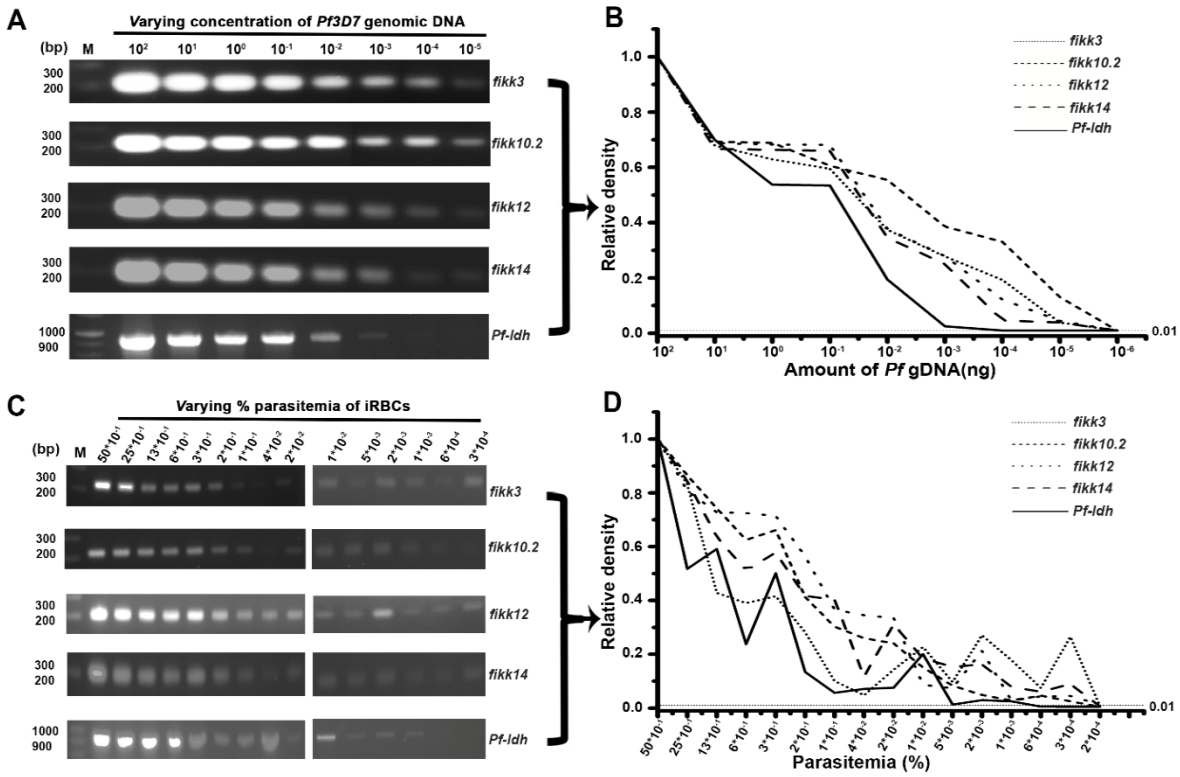

Figure 4.7: Sensitivity analysis of shortlisted primers for the detection of *Plasmodium falciparum*. (A) Sensitivity based on amount of DNA at genomic/molecular level: Gel images showing amplification results with eight-fold dilutions of *Pf* genomic DNA, ranging from 100 ng to 10 fg per reaction in the lanes 1 to 8 as indicated. The lanes correspond to

amplification using shortlisted primers (*fikk3, fikk10.2, fikk12,* & *fikk14*), along with positive control primers (*Pf-ldh*). **(B)** Densitometry analysis graph displaying the relative density of the bands from the shortlisted primers above the threshold level showing the sensitivity for *Pf* at the genomic level.; **(C) Sensitivity based on parasitemia at organism or cellular level:** Gel images showing amplification results with decreasing levels of parasitemia, starting from 5% to 0.0003% in the lanes 1 to 15 as indicated. The lanes correspond to amplification using shortlisted primers (*fikk3, fikk10.2, fikk12,* & *fikk14*), along with positive control primers (*Pf-ldh*). **(D)** Densitometry analysis graph displaying the relative density of the bands from the shortlisted primers well above the threshold level showing the sensitivity for *Pf* at the organism level. 'M' in each panel denote 100 bp DNA marker.

Sensitivity of isolated genomic DNA is very high but it is relevant to explore the sensitivity of PCR methods to the detection of malaria infected RBCs. A series of concentration of infected RBCs (5% to 0.0003% parasitemia) were used in the series of PCR reaction using selected *fikk* primers and *Pf-ldh* primers. The *fikk* primers could be able to detect parasitemia as low as 0.0003% (**Figure 4.7C**). The *Pf-ldh* primers gives detectable PCR product till parasite concentration of 0.0048% parasitemia (**Figure 4.7D**). *fikk3* or *fikk 10.2* primers gives detectable PCR product till parasite concentration of 0.0391% parasitemia whereas PCR with *fikk 10.2* primers allow to detect parasite concentration up to 0.0096% parasitemia (**Figure 4.7D**). Interestingly, PCR with *fikk 12/fikk 14* primers can detect parasite concentration till 0.0003% parasitemia (**Figure 4.7D**). Hence our results indicate that PCR based assay with the shortlisted primer sets can be able to detect *P. falciparum* genome as low as 10 femtogram (fg), and they can be able to detect parasite infected RBCs as low as 0.0003 % parasitemia which is nearly equal to presence of three parasites in one million normal RBCs.

4.3.5 Shortlisted primers are highly selective and sensitive in detecting *Plasmodium falciparum* in Mock patient samples:

Mock patient samples were prepared to mimic different conditions: different infectious agents in the blood, samples with varying parasite concentrations, co-infection with other organisms or blood samples contaminated with other biological fluids like saliva, etc. The mock patient samples were processed in a double blind mode to assess the utility of PCR based malaria detection using *fikk* primers. The present gold standard *Pf-ldh* primers were used to compare the results of *fikk 3* primer based detection of parasite in PCR reaction (**Table 4.2**).

Table 4.2: Validation of *fikk3* for detecting *P.falciparum* malaria via blind test.						
S.No.	**Mock Samples**	**Sample Type**	**Result (P/N)**		**Accuracy of Prediction by PCR (%)**	
			Reported	**Expected**	**Pf-FIKK 3 Primer**	**Pf-ldh Primer**
1	PAT140X	Only RBCs + *Duck enteritis virus*	Negative	Negative	100	100
2	PAT141X	Malaria Parasites - Parasitemia 1 %	Positive	Positive	100	100
3	PAT142X	Only RBCs	Negative	Negative	100	100
4	PAT143X	Malaria Parasites - Parasitemia 0.2 % + *Acinetobacter baylyi*	Positive	Positive	100	100
5	PAT144X	Only RBCs	Negative	Negative	100	100
6	PAT145X	Malaria Parasites - Parasitemia 0.2 % + *Rhodococcus opacus*	Positive	Positive	100	100
7	PAT146X	Clot RBCs	Negative	Negative	100	100
8	PAT147X	Only RBCs + *Influenza virus*	Negative	Negative	100	100
9	PAT148X	Only RBCs + *Japanese encephalitis*	Negative	Negative	100	100
10	PAT149X	Malaria Parasites - Parasitemia 0.2 %	Positive	Positive	100	0
11	PAT150X	Malaria Parasites - Parasitemia 0.4 %	Positive	Positive	100	0
12	PAT151X	Only RBCs (Dried sample - Slide)	Negative	Negative	100	100
13	PAT152X	Malaria Parasites - Parasitemia 0.4 % + *Herpes simplex virus* and *Scenedesmus*	Positive	Positive	100	100
14	PAT153X	RBCs + Saliva	Negative	Negative	100	100
15	PAT154X	Malaria Parasites - Parasitemia 0.6 % + *Bacillus megaterium*	Positive	Positive	100	100
16	PAT155X	Only RBCs + *Newcastle disease virus*	Negative	Negative	100	100
17	PAT156X	Malaria Parasites - Parasitemia 0.6 %	Positive	Positive	100	100

18	PAT157X	Malaria Parasites - Parasitemia 0.6 % + *E. coli-DH5α*	Positive	Positive	100	100
19	PAT158X	Only RBCs + *Aspergillus terreus* and *S. cerevisiae*	Negative	Negative	100	100
20	PAT159X	Malaria Parasites - Parasitemia 0.8 %	Positive	Positive	100	100
21	PAT160X	Malaria Parasites - Parasitemia 0.7 %	Positive	Positive	100	100
22	PAT161X	Malaria Parasites - Parasitemia 2 %	Positive	Positive	100	100
23	PAT162X	Malaria Parasites - Parasitemia 1.25 %	Positive	Positive	100	100
24	PAT163X	Malaria Parasites - Parasitemia 0.65 %	Positive	Positive	100	100
25	PAT164X	Malaria Parasites - Parasitemia 0.25 %	Positive	Positive	100	100
26	PAT165X	Malaria Parasites - Parasitemia 1.9 %	Positive	Positive	100	100
27	PAT166X	Malaria Parasites - Parasitemia 1.1 %	Positive	Positive	100	100
28	PAT167X	Malaria Parasites - Parasitemia 0.5 %	Positive	Positive	100	100
29	PAT168X	Malaria Parasites - Parasitemia 0.2 %	Positive	Positive	100	100
30	PAT169X	Malaria Parasites - Parasitemia 1.8 %	Positive	Positive	100	100
31	PAT170X	Malaria Parasites - Parasitemia 0.95 %	Positive	Positive	100	100
32	PAT171X	Malaria Parasites - Parasitemia 1 %	Positive	Positive	100	100
33	PAT172X	Malaria Parasites - Parasitemia 0.3 %	Positive	Positive	100	100
34	PAT173X	Malaria Parasites - Parasitemia 0.4 %	Positive	Positive	100	100
35	PAT174X	Malaria Parasites - Parasitemia 1.75 %	Positive	Positive	100	100
36	PAT175X	Malaria Parasites - Parasitemia 1.5 %	Positive	Positive	100	100
37	PAT176X	Malaria Parasites - Parasitemia 1.3 %	Positive	Positive	100	100
38	PAT177X	Malaria Parasites - Parasitemia 1.6 %	Positive	Positive	100	100
39	PAT178X	Malaria Parasites - Parasitemia 1.4 %	Positive	Positive	100	100
40	PAT179X	Malaria Parasites - Parasitemia 0.8 %	Positive	Positive	100	100

PCR using *fikk3* primers was robust method to detect malaria parasite in different types of mock patient samples such as co-infection of malaria with other organisms (Herpes simplex virus, Duck enteritis virus, Influenza virus, Japanese encephalitis, Newcastle disease virus, *Scenedesmus* , *Aspergillus terreus*, *Pichia pastoris*, *Saccharomyces cerevisiae*, *Acinetobacter baylyi*, *Rhodococcus opacus*, *Bacillus megaterium*, & *E. coli-DH5α*), mock patients samples mixed with biological fluids (saliva) or blood clotted due to improper treatment (scrapped clot).

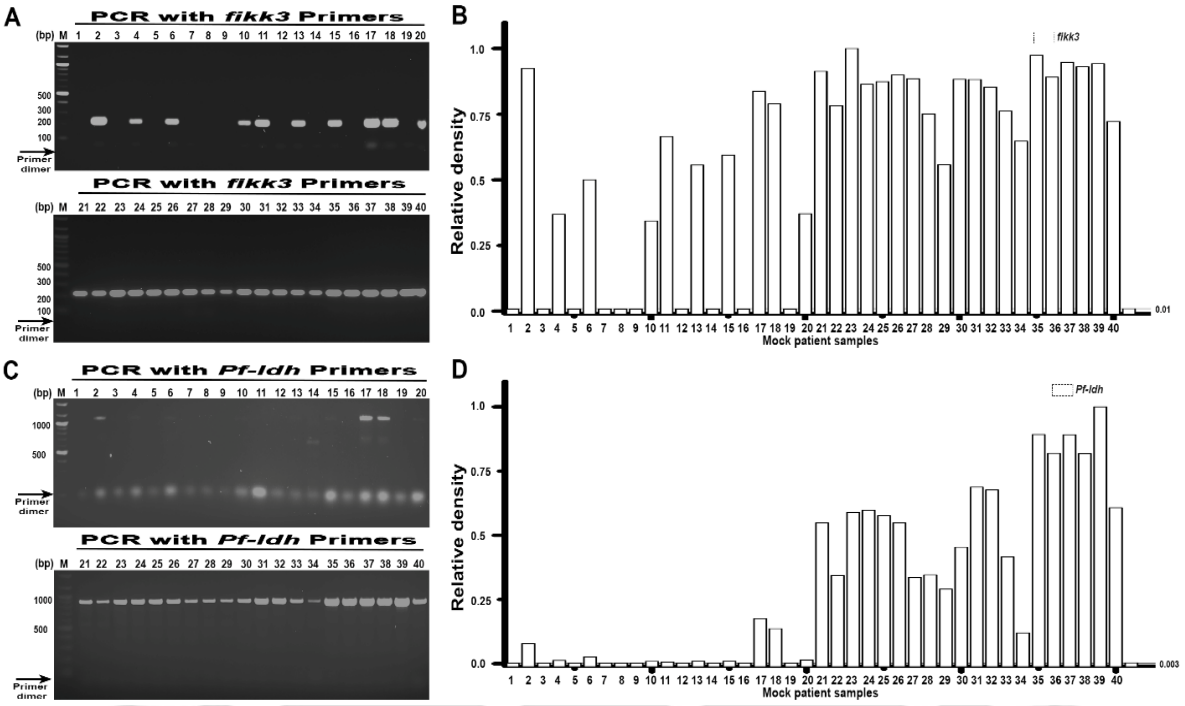

Figure 4.8: Validation of shortlisted primers (*fikk3*) in mock patient samples. (A) PCR results using *fikk3* primers with 2 % agarose gel images displaying amplification at specified product size of 225 bp for 40 mock samples (from Lane 1 to 40), those spiked with in-vitro cultured parasites to mimic malaria mock patient blood, with parasitemia ranging from 0.1% to 2% and also including uninfected RBC lysate, serving as a negative which is below the threshold value of 0.01.; **(B)** Densitometry analysis graph for *fikk3* primers showing the relative density of bands corresponding to absence and presence of varying levels of parasitemia as indicated.; **(C)** PCR results using positive control primers, *Pf-ldh* with 2 % agarose gel images displaying amplification at specified product size of 951 bp for 40 mock samples (from Lane 1 to 40), those spiked with in-vitro cultured parasites to mimic malaria patient blood, with parasitemia ranging from 0.1% to 2% and also including uninfected RBC lysate, serving as a negative which is below the threshold value of 0.003 with faint signals.; **(D)** Densitometry analysis graph for *Pf-ldh* primers showing the relative density of bands corresponding to

absence and presence of varying levels of parasitemia with respect to threshold value as indicated. 'M' in each panel denote 100 bp DNA marker.

In most of these cases, presence of parasite gives very high signal and accuracy of prediction is 100% with *fikk3* primers (**Figure 4.8A, B** and **Table 4.2**). In contrast, *Pf-ldh* primers gives reliable result but PCR product intensity was low and in few cases (4, 6, 15), it was giving false results or doubtful results like patient sample 2, 6, 10, 13, 20 (**Figure 4.8C, D** and **Table 4.2**). Hence, current findings underscore the potential of these *fikk* kinase-based molecular diagnostics for accurate detection and surveillance of malaria, particularly in endemic regions with limited access to advanced diagnostic facilities.

4.4 Discussion

Malaria parasite propagation into the host involves multiple organs [37], and parasite growth within the host produces different types of haemoglobin (Hb) degradation products and pro-oxidant molecules [37]. Malaria parasite appearance in the blood is a late stage of the disease, and detection of the parasite in the blood is the standard procedure with multiple detection methods [38]. DNA is a robust molecule, and it can withstand the harsh conditions of biological fluids like blood, saliva and urine [39]. Detection of *P. falciparum* DNA in saliva and urine is found to be a robust and easy method to detect malaria parasites [40]. The coexistence of malaria with other bacterial, fungal and viral diseases makes malaria detection difficult, and it often misguides the final conclusions [41, 42]. The co-infections reduce the sensitivity of diagnostic tests by suppressing parasitemia or altering immune responses, which lowers the detectable levels of malaria antigens or DNA by interfering during malaria detection, resulting in false-negative results [43]**.** Conversely, specificity is compromised due to cross-reactivity between antigens from non-malaria pathogens (bacterial, viral or fungal) [42] and malaria-specific antibodies, leading to false-positive results. Cross-reactivity between non-malaria pathogens and malaria-specific antibodies increases the likelihood of false-positive results and the complexity increases because co-infections often present with overlapping symptoms, making clinical differentiation challenging and late-stage parasite detection issues. Thus stressing the need for more accurate and robust diagnostic tools to manage malaria effectively in co-infected patients [43, 44].

FIKK kinase is unique to the plasmodium genus, and it has a well-C-terminal conserved kinase domain and a unique N-terminus domain with an unknown function [45, 46]. Exploiting the N-terminus unique region, we have designed diagnostic primers for all FIKK kinases and

screened these primers using in-silico PCR (Figure 4.2). The diagnostic primers targeting *Plasmodium falciparum fikk* kinases demonstrate impressive sensitivity and selectivity, making it a potential biomarker in malaria diagnostics. The assay could detect as low as 10 fg of *P. falciparum* genomic DNA and as few as 0.0003% parasitemia, which translates to identifying approximately three parasites among one million red blood cells (RBCs). This high sensitivity is noteworthy, as gold-standard diagnostic methods like microscopy often struggle to detect such low levels of parasitemia, particularly in the early stages of infection or asymptomatic carriers [18]. The specificity of the designed *fikk* primers was demonstrated through their ability to specifically amplify *P. falciparum* DNA without cross-reacting with human DNA or other most common human infecting malaria strain *P. vivax*, bacterial species, viral species, fungi and algae (Figure 4). Although many infectious organisms co-exist with malaria infection could not be tested due to biosafety concerns. Co-infections were selected based on their clinical relevance and epidemiological prevalence in malaria-endemic regions, where multiple pathogens frequently coexist and influence disease outcomes. The in vitro co-infection models employed in this study served as controlled systems to evaluate the assay's specificity under mixed-pathogen conditions rather than to replicate the full complexity of in vivo interactions. The selected pathogens, known to exhibit bloodstream phases during active infection, represent realistic scenarios in which diagnostic cross-reactivity could occur. The findings demonstrated that FIKK-based detection remained unaffected by the presence of these co-infections, underscoring its potential diagnostic reliability and species specificity for *P. falciparum*. Nevertheless, future clinical validation using patient-derived samples under field and mixed-infection conditions is essential to substantiate these results, ultimately advancing toward the development of species-resolved and field-applicable malaria diagnostics.

This specificity was confirmed through PCR experiments and cross-reactivity tests, which showed no amplification with non-target organisms, thereby preventing false positives. The isothermal thermophilic helicase–dependent amplification (tHDA) study also highlights high sensitivity and specificity. It reports a sensitivity of 96.6% and a specificity of 100%, detecting samples with parasitemia levels around 1% and 50 copies of DNA per assay or 200 parasites per microliter of blood [47]. Rapid diagnostic tests (RDTs) provide quick, point-of-care testing but may not always detect low parasitemia or differentiate between *Plasmodium* species [48]. Sensitivity and selectivity of RDT assay developed so far drops sharply for parasite levels below 100 parasites/µL, often resulting in false negatives, with studies showing that RDTs miss 30-40% of infections in these cases. Additionally, RDTs commonly struggle to identify non-*Plasmodium falciparum* species, detecting mixed infections in only 5-10% of

cases, compared to 20% identified by PCR. Geographic variability further complicates diagnosis, with *hrp2* gene deletions causing up to 40% of *P. falciparum* cases to go undetected in some regions, like the Amazon Basin [12, 49]. While PCR-based methods offer superior sensitivity and specificity, their adoption in malaria-endemic regions faces significant challenges. These methods require specialized equipment, such as thermal cyclers, which are costly to acquire and maintain, especially in remote areas with unreliable electricity [50]. Additionally, the need for expensive reagents and trained personnel with expertise in molecular biology limits their practicality in point-of-care settings where simple, rapid diagnostics are crucial. Transporting samples to centralized labs can also delay treatment, which is critical in managing malaria cases [51]. To address these limitations, we emphasize the potential of isothermal amplification techniques like LAMP and Recombinase Polymerase Amplification (RPA), which do not require thermal cyclers and can be performed with simpler equipment [52] and similar approaches, such as emulsion systems or targeted delivery, could enhance the specificity and effectiveness of *Plasmodium*-specific diagnostic tools [53]. By integrating these concepts, we address challenges in current diagnostic methods and explore innovative strategies to improve detection accuracy [54]. Adapting the *fikk* kinase-based assay for these methods could enable faster, more accessible diagnostics in resource-limited settings, bridging the gap between high accuracy and field feasibility. PCR assay developed with primers designed against lactate dehydrogenase (*ldh*) faces several limitations, including reduced species specificity, particularly when detecting non-*Plasmodium falciparum* species, and lower sensitivity in identifying low-density infections. These assays can also struggle to detect mixed infections, as primers may preferentially amplify one species over another, leading to missed coinfections. Genetic variability in the *ldh* gene may further hinder primer binding, resulting in false negatives, especially in regions with emerging mutations. These limitations underscore the need for novel targets for better sensitivity and species differentiation in diverse malaria-endemic regions that exhibit greater selectivity and sensitivity [55]. Thus, the molecular target of *fikk* kinases demonstrates the assay's robustness through cross-reactivity tests, confirming the primers' specificity compared to traditional diagnostic methods, particularly for detecting low-density infections and mixed-species malaria. However, its implementation is more technically demanding, requiring specialized equipment and expertise [56]. While the upfront costs of PCR-based diagnostics are higher, they may prove more cost-effective over the long term, especially in challenging diagnostic scenarios, by reducing the need for confirmatory tests and improving patient management [56, 57]. In low-resource settings, where microscopy and RDTs are more accessible, adopting PCR methods would require significant infrastructure

and trained personnel. To address these challenges, we propose solutions such as portable PCR devices and cost-reduction strategies [57] to enhance the feasibility of *fikk* kinase-based PCR. Ultimately, this method has the potential to replace conventional diagnostics in complex clinical cases that require higher sensitivity.

The *fikk* kinase-based PCR assay has heightened accuracy that can lead to more precise treatment decisions, better patient outcomes, and reduced misdiagnoses, which is critical in preventing complications and drug resistance. Additionally, early detection of asymptomatic carriers can facilitate timely interventions, enhancing overall patient care. Beyond individual patient benefits, this assay could substantially support malaria elimination efforts by accurately identifying cases, including asymptomatic infections, thereby reducing the parasite reservoir in endemic regions. Its high specificity also ensures efficient use of limited healthcare resources by minimizing false positives. Ultimately, this diagnostic advancement could play a pivotal role in achieving the global goal of malaria eradication through better surveillance and targeted interventions. PCR methods developed using *fikk*-based primers are robust enough to detect malaria in mock patient samples contaminated with other pathogens, clotted blood, blood cells extracted from thin smears and samples mixed with other biological fluids like saliva (Table 4.4). Compared with existing diagnostic methods, the study highlights the limitations of traditional microscopy, which, while specific, often lacks the sensitivity of molecular methods like PCR. Additionally, combining molecular markers and *fikk* kinases with isothermal amplification techniques could provide a hybrid approach that leverages the strengths of both methods where it offers a significant advantage by eliminating the need for sample preparation, making it more convenient for field applications. Using molecular markers like *fikk* kinases thus offers an advantage in both sensitivity and specificity, making it a valuable tool for accurate malaria diagnosis, especially in low-resource settings where mixed infections and low parasitemia complicate diagnosis. Developing such highly sensitive and specific diagnostic tools can significantly aid in the early detection, monitoring, and management of malaria, contributing to better public health outcomes in affected areas.

4.5. REFERENCES:

1. Organization, W.H., *World malaria report 2023*. 2023: World Health Organization.
2. Sinden, R., *The cell biology of malaria infection of mosquito: advances and opportunities.* Cellular microbiology, 2015. **17**(4): p. 451-466.
3. White, N., et al., *Erratum: Malaria (The Lancet (2014) 383 (723-735)).* Lancet, 2014. **383**(9918).
4. Maturana, C.R., et al., *Advances and challenges in automated malaria diagnosis using digital microscopy imaging with artificial intelligence tools: A review.* Frontiers in microbiology, 2022. **13**: p. 1006659.
5. Mirahmadi, H., et al., *Detection of malaria using blood smear by light microscopy, RDT and nested-PCR for suspected patients in south-eastern Iran.* Gene Reports, 2021. **25**: p. 101339.
6. Parra, M.E., C.B. Evans, and D.W. Taylor, *Identification of Plasmodium falciparum histidine-rich protein 2 in the plasma of humans with malaria.* Journal of clinical microbiology, 1991. **29**(8): p. 1629-1634.
7. Makler, M.T., C.J. Palmer, and A.L. Ager, *A review of practical techniques for the diagnosis of malaria.* Annals of tropical medicine and parasitology, 1998. **92**(4): p. 419-434.
8. JM, R., *Usefulness of seminested multiplex PCR in surveillance of imported malaria in Spain.* J Clin Microbiol, 1999. **37**: p. 3260-3264.
9. Piper, R., et al., *Immunocapture diagnostic assays for malaria using Plasmodium lactate dehydrogenase (pLDH).* The American journal of tropical medicine and hygiene, 1999. **60**(1): p. 109-118.
10. Opoku Afriyie, S., et al., *Accuracy of diagnosis among clinical malaria patients: comparing microscopy, RDT and a highly sensitive quantitative PCR looking at the implications for submicroscopic infections.* Malaria Journal, 2023. **22**(1): p. 76.
11. Mukkala, A.N., et al., *An update on malaria rapid diagnostic tests.* Current infectious disease reports, 2018. **20**: p. 1-8.
12. Amoah, L.E., et al., *Diagnostic performance of an ultra-sensitive RDT and a conventional RDT in malaria mass testing, treatment and tracking interventions in southern Ghana.* Parasites & Vectors, 2024. **17**(1): p. 280.
13. Gamboa, D., et al., *A large proportion of P. falciparum isolates in the Amazon region of Peru lack pfhrp2 and pfhrp3: implications for malaria rapid diagnostic tests.* PloS one, 2010. **5**(1): p. e8091.
14. Fontecha, G., et al., *Deletions of pfhrp2 and pfhrp3 genes of Plasmodium falciparum from Honduras, Guatemala and Nicaragua.* Malaria journal, 2018. **17**: p. 1-10.
15. Okangba, C., et al., *Comparative Evaluation of BinaxNOW™ Malaria Rapid Diagnostic Test, Microscopy and Polymerase Chain Reaction for Plasmodium falciparum Detection among Individuals Suspected with Malaria in Lagos, Southwest Nigeria.* Nigerian Journal of Parasitology, 2022. **43**(2).
16. Leski, T.A., et al., *Use of real-time multiplex PCR, malaria rapid diagnostic test and microscopy to investigate the prevalence of Plasmodium species among febrile hospital patients in Sierra Leone.* Malaria journal, 2020. **19**: p. 1-8.
17. Chebore, W., et al., *Assessment of molecular markers of anti-malarial drug resistance among children participating in a therapeutic efficacy study in western Kenya.* Malaria Journal, 2020. **19**: p. 1-12.
18. Berzosa, P., et al., *Comparison of three diagnostic methods (microscopy, RDT, and PCR) for the detection of malaria parasites in representative samples from Equatorial Guinea.* Malaria journal, 2018. **17**: p. 1-12.

19. Ward, P., et al., *Protein kinases of the human malaria parasite Plasmodium falciparum: the kinome of a divergent eukaryote.* BMC genomics, 2004. **5**: p. 1-19.
20. Nunes, M.C., et al., *Plasmodium falciparum FIKK kinase members target distinct components of the erythrocyte membrane.* PloS one, 2010. **5**(7): p. e11747.
21. Nunes, M.C., et al., *A novel protein kinase family in Plasmodium falciparum is differentially transcribed and secreted to various cellular compartments of the host cell.* Molecular microbiology, 2007. **63**(2): p. 391-403.
22. Davies, H., et al., *An exported kinase family mediates species-specific erythrocyte remodelling and virulence in human malaria.* Nature microbiology, 2020. **5**(6): p. 848-863.
23. Schneider, A.G. and O. Mercereau-Puijalon, *A new Apicomplexa-specific protein kinase family: multiple members in Plasmodium falciparum, all with an export signature.* BMC genomics, 2005. **6**: p. 1-12.
24. Siddiqui, G., N.I. Proellochs, and B.M. Cooke, *Identification of essential exported Plasmodium falciparum protein kinases in malaria-infected red blood cells.* British Journal of Haematology, 2020. **188**(5): p. 774-783.
25. Kalendar, R., *A guide to using FASTPCR software for PCR, in silico PCR, and oligonucleotide analysis.* PCR Primer Design, 2022: p. 223-243.
26. Trivedi, V., et al., *Clotrimazole inhibits hemoperoxidase of Plasmodium falciparum and induces oxidative stress: proposed antimalarial mechanism of clotrimazole.* Journal of Biological Chemistry, 2005. **280**(50): p. 41129-41136.
27. Chan, S., *I. DNA isolation from Plasmodium falciparum.* METHODS IN MALARIA RESEARCH, 2013: p. 259.
28. Bharatha, A., S. Suguna, and N.D.S.K.R. Kunkulol, *Genomic DNA isolation from human whole blood samples by non enzymatic salting out method.* 2014.
29. Bhardwaj, B., et al., *An efficient method for DNA extraction from cyanobacteria isolated from hypersaline and marine environments.* Journal of Phycology, 2019. **55**(3): p. 733-737.
30. Pattern, R., *RNA isolation and reverse transcription protocol: Cells in culture.* Boston: Abcam, 2019.
31. Lõoke, M., K. Kristjuhan, and A. Kristjuhan, *Extraction of genomic DNA from yeasts for PCR-based applications.* Biotechniques, 2011. **50**(5): p. 325-328.
32. Mahesh, R., V.R. Naira, and S.K. Maiti, *Concomitant production of fatty acid methyl ester (biodiesel) and exopolysaccharides using efficient harvesting technology in flat panel photobioreactor with special sparging system via Scenedesmus abundans.* Bioresource technology, 2019. **278**: p. 231-241.
33. Keluskar, P., et al., *Plasmodium falciparum and Plasmodium vivax specific lactate dehydrogenase: genetic polymorphism study from Indian isolates.* Infection, Genetics and Evolution, 2014. **26**: p. 313-322.
34. Gadia, C.L.B., et al., *Identification of pathogens for differential diagnosis of fever with jaundice in the Central African Republic: a retrospective assessment, 2008–2010.* BMC Infectious Diseases, 2017. **17**: p. 1-5.
35. Gómez-Pérez, G.P., et al., *Plasmodium falciparum malaria and invasive bacterial co-infection in young African children: the dysfunctional spleen hypothesis.* Malaria journal, 2014. **13**: p. 1-15.
36. Heinig, R.L. and M.B. Thomas, *Interactions between a fungal entomopathogen and malaria parasites within a mosquito vector.* Malaria journal, 2015. **14**: p. 1-10.
37. Tripathy, S. and S. Roy, *Redox sensing and signaling by malaria parasite in vertebrate host.* Journal of Basic Microbiology, 2015. **55**(9): p. 1053-1063.

38. Tek, F.B., A.G. Dempster, and I. Kale, *Parasite detection and identification for automated thin blood film malaria diagnosis.* Computer vision and image understanding, 2010. **114**(1): p. 21-32.
39. Chakraborty, S., *Democratizing nucleic acid-based molecular diagnostic tests for infectious diseases at resource-limited settings–from point of care to extreme point of care.* Sensors & Diagnostics, 2024. **3**(4): p. 536-561.
40. Chai, H.C. and K.H. Chua, *Urine and saliva: relevant specimens for malaria diagnosis?* Diagnostics, 2022. **12**(12): p. 2989.
41. Salam, N., et al., *Global prevalence and distribution of coinfection of malaria, dengue and chikungunya: a systematic review.* BMC public health, 2018. **18**: p. 1-20.
42. Wilairatana, P., et al., *The prevalence of malaria and bacteremia co-infections among febrile patients: a systematic review and meta-analysis.* Tropical medicine and infectious disease, 2022. **7**(9): p. 243.
43. Forero-Peña, D.A., et al., *Seroprevalence of viral and bacterial pathogens among malaria patients in an endemic area of southern Venezuela.* Infectious Diseases of Poverty, 2023. **12**(1): p. 33.
44. Ornellas-Garcia, U., P. Cuervo, and F.L. Ribeiro-Gomes, *Malaria and leishmaniasis: Updates on co-infection.* Frontiers in Immunology, 2023. **14**: p. 1122411.
45. Osman, K.T., et al., *Biochemical characterization of FIKK8–A unique protein kinase from the malaria parasite Plasmodium falciparum and other apicomplexans.* Molecular and biochemical parasitology, 2015. **201**(2): p. 85-89.
46. Kumar, D.A., et al., *Plasmodium falciparum FIKK 9.1 kinase modeling to screen and identify potent antimalarial agents from chemical library.* 3 Biotech, 2023. **13**(8): p. 277.
47. Li, Y., et al., *Detection and species identification of malaria parasites by isothermal tHDA amplification directly from human blood without sample preparation.* The Journal of Molecular Diagnostics, 2013. **15**(5): p. 634-641.
48. Kavanaugh, M.J., S.E. Azzam, and D.M. Rockabrand, *Malaria rapid diagnostic tests: literary review and recommendation for a quality assurance, quality control algorithm.* Diagnostics, 2021. **11**(5): p. 768.
49. Golassa, L., et al., *High prevalence and extended deletions in Plasmodium falciparum hrp2/3 genomic loci in Ethiopia.* PloS one, 2020. **15**(11): p. e0241807.
50. Mediavilla, A., et al., *Real-time PCR for malaria diagnosis and identification of Plasmodium species in febrile patients in Cubal, Angola.* Parasites & Vectors, 2024. **17**(1): p. 384.
51. Yang, S. and R.E. Rothman, *PCR-based diagnostics for infectious diseases: uses, limitations, and future applications in acute-care settings.* The Lancet infectious diseases, 2004. **4**(6): p. 337-348.
52. De Koninck, A.-S., et al., *Diagnostic performance of the loop-mediated isothermal amplification (LAMP) based illumigene® malaria assay in a non-endemic region.* Malaria journal, 2017. **16**: p. 1-9.
53. Khan, B.A., et al., *Fabrication and Evaluation of W/O Emulsion Loaded with Linum usitatissimum Seeds Extract for Anti-Leishmaniasis Efficacy.* Antibiotics, 2022. **11**(4): p. 432.
54. Roberts, A., et al., *A recent update on advanced molecular diagnostic techniques for COVID-19 pandemic: an overview.* Frontiers in immunology, 2021. **12**: p. 732756.
55. Tang, J., et al., *Assessment of false negative rates of lactate dehydrogenase-based malaria rapid diagnostic tests for Plasmodium ovale detection.* PLoS Neglected Tropical Diseases, 2019. **13**(3): p. e0007254.

56. He, W., et al., *Development of new real-time PCR assays for detection and species differentiation of Plasmodium ovale.* PLoS neglected tropical diseases, 2024. **18**(9): p. e0011759.
57. Costa, G.L., et al., *Improving the molecular diagnosis of malaria: droplet digital PCR-based method using saliva as a DNA source.* Frontiers in Microbiology, 2022. **13**: p. 882530.

ANNEXURE-I

Supplementary Figures:

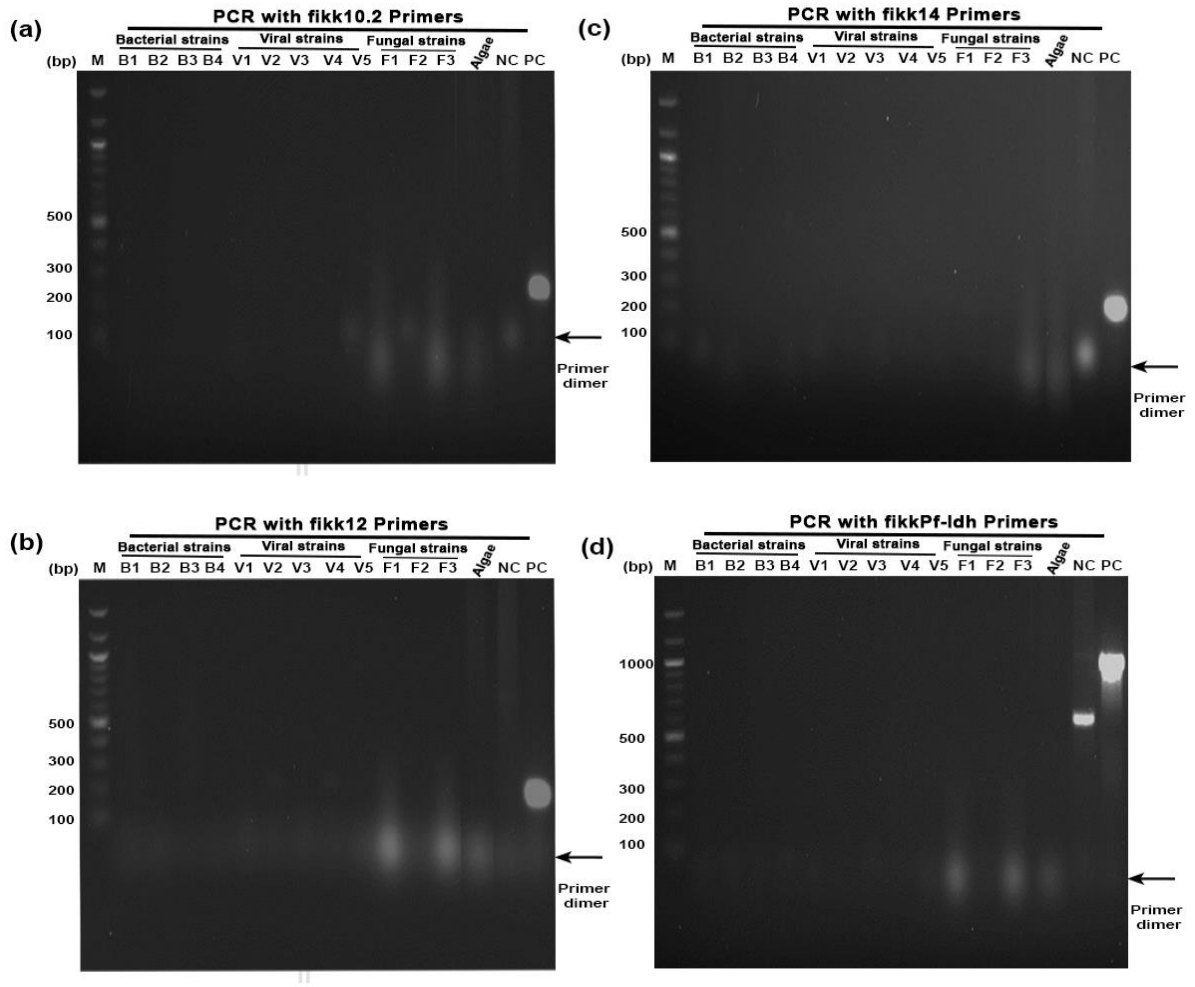

Figure S1: The primers designed for specific amplification from *Plasmodium falciparum* genome does not show any amplification with various pathogenic bacteria, virus, fungi and algae at the genomic/molecular level. PCR reactions were setup with *fikk 10.2* **(a)**, *fikk 12* **(b)**, *fikk 14* **(c)**, *& Pf-ldh* **(d)** primers and template DNA from different bacterial species, fungal species, viral species, & algae. Amplified product was loaded into the agarose gel from

different PCR reactions where template DNA/cDNA was used as follows; *Acinetobacter baylyi* DNA in lane B1, *Rhodococcus opacus* DNA in lane B2, *Bacillus megaterium* DNA in lane B3, & *E. coli-DH5α* DNA in lane B4, cDNA from Herpes simplex virus in lane V1, Duck enteritis virus in lane V2, Influenza virus in lane V3, Japanese encephalitis in lane V4, & Newcastle disease virus in lane V5, genomic DNA from fungal species as *Aspergillus terreus* in lane F1, *Pichia pastoris* in lane F2, & *Saccharomyces cerevisiae* in lane F3 & genomic DNA from Algae, *Scenedesmus* in lane Algae. Lane NC and PC in each panel denote negative (no template used) and positive (*Pf* gDNA of 1 ng used) controls, respectively and 'M' as 100 bp DNA marker.

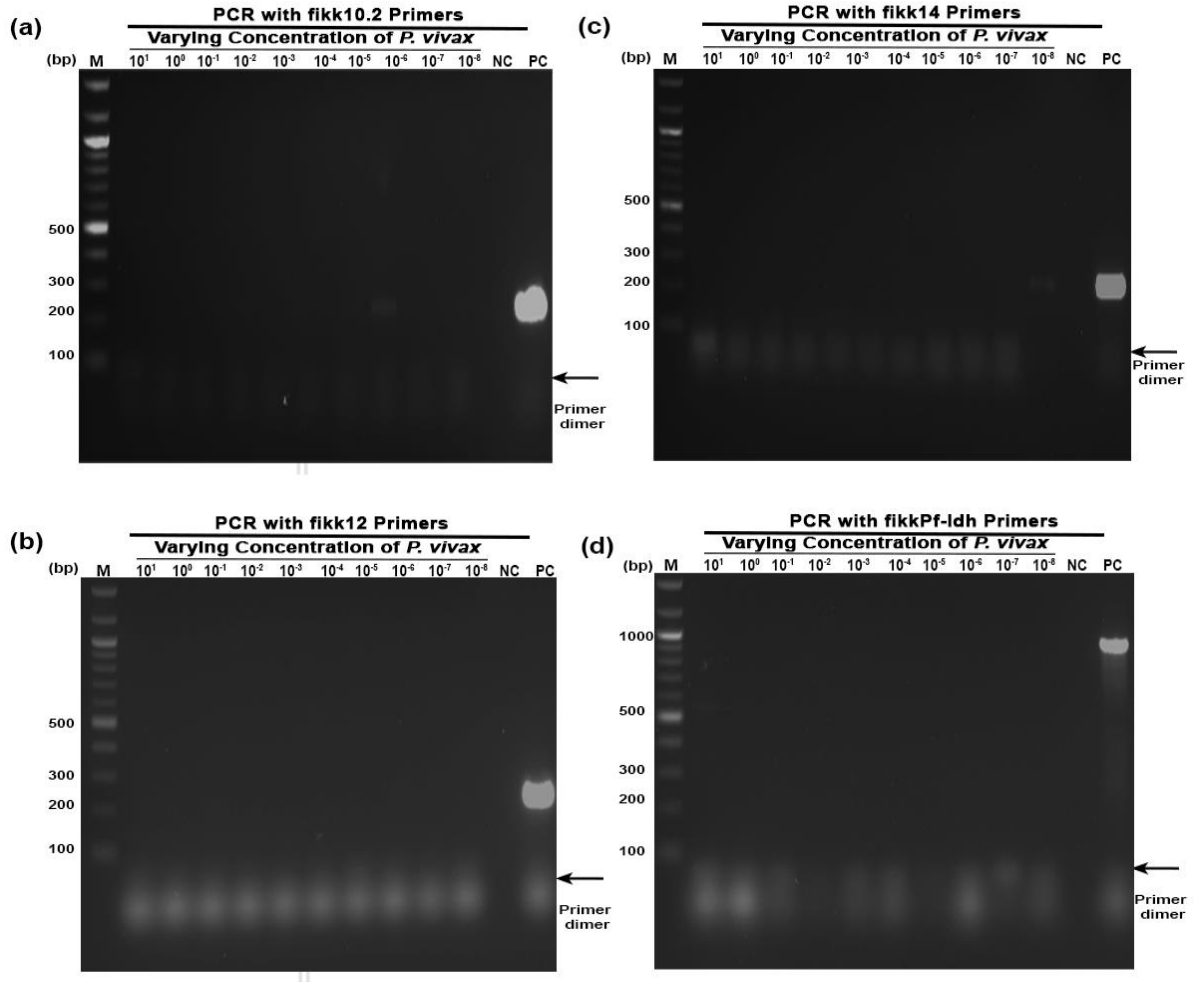

Figure S2: The primers designed for specific amplification from *Plasmodium falciparum* genome does not show any amplification with the *Plasmodium vivax* at the molecular level. PCR reactions were setup with *fikk 10.2* **(a)**, *fikk 12* **(b)**, *fikk 14* **(c)**, *& Pf-ldh* **(d)** primers and *Plasmodium vivax* gDNA as template DNA of various dilutions ranging from 10 ng to 10 ag

and amplified product was loaded into the agarose gel. Lane NC and PC in each panel denote negative (no template used) and positive (*Pf* gDNA of 1 ng used) controls, respectively and 'M' as 100 bp DNA marker.

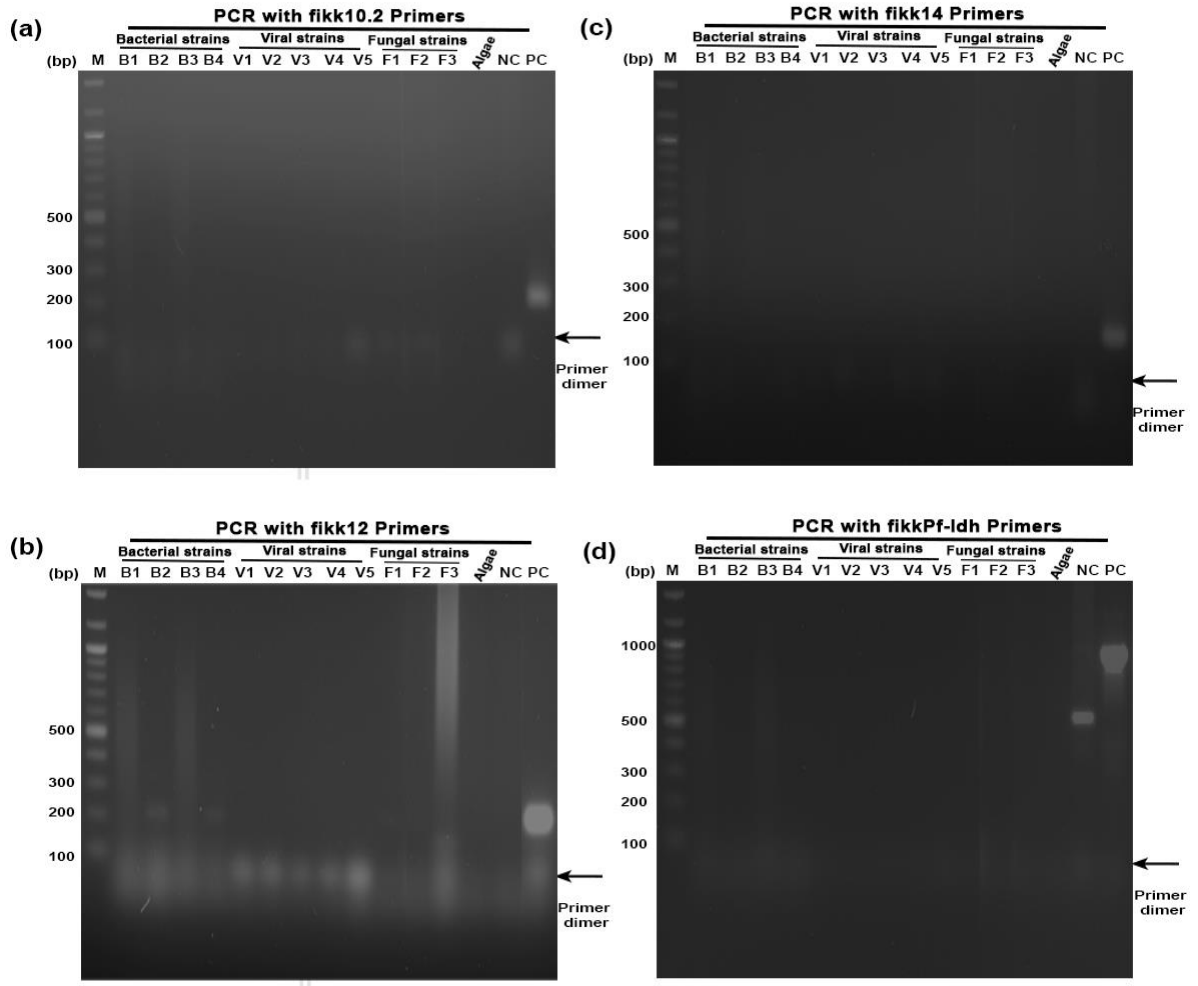

Figure S3: The primers designed for specific amplification from *Plasmodium falciparum* genome does not show any amplification with various pathogenic bacteria, virus, fungi and algae at the cellular/organism level. PCR reactions were setup with *fikk 10.2* **(a)**, *fikk 12* **(b)**, *fikk 14* **(c)**, *& Pf-ldh* **(d)** primers with culture from different bacterial species, fungal species, viral species, & algae. Amplified product was analysed on 2% agarose gel with *Acinetobacter baylyi* in lane B1, *Rhodococcus opacus* in lane B2, *Bacillus megaterium* in lane B3, & *E. coli-DH5α* in lane B4, viral species Herpes simplex virus in lane V1, Duck enteritis virus in lane V2, Influenza virus in lane V3, Japanese encephalitis in lane V4, & Newcastle disease virus in lane V5, fungal species as *Aspergillus terreus* in lane F1, *Pichia pastoris* in lane F2, & *Saccharomyces cerevisiae* in lane F3 & Algae *Scenedesmus* in lane Algae. Lane

NC and PC in each panel denote negative (no template used) and positive (*Pf* gDNA of 1 ng used) controls, respectively and 'M' as 100 bp DNA marker.

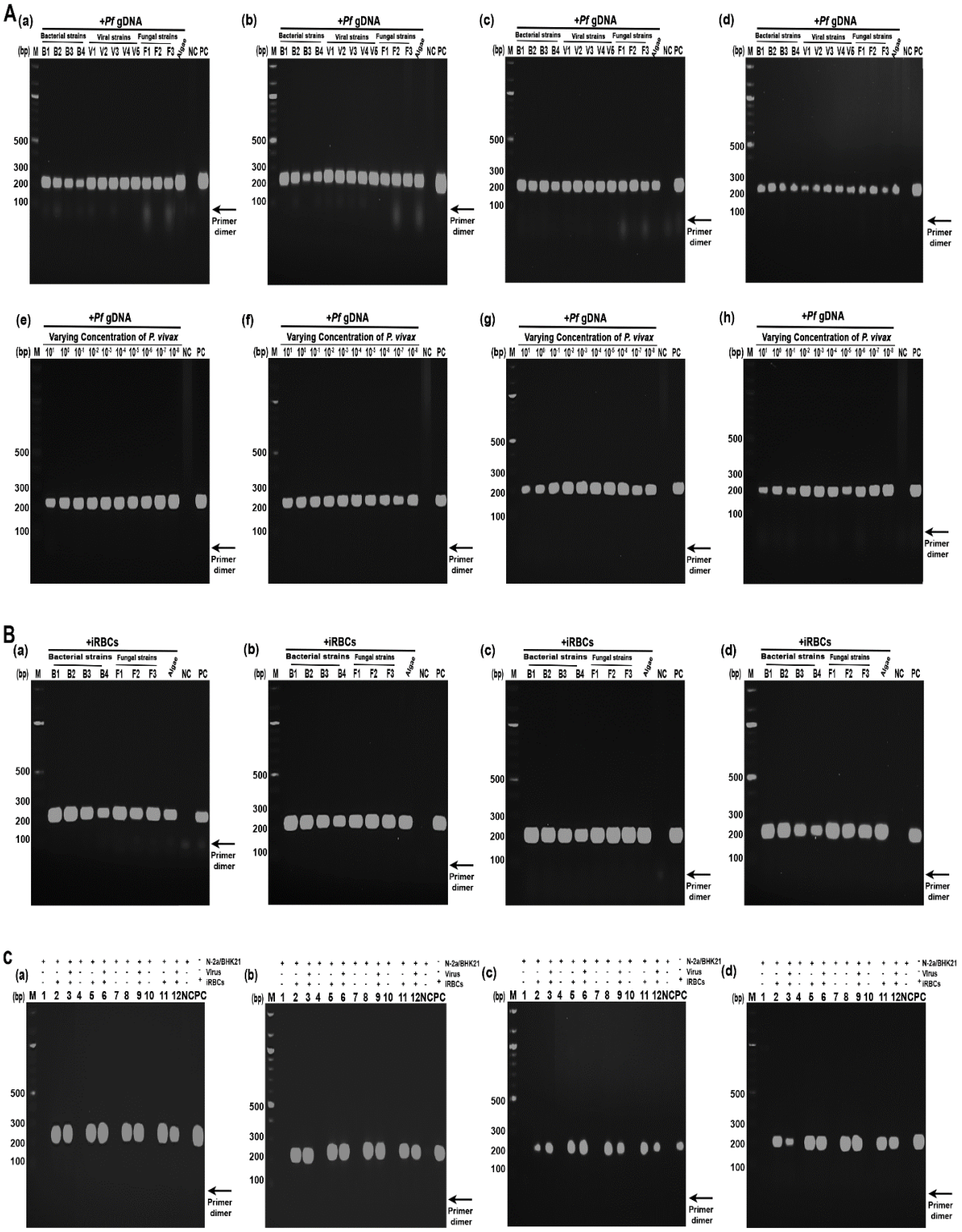

Figure S4: Shortlisted *fikk* primers are specific to detect *P.f* gDNA /*P. f* infected RBCs in the presence of other pathogens both at genomic level and organism level. (A) Specificity

of *fikk*-based PCR assay at genomic level: Shortlisted primers gives amplified product from *P. falciparum* genome in the presence of DNA from other pathogens. PCR reactions were setup with *fikk 3* **(a)**, *fikk 10.2* **(b)**, *fikk 12* **(c)**, & *fikk 14* **(d)**, primers and *P. falciparum* genome mixed with DNA from other pathogens in the ratio of 1:100 and resulting mixture was used as a template DNA. Amplified product was loaded into the agarose gel from different PCR reactions into different lanes in the same manner as described in panel **'a'**, **of Figure 3**. Similarly, PCR reactions were setup with *fikk 3* **(e)**, *fikk 10.2* **(f)**, *fikk 12* **(g)**, & *fikk 14* **(h)**, primers and *P. falciparum* genome mixed with *P. vivax* gDNA (varying concentration from 10 ng to 10 ag) as template DNA and amplified product was loaded into the agarose gel. **(B) Specificity of *fikk*-based PCR assay at cellular/organism level:** Shortlisted primers gives amplified product from *Plasmodium falciparum* infected RBCs in the presence of cells from other pathogens. PCR reactions were setup with *fikk 3* **(a)**, *fikk 10.2* **(b)**, *fikk 12* **(c)**, & *fikk 14* **(d)**, primers and *Plasmodium falciparum* infected RBCs in the presence of other pathogens, extracted and used as a template DNA. Amplified product was loaded into the agarose gel from different PCR reactions into different lanes as *Acinetobacter baylyi* in lane B1, *Rhodococcus opacus* in lane B2, *Bacillus megaterium* in lane B3, & *E. coli-DH5α* in lane B4, fungal species as *Aspergillus terreus* in lane F1, *Pichia pastoris* in lane F2, & *Saccharomyces cerevisiae* in lane F3 & Algae, *Scenedesmus* in lane Algae. **(C) Shortlisted *fikk* primers are specific to detect *Plasmodium falciparum* infected RBCs in the presence of virus infected mammalian cells.** Shortlisted *fikk 3* **(a)**, *fikk 10.2* **(b)**, *fikk 12* **(c)**, & *fikk 14* **(d)**, primers gives amplified product from *Plasmodium falciparum* infected RBCs in the presence of mammalian cells (mammalian cells alone in Lane 1, 4, 7, & 10, or in combination with iRBCs in Lane 2, 5, 8, & 11 as denoted in the respective lane of each image) infected with different viruses (Lanes 3: Herpes simplex virus+iRBCs, Lanes 6: Influenza virus+iRBCs, Lanes 9: Japanese encephalitis virus+iRBCs, Lane NC and PC in each panel denote negative (no template used) and positive (*Pf* gDNA of 1 ng / *Pf* gDNA of 0.2 % parasitemia used) controls, respectively and 'M' as 100 bp DNA marker.

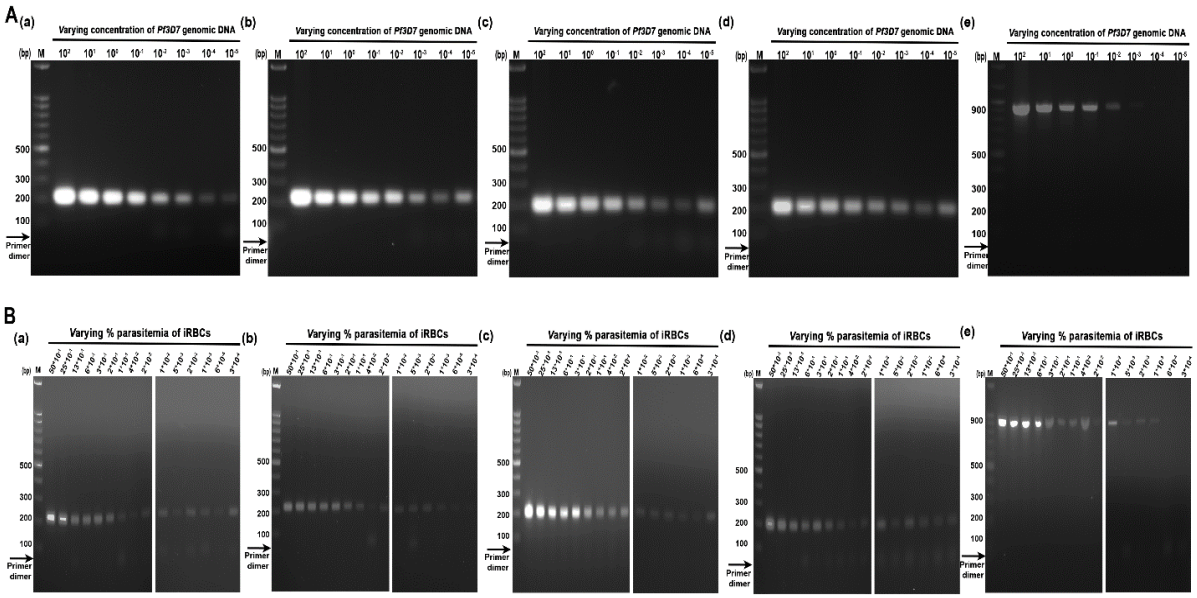

Figure S5: Sensitivity analysis of shortlisted primers for the detection of *Plasmodium falciparum*. (A) Sensitivity based on amount of DNA at genomic level: Gel image showing amplification results using *fikk 3* **(a)**, *fikk 10.2* **(b)**, *fikk 12* **(c)**, *fikk 14* **(d)**, & *Pf-ldh* **(e)**, primers with eight-fold dilutions of *Pf* genomic DNA, ranging from 100 ng to 10 fg per reaction in the lanes 1 to 8 as indicated. Gel images showing amplification results with eight-fold dilutions of *Pf* genomic DNA, ranging from 100 ng to 10 fg per reaction in the lanes 1 to 8 as indicated. **(B) Sensitivity based on parasitemia at cellular/organism level:** Gel images showing amplification results using *fikk 3* **(a)**, *fikk 10.2* **(b)**, *fikk 12* **(c)**, *fikk 14* **(d)**, & *Pf-ldh* **(e)**, primers with decreasing levels of parasitemia, starting from 5% to 0.0003% in the lanes 1 to 15 as indicated. 'M' in each panel denote 100 bp DNA marker.

ANNEXURE-II

Supplementary Tables:

The reader can find the following supplementary tables of S1 to S6 from the published article, Prasad, M. R., & Trivedi, V. (2024). **Molecular Investigation of FIKK Kinase Family to Develop PCR-Based Diagnosis of Plasmodium falciparum**. *Molecular Biotechnology*, 1-17.

Table S1: Results of the In-silico PCR (of *fastPCR* tool & Primer-BLAST) from the designed primers of *fikk3* verifying the specific amplification in *Plasmodium falciparum* and non-specific amplification in *Homo sapiens*

Table S2: Results of the In-silico PCR (of fastPCR tool & Primer-BLAST) from the designed primers of *fikk4.2* verifying the specific amplification in *Plasmodium falciparum* and non-specific amplification in *Homo sapiens*

Table S3: Results of the In-silico PCR (of fastPCR tool & Primer-BLAST) from the designed primers of *fikk8* verifying the specific amplification in *Plasmodium falciparum* and non-specific amplification in *Homo sapiens*

Table S4: Results of the In-silico PCR (of fastPCR tool & Primer-BLAST) from the designed primers of *fikk10.2* verifying the specific amplification in *Plasmodium falciparum* and non-specific amplification in *Homo sapiens*

Table S5: Results of the In-silico PCR (of fastPCR tool & Primer-BLAST) from the designed primers of *fikk12* verifying the specific amplification in *Plasmodium falciparum* and non-specific amplification in *Homo sapiens*

Table S6: Results of the In-silico PCR (of fastPCR tool & Primer-BLAST) from the designed primers of *fikk14* verifying the specific amplification in *Plasmodium falciparum* and non-specific amplification in *Homo sapiens*

Chapter 5

Characterization of Antigenic Determinants of FIKK Kinase(s) to Detect *Plasmodium falciparum*

*The contents of this chapter is published as **Prasad, M. R., Kumar, D. A, Eena Dodwani, Sukhwinder Singh, & Trivedi, V.** (2025). Antigenic determinant analysis of FIKK Kinase family to identify novel candidates for diagnosis of *Plasmodium falciparum*. *Microbial Pathogenesis*

SUMMARY

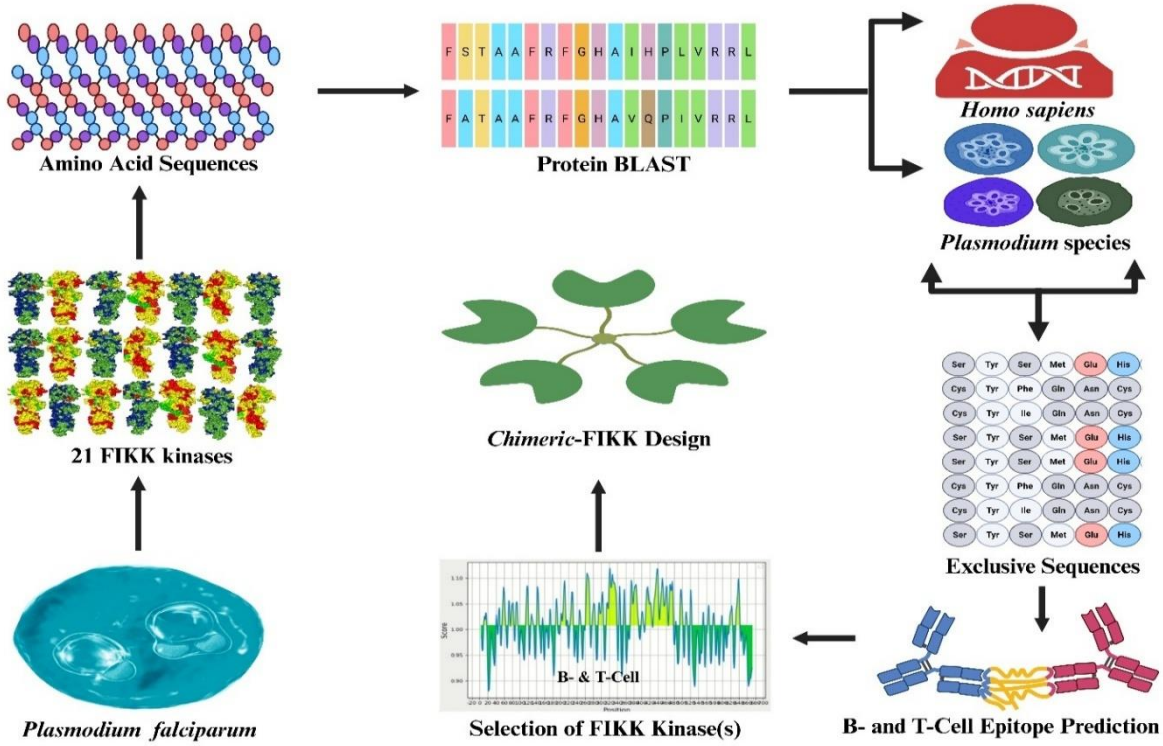

Figure: The research flowchart illustrates the gene selection to the engineered C-FIKK construct ready for diagnostic evaluation.

This chapter explores the diagnostic potential of the *P. falciparum*-specific FIKK kinase protein family using an integrated immunoinformatics approach to identify novel antigenic determinants suitable for species-specific malaria detection. A total of 21 FIKK kinase proteins were retrieved from PlasmoDB and evaluated for conserved, unique, and immunogenic regions using PSI-BLAST against *Homo sapiens* and other *Plasmodium* species. Linear B-cell and T-cell epitopes were predicted using IEDB tools based on surface accessibility, flexibility, hydrophilicity, and MHC class I and II binding affinities. Several highly antigenic, surface-accessible epitopes with strong global HLA coverage were identified. The six FIKK kinases containing overlapping B- and T-cell epitopes from FIKK7.1, FIKK8, FIKK9.1, FIKK9.3, FIKK9.7, and FIKK13 were selected to design a multi-epitope *chimeric*-FIKK (C-FIKK) construct. This construct was codon-optimized for recombinant expression in *E. coli* and intended for polyclonal antibody generation. Thus this chapter provides a detailed approach in exploiting FIKK kinases as precise diagnostic markers with the engineered *chimeric*-FIKK protein holding significant promise for advancing malaria diagnostics, particularly in low-resource and field settings.

5.1 INTRODUCTION

Malaria continues to be a major global health burden, with majority of these cases caused by *P. falciparum*, the most virulent species responsible for severe and fatal malaria, especially in sub-Saharan Africa, Southeast Asia, and parts of South America (WHO, 2023). Accurate and timely diagnosis is essential for malaria case management, disease surveillance, and the interruption of transmission. However, the current diagnostic landscape faces multiple challenges, particularly in detecting low-density parasitemia, distinguishing between species during coinfection, and identifying mixed infections (Ippolito, M.M., et al., 2021 ; Zimmerman, P.A. et al., 2015).

The conventional diagnostic approaches such as light microscopy and RDTs are limited in their effectiveness. Microscopy, though considered the gold standard, is time-consuming, requires skilled personnel, and has reduced sensitivity in low parasitemia conditions. RDTs, commonly based on detecting *Pf*-HRP2 or pLDH antigens, are simple and rapid but suffer from reduced sensitivity in early infections and may give false negatives due to gene deletions (e.g., HRP2/HRP3 deletions in *P. falciparum*) (WHO, 2023; Wongsrichanalai et al., 2007). Furthermore, RDTs generally lack the specificity to differentiate among *Plasmodium* species or detect co-infections, which is crucial in regions with multiple endemic species. To address these limitations, there is a growing interest in leveraging bioinformatic approaches to identify novel, species-specific, and immunologically relevant targets. In this context, the *P. falciparum* FIKK kinase protein family represents a promising set of antigens due to their unique presence in the parasite, surface localization, and role in host cell modification. FIKK kinases are exported into the host erythrocyte cytoplasm and have been implicated in immune evasion and cytoadherence features that make them ideal candidates for diagnostic and vaccine development (Ward, P., et al., 2004 ; Nunes, M.C., et al., 2007 & 2010 ; Schneider, A.G. et al., 2005 ; Davies, H., et al., 2020).

This chapter presents a comprehensive immunoinformatic characterization of 21 FIKK kinases from *P. falciparum*, aiming to identify B-cell and T-cell epitopes with high antigenicity and MHC-binding potential. Using a multi-parametric strategy involving tools such as the IEDB analysis resource, Bepipred 2.0, NetMHCpan EL 4.1, and structural prediction tools, linear B- and T-cell epitopes were mapped for their surface accessibility, hydrophilicity, flexibility, and antigenic potential (Emini et al., 1985; Kolaskar & Tongaonkar, 1990; Reynisson et al., 2020; Jespersen et al., 2017). A *chimeric*-FIKK construct (C-FIKK) was designed by fusing the most promising immunogenic peptide regions from six selected FIKK kinases. This construct was codon-optimized for recombinant expression in *E. coli*, offering a

platform for antibody generation and future development of lateral-flow immunoassays or ELISA-based diagnostics. Unlike HRP2 or pLDH, FIKK-derived diagnostic antigens promise improved specificity, resistance to gene deletion artifacts, and the ability to detect multiple *Plasmodium* species. Additionally, the immunoinformatic approach enhances diagnostic sensitivity by targeting highly immunogenic, population-relevant epitopes (Southwood et al., 1998; Hoof et al., 2009). Overall, this work addresses the diagnostic gaps in current malaria detection systems and lays the groundwork for a next-generation diagnostic platform capable of sensitive and species-specific detection of *P. falciparum* and potentially other malaria-causing parasites.

5.2 EXPERIMENTAL PROCEDURES

5.2.1 Comparative Analysis of *FIKK* Kinase Proteins: Retrieval from PlasmoDB and Protein BLAST Evaluation

The procedure for comparative analysis of all the 21 FIKK kinase(s) using protein BLAST was detailed in the section 3.8.1 of chapter 3: Experimental Procedures

5.2.2 Computational Prediction of Linear B-Cell Epitopes in *FIKK* Kinase Proteins

The procedure for predicting linear B-Cell epitopes of all the 21 FIKK kinase(s) using IEDB tools was detailed in the section 3.8.2 of chapter 3: Experimental Procedures

5.2.3 Computational Prediction of MHC Class I and II Binding Epitopes for T-Cell Immunogenicity

The procedure for predicting MHC Class I and II binding epitopes for T-Cell immunogenicity of all the 21 FIKK kinase(s) using IEDB tools was detailed in the section 3.8.3 of chapter 3: Experimental Procedures

5.2.4 Computational Design of *Chimeric*-FIKK Protein and Plasmid Assembly

Selected FIKK kinases were analyzed for overlapping residues forming linear B-cell epitopic peptides using the Emini Surface Accessibility (Emini et al., 1985) and Kolaskar & Tongaonkar Antigenicity methods (Kolaskar & Tongaonkar, 1990). These B-cell epitopes were compared with predicted T-cell epitopes (Sette et al., Year) to evaluate their surface accessibility and antigenic properties. Overlapping residues shared by both B-cell and T-cell epitopes (MHC-I and MHC-II immunogenicity) with the highest antigenicity were selected for designing a chimeric FIKK (C-FIKK) protein. The chimeric construct was generated by fusing peptides from six selected FIKK kinases using appropriate peptide linkers. The recombinant gene sequence (575 bp) was codon-optimized for *E. coli* expression using OPTIMIZER (Puigbò et al., 2007) and the GeneScript rare codon analysis tool to enhance expression efficiency. The optimized gene was synthesized (by Gene Script) and cloned into the pET28a (+) expression vector for further experimental validation.

5.3 RESULTS

The species-specific expression and essential function in erythrocyte modification make FIKK kinases of *Plasmodium* species an attractive candidate for diagnostic applications [12, 15]. Unlike conventional diagnostic markers such as *Pf*-HRP-II and pLDH, FIKK kinases exhibited unique immunogenic regions that had improved the specificity and sensitivity of malaria detection, particularly for *P. falciparum* at the molecular level [17]. Leveraging the distinct sequence and antigenic properties of FIKK kinases for the development of advanced diagnostic tools suggests their suitability for lateral-flow immunoassays with higher sensitivity, species differentiation, and applicability in field settings.

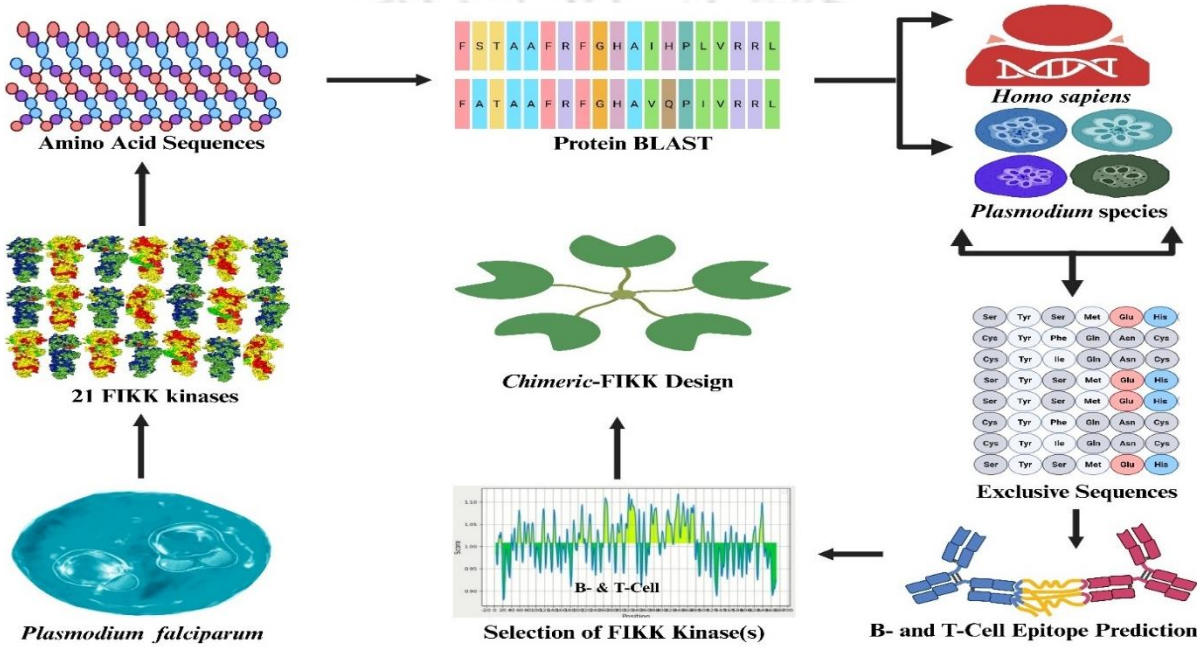

Figure 5.1: The illustration of the research design visually outlines the step-by-step process, starting from FIKK selection to final C-FIKK design.

From a total of 21 FIKK kinases of *Plasmodium falciparum*, we explored the applicability of these enzymes, focusing on specific regions for diagnosing malaria, particularly *P. falciparum*, in biological samples. In the designed study (Figure 5.1), protein sequences were analysed to identify regions within each kinase enzyme that are exclusive to the FIKK kinases of *Plasmodium* species causing malaria in humans. Peptide sequences were selected based on B-cell and T-cell epitope predictions, prioritizing those with higher antigenicity scores against humans. The chosen peptides were then linked using appropriate linkers to generate a chimeric FIKK that is used to detect *P. falciparum* as well other *Plasmodium* species causing malaria in humans by in-vitro dot blot assay.

5.3.1 Exclusive Amino Acid Profiles of *P. falciparum* FIKK Kinase(s)

The process begins with a protein BLAST analysis of 21 FIKK kinase(s) from *P. falciparum* against human counterparts and other *Plasmodium* species that cause malaria in humans (Table 5.1). The table provides the information on the 21 FIKK kinase(s) with exclusive regions for individual *P. falciparum* FIKK kinases, conserved FIKK kinases across *Plasmodium* species, and homologous regions to human counter parts.

Figure 5.2: FIKK9.1 includes distinctive regions with potential applications in malaria detection. The FIKK9.1 sequence is categorized based on its characteristics: regions exclusive to *Plasmodium falciparum* are marked in pink, those conserved across *Plasmodium* species are shown in blue, regions similar to humans are indicated in yellow, and areas conserved in both *Plasmodium* species and humans are highlighted in green. Epitope prediction identifies antigenic values greater than 1.12, which are represented by pink rectangles with a pink star, accompanied by the epitope symbol. Regions with antigenic values between 0.9 and 1.1 are shown in green rectangular boxes, also with the epitope symbol.

Table 5.1: Analysis of *Plasmodium falciparum* 3D7 FIKK kinase(s) protein sequence.

FIKK Kinase	Gene ID	Exclusive region to *Plasmodium* genus	Exclusive Region to Plasmodium Falciparum	Homologous Region to *Homo sapiens*
FIKK1	PF3D7_0102600	40-278	1-39	279-629
FIKK3	PF3D7_0301200	116-257	1-115	258-610
FIKK4.1	PF3D7_0424500	43-277	1-42	278-622
FIKK4.2	PF3D7_0424700	10-327	1-9; 1219-1222	328-1217
FIKK5	PF3D7_0500900	120-267	1-119; 598-600	267-597
FIKK7.1	PF3D7_0726200	28-530;769-841	1-27; 842-845	531-768
FIKK7.2	PF3D7_0731400	106-198	1-105	199-531
FIKK8	PF3D7_0805700	1-1097	Nil	1098-1454
FIKK9.1	PF3D7_0902000	41-180	1-40	181-542
FIKK9.2	PF3D7_0902100	91-164	1-90	165-520
FIKK9.3	PF3D7_0902200	41-303	1-40	304-632
FIKK9.4	PF3D7_0902300	195-238	1-194	239-607
FIKK9.5	PF3D7_0902400	109-148	1-108	149-540
FIKK9.6	PF3D7_0902500	33-309	1-32	310-589
FIKK9.7	PF3D7_0902600	95-285	1-94	286-614
FIKK10.1	PF3D7_1016400	119-324	1-118	325-607
FIKK10.2	PF3D7_1039000	34-561	1-33	562-911
FIKK11	PF3D7_1149300	76-346	1-75	347-560
FIKK12	PF3D7_1200800	139-250	1-138	251-564
FIKK13	PF3D7_1371700	124-215	1-123	216-561
FIKK14	PF3D7_1476400	87-254	1-86	255-622

To evaluate the diagnostic relevance of the selected epitopes, we initially performed a comprehensive BLAST analysis of all 21 FIKK kinases from *Plasmodium falciparum* against human proteins and other *Plasmodium* species known to infect humans (Table 5.1). The analysis revealed that regions located in the N-terminal domain (approximately amino acids 1–100) were uniquely conserved among *P. falciparum* strains, while the central regions (50–300 amino acids) showed conservation across the *Plasmodium* genus, and the C-terminal domains exhibited partial homology with human proteins (Table 5.1). Notably, the epitopes chosen for inclusion in the C-FIKK construct were specifically conserved among *P. falciparum* field isolates, including NF135/5.C10, UGT5.1, Santa Lucia, 3D7, NF54, CAMP/Malaysia, 7G8, Tanzania (2000708), HB3, Palo Alto/Uganda, and Vietnam Oak-Knoll (FVO). However, these epitopes did not exhibit significant similarity with sequences from other *Plasmodium* species such as *P. vivax*, *P. ovale*, *P. malariae*, or *P. knowlesi*, thereby supporting their species specificity. The protein BLAST output (Figure 5.2) visually differentiates these findings, where pink regions represent *P. falciparum*-specific sequences, blue regions indicate homology with other *Plasmodium* species, yellow marks homology with human proteins, and green highlights sequences common to both *Plasmodium* and human genomes.

5.3.2 Computational Prediction of Linear B-Cell Epitopes in *P. falciparum* FIKK Kinase(s)

The maximum and minimum hydrophilicity scores for all FIKK kinase proteins are summarized in Table 5.2. Among the predicted epitopes, amino acid positions 217-DDDDDDD-223 of the protein FIKK10.2 with the highest of 10.00 and amino acid positions 10-IFWFLFL-16 of the protein FIKK11 with lowest scores of -9.143 were recorded.

Table 5.2: Characterization of predicted B-cell epitopes of FIKK kinase from *P. falciparum*.

FIKK NAME	HYDROPHILICITY		SURFACE FLEXIBILITY	
	EPITOPE	SCORE (Max./Min.)	EPITOPE	SCORE (Max./Min.)
FIKK1	131-NDSNSDN-137 554-IFFIFLW-560	7.714/-8.971	NDSNSDN (131-137) YVVMVCE (395-401)	1.115 0.884
FIKK3	DDDCDDN (187-193) LYFILIF (61-67)	8.343/-7.814	DNKNSSD (339-345) VFFIWVW (533-539)	1.122 0.884
FIKK4.1	DNNNNND (63-69) IFFIWVW (547-553)	7.857/-8.300	KEKSKKK (115-121) IFFIWVW (547-553)	1.111 0.881
FIKK4.2	DDNDDSD (943-949) IFYIWIW (1145-1151)	9.071 -7.871	KGSKGKS (943-949) IFYIWIW (1145-1151)	1.119 0.862
FIKK5	DASTDEN (535-541) ILFIWIW (519-525)	6.943 -8.914	LENSNKN (138-144) ILFIWIW (519-525)	1.101 0.877
FIKK7.1	EDEKNED (307-313) LIIFLIL (24-30)	8.014 -8.686	DNSNKEQ (391-397) VLFIWIW (768-774)	1.121 0.879
FIKK7.2	DRTNDTD (82-88) IVFIWIW (456-462)	7.371 -8.129	SSKNGNG (194-200) VFIWIWN (457-463)	1.115 0.872
FIKK8	DDEDNSN (150-156) VFFFWIW (1380-1386)	8.329 -8.471	NNNSNNN (213-219) IPIYIWV (1131-1137)	1.130 0.877
FIKK9.1	DKDSDES (93-99) ILFIWIW (466-472)	8.071 -8.914	NKKSKKK (335-341) ILFIWIW (466-472)	1.106 0.877
FIKK9.2	KDGSNKN (116-122) LGILFIW (442-448)	6.800 -6.843	KDGSNKN (116-122) DIYMLGI(438-444)	1.120 0.879
FIKK9.3	DNNKDEE (41-47) VLFLFLL (6-12)	7.900 -8.414	KDGSGND (294-300) TFFIWLW (557-563)	1.126 0.885
FIKK9.4	GGDKKDD (269-275) IMLIWIW (531-537)	7.543 -8.200	PSNGGDK (266-272) IMLIWIW (531-537)	1.120 0.864
FIKK9.5	DDEERKQ (443-449) ILFIAIW (464-470)	7.357 -7.186	SPNNNPI (136-142) VFFMIIR (6-12)	1.087 0.875
FIKK9.6	DEEERKK (495-501) IVFIAIW (516-522)	7.000 -6.400	NSSPSTS (153-159) SYLWYIS (525-531)	1.111 0.889
FIKK9.7	SDEKDDE (89-95) ILFILIW (525-531)	8.257 -8.800	NENGNGN (312-318) ILIWVYH (528-534)	1.123 0.866
FIKK10.1	EDDEEDT (119-125) VLFIWIW (532-538)	8.371 -8.300	SKEGDGS (265-271) LYFIWFV (51-57)	1.110 0.876
FIKK10.2	DDDDDDD (217-223) ILYIWIW (836-842)	10.000 -7.871	TSQNKTK (198-204) ILYIWIW (836-842)	1.116 0.863
FIKK11	NDDNKNN (212-218) IFWFLFL (10-16)	7.671 -9.143	LKSGSNL (109-115) YIFWFLF (9-15)	1.105 0.877
FIKK12	EDESKEN (160-166) VLFIWIW (491-497)	7.514 -8.300	ENKSKGR (208-214) LFIWIWN (492-498)	1.117 0.872
FIKK13	NKNDDQS (132-138) IFFIWMW (484-490)	7.457 -8.371	HGGSKND (38-44) FFIWMWN (485-491)	1.111 0.864
FIKK14	MDDDDDD (405-411) IFFIWIW (546-552)	7.971 -8.914	SSKKSNE (185-191) IFFIWIW (546-552)	1.125 0.876

The surface flexibility of the epitopes using a threshold value of 1, the maximum predicted flexibility scores for FIKK kinase proteins are also presented in Table 5.2. Among the predicted epitopes, amino acid positions 213-NNNSNNN-219 of the protein FIKK8 with the highest of 1.130 and amino acid positions 1145-IFYIWIW-1151 of the protein FIKK4.2 with lowest scores of 0.862 were recorded.

For the surface accessibility using the threshold value set at 1 among the predicted proteins, epitopes with the highest predicted scores was amino acid positions 23-KKKKKK-28 of the protein FIKK10.1 with the highest of 11.969 and amino acid positions 26-FVFLCC-31 of the protein FIKK4.1 with lowest scores of 0.017 were recorded along with other proteins were detailed in Table 5.3.

Table 5.3: Characterization of predicted 21 FIKK kinase B-cell epitopes of *P. falciparum* 3D7 strain (PF3D7) based on their innate physiochemical properties (surface accessibility and antigenicity).

FIKK NAME	SURFACE ACCESSIBILITY		ANTIGENICITY	
	EPITOPE	SCORE (Max./Min.)	EPITOPE	SCORE (Max./Min.)
FIKK1	KEKDDK (258-263)	6.484 0.044	SVVLAFL (329-335)	1.205 0.835
	IFFIFL (554-559)		DENNRKN (608-614)	
FIKK3	KNKKKK (403-408)	8.477 0.050	LHLLVKL (414-420)	1.203 0.833
	VFFIWV (533-538)		NNNKNDK (250-256)	
FIKK4.1	KNKRKE (405-410)	5.519 0.017	VFVFLCC (25-31)	1.289 0.800
	FVFLCC (26-31)		NNNNNDE (64-70)	
FIKK4.2	QEERKK (1125-1130)	4.403 0.015	VVLVTEL (986-992)	1.201 0.811
	CIIFFI (53-58)		NNNNNKD (933-939)	
FIKK5	QDERKK (499-504)	6.904 0.040	SLLVIFV (59-65)	1.217 0.856
	LLVIFV (60-65)		KNNKKGN (354-360)	
FIKK7.1	KDENKK (538-543)	5.063 0.028	CGYVVMV (607-613)	1.203 0.789
	ILIIFL (23-28)		NNNNDNN (596-602)	
FIKK7.2	KKKKKK (327-332)	11.542 0.042	SCAPCVG (397-403)	1.174 0.864
	IVFIWI (456-461)		EDRTNDT (81-87)	
FIKK8	EKEKKR (859-864)	5.810 0.044	FILYQCL (1255-1261)	1.190 0.776
	VFFFWI (1380-1385)		NNNNNNN (217-223)	
FIKK9.1	KKKKKK (48-53)	10.791 0.031	VIVSELY (309-315)	1.170 0.810
	LIIVFI (13-18)		NNEEDNN (109-115)	

FIKK9.2	KKKYKE (403-408) ILFIWI (444-449)	7.912 0.047	ILVYTYL (60-66) NESGGRN (166-172)	1.181 0.862
FIKK9.3	KKKKKR (150-155) IGVLFL (4-9)	9.862 0.048	VLFLFLL (6-12) DNNNNNN (164-5170)	1.224 0.789
FIKK9.4	KRQKRK (90-95) CVNIIC (56-61)	7.974 0.025	CLFQSCC (467-473) PNKNNEN (178-184)	1.229 0.850
FIKK9.5	KKNDKK (333-338) LICVFF (3-8)	7.634 0.031	YFDVSCV (451-457) NINDEKN (64-70)	1.187 0.875
FIKK9.6	KKNKKK (386-391) IVFIAI (516-521)	9.269 0.040	LCLFQSC (451-457) TGNDGNN (250-256)	1.206 0.836
FIKK9.7	QDERKK (505-510) IILFII (9-14)	7.080 0.031	LILYFYL (2-8) NENGNEN (274-280)	1.188 0.811
FIKK10.1	KKKKKK (23-28) VLFIWI (532-537)	11.969 0.051	VSDLVII (76-82) DENNINN (196-202)	1.171 0.853
FIKK10.2	NKKRKK (124-129) GIIGLI (443-448)	6.176 0.034	KLYKVVY (1591-597) NNNTNNN (601-607)	1.171 0.795
FIKK11	DKKKKK (77-82) LFLILL (14-19)	9.406 0.049	CLFESCV (421-427) NDDNKNN (212-218)	1.202 0.824
FIKK12	KKKKKK (420-425) VLFIWI (491-496)	10.816 0.046	LLYLLFL (19-25) DNNKGNK (59-65)	1.215 0.847
FIKK13	QEERKK (464-469) LGIFFI (482-487)	6.663 0.049	LLYIFLL (26-32) NNMNEKN (289-295)	1.201 0.816
FIKK14	RRERKK (526-531) LLIFVI (59-64)	8.545 0.035	LLLLIFV (57-63) MDDDDDD (405-411)	1.232 0.860

Additionally, the potential of these epitopes to elicit B-cell immune responses was evaluated using the Kolaskar and Tongaonkar antigenicity method [24]. Notably, the FIKK proteins exhibited the most antigenic epitope with scores above the set threshold of 1, as shown in Table 5.3. Among the predicted epitopes, amino acid positions 25-VFVFLCC-31 of the protein FIKK4.1 with the highest of 1.289 and amino acid positions 164-DNNNNNN-170 of the protein FIKK9.3 with lowest scores of 0.789 were recorded.

Using the B-Cell predictive server [18], the epitopes were predicted for the 21 FIKK kinase proteins, among which most of the predictive scores were 12mer peptides. The most

potentially antigenic B-cell epitopes predicted were those with predictive values >0.5 and the least <0.5 are presented in Table 5.4. Among the predicted epitopes, amino acid positions 306-NGNENGNENGNG-317 of the protein FIKK9.7 with the highest of 0.754 and amino acid positions 55-ILFTLTFLF-63 of the protein FIKK10.2 with lowest scores of 0.154 were recorded.

Table 5.4: Predicted linear B-cell epitopes of antigenic FIKK proteins of *P. falciparum* (*PF3D7* strain)

FIKK NAME	SEQUENCES	EPITOPE LENGTH	B-CELL PREDICTED SCORE
FIKK1	NSDNNYNNDNNI (134-145) SFLGILYLFFYN (24-39)	12 12	0.713 0.213
FIKK3	KYKKMKIKDPMRNLNY (493-509) CTVTFLGILYFILIFS (53-68)	16 16	0.686 0.191
FIKK4.1	NNKNSKSYN (170-178) VFVFLCCFL (25-33)	9 9	0.705 0.157
FIKK4.2	NKKNQVKNKNES (31-42) FFIIYFLFIIPL (56-67)	12 12	0.705 0.275
FIKK5	RKLRHVQETKGL (443-504) SFVSVLIFSLLV (51-62)	12 12	0.686 0.207
FIKK7.1	KKLDSVHNFEMN (412-423) SILIIFLILYLR (22-33)	12 12	0.682 0.208
FIKK7.2	KSITDQEER (431-439) MPILVVMDK (1-9)	9 9	0.695 0.201
FIKK8	NNNNNNINNNSN (1012-1023) FVMEATALAFLN (1157-1168)	12 12	0.731 0.231
FIKK9.1	DVNNEEDNN (107-115) LIFASLIIV (9-17)	9 9	0.696 0.170
FIKK9.2	KKKKDGSNKNKK (113-124) TIILVYTYLFHL (58-69)	12 12	0.649 0.197
FIKK9.3	TEKIRNPYTSLR (521-532) VLFLFLLNVIIY (6-17)	12 12	0.725 0.159
FIKK9.4	NKNNENLNA (179-187)	9 9	0.706 0.156

	LLVISLYFF (32-40)		
FIKK9.5	NNDYNSFTH (17-25) MELICVFFM (3-8)	9 9	0.686 0.200
FIKK9.6	KRYVEVGTK (476-484) LGIVFIAIW (514-522)	9 9	0.692 0.228
FIKK9.7	NGNENGNENGNG (306-317) YVMEAVVSAFLS (242-253)	12 12	0.754 0.201
FIKK10.1	TNNLRHLKNMNG (455-466) WFVLGTLYFFLS (55-66)	12 12	0.688 0.204
FIKK10.2	DEKKSFLFQ (767-775) ILFTLTFLF (55-63)	9 9	0.686 0.154
FIKK11	KLNGENTGI (126-134) WFLFLILLN (12-20)	9 9	0.691 0.180
FIKK12	KKLREKNIT (451-463) YFLWLLYLL (15-22)	9 9	0.703 0.204
FIKK13	TNKLRHKEKLNS (407-418) FIVGLLYIFLLN (22-33)	12 12	0.702 0.168
FIKK14	KEYRKMKVSSPF (506-517) LLLLIFVILTIG (57-68)	12 12	0.680 0.163

Each parameter used to characterize the selected epitopes including hydrophilicity, surface flexibility, surface accessibility, and antigenicity has been graphically illustrated in Supplementary Figures S1–S5 (Annexure 1), corresponding to their respective data in Tables 5.2-5.4. Along with this a detailed summary of predicted epitope characteristics having antigenicity using VaxiJen score (v2.0) was provided in Supplementary Table 1 (Annexure 1) for all 21 FIKK kinases to support its selection.

5.3.3 Computational Prediction of T-Cell Immunogenicity in *P. falciparum* FIKK Kinase(s)

The binding affinities of MHC class I molecules were scored against HLA alleles, prioritizing the most common haplotypes across diverse populations to identify potential T-cell epitopes. The analysis provided binding affinities and percentile ranks for major HLA class I super types, including HLA-A*01:01*, *HLA-A*02:01, HLA-A*03:01*, *HLA-A*24:02, HLA-B*07:02*, *HLA-B*08:01, HLA-B*27:05*, *HLA-B*40:01, HLA-B*58:01*, *and HLA-B*15:01, which together represent

the majority of class I alleles found in the human population [22]. Among the identified MHC class I epitopes, the two highest-ranked epitopes with highest binding affinity were selected (Table 5.5). The class II T-cell epitope clusters were identified based on their ability to bind multiple HLA-DRB1 alleles, including HLA-DRB1*03:01*, *HLA-DRB1*07:01, HLA-DRB1*15:01*, *HLA-DRB3*01:01, HLA-DRB3*02:02*, *HLA-DRB4*01:01, and HLA-DRB5*01:01.

Table 5.5: Prediction of potential T-cell epitopes (MHC-I binding predictions) of FIKK kinases of *P. falciparum* 3D7 strain (PF3D7).

FIKK NAME	MHC-I BINDING PREDICTIONS			
	ALLELE	T- CELL EPITOPE	BINDING AFFINITY	RANK
FIKK1	HLA-A*11:01	KSAPVYTTK (471-479)	0.96	0.01
	HLA-B*15:01	KQYDLMKEY (306-314)	0.98	0.01
FIKK3	HLA-A*11:01	KTMKFFIKK (275-283)	0.99	0.01
	HLA-B*40:01	TEYDGEYLL (297-305)	0.98	0.01
FIKK4.1	HLA-A*24:02	YYPGIAPKF (335-343)	0.99	0.01
	HLA-B*57:01	KTREEIIIF (4-12)	0.98	0.01
FIKK4.2	HLA-A*01:01	YSDSDVEYDY (171-180)	0.98	0.01
	HLA-B*44:03	EENSEEIRKY (120-129)	0.99	0.01
FIKK5	HLA-A*11:01	AVTSAFLTK (300-308)	0.96	0.01
	HLA-B*44:03	EEIKDKTIY (190-198)	0.98	0.01
FIKK7.1	HLA-A*68:01	DIFDFIIKR (620-628)	0.98	0.01
	HLA-B*58:01	SAYTPPECW (716-724)	0.97	0.01
FIKK7.2	HLA-A*01:01	RSDPSYDLQY (470-479)	0.98	0.01
	HLA-B*15:01	KQYKLMNEY (215-223)	0.98	0.01
FIKK8	HLA-A*01:01	YIDKNGSKY (563-571)	0.97	0.01
	HLA-B*44:03	NEEDIFMKY (231-239)	0.97	0.01
FIKK9.1	HLA-A*03:01	KVYPKVFNK (328-336)	0.99	0.01
	HLA-B*51:01	EPLKYLHSI (435-443)	0.92	0.01
FIKK9.2	HLA-A*24:02	KYHPGITPKF (236-245)	0.98	0.01
	HLA-B*40:01	SELKGLNEL (257-265)	0.98	0.01
FIKK9.3	HLA-A*01:01	TTDSTKFHIY (94-103)	0.99	0.01
	HLA-B*57:01	KALELTRKW (591-599)	0.99	0.01
FIKK9.4	HLA-A*03:01	RIYDNGMNK (145-153)	0.99	0.01
			0.99	0.01

	HLA-B*44:03	SENKIIYNW (205-213)		
FIKK9.5	HLA-A*02:03	KLINKLHQV (346-354)	0.99	0.01
			0.98	0.01
	HLA-B*44:03	KEINNIKNY (74-82)		
FIKK9.6	HLA-A*24:02	RYVEVGTKF (477-485)	0.98	0.01
			0.99	0.01
	HLA-B*51:01	FPFEYLQEI (485-493)		
FIKK9.7	HLA-A*03:01	KIYKELKITK (485-494)	0.95	0.01
			0.99	0.01
	HLA-B*57:01	MSVENVFNW (138-146)		
FIKK10.1	HLA-A*11:01	SVFTHVFEK (102-110)	0.99	0.01
			0.98	0.01
	HLA-B*15:01	KQFELMNAY (288-296)		
FIKK10.2	HLA-A*02:01	GLIPKLYKV (587-595)	0.99	0.01
			0.98	0.01
	HLA-B*15:01	KQYKLMNEY (552-560)		
FIKK11	HLA-A*01:01	LTDRKIFEY (23-31)	0.99	0.01
			0.99	0.01
	HLA-B*40:01	YEYNGINKL (43-51)		
FIKK12	HLA-A*02:03	FLSEHHPGI (276-284)	0.96	0.01
			0.99	0.01
	HLA-B*57:01	LSCYPSTKSW (524-533)		
FIKK13	HLA-A*24:02	YYPGITPKF (271-279)	0.99	0.01
			0.99	0.01
	HLA-B*08:01	YIKRKKNTL (337-345)		
FIKK14	HLA-A*03:01	KVVKKVMKK (239-247)	0.98	0.01
			0.98	0.01
	HLA-B*44:03	QEHQNYIKY (374-382)		

These specific alleles were chosen because they represent the most common HLA molecules within each HLA-DRB1 supertype and collectively account for over 95% of the human population globally, eliminating the need to analyze every individual haplotype [23]. Among the identified MHC class II epitopes, the two highest-ranked epitopes with highest binding affinity were selected (Table 5.6). Now the overlapping residues that constitute linear B-cell epitopic peptides with the T-cell predicted epitopes were shortlisted based on the threshold value of >0.5 from Table 5 and Table 6 for the 6 selected proteins as FIKK7.1 (205-KNKEDVLLNK-214, & 243-QLKGNTLITT-252), FIKK8 (532-HEIDDNGYII-541, & 572-NVDISNDLF-580), FIKK9.1 (77-GIIFKSTKEK-86), FIKK9.3 (67-KDVRNDYMND-76), FIKK9.7 (2-LILYFYLIIL-11, 46-FFSRIVNKIH-55, 65-TKYIKEIIYK-74, & 81-INFCKDFSSD-90) and FIKK13 (21-TFIVGLLYIF-30, & 119-GCSDINFLDR-128) having the greater binding affinity.

Table 5.6: Prediction of potential T-cell epitopes (MHC-II binding predictions) of FIKK kinases of *P. falciparum* 3D7 strain (PF3D7).

FIKK NAME	MHC-II BINDING PREDICTIONS			
	ALLELE	T- CELL EPITOPE	BINDING AFFINITY	RANK
FIKK1	HLA-DRB1*15:01	ERKIYYFDVRSADKY (536-550)	0.91	0.08
	HLA-DRB4*01:01	LKVILKQLLDENNRK (599-613)	0.88	0.09
FIKK3	HLA-DRB1*15:01	MYNIKLLKNEKIEVN (167-181)	0.90	0.13
	HLA-DRB3*02:02	FLNEYHPNIAPKFYK (319-333)	0.91	0.05
FIKK4.1	HLA-DRB1*15:01	NSAPIYTYNNRHLKG (464-478)	0.94	0.01
	HLA-DRB5*01:01	GEDVFKYVKNKRKEG (397-411)	0.97	0.01
FIKK4.2	HLA-DRB1*15:01	SEEIRKYLSDKTKKR (171-180)	0.94	0.04
	HLA-DRB3*02:02	YDNYFININKKNQVK (23-37)	0.95	0.01
FIKK5	HLA-DRB3*01:01	KKKKIIYDSLNLLIR (391-405)	0.74	0.26
	HLA-DRB5*01:01	QKMFKTIIDPKKENA (245-259)	0.81	0.11
FIKK7.1	HLA-DRB3*02:02	NKEYIKDENKKFQNI (533-547)	0.95	0.05
	HLA-DRB5*01:01	KMKFRKSKNEKKNEQ (67-81)	0.86	0.06
FIKK7.2	HLA-DRB1*03:01	TSHNILISDKHEIRL (355-369)	0.95	0.19
	HLA-DRB3*02:02	EGEYIINAENYVMEA (224-238)	0.86	0.01
FIKK8	HLA-DRB3*01:01	GSKYNVDISNDLFKK (568-582)	0.96	0.01
	HLA-DRB5*01:01	EEEYEKLGNERRDVQ (215-223)	0.89	0.03
FIKK9.1	HLA-DRB1*07:01	DGEYMYTKDNFVMEA (563-571)	0.97	0.01
	HLA-DRB3*01:01	LDTFRVTKSWPEDIK (231-239)	0.97	0.01
FIKK9.2	HLA-DRB1*15:01	FCDIDIFKNELIKIR (267-281)	0.92	0.08
	HLA-DRB5*01:01	YSEIKIIAPFHKNVE (22-36)	0.79	0.13
FIKK9.3	HLA-DRB1*03:01	TNIILNDKIFERYNR (94-103)	0.94	0.11
	HLA-DRB3*01:01	KTNIISDLEQEIKNK (591-599)	0.80	0.17
FIKK9.4	HLA-DRB3*02:02	DYKYLWNKADSLEDN (538-552)	0.92	0.05
	HLA-DRB5*01:01	GGIYRDISENERKKI (393-407)	0.78	0.16
FIKK9.5	HLA-DRB1*15:01	INNIKNYENNLYCNH (76-90)	0.88	0.17
	HLA-DRB3*02:02	EPYFKENIIENVNYV (114-128)	0.69	0.38
FIKK9.6	HLA-DRB3*02:02	ESHLYLNSSPSTSHS (147-161)	0.88	0.10
	HLA-DRB4*01:01	LKRILRQLLDLDRRK (562-576)	0.85	0.11
FIKK9.7	HLA-DRB1*15:01	GNAIRSYENNIPNLN (335-349)	0.93	0.04

	HLA-DRB3*02:02	IRSYENNIPNLNVFN (338-352)	0.95	0.01
FIKK10.1	HLA-DRB3*02:02	SDNYYINGVKYSDWK (225-239)	0.85	0.12
	HLA-DRB5*01:01	PKLYKILYEPEKKEY (326-340)	0.82	0.10
FIKK10.2	HLA-DRB3*01:01	SVKYDSDESEELSEA (362-376)	0.93	0.08
	HLA-DRB5*01:01	NEKIELVNGNSKDKG (233-247)	0.85	0.08
FIKK11	HLA-DRB3*02:02	NGEYLVNAENYVMEA (242-256)	0.89	0.07
	HLA-DRB5*01:01	FDKFVIAKNWPKEFK (518-532)	0.92	0.01
FIKK12	HLA-DRB1*07:01	ITDPFEHVKTISMQR (458-472)	0.94	0.07
	HLA-DRB5*01:01	FKTFQSLVSYDRPSK (32-46)	0.88	0.04
FIKK13	HLA-DRB3*01:01	YEGEYLIDKENYVME (247-261)	0.97	0.01
	HLA-DRB5*01:01	DHKTYKSIINSKKGN (206-220)	0.92	0.01
FIKK14	HLA-DRB1*15:01	GRNIRIYMTIHGGPP (680-694)	0.96	0.02
	HLA-DRB5*01:01	VEYFIYSNSNLKKNN (374-382)	0.88	0.04

5.3.4 Screening and Selection of Suitable FIKK Kinase(s) based on Physico-Chemical Properties of B- & T-Cell Epitopes.

A total of 12 peptides were shortlisted from the 6 selected proteins of FIKK7.1, FIKK8, FIKK9.1, FIKK9.3, FIKK9.7 AND FIKK13 based on its characteristic surface accessibility with a B-Cell predictive score. These were cross-referenced with overlapping residues that constitute linear B-cell epitopic peptides predicted by the Emini Surface Accessibility [21] and Kolaskar & Tongaonkar Antigenicity methods [24] and later with T-cell predicted epitopes. Relatively, we checked for surface accessibility and antigenic properties possessed by the B-cell epitopes predicted for the respective FIKK proteins (Figure 5.3).

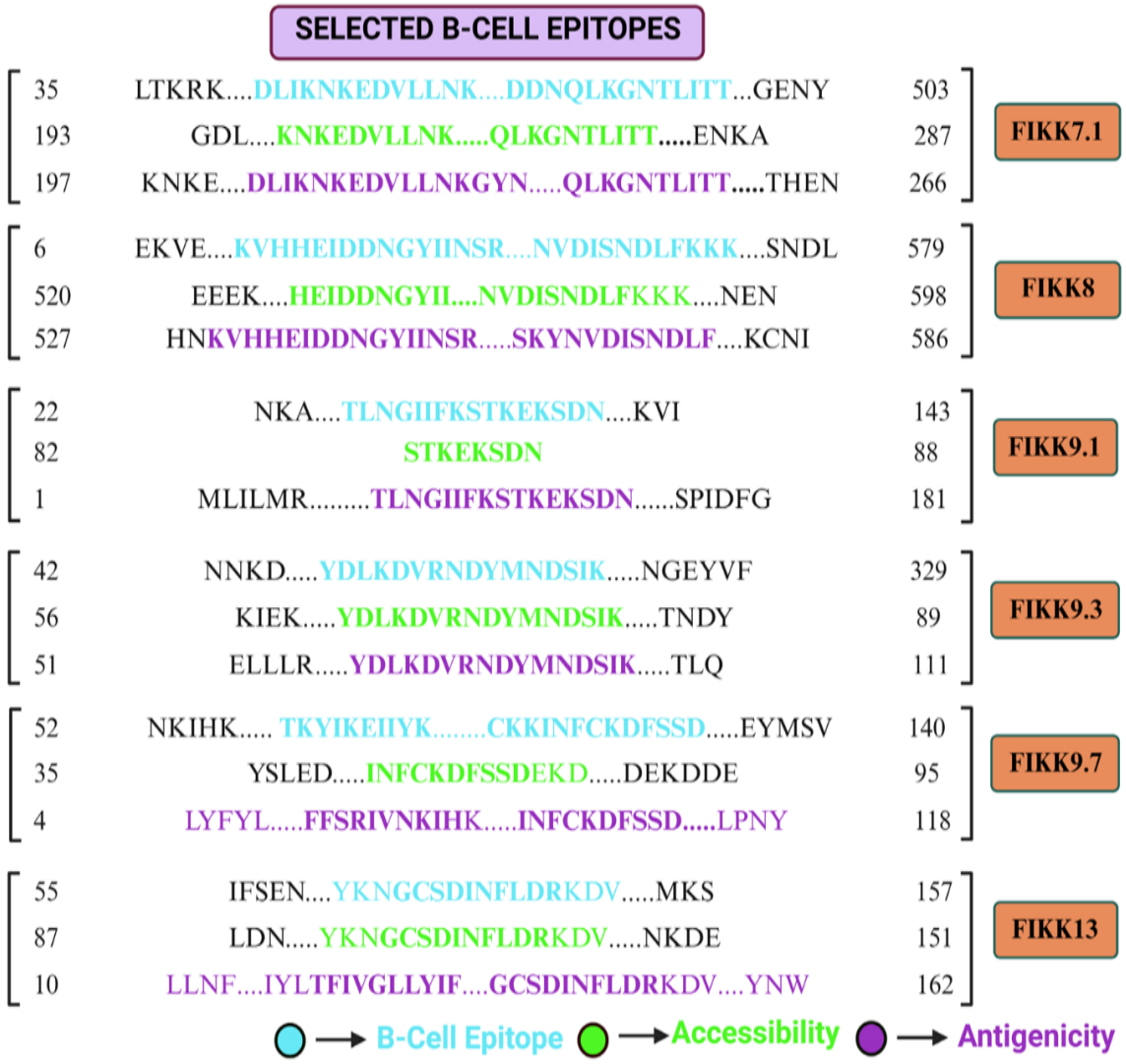

Figure 5.3: B-Cell Epitope analysis of different FIKK kinases. Sequential and overlapping analysis of predicted linear B-cell epitopes to identify their surface accessibility and antigenic potential.

The overlapping residues that constitute of B-cell epitopic peptides with T-cell epitopes (MHC-I & MHC-II) for the selected FIKK proteins are shown in the Figure 5.4. Now these selected epitopes having highest antigenicity were incorporated into a *chimeric*-FIKK (C-FIKK) design, which was expressed in *E. coli* strains, purified, and used to generate polyclonal antibodies in rabbits that subsequently was characterized to evaluate their sensitivity and specificity in detecting *P. falciparum*.

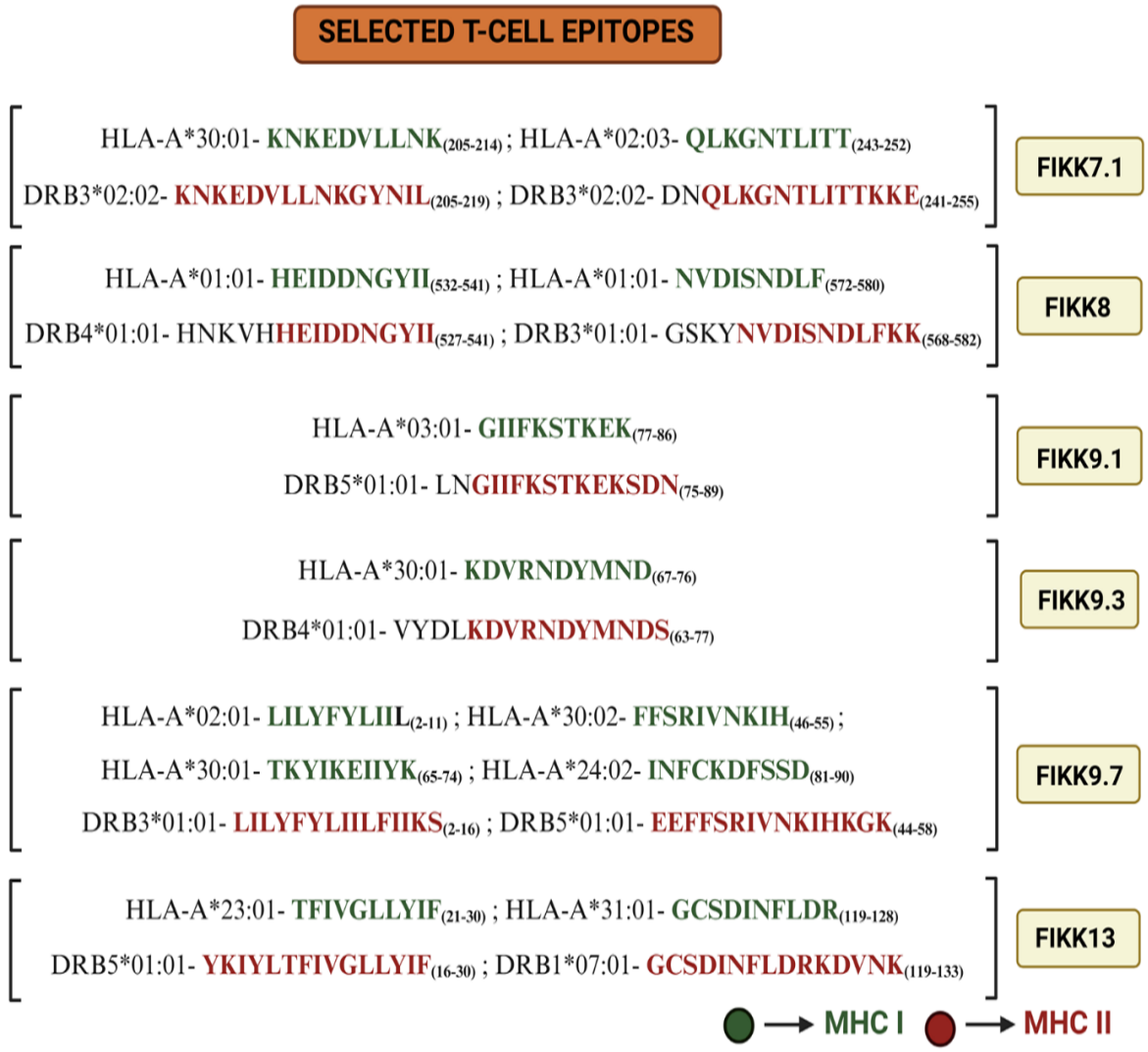

Figure 5.4: T-Cell Epitope analysis of different FIKK kinases. Sequential and overlapping analysis of predicted linear T-cell epitopes to identify potential MHC-1 & II with greater binding affinities.

5.3.5 Computational Design of *Chimeric*-FIKK and Plasmid Assembly

Now the shortlisted epitopes from the selected FIKK kinases having highest antigenicity of the overlapping residues in both B-cell and T-cell epitopes were incorporated into a *chimeric*-FIKK (C-FIKK) design. The chimeric construct was generated by fusing peptides from six selected FIKK kinases (FIKK7.1, FIKK8, FIKK9.1, FIKK9.3, FIKK9.7 and FIKK13) using appropriate peptide linkers (Figure 5.5). The recombinant gene sequence (575 bp) was codon-optimized for *E. coli* expression to enhance expression efficiency. The optimized gene was synthesized (by Gene Script) and was directly cloned into the pET28a (+) expression vector.

Now it can be expressed in *E. coli* strains, purified, and used to generate polyclonal antibodies in rabbits that subsequently can be characterized to evaluate their sensitivity and specificity in detecting *P. falciparum*.

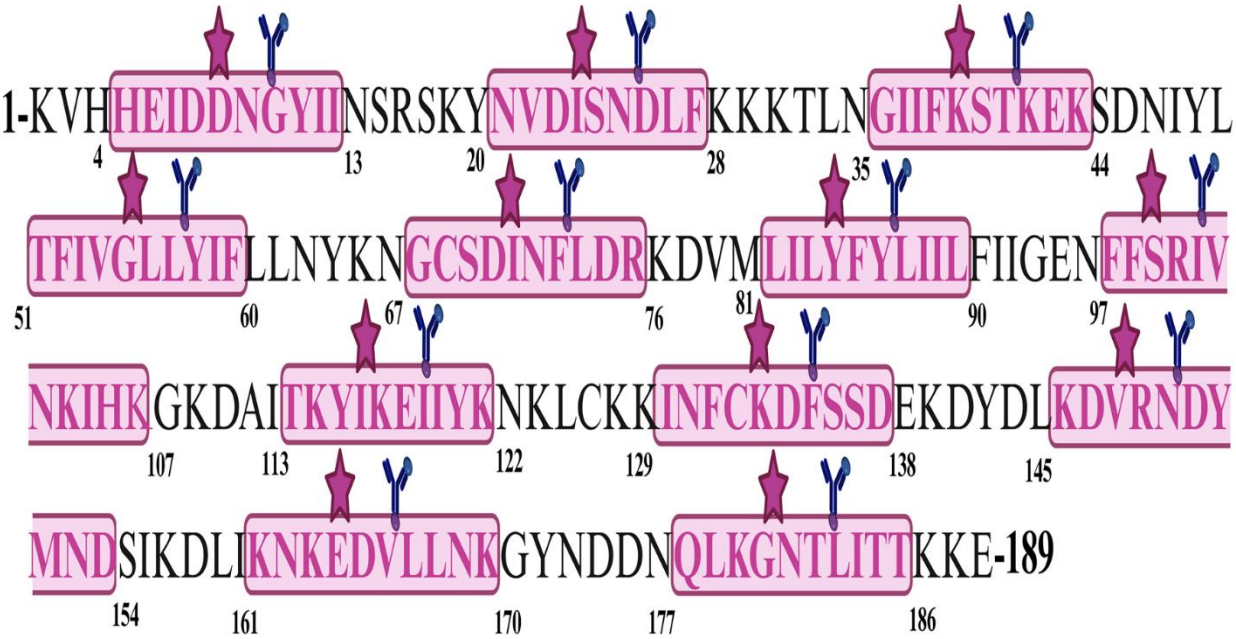

Figure 5.5: Construction of *Chimeric*-FIKK kinase. The amino acid sequence of the chimeric FIKK prepared by taking amino acids sequences selected from different FIKK proteins based on the physicochemical properties of B-cell epitope and T-Cell epitope.

5.4 DISCUSSION

This study systematically characterized the immunogenic and diagnostic potential of the FIKK kinase protein family in *P. falciparum*, addressing key limitations in conventional malaria diagnostic strategies. Through a rigorous bioinformatics pipeline, 21 FIKK kinases were analyzed for conserved, unique, and immunodominant regions based on sequence homology, antigenicity, and MHC binding properties. The findings demonstrate that FIKK kinases harbor multiple antigenic determinants, both B- and T-cell epitopes that are structurally accessible, immunogenic, and distinguishable from human homologs and other *Plasmodium* species.

The sequence alignment using PSI-BLAST revealed three major domains across most of the FIKK kinases: An N-terminal region with species-specific sequences unique to *P. falciparum*, a central domain conserved across *Plasmodium* species, and a C-terminal region with homology to human proteins (Table 5.1; Figure 5.2). This domain-specific classification is crucial for identifying diagnostic epitopes that are both species-specific and free from cross-reactivity with host proteins, a common limitation in HRP2- and pLDH-based diagnostics (Mens et al., 2006; WHO, 2022).

Using IEDB-based algorithms, high-scoring linear B-cell epitopes were identified, characterized by their surface accessibility, flexibility, hydrophilicity, and antigenicity (Emini et al., 1985; Karplus,P et al 1985; Parker et al., 1986; Kolaskar & Tongaonkar, 1990). Notable findings include FIKK10.2, which showed the highest hydrophilicity score (10.00 at residues 217–223), and FIKK10.1, with the highest surface accessibility (11.969 at residues 23–28) (Tables 2–3). The overlapping of high surface-accessibility and antigenicity in regions devoid of human or inter-species homology confirms their utility as safe and effective diagnostic targets. Further refinement using BepiPred 2.0 allowed the identification of linear B-cell epitopes ranging from 9 to 16 amino acids with predictive scores above 0.7—indicative of strong antigenic potential (Jespersen et al., 2017). Among these, the peptide NGNENGNENGNG (FIKK9.7) showed the highest BepiPred score (0.754), signifying a strong candidate for antibody-based detection (Table 4).

T-cell immunogenicity was evaluated using NetMHCpan EL 4.1, which highlighted high-affinity peptide binding to common HLA class I and II alleles, covering >95% of the global population (Reynisson et al., 2020; Southwood et al., 1998). The MHC-I epitope 471-KSAPVYTTK-479 (FIKK1) and the MHC-II epitope 247-YEGEYLIDKENYVME-261 (FIKK13) both exhibited top-ranking binding affinities across diverse HLA subtypes (Tables 5–6). These epitopes were further cross-matched with B-cell epitopes to identify overlapping sequences, maximizing diagnostic sensitivity through both humoral and cell-mediated immune

recognition. Based on these analyses, six FIKK kinases of FIKK7.1, FIKK8, FIKK9.1, FIKK9.3, FIKK9.7, and FIKK13 were shortlisted for chimeric construct design. Twelve overlapping epitope regions were fused using peptide linkers to form a single *chimeric*-FIKK (C-FIKK) construct (Figure 5). The construct was codon-optimized for *E. coli* expression using the OPTIMIZER tool (Puigbò et al., 2007), facilitating downstream polyclonal antibody generation and enabling compatibility with immunoassay platforms such as dot-blot or lateral-flow devices.

The integration of high-throughput in silico epitope prediction and rational chimeric design overcomes critical challenges in current malaria diagnostics. These advantages position the FIKK-based diagnostic system as a robust alternative to HRP2-based tests, which suffer from deletions and false-negative results (Gatton et al., 2020). Moreover, the potential to detect conserved but immunogenic epitopes offers utility in mixed infections and low-parasitemia settings, where conventional RDTs underperform. Thus this chapter validates the utility of the FIKK kinase family as a rich source of antigenic markers and supports the development of a novel, multi-epitope chimeric diagnostic antigen for advanced detection of *P. falciparum*. Future experimental validation of C-FIKK in clinical settings and comparison with standard diagnostics will determine its translational potential in endemic and resource-limited regions.

5.5 REFERENCES:

1. Mens, P.F., et al. (2006). Detection of *Plasmodium falciparum* DNA in saliva samples from malaria patients using nested PCR. *Trans R Soc Trop Med Hyg*, 100(7), 669–671.
2. Gatton, M.L., et al. (2020). Implications of PfHRP2 and PfHRP3 gene deletions for malaria rapid diagnostic tests. *Lancet Infect Dis*, 20(5), e133–e142.
3. Wongsrichanalai, C., et al. (2007). A Review of Malaria Diagnostic Tools: Microscopy and RDTs. *Am J Trop Med Hyg*, 77(6 Suppl), 119–127.
4. Moody, A., *Rapid diagnostic tests for malaria parasites.* Clinical microbiology reviews, 2002. **15**(1): p. 66-78.
5. Cunningham, J., et al., *A review of the WHO malaria rapid diagnostic test product testing programme (2008–2018): performance, procurement and policy.* Malaria journal, 2019. **18**: p. 1-15.
6. Zimmerman, P.A. and R.E. Howes, *Malaria diagnosis for malaria elimination.* Current opinion in infectious diseases, 2015. **28**(5): p. 446-454.
7. Murray, C.K., et al., *Update on rapid diagnostic testing for malaria.* Clinical microbiology reviews, 2008. **21**(1): p. 97-110.
8. Poti, K.E., et al., *HRP2: transforming malaria diagnosis, but with caveats.* Trends in parasitology, 2020. **36**(2): p. 112-126.
9. Ippolito, M.M., et al., *Antimalarial drug resistance and implications for the WHO global technical strategy.* Current epidemiology reports, 2021. **8**: p. 46-62.
10. Hoof, I., et al. (2009). NetMHCpan, a method for MHC class I binding prediction beyond humans. *Immunogenetics*.
11. Ward, P., et al., *Protein kinases of the human malaria parasite Plasmodium falciparum: the kinome of a divergent eukaryote.* BMC genomics, 2004. **5**: p. 1-19.
12. Nunes, M.C., et al., *Plasmodium falciparum FIKK kinase members target distinct components of the erythrocyte membrane.* PloS one, 2010. **5**(7): p. e11747.
13. Schneider, A.G. and O. Mercereau-Puijalon, *A new Apicomplexa-specific protein kinase family: multiple members in Plasmodium falciparum, all with an export signature.* BMC genomics, 2005. **6**: p. 1-12.
14. Nunes, M.C., et al., *A novel protein kinase family in Plasmodium falciparum is differentially transcribed and secreted to various cellular compartments of the host cell.* Molecular microbiology, 2007. **63**(2): p. 391-403.
15. Davies, H., et al., *An exported kinase family mediates species-specific erythrocyte remodelling and virulence in human malaria.* Nature microbiology, 2020. **5**(6): p. 848-863.
16. Balaji, S. and V. Trivedi, *Extracellular methemoglobin primes red blood cell aggregation in malaria: an in vitro mechanistic study.* FEBS letters, 2013. **587**(4): p. 350-357.
17. Prasad, M.R. and V. Trivedi, *Molecular Investigation of FIKK Kinase Family to Develop PCR-Based Diagnosis of Plasmodium falciparum.* Molecular Biotechnology, 2024: p. 1-17.
18. Jespersen, M.C., et al., *BepiPred-2.0: improving sequence-based B-cell epitope prediction using conformational epitopes.* Nucleic acids research, 2017. **45**(W1): p. W24-W29.
19. Parker, J., D. Guo, and R. Hodges, *New hydrophilicity scale derived from high-performance liquid chromatography peptide retention data: correlation of predicted surface residues with antigenicity and X-ray-derived accessible sites.* Biochemistry, 1986. **25**(19): p. 5425-5432.

20. Karplus, P. and G. Schulz, *Prediction of chain flexibility in proteins: a tool for the selection of peptide antigens.* Naturwissenschaften, 1985. **72**(4): p. 212-213.
21. Emini, E.A., et al., *Induction of hepatitis A virus-neutralizing antibody by a virus-specific synthetic peptide.* Journal of virology, 1985. **55**(3): p. 836-839.
22. Karosiene, E., et al., *NetMHCcons: a consensus method for the major histocompatibility complex class I predictions.* Immunogenetics, 2012. **64**: p. 177-186.
23. Nielsen, M., C. Lundegaard, and O. Lund, *Prediction of MHC class II binding affinity using SMM-align, a novel stabilization matrix alignment method.* BMC bioinformatics, 2007. **8**: p. 1-12.
24. Kolaskar, A.S. and P.C. Tongaonkar, *A semi-empirical method for prediction of antigenic determinants on protein antigens.* FEBS letters, 1990. **276**(1-2): p. 172-174.
25. Puigbò, P., et al. (2007). OPTIMIZER: A web server for optimizing the codon usage of DNA sequences. *Nucleic Acids Res*, 35(Web Server issue), W126–W131.
26. Southwood, S., et al. (1998). Several common HLA-DR types share largely overlapping peptide binding repertoires. *J Immunol*, 160(7), 3363–3373.
27. Reynisson, B., et al. (2020). NetMHCpan-4.1 and NetMHCIIpan-4.0: Improved predictions of MHC antigen presentation. *Nucleic Acids Res*, 48(W1), W449–W454.
28. Jespersen, M.C., et al. (2017). BepiPred-2.0: Improving sequence-based B-cell epitope prediction using conformational epitopes. *Nucleic Acids Res*, 45(W1), W24–W29.
29. Adu-Gyasi, D., et al., *Assessing the performance of only HRP2 and HRP2 with pLDH based rapid diagnostic tests for the diagnosis of malaria in middle Ghana, Africa.* PLoS One, 2018. **13**(9): p. e0203524.
30. Park, S.H., et al., *Diagnostic Performance of Three Rapid Diagnostic Test Kits for Malaria Parasite Plasmodium falciparum.* Korean J Parasitol, 2020. **58**(2): p. 147-152.
31. Kavanaugh, M.J., S.E. Azzam, and D.M. Rockabrand, *Malaria rapid diagnostic tests: literary review and recommendation for a quality assurance, quality control algorithm.* Diagnostics, 2021. **11**(5): p. 768.
32. Oyegoke, O.O., et al., *Malaria diagnostic methods with the elimination goal in view.* Parasitology research, 2022. **121**(7): p. 1867-1885.
33. Gilani, S.T.A., et al., *COMPARISON OF IMMUNOCHROMATOGRAPHY AND MICROSCOPIC FILM METHOD FOR THE DIAGNOSIS OF MALARIA IN LIBERIA.* Pakistan Armed Forces Medical Journal, 2020. **70**(4): p. 1201-05.
34. Lee, W.S., et al., *Simple, rapid, and accurate malaria diagnostic platform using microfluidic-based immunoassay of Plasmodium falciparum lactate dehydrogenase.* Nano Convergence, 2020. **7**: p. 1-8.
35. Shrivastava, D., et al., *Plasmodium falciparum FIKK9. 1 is a monomeric serine–threonine protein kinase with features to exploit as a drug target.* Chemical Biology & Drug Design, 2021. **97**(4).
36. WHO. World Malaria Report 2023.

ANNEXURE-I

Supplementary Figures:

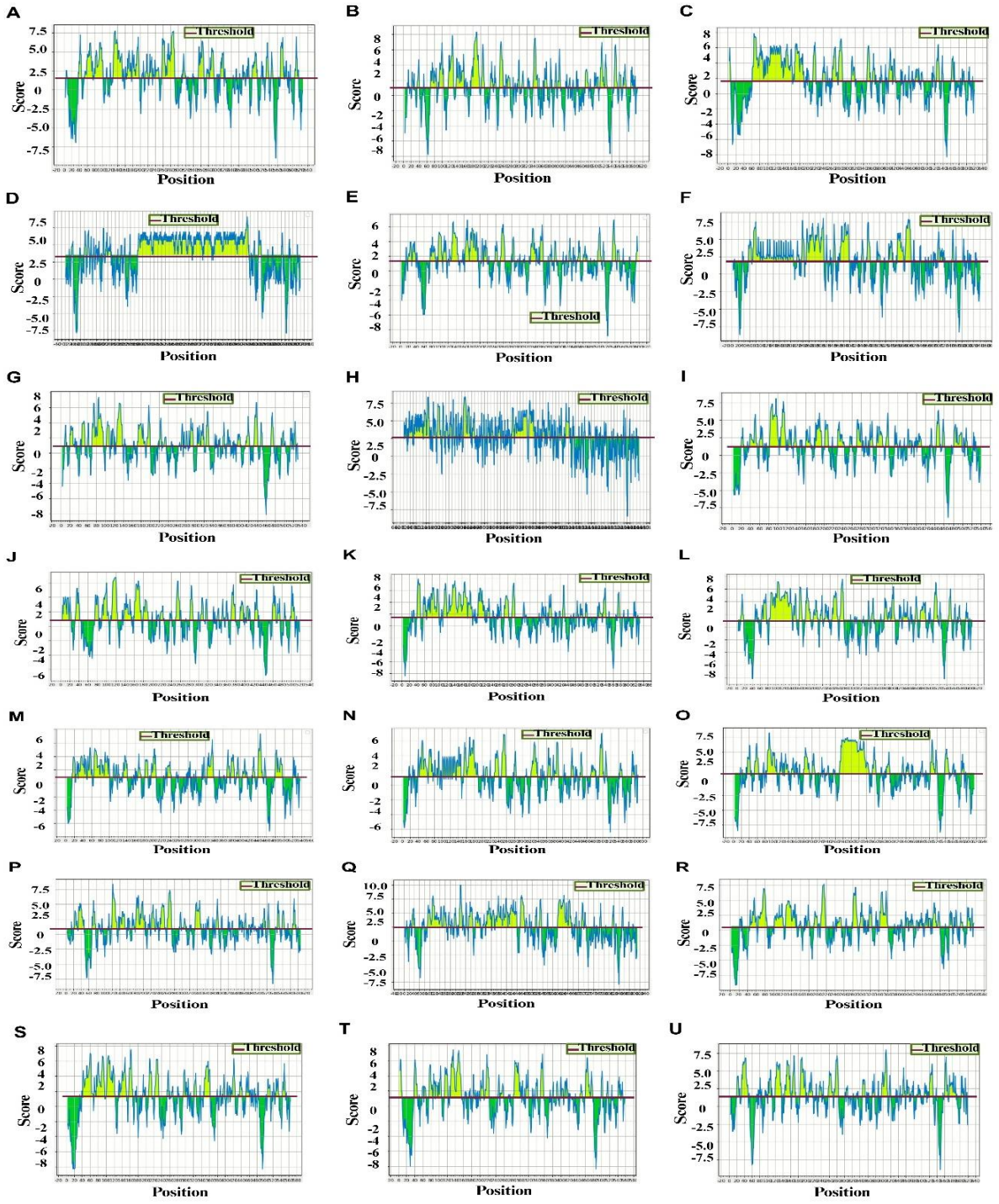

Figure S1: Graphical representation of all 21 FIKK kinase protein residues of *P. falciparum* predicted for their hydrophilicity using the Parker method.

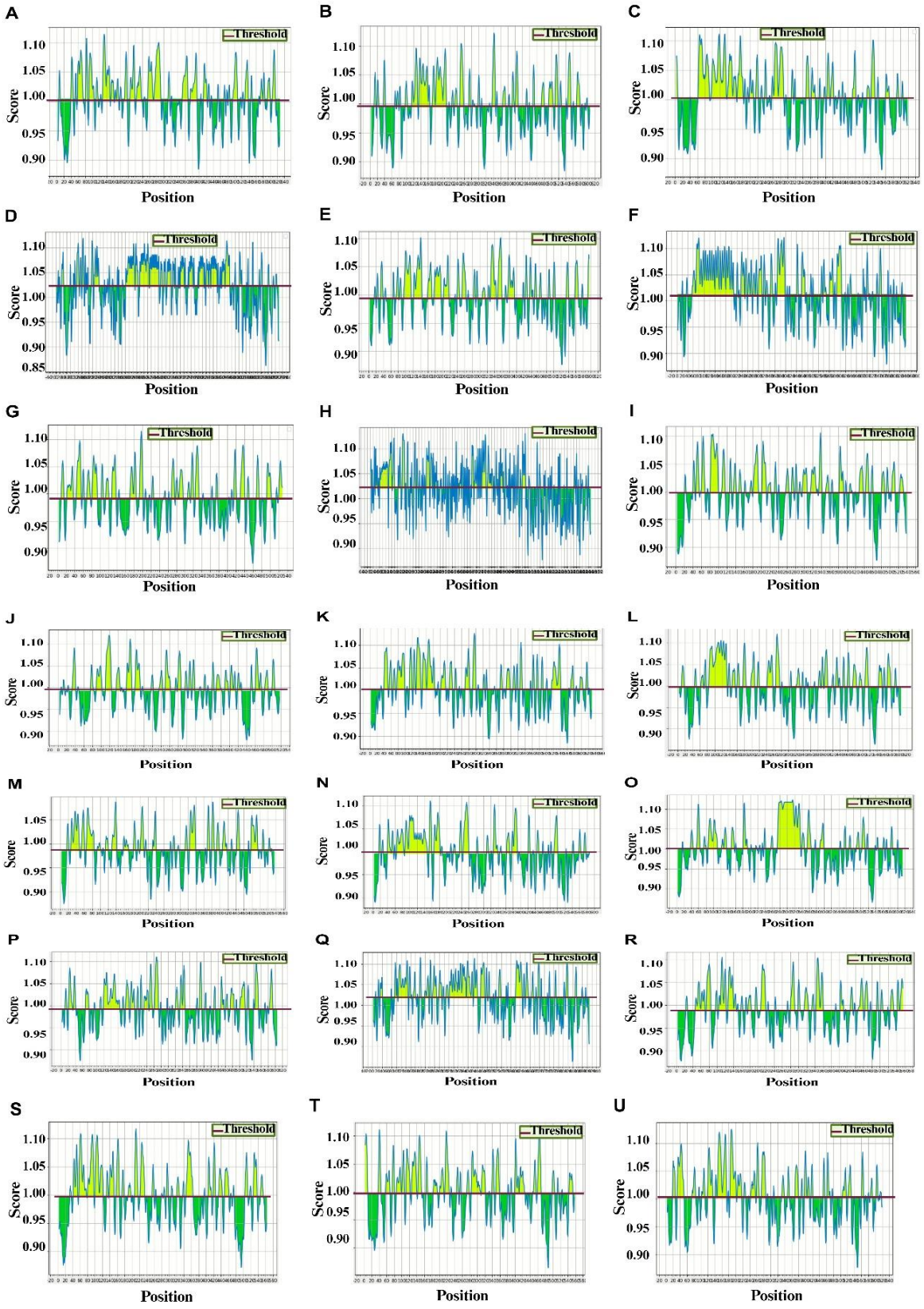

Figure S2: Graphical representation of all 21 FIKK kinase protein residues of *P. falciparum* predicted for their flexibility using the Karplus and Schulz method.

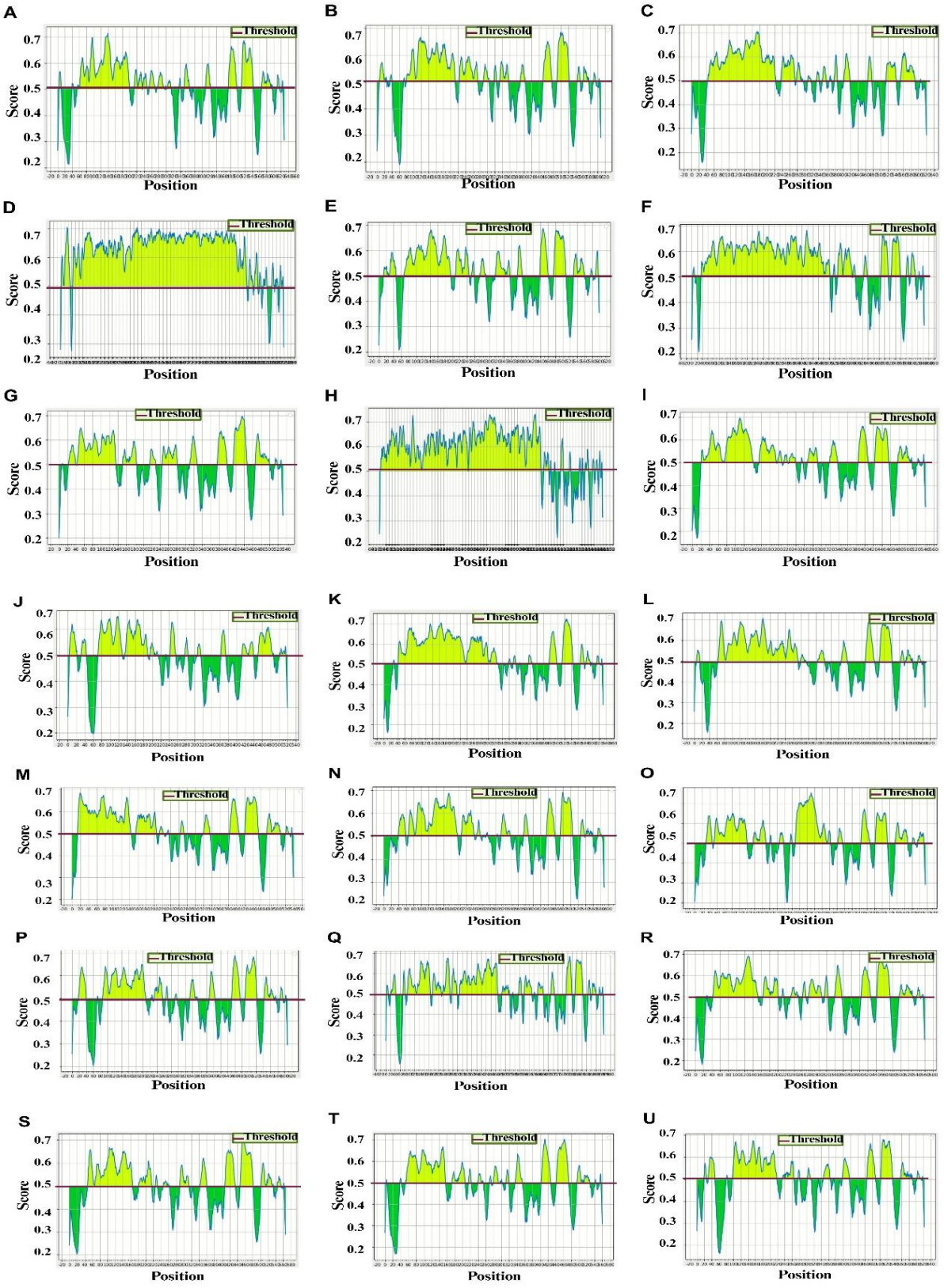

Figure S3: Graphical representation of all 21 FIKK kinase protein residues of *P. falciparum* predicted for their antigenicity using the BepiPred-2.0 method of Jespersen MC.

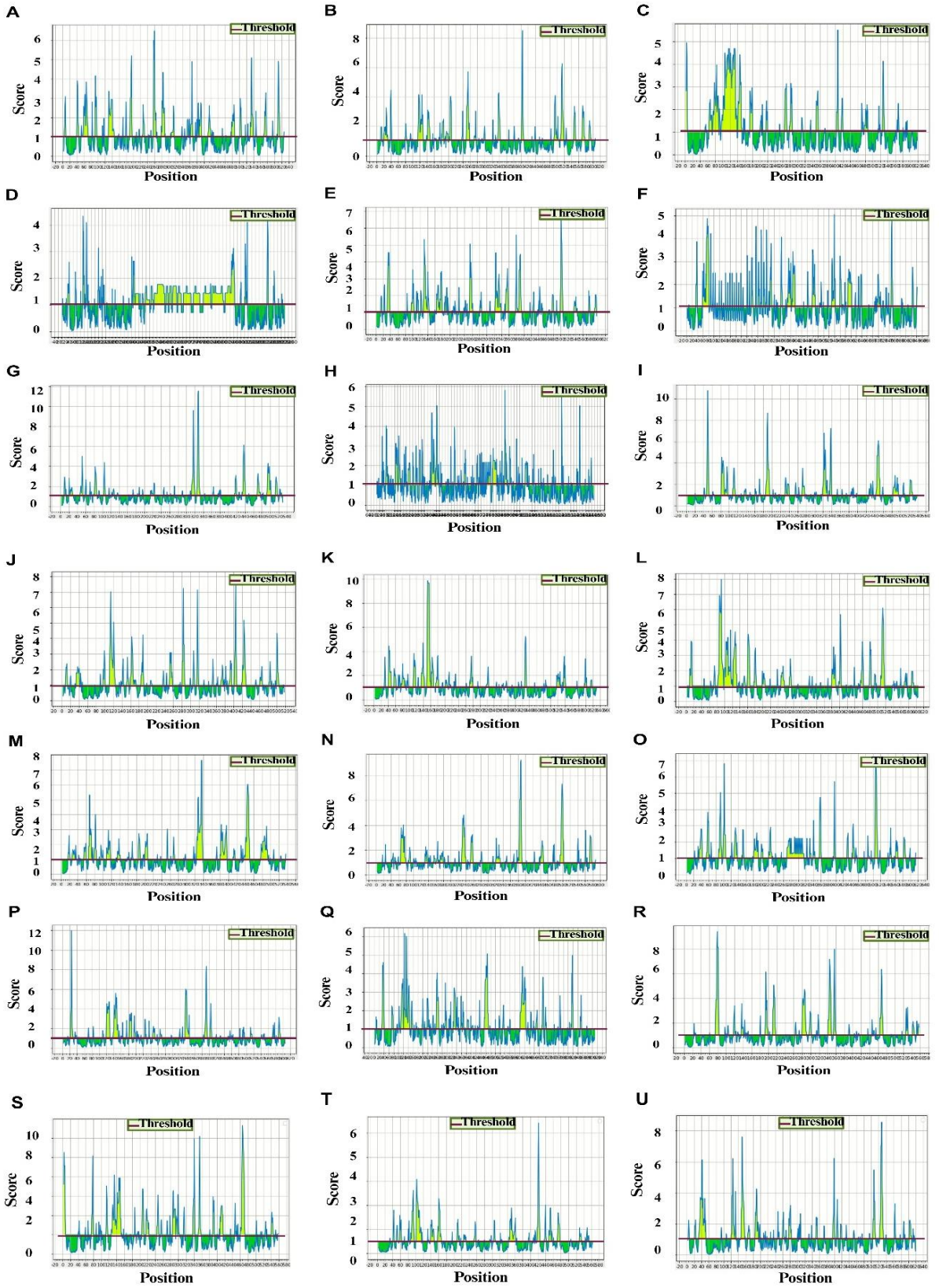

Figure S4: Graphical representation of all 21 FIKK kinase protein residues of *P. falciparum* predicted for their surface acccessibility using the Emini method

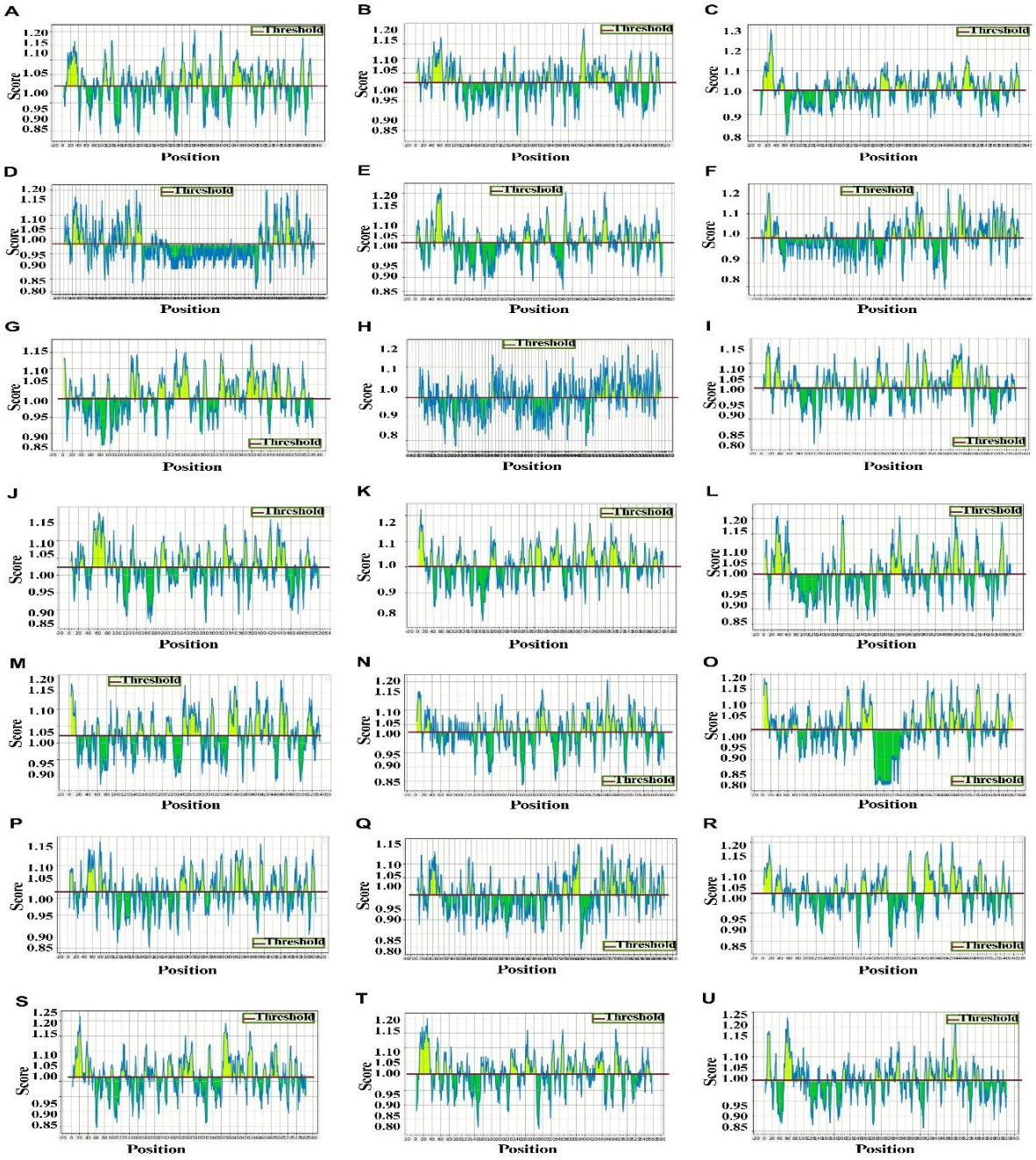

Figure S5: Graphical representation of all 21 FIKK kinase protein residues of *P. falciparum* predicted for their antigenicity using the Kolaskar & Tongaonkar antigenicity method.

Note: In each of the supplementary figures (S1, S2, S3, S4 & S5), the 21 FIKK kinase(s) are denoted as (A) FIKK1, (B) FIKK3, (C) FIKK4.1, (D) FIKK4.2, (E) FIKK5, (F) FIKK7.1, (G) FIKK7.2, (H) FIKK8, (I) FIKK9.1, (J) FIKK9.2, (K) FIKK9.3, (L) FIKK9.4, (M) FIKK9.5, (N) FIKK9.6, (O) FIKK9.7, (P) FIKK10.1, (Q) FIKK10.2, (R) FIKK11, (S) FIKK12, (T) FIKK13, and (U) FIKK14

Supplementary Table-1

The predicted antigenicity scores (VaxiJen v2.0) identified from all the 21 FIKK kinases of *P. falciparum*. VaxiJen scores >0.5 were considered probable antigens.				
FIKK Name	**Gene ID**	**VaxiJen Score (Threshold: 0.5)**	**Antigen/Non-Antigen**	**Length (AA-Amino Acids)**
FIKK1	PF3D7_0102600	0.5025	Antigen	630AA
FIKK3	PF3D7_0301200	0.4751	Non-Antigen	610AA
FIKK4.1	PF3D7_0424500	0.6539	Antigen	622AA
FIKK4.2	PF3D7_0424700	0.8825	Antigen	1222AA
FIKK5	PF3D7_0500900	0.4719	Non-Antigen	600AA
FIKK7.1	PF3D7_0726200	0.5775	Antigen	845AA
FIKK7.2	PF3D7_0731400	0.3377	Non-Antigen	1605AA
FIKK8	PF3D7_0805700	0.5880	Antigen	1457AA
FIKK9.1	PF3D7_0902000	0.4962	Non-Antigen	542AA
FIKK9.2	PF3D7_0902100	0.4568	Non-Antigen	521AA
FIKK9.3	PF3D7_0902200	0.5025	Antigen	633AA
FIKK9.4	PF3D7_0902300	0.5473	Antigen	608AA
FIKK9.5	PF3D7_0902400	0.5093	Antigen	540AA
FIKK9.6	PF3D7_0902500	0.5710	Antigen	591AA
FIKK9.7	PF3D7_0902600	0.5411	Antigen	617AA
FIKK10.1	PF3D7_1016400	0.3538	Non-Antigen	609AA
FIKK10.2	PF3D7_1039000	0.6264	Antigen	913AA
FIKK11	PF3D7_1149300	0.5271	Antigen	560AA
FIKK12	PF3D7_1200800	0.5820	Antigen	567AA
FIKK13	PF3D7_1371700	0.4006	Non-Antigen	561AA
FIKK14	PF3D7_1476400	0.4974	Non-Antigen	623AA

Chapter 6

Diagnostic Validation of *Chimeric*-FIKK in *Plasmodium falciparum* Malaria Detection

*The contents of this chapter are published as **Prasad, M. R., Kumar, D. A, Eena Dodwani, Sukhwinder Singh, & Trivedi, V.** (2025). Antigenic determinant analysis of FIKK Kinase family to identify novel candidates for diagnosis of *Plasmodium falciparum*. *Microbial Pathogenesis*

SUMMARY

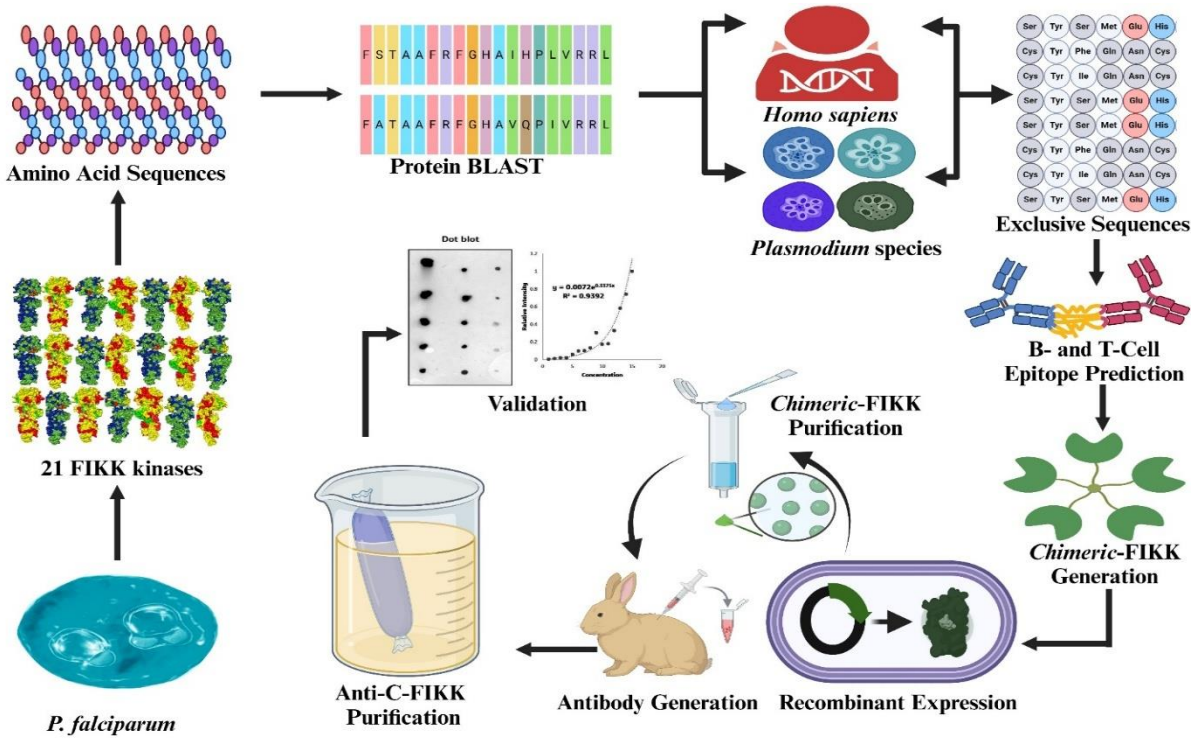

Figure: Workflow and design strategy for selecting FIKK kinases and validating C-FIKK as diagnostic targets in detection of *P. falciparum* malaria.

Malaria diagnosis remains challenging, especially in sub-Saharan Africa, where current methods like microscopy and RDTs face limitations such as low sensitivity and *Pf*-HRP2 gene deletions. Molecular techniques offer higher accuracy but are impractical in resource-limited settings. However, limitations in sensitivity, especially for low-density infections, and specificity for mixed infections underscore the need for novel biomarkers. In our study, *chimeric-FIKK* (C-FIKK) was generated as a promising target for malaria diagnosis that comprises highly immunogenic epitopes derived from the N-terminal regions of selected FIKK kinases of *P. falciparum* with no homology with the human counter parts. The polyclonal antibodies (anti-C-FIKK) that were generated, purified, and characterized for diagnostic applications demonstrated high sensitivity with a detection limit of 4 nM and exhibited remarkable specificity for *P. falciparum* in the presence of proteins from human serum, parasites culture media and few other bacterial, viral, fungal and algal organisms. These findings suggest that FIKK kinase-based rapid diagnostic tests is a robust and reliable diagnostic target for malaria detection, paving the way for the development of next-generation diagnostic systems with enhanced sensitivity and specificity.

6.1 INTRODUCTION

Effective malaria diagnosis is critical for disease management and eradication [1, 2]. While microscopy remains the gold standard, it has limitations in sensitivity, requiring skilled personnel and struggling with low-density infections [3]. Rapid diagnostic tests (RDTs) have emerged as a practical alternative [4], detecting key antigens such as *Plasmodium* lactate dehydrogenase (pLDH), histidine-rich protein II (*Pf*-HRP-II), and aldolase [5, 6]. However, RDTs face challenges, including a high detection threshold (>100 parasites/μL), limited species differentiation, failure to reliably detect co-infections, and reduced sensitivity due to *pf-hrp2* gene deletions, leading to false-negative results [7, 8]. These issues underscore the need for novel biomarkers with improved sensitivity and specificity [9, 10].

To address these limitations, we explored the potential of FIKK kinases of *P. falciparum*-specific serine/threonine protein kinases that play a critical role in parasite survival and host cell remodelling [11]. Unlike other *Plasmodium* species, which typically have a single FIKK kinase, *P. falciparum* harbours 21 FIKKs, many of which are exported into infected erythrocytes [12, 13]. These kinases possess a conserved C-terminal kinase domain and a variable N-terminal region, contributing to substrate specificity [13]. Functionally, FIKK kinases phosphorylate host cytoskeletal and membrane-associated proteins, altering erythrocyte deformability and cytoadhesion properties, which are crucial for parasite virulence and severe malaria pathogenesis [14-16]. Their absence in humans and one conserved FIKK in non-*falciparum Plasmodium* species makes them promising candidates for diagnostic and therapeutic interventions in overcoming the challenges.

Targeting *Plasmodium*-specific FIKK kinases presents a promising diagnostic approach. Unlike conventional biomarkers, FIKK kinases had shown a higher sensitivity and enhanced specificity without any cross-reactivity in *P. falciparum* detection [17]. The study had demonstrated the in-silico and in-vitro PCR analyses that FIKK-based primers selectively detected *P. falciparum* even in the presence of *P. vivax* and other pathogens, addressing the co-infection challenge in malaria diagnosis at the molecular level. The assay achieved remarkable sensitivity, detecting parasitemia as low as 0.0003%, significantly surpassing the detection limits of present PCR-based methods, RDTs and microscopy. Additionally, FIKK primers exhibited robust performance in mock patient samples contaminated with bacterial, viral, and fungal species, confirming their clinical reliability [17]. The integration of FIKK kinase-based PCR into malaria rapid diagnostic workflows could significantly enhance detection accuracy by reliably detecting co-infections with increased sensitivity particularly in resource-limited settings where mixed infections and low parasitemia complicate diagnosis [8, 17]. Moreover,

its adaptability to isothermal amplification methods like Loop-Mediated Isothermal Amplification (LAMP) and Recombinase Polymerase Amplification (RPA) could enable rapid, field-deployable testing, bridging the gap between high sensitivity and practical usability [3, 6]. Given its superior performance over existing diagnostic tools, FIKK kinase-targeted PCR holds great potential for improving malaria surveillance, guiding effective treatment, and contributing to global eradication efforts.

To further explore the translational potential of FIKK kinases from the designed *chimeric*-FIKK (C-FIKK) using IEDB tools, that identified the exclusive B-cell [18-21] and T-cell epitopes [22, 23] with high antigenicity [24] was investigated. Through extensive analysis and effective selection from all the 21 FIKK kinase proteins of *P. falciparum* and one conserved FIKK from other *Plasmodium* species causing malaria in humans that selected the FIKK7.1, FIKK8, FIKK9.1, FIKK9.3, FIKK9.7, and FIKK13 incorporating highly immunogenic peptide sequences. The recombinant C-FIKK protein was then expressed, purified, and used to generate polyclonal antibodies in rabbits. The sensitivity and selectivity of the anti-C-FIKK antibody were rigorously evaluated, showing suitability for *P. falciparum* malaria detection. The dot blot analysis revealed that the anti-C-FIKK antibody could detect as low as 4 nM of the target protein, with stable performance across multiple trials. This detection threshold is comparable to or better than traditional diagnostic methods like RDTs, which often struggle with low parasitemia detection. These findings underscore the potential of FIKK kinases as a potential diagnostic biomarker for *P. falciparum*-specific malaria detection. Beyond PCR applications, the high specificity of anti-FIKK antibodies suggests their suitability for lateral-flow immunoassays, paving the way for next-generation RDTs with improved sensitivity, species differentiation, and applicability in field settings. By bridging molecular and protein-level diagnostics, FIKK-based strategies offer a transformative approach to overcoming existing challenges in malaria detection, contributing to more effective surveillance and eradication efforts.

6.2 EXPERIMENTAL PROCEDURES

6.2.1 Materials and Strains

The various materials and reagents used in this study are comprehensively detailed in the section 3.1, with specific strains employed for the study as listed in Table 3.1 of the same section of chapter 3: Experimental Procedures.

6.2.2 Parasite culture

Plasmodium falciparum (3D7), a drug-sensitive strain is cultured as described in the section 3.3 of chapter 3: Experimental Procedures.

6.2.3 Recombinant *Chimeric*-FIKK Expression: Optimization and Analysis

C-FIKK protein expression was optimized by evaluating different *E. coli* hosts, growth media, inducer concentrations, additives, and incubation temperatures as described in the sub-sections of 3.9.1 to 3.9.7 of section 3.9 under chapter 3: Experimental Procedures.

6.2.4 Purification of *Chimeric*-FIKK and Polyclonal Antibody Generation in Rabbit

Following optimization in *E. coli* BL21(DE3) CodonPlus, C-FIKK was purified as described in the sub-section of 3.9.8 of section 3.9, and section 3.10 to 3.12 followed by protein quantification (section 3.13) and their by generating polyclonal antibody in rabbit (section 3.14) under chapter 3: Experimental Procedures.

6.2.5 Purification of Polyclonal antibody of C-FIKK by ammonium sulphate precipitation

The ammonium sulphate precipitation was carried out as detailed in the section 3.15 of chapter 3: Experimental Procedures.

6.2.6 Evaluation of purified anti-C-FIKK polyclonal antibodies titre

An ELISA (Enzyme-Linked Immunosorbent Assay) was performed to evaluate the titration of purified anti-C-FIKK polyclonal antibody [27] as detailed in the section 3.16 of chapter 3: Experimental Procedures.

6.2.7 Sensitivity of anti-C-FIKK polyclonal antibodies

The sensitivity of purified anti-C-FIKK antibody, was performed as detailed in the section 3.17 of chapter 3: Experimental Procedures.

6.2.8 Detection of parasite protein using purified anti-C-FIKK polyclonal antibody

The specificity of the anti-C-FIKK antibody was evaluated by probing them against various samples, including complete media, human serum, parasite culture media, and parasite culture as detailed in the section 3.18 of chapter 3: Experimental Procedures.

6.2.9 Selectivity of anti-C-FIKK during other infectious diseases by mocking coinfection

The selectivity of the anti-C-FIKK antibody was evaluated as described in the section 3.19 of chapter 3: Experimental Procedures.

6.3 RESULTS

6.3.1 Recombinant C-FIKK Expression

The nucleotide sequence corresponding to the chimeric-FIKK protein was optimized for expression in *E.coli* and synthetic gene was cloned into pET28a (+) and resulting clone as termed as "C-FIKK". It was transformed into DH5α, and the plasmid (C-FIKK_pET28a+) was verified for its integrity (Figure 6.1, panel A) with expected band at ~6 kb and further confirmed by PCR using insert specific primers (Figure 6.1, panel B) with expected band at ~600 bp size. The C-FIKK was transformed into BL21Codon+ and it gives low levels of C-FIKK expression (Figure 6.1, panel C) with a molecular weight of 22.31kDa (where UN-Un-Induced, IN-Induced, SP-Induced Sonicated Pellet & SS- Induced Sonicated Supernatant). The expression of C-FIKK was further confirmed by western blotting using anti-His antibodies (Figure 6.1, panel D) along with the non/un-transformed pET28a (+) vector (as control).

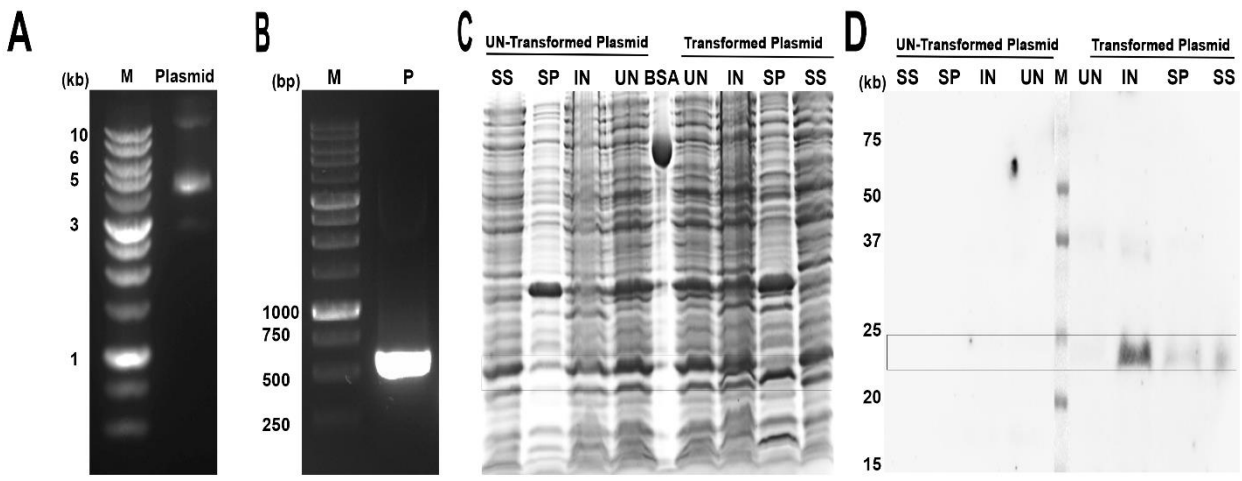

Figure 6.1: *Chimeric*-FIKK Expression. The E. coli strains of DH5α were transformed with the recombinant plasmid carrying the *c-fikk* gene (582 bp). Plasmid DNA was isolated **(A)** of size ~6 kb (~5.5 kb +582 bp) and analyzed by gel electrophoresis to verify the presence of the *c-fikk* insert **(B)**. The recombinant E. coli (in BL21(DE3) CodonPlus_pET28a+vector) was induced with 1 mM IPTG, and protein expression was confirmed through 15% SDS-PAGE analysis **(C)** of the protein lysate. The expression was confirmed by Western blotting **(D)** using anti-His antibody (1:7000 dilution), detecting the His-tagged C-FIKK protein at ~23 kDa in induced (IN), and induced supernatant (SS) lane in comparison to the non/un-transformed pET28 a (+) vector with the lanes UN-uninduced, IN-induced, SP-induced sonicated pellet and SS-induced sonicated supernatant lanes without bands and marker (M) at the centre.

6.3.2 *Chimeric* FIKK: Purification and Antibody Production

The affinity chromatography using Ni-NTA agarose was employed to purify the C-FIKK protein from the supernatant (Figure 6.2, panel A). However, due to weak binding, the protein eluted in the first wash (W1), as confirmed by western blotting. To address this, the protein was purified through electro elution from gel slices as detailed in the 'Experimental Procedures,' in chapter-3 and then recovered sample was analyzed (Figure 6.2, panel B). Further purification was achieved through ammonium sulfate precipitation of the electro eluted protein. The C-FIKK protein was fractionated to optimize precipitation at 25% saturation (Figure 6.2, panel C) and verified at subsequent steps (Figure 6.2, panel D) in the Pellet-P and Supernatant-S during ammonium sulfate precipitation. The final purified C-FIKK protein (Figure 6.2, panel E) was obtained through dialysis and confirmed by western blotting, yielding 2.8 mg of total protein after four buffer changes in 1x PBS (Phosphate Buffered Saline).

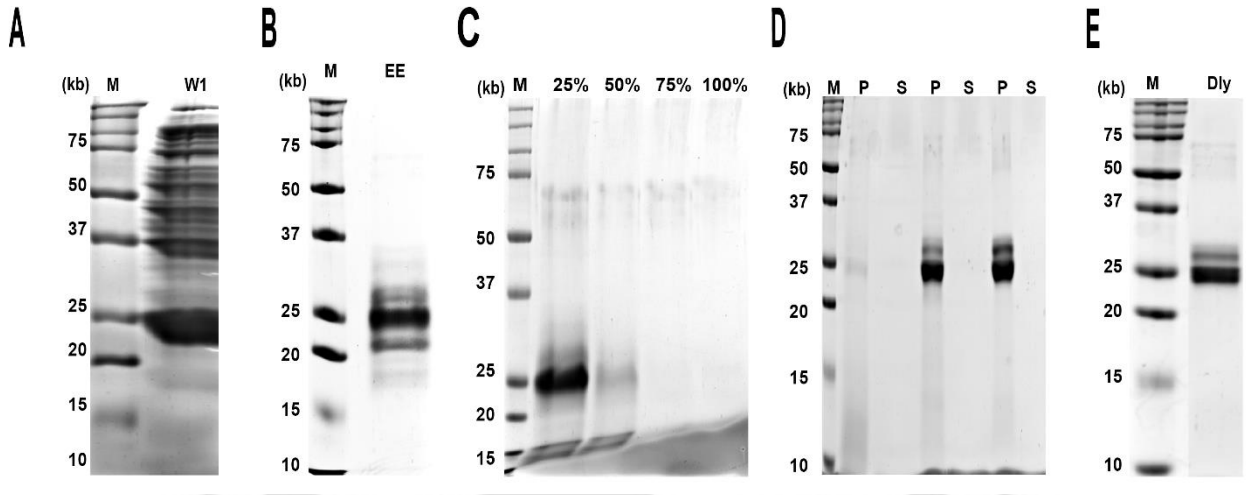

Figure 6.2: Purification, and Antibody Generation of C-FIKK. The purification of C-FIKK was performed using Ni-NTA affinity chromatography with C-FIKK weak binding and eluting in wash 1 (W1) itself **(A)** followed by EE-electroelution **(B)**, ammonium sulfate fractionation **(C)** to confirm at 25% and then precipitation **(D)** by verifying in pellet -P and Supernatant-S before going to the dialysis-Dly and final confirmation **(E).**

The serum of ~6 mL was collected post- immunization and the presence of anti-C-FIKK antibodies was confirmed using ELISA at dilutions ranging from 1:100 to 1: 80,000, where a decrease in absorbance values was observed (Figure 6.3, panel A) with increasing dilution in two separate stocks of serum (S1 & S2). The anti-C-FIKK antibodies were thus purified using ammonium sulfate precipitation and verified through SDS-PAGE (Figure 6.3, panel B). Confirmation was performed initially with anti-His antibodies (Figure 6.3, panel C)

and later with purified anti-C-FIKK antibodies at a 1:5000 dilutions (Figure 6.3, panel D) and thus enabling the purified protein for further validation.

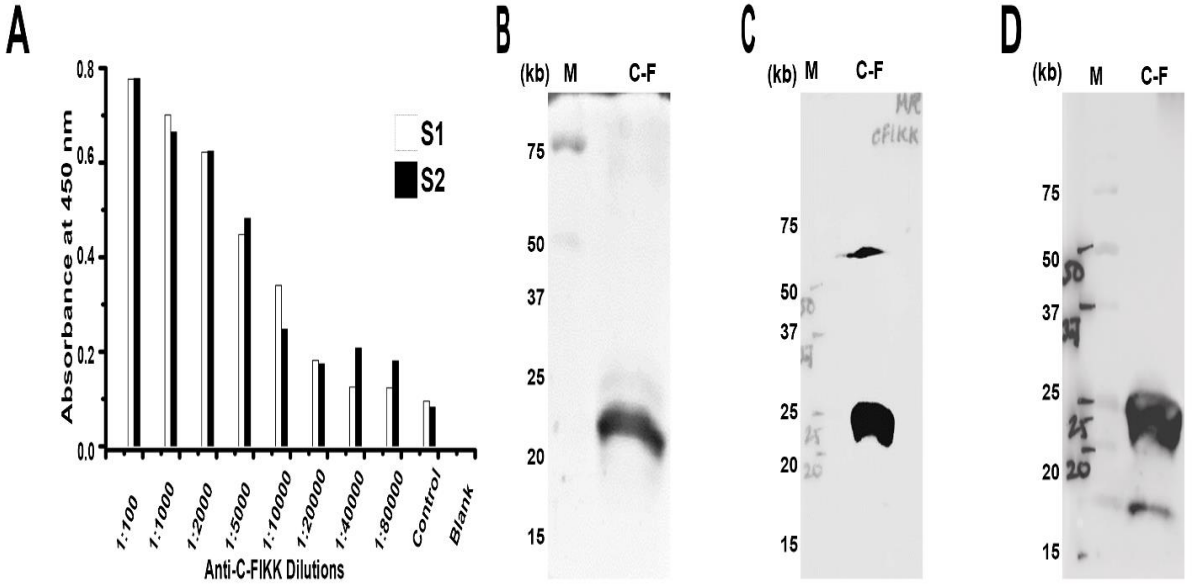

Figure 6.3: Antibody Titration and Specificity Validation of Anti-C-FIKK Sera by ELISA and Western Blot. The determination of anti-C-FIKK serum titer against purified C-FIKK by ELISA shows linear decrease of absorbance value with increase of antisera dilution. The titre of 1:5000 dilution of antisera (of serum 1-S1, & serum 2-S2 stock) was found to be optimal for further studies **(A)**. The antibody specificity was verified through SDS-PAGE **(B)** and confirmed initially with anti-His antibodies **(C)** and later with purified anti-C-FIKK antibodies **(D).**

6.3.3 Diagnostic Validation: Sensitivity and Selectivity of *Chimeric* FIKK

The sensitivity of the polyclonal anti-C-FIKK antibody was assessed using purified protein samples. Different concentrations of the purified protein, ranging from 250 nano Mol to 0.02 nano Mol (as 1 is 250 nM; 2 is 125 nM ; 3 is 63 nM ; 4 is 32 nM ; 5 is 16 nM ; 6 is 8 nM ; 7 is 4 nM ; 8 is 2 nM ; 9 is 1 nM; 10 is 0.5 nM ; 11 is 0.25 nM ; 12 is 0.13 nM; 13 is 0.07 nM ; 14 is 0.04 nM ; 15 is 0.02 nM), were applied onto a membrane (Figure 6.4, panel A) and probed with the anti-C-FIKK antibody. The antibody's sensitivity was observed to decrease proportionally with the reduction in protein concentration (Figure 6.4, panel B). Dot blot analysis indicated that the detection threshold of the anti-C-FIKK antibody was approximately 4 nM of protein, with stable performance across multiple trials. The anti-C-FIKK antibody detects C-FIKK antigen at least to 0.02% parasitemia grown under *in-vitro* conditions

(Figure6.4,panelC&D).

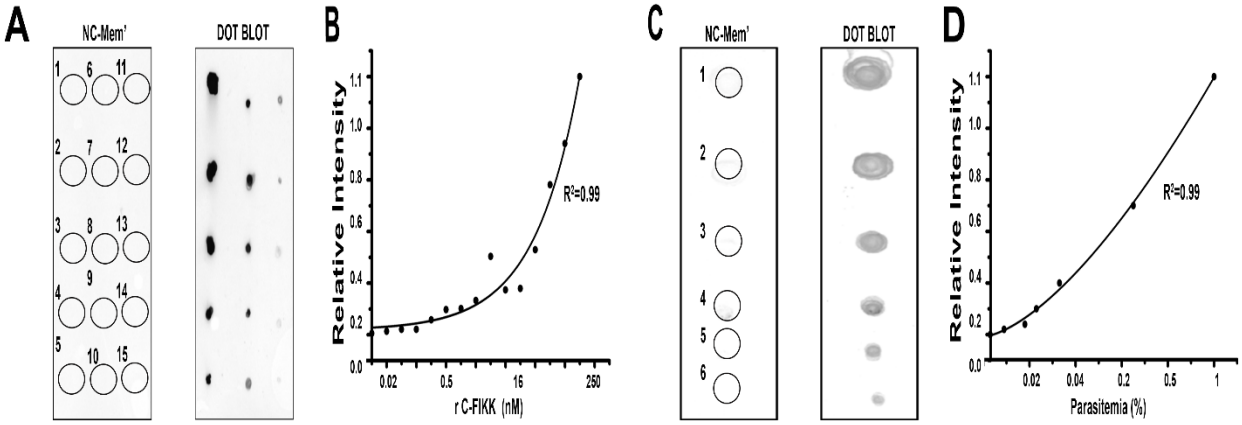

Figure 6.4: Sensitivity of *Chimeric*-FIKK. The sensitivity of purified C-FIKK antigen was assessed across a concentration range from 250 nM to 0.02 nM, **(A)** with a R^2 = 0.99, demonstrating a strong correlation **(B)**. The Anti-C-FIKK antibody detection of C-FIKK antigen in parasite samples, showing detection at parasitemia levels as low as 0.02%, spanning from 0.02% to 1% parasitemia **(C)** as 1 is 1 %, 2 is 0.5%, 3 is 0.2%, 4 is 0.1 %, 6 is 0.04% and 7 is 0.02 %. The corresponding graph **(D)** also exhibits with R^2 = 0.99, confirming strong correlation for detection.

We then assessed the selectivity of C-FIKK using human serum obtained from whole blood and the complete medium used for *in vitro* parasite culture that were tested for potential cross-reactivity. These samples, along with 0.02 % parasites as positive control as 1, BSA as negative control as 2, and serum of various dilutions, were spotted onto a nitrocellulose membrane at dilutions ranging from 1:1 to 1:20 (from 3 to 7). A plain blot confirmed uniform application of all samples on the membrane. Probing and chemiluminescent detection showed no signal in the human serum (Figure 6.5, panel A) or culture medium (Figure 6.5, panel B) samples at any dilution. These results clearly demonstrate that the anti-C-FIKK antibody does not cross-react with human serum proteins or components of the parasite culture medium.

Inaccurate diagnosis in the presence of co-infecting pathogens can significantly impact disease outcomes, treatment efficacy, and the development of drug resistance. Therefore, it is essential to evaluate the performance of the detection system in the presence of other infectious agents. This study focused on assessing potential interference caused by organisms such as *Bacillus vallismortis, Bacillus subtilis, Staphylococcus aureus, Listeria monocytogenes, Bacillus tequilensis, Lactobacillus, Rhodococcus opacus,* several *E. coli* strains (BL21(DE3), BL21(DE3) CodonPlus, Rosetta(DE3), DH5α), *Mycobacterium smegmatis,* yeast (*Aspergillus terreus, Neurospora crassa, Saccharomyces cerevisiae, Pichia pastoris*), viruses (Influenza

virus, Newcastle disease virus, Japanese encephalitis virus, Duck enteritis virus, Herpes simplex virus), and algae (*Scenedesmus*).

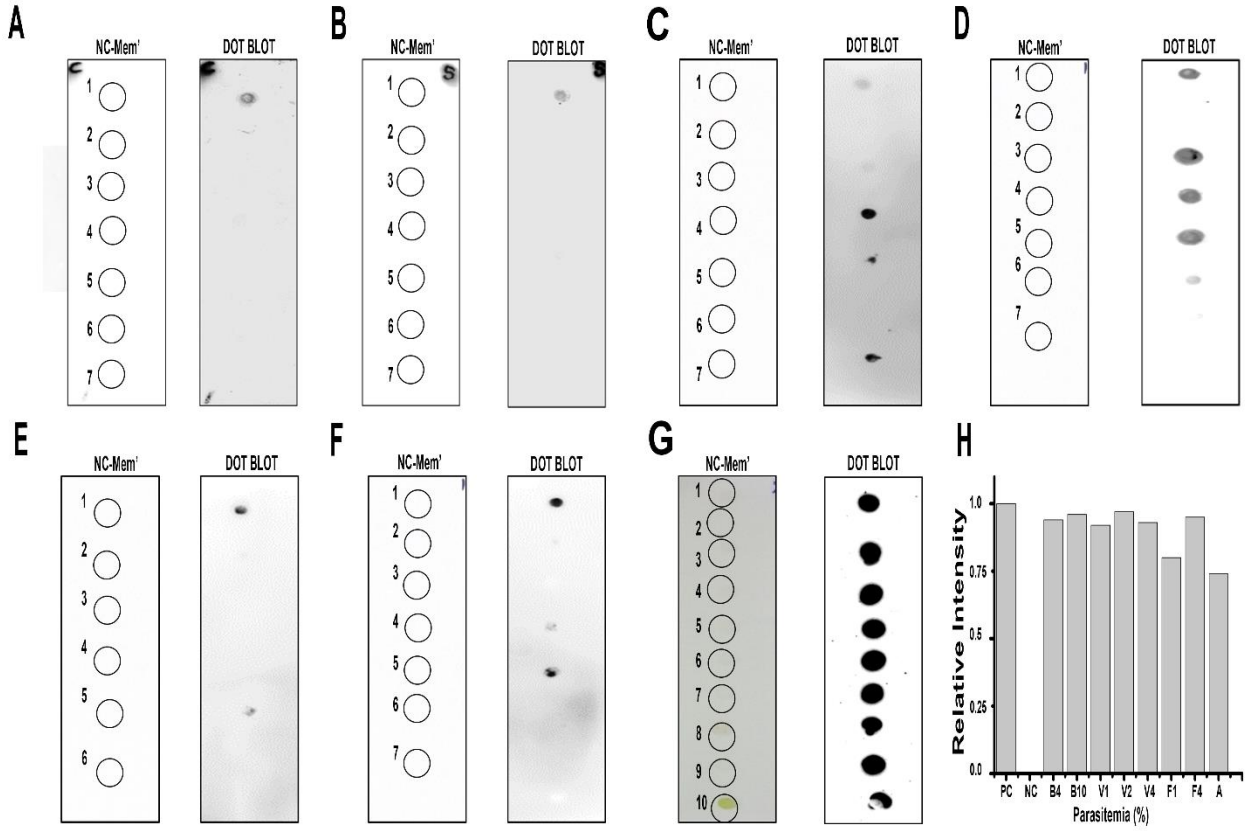

Figure 6.5: Selectivity of *Chimeric*-FIKK. The serum samples of various dilution (1:1 to 1:20 dilution) was analyzed through dot blotting technique **(A)** with 0.02 % parasites as positive control as 1, BSA as negative control as 2, with undiluted serum as 3 and of various dilutions (4 as 1:1, 5 as 1:5, 6 as 1:10, & 7 as 1:20). Similarly, with culture media was analyzed through dot blotting technique **(B)** with 0.02 % parasites as positive control as 1, BSA as negative control as 2 in all the panels, with undiluted culture media as 3 and of various dilutions (4 as 1:1, 5 as 1:5, 6 as 1:10, & 7 as 1:20). The lysates of bacterial organisms **(C)** *Bacillus vallismortis* as 3, *Bacillus subtilis* as 4, *Staphylococcus aureus* as 5, *Listeria monocytogenes* as 6, *Bacillus tequilensis* as 7, with 0.02 % parasites as positive control as 1, and BSA as negative control as 2. The other bacterial strains **(D)** include *Bacillus megaterium* as 3, *Acinetobacter baylyi* as 4, *Methylobacterium extorquens* as 5, *Lactobacillus lactis* as 6, and *Rhodococcus opacus* as 7 was analyzed through dot blotting technique. The lysates of viral pathogens in panel **(E)** with, Duck enteritis virus as 3, Influenza virus as 4, Japanese encephalitis virus as 5, Newcastle disease virus as 6 was analyzed through dot blotting technique and lysates of fungal and algal pathogens in panel **(F)** with *Aspergillus terreus* as 3, *Neurospora crassa* as 4, *Pichia*

pastoris as 5, *Saccharomyces cerevisiae* as 6, and *Scenedesmus* as 7 was analyzed through dot blotting technique. The Parasitized RBC contaminated **(G)** with different concentrations of bacteria (*Listeria monocytogenes* as 3, and *Rhodococcus opacus* as 4*)*, virus (*Duck enteritis virus* as 5, *Influenza virus* as 6, *Newcastle disease virus* as 7,), yeast (*Aspergillus terreus* as 8, and *Saccharomyces cerevisiae* as 9, and *Scenedesmus* as 10 and are studied for its interference in the detection of C-FIKK. The RBC lysate and parasitized RBC lysate are used as Negative control (NC as 2) and Positive control (PC as 1). The signal intensities are measured and compared to positive control **(H)**. The blot is developed using chemiluminescence substrate (dot blot) and as a control before applying substrate the image of blot spotted with is acquired (Nitrocellulose membrane-NC-Mm').

To confirm the specificity of the anti-C-FIKK antibody, a dot blot analysis was initially performed using infectious agents alone, including bacteria (Figure 6.5, panels C & D), viruses (Figure 6.5, panel E), fungi, and algae (Figure 6.5, panel F). No signal was detected for organisms such as *Listeria monocytogenes* (6 of panel G), *Rhodococcus opacus* (7 of panel H), *Duck enteritis virus* (3 of panel I), *Influenza virus* (4 of panel I), *Newcastle disease virus* (6 of panel I), *Aspergillus terreus* (3 of panel J), *Saccharomyces cerevisiae* (6 of panel J), and *Scenedesmus* (7 of panel J), indicating no cross-reactivity with the antibody. However, cross-reactivity was observed with *Bacillus vallismortis* (3 of panel G), *Bacillus subtilis* (4 of panel G), *Staphylococcus aureus* (5 of panel G), *Bacillus tequilensis* (7 of panel G), *Lactobacillus* (3 of panel H), BL21(DE3) (4 of panel H), BL21(DE3) CodonPlus (5 of panel H), *Mycobacterium smegmatis* (6 of panel H), yeast (*Neurospora crassa* (4 of panel J), *Pichia pastoris* (5 of panel J)), and *Japanese encephalitis virus* (5 of panel I). This cross-reactivity is likely due to the presence of residual bacterial proteins in the gel-eluted C-FIKK preparation used for immunization, as the electro elution process may have co-purified host strain proteins along with C-FIKK. Under the same experimental conditions, the antibody's ability to detect the C-FIKK protein was further tested by mixing parasite lysates with high concentrations of non-reactive infectious agents (Figure 6.5, panel G). The chemiluminescent signals obtained from the blot confirmed that the presence of these non-cross-reactive organisms did not interfere with the detection of the C-FIKK protein in the parasite lysate (Figure 6.5, panel H).

6.4 DISCUSSION

Although microscopy remains the gold standard, its reliance on skilled personnel and limitations in detecting low-parasitemia and mixed infections make it impractical in many endemic regions [6]. RDTs, though widely used, are hindered by high detection thresholds, antigenic variability, and *pfhrp2* gene deletions, leading to false negatives and reduced diagnostic reliability [5, 8]. The species-specific nature of FIKK kinases, unique to *P. falciparum*, makes them ideal targets for both molecular and immunodiagnostic approaches [11, 13]. The development of a FIKK-based PCR assay demonstrated enhanced sensitivity, detecting parasitemia as low as 0.0003% and distinguishing *P. falciparum* even in mixed infections [17], surpassing conventional PCR and RDT methodologies detect malarial antigens that paves way to detecting malaria with >98% accuracy and potential to differentiate among mixed species [29-31].

The current study bridges the gap between the molecular, & protein-level diagnostics, suggesting the suitability of FIKK kinases for next-generation lateral-flow immunoassays for the specific detection of *Plasmodium falciparum*, addressing key limitations associated with conventional malaria diagnostic markers like HRP-II and pLDH. While these markers have been widely employed, their diagnostic performance is often hindered by issues such as cross-reactivity and low sensitivity, particularly in low-parasitemia infections [12]. By leveraging the unique sequence and antigenic properties of FIKK kinases, this study demonstrates their ability to serve as reliable and specific markers for malaria diagnosis. The bioinformatics-driven approach employed in this study enabled the identification of exclusive antigenic regions within the 21 FIKK kinases of *P. falciparum*. These regions, characterized by high hydrophilicity, surface accessibility, and B-cell and T-cell epitope-binding potential, were integrated into the design of a *chimeric*-FIKK protein. This strategy contrasts with earlier diagnostic tools that primarily rely on broadly conserved antigens, often leading to cross-reactivity with non-target species [31]. The incorporation of highly specific epitopes ensured robust immunogenicity, as evidenced by the production of polyclonal anti-C-FIKK antibodies with high specificity and sensitivity. The dot blot analysis revealed that the anti-C-FIKK antibody could detect as low as 4 nMol of the target protein, with stable performance across multiple trials. This detection threshold is comparable to or better than traditional diagnostic methods like RDTs, which often struggle with low parasitemia detection [32].

Moreover, the antibody exhibited no cross-reactivity with human serum proteins, parasite culture media, and non-target infectious agents such as *Listeria monocytogenes*, *Saccharomyces cerevisiae*, and various viruses. However, cross-reactivity with certain

bacterial strains (*Bacillus subtilis*, *Mycobacterium smegmatis*, and *E. coli*) underscores the importance of further refining the purification process to eliminate residual host proteins during immunogen preparation. The ability of the anti-C-FIKK antibody to detect *P. falciparum* antigen even in the presence of high concentrations of non-cross-reactive organisms highlights its potential utility in complex biological samples. This is particularly significant in resource-limited settings where mixed infections and non-specific background signals can complicate diagnostics. Compared to earlier studies [33], which often focused on single antigen targets (HRP-II or pLDH), the chimeric approach employed here provides a novel platform for malaria diagnosis with enhanced specificity and reduced likelihood of false positives. While previous studies have reported promising results for HRP-II-based diagnostics, these tools are prone to degradation under storage conditions and show reduced efficacy in detecting low parasitemia levels [33]. Similarly, pLDH-based assays, although species-specific, often fail to distinguish between active and resolved infections due to the persistence of antigens in circulation [34]. The C-FIKK approach, by contrast, directly targets parasite-specific epitopes with no homology to human and other *Plasmodium* proteins, offering a significant advancement in diagnostic accuracy. The findings from this study underscore the diagnostic utility of FIKK kinases as specific and sensitive markers for malaria detection. By addressing the limitations of conventional diagnostic tools, the FIKK approach has the potential to transform malaria diagnostics, contributing to improved disease management and elimination efforts. In conclusion, our study suggests FIKK could be used as a platform to develop immuno-chromatographic strips for the detection of species-specific malaria detection.

6.5 REFERENCES:

1. Hatherell, H.-A., et al., *Sustainable surveillance of neglected tropical diseases for the post-elimination era.* Clinical Infectious Diseases, 2021. **72**(Supplement_3): p. S210-S216.
2. Lourenço, C., et al., *Strengthening surveillance systems for malaria elimination: a global landscaping of system performance, 2015–2017.* Malaria journal, 2019. **18**: p. 1-11.
3. Tangpukdee, N., et al., *Malaria diagnosis: a brief review.* The Korean journal of parasitology, 2009. **47**(2): p. 93.
4. Moody, A., *Rapid diagnostic tests for malaria parasites.* Clinical microbiology reviews, 2002. **15**(1): p. 66-78.
5. Cunningham, J., et al., *A review of the WHO malaria rapid diagnostic test product testing programme (2008–2018): performance, procurement and policy.* Malaria journal, 2019. **18**: p. 1-15.

6. Zimmerman, P.A. and R.E. Howes, *Malaria diagnosis for malaria elimination.* Current opinion in infectious diseases, 2015. **28**(5): p. 446-454.
7. Murray, C.K., et al., *Update on rapid diagnostic testing for malaria.* Clinical microbiology reviews, 2008. **21**(1): p. 97-110.
8. Poti, K.E., et al., *HRP2: transforming malaria diagnosis, but with caveats.* Trends in parasitology, 2020. **36**(2): p. 112-126.
9. Ippolito, M.M., et al., *Antimalarial drug resistance and implications for the WHO global technical strategy.* Current epidemiology reports, 2021. **8**: p. 46-62.
10. El-Zawahry, Y.A., et al., *Phenotypic detection of extended spectrum β-lactamase and Metallo β-lactamase production by Gram negative uropathogens after exposure to gamma radiation.* 2020.
11. Ward, P., et al., *Protein kinases of the human malaria parasite Plasmodium falciparum: the kinome of a divergent eukaryote.* BMC genomics, 2004. **5**: p. 1-19.
12. Nunes, M.C., et al., *Plasmodium falciparum FIKK kinase members target distinct components of the erythrocyte membrane.* PloS one, 2010. **5**(7): p. e11747.
13. Schneider, A.G. and O. Mercereau-Puijalon, *A new Apicomplexa-specific protein kinase family: multiple members in Plasmodium falciparum, all with an export signature.* BMC genomics, 2005. **6**: p. 1-12.
14. Nunes, M.C., et al., *A novel protein kinase family in Plasmodium falciparum is differentially transcribed and secreted to various cellular compartments of the host cell.* Molecular microbiology, 2007. **63**(2): p. 391-403.
15. Davies, H., et al., *An exported kinase family mediates species-specific erythrocyte remodelling and virulence in human malaria.* Nature microbiology, 2020. **5**(6): p. 848-863.
16. Balaji, S. and V. Trivedi, *Extracellular methemoglobin primes red blood cell aggregation in malaria: an in vitro mechanistic study.* FEBS letters, 2013. **587**(4): p. 350-357.
17. Prasad, M.R. and V. Trivedi, *Molecular Investigation of FIKK Kinase Family to Develop PCR-Based Diagnosis of Plasmodium falciparum.* Molecular Biotechnology, 2024: p. 1-17.
18. Jespersen, M.C., et al., *BepiPred-2.0: improving sequence-based B-cell epitope prediction using conformational epitopes.* Nucleic acids research, 2017. **45**(W1): p. W24-W29.
19. Parker, J., D. Guo, and R. Hodges, *New hydrophilicity scale derived from high-performance liquid chromatography peptide retention data: correlation of predicted surface residues with antigenicity and X-ray-derived accessible sites.* Biochemistry, 1986. **25**(19): p. 5425-5432.
20. Karplus, P. and G. Schulz, *Prediction of chain flexibility in proteins: a tool for the selection of peptide antigens.* Naturwissenschaften, 1985. **72**(4): p. 212-213.
21. Emini, E.A., et al., *Induction of hepatitis A virus-neutralizing antibody by a virus-specific synthetic peptide.* Journal of virology, 1985. **55**(3): p. 836-839.
22. Karosiene, E., et al., *NetMHCcons: a consensus method for the major histocompatibility complex class I predictions.* Immunogenetics, 2012. **64**: p. 177-186.
23. Nielsen, M., C. Lundegaard, and O. Lund, *Prediction of MHC class II binding affinity using SMM-align, a novel stabilization matrix alignment method.* BMC bioinformatics, 2007. **8**: p. 1-12.
24. Kolaskar, A.S. and P.C. Tongaonkar, *A semi-empirical method for prediction of antigenic determinants on protein antigens.* FEBS letters, 1990. **276**(1-2): p. 172-174.
25. Kolaskar, A.S. and P.C. Tongaonkar, *A semi-empirical method for prediction of antigenic determinants on protein antigens.* FEBS Lett, 1990. **276**(1-2): p. 172-4.

26. Vázquez-Iglesias, L., et al., *A simple electroelution method for rapid protein purification: isolation and antibody production of alpha toxin from Clostridium septicum.* PeerJ, 2017. **5**: p. e3407.
27. Wingfield, P., *Protein precipitation using ammonium sulfate.* Current protocols in protein science, 1998. **13**(1): p. A. 3F. 1-A. 3F. 8.
28. Singh, G., et al., *Development of an indirect competitive ELISA for analysis of alternariol in bread and bran samples.* Food analytical methods, 2018. **11**: p. 1444-1450.
29. Adu-Gyasi, D., et al., *Assessing the performance of only HRP2 and HRP2 with pLDH based rapid diagnostic tests for the diagnosis of malaria in middle Ghana, Africa.* PLoS One, 2018. **13**(9): p. e0203524.
30. Park, S.H., et al., *Diagnostic Performance of Three Rapid Diagnostic Test Kits for Malaria Parasite Plasmodium falciparum.* Korean J Parasitol, 2020. **58**(2): p. 147-152.
31. Kavanaugh, M.J., S.E. Azzam, and D.M. Rockabrand, *Malaria rapid diagnostic tests: literary review and recommendation for a quality assurance, quality control algorithm.* Diagnostics, 2021. **11**(5): p. 768.
32. Oyegoke, O.O., et al., *Malaria diagnostic methods with the elimination goal in view.* Parasitology research, 2022. **121**(7): p. 1867-1885.
33. Gilani, S.T.A., et al., *COMPARISON OF IMMUNOCHROMATOGRAPHY AND MICROSCOPIC FILM METHOD FOR THE DIAGNOSIS OF MALARIA IN LIBERIA.* Pakistan Armed Forces Medical Journal, 2020. **70**(4): p. 1201-05.
34. Lee, W.S., et al., *Simple, rapid, and accurate malaria diagnostic platform using microfluidic-based immunoassay of Plasmodium falciparum lactate dehydrogenase.* Nano Convergence, 2020. **7**: p. 1-8.
35. Shrivastava, D., et al., *Plasmodium falciparum FIKK9. 1 is a monomeric serine–threonine protein kinase with features to exploit as a drug target.* Chemical Biology & Drug Design, 2021. **97**(4).

Annexure I

Preparation of Reagents and Buffers

i. Lysis Buffer
20 mM Tris-HCl, 300 mM NaCl, pH 7.8

ii. Elution Buffer
20 mM Tris-HCl, 300 mM NaCl, and varying concentration (10mM, 20mM, 50mM, 100mM, 150mM, 200mM, & 250mM,) of imidazole, pH 8.0

iii. SDS-PAGE Running Buffer
0.25 M Tris-HCl, 1.92 M Glycine, and 1 % SDS-PAGE (w/v), pH 8.3

iv. Staining Solution
0.05 % Coomassie Brilliant Blue R-250, 10 % glacial acetic acid, & 45 % (v/v) methanol

v. De-Staining Solution
10 % glacial acetic acid, & 45 % (v/v) methanol

vi. Composition of 15 % SDS-PAGE Resolving Gel & 5 % Stacking Gel

S. No	Component	15% Resolving Gel (For 10 mL)	5% Stacking Gel
1	Distilled Water	2.290 mL	3.435 mL
2	30 % Acrylamide	5 mL	830 µL
3	Tris-HCl (pH 8.8)	2.5 mL	(pH 6.8) 630 µL
4	10 % SDS	100 µL	50 µL
5	10 % APS	100 µL	50 µL
6	TEMED	10 µL	5 µL

vii. Reagents for Competent Cell Preparation
0.1 M CaCl2, 20% glycerol, autoclaved and stored at 4 ºC

viii. PBS & PBST Preparation
137 mM NaCl, 27 mM KCl, 100 mM Na2HPO4, 20 mM KH2PO4, pH 7.4
0.1 % Tween 20 additionally added for PBST

ix. TBS & TBST Preparation
20 mM Tis-HCl, 150 mM NaCl, pH 7.4
0.1 % Tween 20 additionally added for TBST

x. Antibiotic Preparation
50 mg/mL for Kanamycin
50 mg/mL for Chloramphenicol
100 mg/mL for Ampicillin

xi. Electro elution buffer
0.25 M Tris-HCl, 1.92 M Glycine, and 0.1 % SDS (w/v), pH 7.8

xii. Transfer buffer
0.25 M Tris-HCl, 1.92 M Glycine, and 20 % methanol (v/v), pH 8.3

xiii. Blocking buffer
3 % Bovine Serum Albumin (BSA) in PBST/TBST

xiv. SDS-PAGE Gel Loading Dye
10% SDS, 500mM DTT/BME, 50% Glycerol, 0.2% bromophenol blue dye, 250mM Tris-HCl, pH 6.8.

xv. Reagent for Inducing Protein Expression
A stock of 1 M IPTG (Isopropyl β-D-1-thiogalactopyranoside)

xvi. Reagent for Charging Ni Beads
0.2 M NiSO4

xvii. Reagent for Protease Inhibitor

A stock of 100 mM PMSF (phenylmethylsulfonyl fluoride)

xviii. Luria-Bertani (LB) Media Preparation

Per 1 liter, bacto tryptone/peptone: 10 grams, NaCl: 5 grams, and Yeast extract: 10 grams

xix. Super Broth (SB) Media Preparation

Per 1 liter, bacto tryptone/peptone: 32 grams, NaCl: 5 grams, Yeast extract: 20 grams, and NaOH (1 Normal): 0.5 mL

xx. Terrific Broth (TB) Media Preparation

Per 1 liter,

TB-A (900 mL)
bacto tryptone/peptone: 12 grams,
Yeast extract: 24 grams
Glycerol: 3.17 mL

TB-B (100 mL)
KH_2PO_4: 2.32 grams
K_2HPO_4: 16.4 gram

Chapter 7

Conclusions

7.1 CONCLUSIONS

This study highlights the critical role of molecular and rapid diagnostics in improving malaria detection, particularly through FIKK kinase-based assays, which offer superior sensitivity and specificity compared to conventional methods. The development of FIKK kinase-based PCR assays has demonstrated exceptional accuracy in detecting *P. falciparum*, even at low parasitemia levels, outperforming traditional microscopy and RDTs. However, the reliance on sophisticated laboratory infrastructure, costs, and the need for trained personnel remain barriers to widespread implementation, particularly in resource-limited settings. Despite these limitations, the specificity of FIKK kinase-based assays ensures no cross-reactivity, making them a promising alternative for malaria diagnosis and surveillance.

To develop a more reliable alternative that can overcome the barriers in resource-limited settings, chimeric FIKK (C-FIKK) was generated. The development of a chimeric FIKK protein (C-FIKK) and its successful detection by generating polyclonal antibodies further demonstrate the potential of novel biomarkers in overcoming the limitations of current diagnostic tools, such as Pf-HRP2 deletions, low-parasitemia detection, and species specific detection failures. Additionally, these biomarkers can provide a more reliable alternative for species differentiation, addressing a major challenge in malaria co-infections. Despite the high accuracy of molecular techniques like PCR, their dependency on expensive equipment, trained personnel, and sophisticated laboratory infrastructure limits widespread application, particularly in resource-constrained regions. To bridge this gap, either portable pocket PCRs with field-applicable diagnostic solutions or RDT FIKK-based assays can be explored. However, these advancements represent a significant step forward in enhancing malaria surveillance, early detection, and case management, potentially reducing mortality and transmission rates.

7.2 FUTURE DIRECTIONS

1. **Large-Scale Clinical Validation**: Multi-site clinical trials can be assessed for the real-world efficacy and reliability of molecular diagnostic approaches before widespread implementation.
2. **Biomarker Exploration**: Further research into one conserved FIKK kinase for other *Plasmodium* species causing malaria for PCR based assay can be applied for species differentiation.
3. **Monoclonal Antibody Development**: Generating monoclonal antibodies against C-FIKK can improve specificity and reduce cross-reactivity in diagnostic applications.
4. **Integration of FIKK-Based Detection into RDTs**: Developing immunochromatographic test strips utilizing FIKK antibodies can enhance the accuracy and reliability along with species specific detection of malaria rapid testing.
5. **Development of Cost-Effective Molecular Assays**: Refining isothermal amplification techniques such as LAMP and RPA, which do not require complex thermal cycling equipment, making them more suitable for field deployment.
6. **Portable and Automated Platforms**: Integrating FIKK molecular diagnostics with handheld biosensors, portable PCRs, and microfluidic devices can improve accessibility and real-time disease monitoring in endemic regions.
7. **Combination Diagnostics**: Integrating FIKK-based detection with existing pLDH- and HRP-II-based tests could provide a comprehensive diagnostic tool to address PfHRP2 deletions and low parasitemia infections.

List of Publications:

1. **Prasad, M. R.,** Kumar, D. A**,** Eena Dodwani**,** Sukhwinder Singh, & Trivedi, V. (2025). Antigenic determinant analysis of FIKK Kinase family to identify novel candidates for diagnosis of *Plasmodium falciparum*. *Microbial Pathogenesis*

2. Prasad, M. R., & Trivedi, V. (2024). Molecular Investigation of FIKK Kinase Family to Develop PCR-Based Diagnosis of *Plasmodium falciparum*. *Molecular Biotechnology*, 1-17.

3. Kumar, D. A., Karjee, P., **Prasad, M. R.,** Punniyamurthy, T., & Trivedi, V. (2023). *Plasmodium falciparum* FIKK 9.1 kinase modeling to screen and identify potent antimalarial agents from chemical library. *3 Biotech*, *13*(8), 277.

Conferences:

1. Oral presentation in International Conference on "**Mechanistic and Therapeutic Approaches in Human and Animal Health**", 6th to 8th December, 2021 at Department of Zoology, Cooch Behar Panchanan Barma University, West Bengal.

2. Oral presentation in **Research and Industrial Conclave, An amalgamation of Academia, Industry & Strat-ups**, Jan, 2022, IIT Guwahati, Guwahati, Assam.

Microbial Pathogenesis 209 (2025) 108070

Contents lists available at ScienceDirect

Microbial Pathogenesis

journal homepage: www.elsevier.com/locate/micpath

Antigenic determinant analysis of FIKK Kinase family to identify novel candidates for diagnosis of *Plasmodium falciparum*

M. Rajendra Prasad [a,1], D. Anil Kumar [a,1], Eena Dodwani [a], Sukhwinder Singh [b], Vishal Trivedi [a,*]

[a] Malaria Research Group, Department of Biosciences and Bioengineering, Indian Institute of Technology-Guwahati, Guwahati, 781039, Assam, India
[b] Department of Microbiology, Panjab University, Chandigarh, India

ARTICLE INFO

Keywords:
Diagnosis
P. falciparum, C-FIKK
RDT
Sensitivity
Selectivity
Biomarker

ABSTRACT

The efforts to eliminate malaria require the development of highly sensitive and specific point-of-care diagnostic systems to enable early detection and prevent severe complications associated with the disease. Current rapid diagnostic tests (RDTs) rely on antigens conserved across *Plasmodium* species or those specific to *Plasmodium falciparum* and *Plasmodium vivax with humans*. In the current study, chimeric FIKK (C-FIKK) was generated as a promising target for malaria diagnosis by selecting highly antigenic, species-specific B- and T-cell epitopes of six selected FIKK kinases using IEDB tools, from the N-terminal regions of *P. falciparum* with no homology with the human counter parts. The antibodies were generated against C-FIKK, purified, and it exhibits high sensitivity with a detection limit of 3 μM for FIKK9.1. In addition, it is very selective for malaria parasite in the presence of bacterial, viral, fungal and algal organisms. Importantly, no cross-reactivity was observed with host blood components or proteins from non-*Plasmodium* organisms with the purified FIKK9.1. Validation with mock patient samples revealed that the purified antibody could semi-quantitatively detect parasite loads with an average accuracy of 95.45 %. These findings suggest that FIKK kinase-based rapid diagnostic tests is a robust and reliable diagnostic target for malaria detection, paving the way for the development of next-generation diagnostic systems with enhanced sensitivity and specificity.

1. Introduction

Effective malaria diagnosis is critical for disease management and eradication (Lourenço et al., 2019; Hatherell et al., 2021). While microscopy remains the gold standard, it has limitations in sensitivity, requiring skilled personnel and struggling with low-density infections (Tangpukdee et al., 2009). Rapid diagnostic tests (RDTs) have provided practical alternatives by targeting antigens such as histidine-rich protein II (Pf-HRP2), *Plasmodium* lactate dehydrogenase (pLDH), and aldolase (Moody, 2002; Cunningham et al., 2019; Zimmerman & Howes, 2015). However, RDTs have expanded access, yet performance is increasingly constrained by pfhrp2/3 deletions, brand variability, and lower sensitivity at sub-patent parasitemia (Poti et al., 2020, 2022; Chiu et al., 2023; Watson et al., 2023). Recent innovation spans ultrasensitive antigen tests, nucleic-acid methods (uPCR, LAMP/RPA), CRISPR-based assays, and emerging affinity reagents such as aptamers (Azizi et al., 2024; Abudulai et al., 2023; Xiong et al., 2023; Otabil et al., 2024). Against this backdrop, parasite proteins with species-restricted expression and host-cell accessibility are being re-evaluated as diagnostic targets. These challenges emphasize the need for novel, species-specific diagnostic markers with improved sensitivity.

To address these limitations, we explored the potential of FIKK kinases of *P. falciparum*-specific serine/threonine protein kinases that play a critical role in parasite survival and host cell remodeling. Unlike other *Plasmodium* species that encode only a single FIKK, *P. falciparum* harbors 21 members, most exported into infected erythrocytes (Ward et al., 2004; Schneider & Mercereau-Puijalon, 2005). These kinases possess a conserved C-terminal kinase domain and a variable N-terminal region, contributing to substrate specificity (Nunes et al., 2007). Functionally, they remodel host erythrocytes by phosphorylating cytoskeletal and membrane-associated proteins, thereby influencing deformability, cytoadhesion, and virulence (Davies et al., 2020; Balaji & Trivedi,

* Corresponding author. Malaria Research Group, Department of Biosciences and Bioengineering, Indian Institute of Technology-Guwahati, Guwahati, 781039, Assam, India.
E-mail addresses: vtrivedi@iitg.ernet.in, Vishalash_1999@yahoo.com (V. Trivedi).
[1] Equal Contribution.

https://doi.org/10.1016/j.micpath.2025.108070
Received 14 April 2025; Received in revised form 3 September 2025; Accepted 28 September 2025
Available online 2 October 2025

Molecular Biotechnology
https://doi.org/10.1007/s12033-024-01335-y

ORIGINAL PAPER

Molecular Investigation of FIKK Kinase Family to Develop PCR-Based Diagnosis of *Plasmodium falciparum*

M. Rajendra Prasad[1] · **Vishal Trivedi**[1]

Received: 24 October 2024 / Accepted: 19 November 2024

Abstract

Accurate malaria diagnosis is crucial for effective disease management as different *Plasmodium* species require specific treatment regimens. Current detection methods have limitations related to sensitivity and specificity. This is mainly due to employing similar targets such as 18S rRNA, *Pf-ldh*, *Pf-hrp-2*, and aldolase with significant homology to human counterparts. Targeting *Plasmodium fikk* kinases that are unique to *P. falciparum* offers a novel approach for developing potential biomarkers. We have identified exclusive regions of *fikk* kinases using in-silico PCR and later validated our findings using in-vitro PCR. We observed exceptional sensitivity with our designed primers of the targeted *fikk* kinases, with the detection limit going as low as 10^{-5} ng level of parasite DNA and 0.0003% parasitemia. The shortlisted primers also selectively identified *P. falciparum* in the presence of *Plasmodium vivax* or several other bacterial, viral, and fungal pathogens. Detection of mock patient samples indicates that the *fikk*-based PCR diagnosis is giving accurate results, and it is much better than the existing method. Thus, we show that the *fikk* kinases from *P. falciparum* are excellent targets for developing novel biomarkers with high sensitivity and specificity.

Keywords Diagnosis · *P. falciparum* · *Fikk* kinases · PCR · Sensitivity · Selectivity · Biomarker

Abbreviations

%	Percent/Percentage
°C	Degree Celsius
µL	Microlitre
18S rRNA	18S ribosomal RNA
BLAST	Basic Local Alignment Search Tool
bp	Base pair
cDNA	Complementary DNA
C	Terminus- carboxyl-terminus
DEV	Duck enteritis virus
DNA	Deoxyribonucleic acid
E. coli	*Escherichia coli*
FIKK	Phenylalanine, Isoleucine, Lysine, Lysine
f 3	*fikk 3 Gene*
f 4.2	*fikk 4.2 Gene*
f 8	*fikk 8 Gene*
f 10.2	*fikk 10.2 Gene*
f 12	*fikk 12 Gene*
f 14	*fikk 14 Gene*
fg	Femtogram
FP	Forward primer
gDNA	Genomic DNA
GC	Guanine-cytosine content
Hb	Haemoglobin
HSV	Herpes simplex virus
HuGAPDH	Human-specific glyceraldehyde-3-phosphate dehydrogenase
iRBCs	Infected red blood cells
JEV	Japanese encephalitis virus
LAMP	Loop-Mediated Isothermal Amplification
M	Marker
NC/N	Negative control
NCBI	National Centre for Biotechnology Information
NDV	Newcastle disease virus
ng	Nanogram
N	Terminus-Amino-terminal
OD	Optical density
PCR	Polymerase Chain Reaction
PC/P	Positive control
Pf-ldh	*Plasmodium falciparum*-Specific Lactate Dehydrogenase

✉ Vishal Trivedi
vtrivedi@iitg.ac.in; Vishalash_1999@yahoo.com

[1] Malaria Research Group, Department of Biosciences and Bioengineering, Indian Institute of Technology-Guwahati, Guwahati 781039, Assam, India

Published online: 02 December 2024

3 Biotech (2023) 13:277
https://doi.org/10.1007/s13205-023-03677-x

ORIGINAL ARTICLE

Plasmodium falciparum FIKK 9.1 kinase modeling to screen and identify potent antimalarial agents from chemical library

D. Anil Kumar[1] · Pallab Karjee[2] · M. Rajendra Prasad[1] · Tharmalingam Punniyamurthy[2] · Vishal Trivedi[1]

Received: 8 December 2022 / Accepted: 18 June 2023

Abstract
The Plasmodium FIKK kinases are diverged from human kinases structurally. They harbour conserved ATP-binding domains that are non-homologous to other existing kinases. FIKK9.1 kinase is considered as an essential protein for parasite survival. It is localized in major organelles present in parasite and trafficked throughout the infected RBC. It is speculated that FIKK9.1 may phosphorylate several substrates in the parasite's proteome and contribute to parasite survival. Therefore, FIKK9.1 is an attractive target that may lead to a novel class of antimalarials. To identify specific FIKK9.1 kinase inhibitors, we virtually screened organic structural scaffolds from a library of 623 entries. The top hits were identified based on conformations and molecular interactions with the ATP biophore. The hits were also validated under in vitro conditions. In this study, we identified seven top hit organic compounds that may arrest the growth of parasites by inhibiting FIKK9.1 kinase. Evaluation of top hit compounds in antimalarial activity assay identifies that the highly substituted 1,3-selenazolidin-2-imine 1 and thiophene 2 are inhibiting parasite growth with an IC_{50} of 3.2 ± 0.27 µg/ml and 3.13 ± 0.16 µg/ml, respectively. These functionalized heterocyclic compounds 1 and 2 kills the malaria parasite with an IC_{50} of 2.68 ± 0.02 µg/ml and 3.08 ± 0.14 µg/ml, respectively. Isothermal titration calorimetry analysis indicate that ATP is binding to the FIKK9.1 kinase. The dissociation constant (K_d) is measured to be 27.8 ± 2.07 µM with a stoichiometry of $n = 1$. The heterocyclic scaffolds 1 and 2 were abolishing the binding of ATP into the binding pocket. They in-turn reduce the ability of FIKK9.1 kinase to phosphorylate its substrate. Our study found that compounds 1 and 2 are potent inhibitor of FIKK9.1 kinase and the inhibition of FIKK9.1 kinase using small molecules disturbs the parasite life cycle and leads to the death of parasites. This provides new insight in development of novel antimalarials.

Keywords Malaria · FIKK kinase · Lead identification and antimalarial

Introduction

Malaria is a pernicious disease causing nearly half million deaths each year (Organization 2020). Although, malaria-associated death may have declined over a few decades through various efforts such as vector control strategies (Mnzava et al. 2014) and stable artemisinin combination therapies (Pousibet-Puerto et al. 2016) there is a steady increase in malarial cases around the globe. This demands extensive efforts to achieve the goal of eradication of malaria. To improve the outcome, we must ensure total cure of disease through safer and efficient development of new treatments. Drugs such as chloroquine, mefloquine, sulfadoxine-pyrimethamine, lumefantrine and quinine are prevalently used in endemic regions as antimalarials. Drug resistance and side effects of those drugs forced the introduction of artemisinin combination therapy (ACT's) in endemic areas (Haldar et al. 2018). However, the resistance and delayed death of parasites to artemisinin with some of its partner drugs are reported in Greater Mekong Sub-region (Menard and Dondorp 2017) and Eastern India (Das et al. 2018). Though the current antimalarial drug pipeline is promising, there is no alternative therapy besides ACT to control malaria (Nsanzabana 2019). Therefore, development of new antimalarials against novel targets is important to control malaria.

✉ Vishal Trivedi
vtrivedi@iitg.ernet.in; Vishalash_1999@yahoo.com

[1] Malaria Research Group, Department of Biosciences and Bioengineering, Indian Institute of Technology Guwahati, Guwahati 781039, Assam, India

[2] Department of Chemistry, Indian Institute of Technology Guwahati, Guwahati 781039, India

Published online: 18 July 2023